Identification and characterisation of toxin-antitoxin systems (TA) in *Burkholderia pseudomallei*

Submitted by Aaron Trevor Butt to the University of Exeter
as a thesis for the degree of
Doctor of Philosophy in Biological Sciences
In February 2013

I certify that all material in this thesis which is not my own work has been identified and that no material has previously been submitted and approved for the award of a degree by this or any other University.

Signature: ……..

Abstract

The aim of this study was to identify and characterise type II toxin-antitoxin (TA) systems in *Burkholderia pseudomallei,* the causative agent of the human disease melioidosis.

8 putative TA systems were identified within the genome of *B. pseudomallei* K96243. 5 of these were located witihn genome islands. Of the candidate toxins, BPSL0175 (RelE1) or BPSS1060 (RelE2) caused growth to cease when expressed in *Escherichia coli*, whereas expression of BPSS0390 (HicA) or BPSS1584 (HipA) (in an *E. coli ΔhipBA* background) caused a reduction in the number of culturable bacteria. HicA also caused growth arrest in *B. pseudomallei* K96243 *ΔhicAB.* These toxin induced phenotypes were enhanced by an <3kDa extracellular factor that accumulated in the spent medium during growth. Expression of the cognate antitoxins could restore growth and culturability of cells.

Expression of *hicA* in *E. coli* gave an increased number of persister cells in response to ciprofloxacin or ceftazidime. Site directed mutagenesis studies identified two key residues within the HicA toxin that were essential for both the reduced culturability and increased persistence phenotypes. Deletion of *hicAB* from *B. pseudomallei* K96243 did not affect persister cell or survival frequencies compared to the wild type following treatment with a variety of stress conditions.

Deletion of the Δ*hipBA* locus from *B. pseudomallei* K96243 also had no affect on bacterial persistence or survival under the conditions tested.

Contents

List of figures

Page number

Chapter 1

Chapter 2

Chapter 3

Chapter 4

Chapter 5

Chapter 6

Chapter 7

List of tables

Chapter 1

Chapter 2

Chapter 3

Chapter 5

Chapter 6

Chapter 7

Publications and posters

Identification of type II toxin-antitoxin modules in *Burkholderia pseudomallei* Butt A, Müller C, Harmer N, Titball RW. *FEMS Microbiol Lett.* 2013 Jan;338(1):86-94

Identifying Toxin- antitoxin modules in *Burkholderia pseudomallei*
Aaron Butt, Claudia Mueller, Nicholas Harmer, Richard Titball
SGM conference - Edinburgh, April 2010

Identifying Toxin- antitoxin modules in *Burkholderia pseudomallei*
Aaron Butt, Claudia Mueller, Nicholas Harmer, Richard Titball
South West and South Wales Microbiology forum - Cardiff, September 2010

Identifying Toxin- antitoxin modules in *Burkholderia pseudomallei*
Aaron Butt, Claudia Mueller, Nicholas Harmer, Richard Titball
World Melioidosis congress - Townsville, Australia, December 2010

Identifying Toxin- antitoxin modules in *Burkholderia pseudomallei*
Aaron Butt, Claudia Mueller, Nicholas Harmer, Richard Titball
Infection and Immunity meeting – Hua Hin, Thailand, December 2010

The *Burkholderia pseudomallei* TA system toxin BPSS0390 causes growth arrest and increases persister cell frequencies: a single amino acid substitution inactivates functionality
Aaron Butt, Claudia Mueller, Nicholas Harmer, Richard Titball
European Melioidosis Network – Amsterdam, Netherlands, February 2012

Declaration

Unless otherwise stated, the results and data presented in this thesis were solely the work of Aaron Butt.

Circular dichroism was performed by Dr Tam Bui at Kings College London. NMR spectroscopy and analysis was carried out by Dr Matt Crump, Dr Chris Williams and Dr Vicky Higman at the University of Bristol.

Transcriptomics data was provided by Dr Catherine Ong from the Genome institute in Singapore.

Dr Claudia Hemsley provided the *B. pseudomallei* Δ*hipBA* strain.

Acknowledgements

I would like to thank my supervisors Professor Rick Titball and Dr Nic Harmer and my training mentor Dr Claudia Hemsley for their continued help and support throughout the PhD project. I would also like to thank everyone I have worked with over the last 3-4 years in the BPRG research group, in particular Dr Monika Bokori-Brown and Dr Sariqa Wagley who have provided invaluable advice and expertise. Thanks to Dr Nicola Senior for proof reading this thesis.

Thanks also go to my family, especially my parents who have always encouraged and supported me. I would also like to thank all of my friends for listening and providing a temporary escape from science.

Abbreviations

%	Percent
Δ	Delta
1D	One dimensional
2D	Two dimensional
^{o}C	Degrees centigrade
α	Alpha
aa	Amino acid
Amp	Ampicillin
ANOVA	Analysis of variance
ATP	Adenosine triphosphate
β	Beta
Bcc	*Burkholderia cepacia* complex
Bf8	Z-4-bromo-5-(bromomethylene)-3-methylfuran-2(5H)-one
BLAST	Basic local alignment search tool
bp	Base pair
BSA	Bovine serum albumin
Bsa	*Burkholderia* secretion apparatus
C10	3-[4-(4-methoxyphenyl)piperazin-1-yl]piperidin-4-yl biphenyl-4-carboxylate
CBP	Chitin binding protein
CD	Circular Dichroism
CD4	Cluster of differentiation 4
CD8	Cluster of differentiation 8
CFU	Colony forming unit
Cm	Chloramphenicol
COSY	Correlation spectroscopy
CRISPR	Clustered Regularly Interspaced Short Palindromic Repeat
CPS	Capsular polysaccharide
CSP	Competence stimulating peptide
DNA	Deoxyribonucleic acid
dH_2O	Deuterium
dNTPs	Deoxynucleotides
ε	Epsilon
EDF	Extracellular death factor
EDTA	Ethylenediaminetera acetic acid
Ef-Tu	Elongation factor thermo unstable
EMSA	Electophoretic mobility shift assay
g	grams
GI	Genomic Island or Gastrointestinal
GST	glutathione-S-transferase
GTP	Guanosine triphosphase
γ	gamma
H_20_2	Hydrogen peroxide
HCl	Hydrogen chloride
HRP	Horseradish peroxidase

HTH	Helix turn helix
HSQC	Heteronuclear Single Quantum Coherence
IFN	Interferon
IgG	Immunoglobulin G
IgM	Immunoglobulin M
IL	Interleukin
IPTG	Isopropyl β-D-1 thiogalactopyranoside
IV	Intravenous
Km	Kanamycin
λ	Lambda
L	Litre
LB	Luria broth
LPS	Lipopolysaccharide
LF	Left flank
MBP	Maltose binding protein
Mb	Mega base
µ	Micro
m	Milli or metres
M	Molar
MDR	Multi drug resistance
MIC	Minimum inhibitory concentration
min	minute(s)
mRNA	messenger ribonucleic acid
MW	Molecular weight
n	Nano
NaOH	Sodium hydroxide
NaCl	Sodium chloride
NCBI	National Centre for Biotechnology Information
NOESY	Nuclear Overhauser effect spectroscopy
NMR	Nuclear magnetic resonance
ω	Omega
OD	Optical density
O-PS	O-polysaccharide
ONCs	Overnight cultures
ORFs	Open reading frames
P	pico or probability
PAGE	Polyacrylamide gel electrophoresis
PBS	Phosphate buffered saline
PBST	Phosphate buffered saline Tween
PCR	Polymerase chain reaction
pH	Potential of hydrogen-measure of hydrogen ions associated with acidity
PI	Isoelectric point
(p)ppGpp	guanosine (penta) or tetraphosphate
PSK	postsegregational killing
PQ	Paraquat
PVDF	Polyvinylidenflouride
qPCR	qualitative real time polymerase chain reaction
RF	Right flank
RHH	Ribbon helix helix

RPM	Revs per minute
RNA	Ribonucleic acid
rRNA	Ribosomal ribonucleic acid
ROS	Reactive oxygen species
RT	Room temperature
s	Subunit
σ	Sigma
secs	Seconds
SDM	Site directed mutagenesis
SDS	Sodium dodecyl sulphate
SEM	Standard error of the mean
TA	Toxin-antitoxin
TAE	Tris-acetate-EDTA
TBS	Tris buffered saline
TBST	Tris buffered saline Tween
Tet	Tetracycline
TLR	Toll- ike receptor
TTSS	Type III secretion system
tRNA	Transfer ribonucleic acid
TNF	Tumour necrosis factor
TOCSY	Total correlation spectroscopy
Tp	Trimethoprim
T6SS	Type VI secretion system
UV	Ultraviolet
UNAG	Uridine diphosphate-N-acetylglucosamine
v	Volume
V	Volts
VBNC	Viable but non culturable
WT	Wildtype
W/V	Weight to volume
x g	Centrifugal force
ζ	Zeta

Chapter 1

Introduction

1.0 *Burkholderia pseudomallei*

Burkholderia pseudomallei is a motile, Gram-negative, environmental bacterium that resides in soil and stagnant water as a saprophyte in south east Asia and northern Australia (Wiersinga*, et al.*, 2006). This bacterium is a member of the *Burkholderia* genus (figure 1.0) which includes over 40 different species including *Burkholderia mallei,* a host specific bacterium which causes glanders in horses and *Burkholderia cenocepacia* and *Burkholderia multivorans*, which are often associated with chronic pneumatic infection in cystic fibrosis patients (Drevinek & Mahenthiralingam, 2010, Galyov*, et al.*, 2010).

B. pseudomallei has adapted to the human host, to become an opportunistic pathogen and through inhalation or cuts in the skin is capable of causing the infectious disease melioidosis, which is responsible for up to 20% of septicemic deaths in endemic areas (Chaowagul*, et al.*, 1989, Galyov*, et al.*, 2010). *Burkholderia thailandensis,* another member of the genus, co-exists with *B. pseudomallei* in the soil but rarely if ever causes disease in humans and is significantly less virulent in mice or hamsters (DeShazer, 2007).

In addition to causing acute illness *B. pseudomallei* can establish an asymptomatic latent infection with symptoms occurring years post exposure, or manifest as a chronic reoccurring infection despite a prolonged course of antibiotic treatment (Currie*, et al.*, 2000).

The potential for the bacterium to cause disease through inhalation has led to the micro-organism being categorised as a category B infectious agent by the Centre of Infectious Disease and in recent months the bacterium has been listed in the top tier of disease agents considered an exceptional threat to security by the US Federal Select

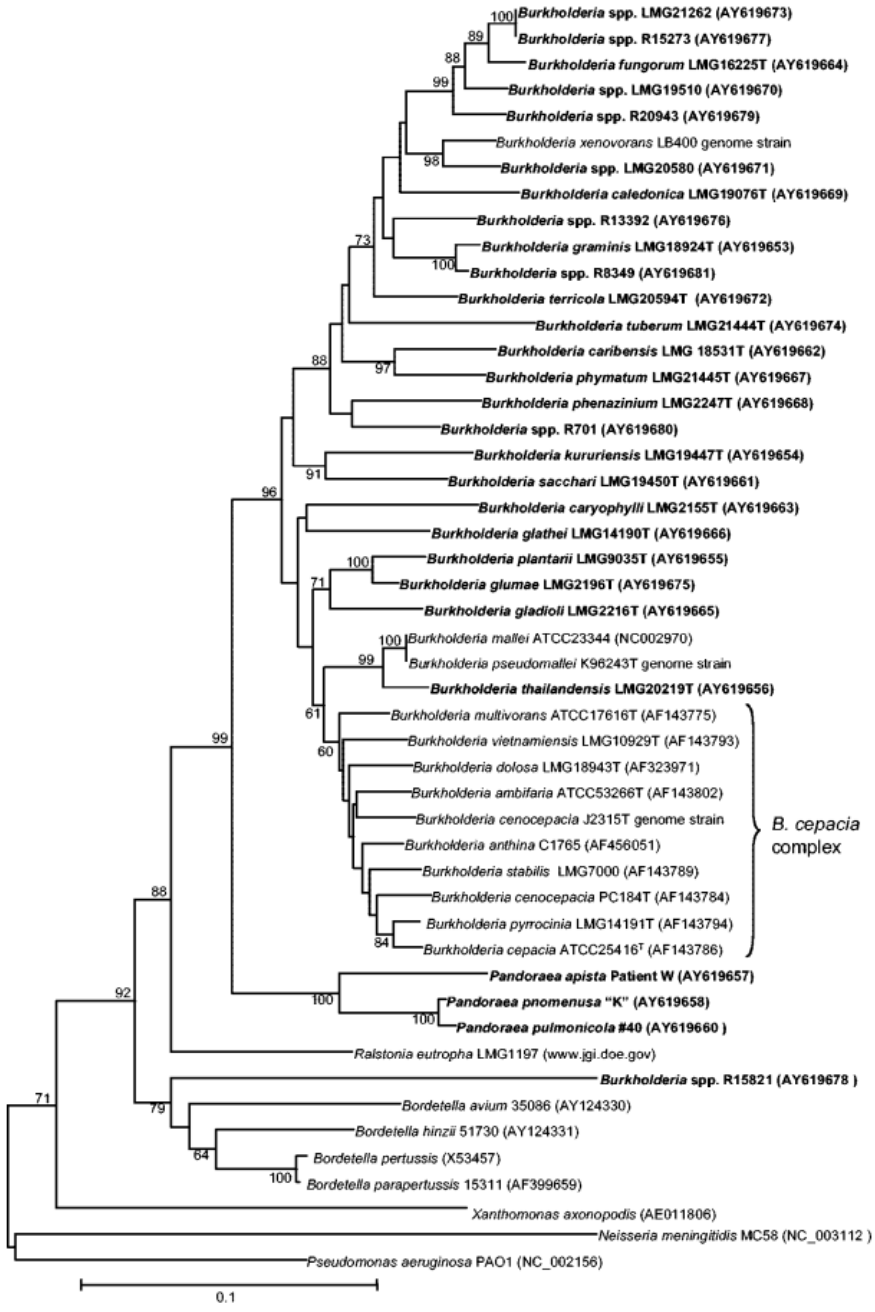

Figure 1.0. The phylogeny of the *Burkholderia* genus. The phylogenetic tree is based on *recA* sequences. Most *Burkholderia* species are plant pathogens, but 2 groups can cause disease in humans. The *Burkholderia cepacia* complex is a group of opportunistic pathogens that can cause infection in cystic fibrosis patients. *Burkholderia pseudomallei* and *Burkholderia mallei* have the potential to cause the diseases melioidosis and glanders respectively. The related species *Burkholderia thailandensis* is rarely pathogenic. The tree was rooted with the *Pseudomonas aeruginosa* PAO1 *recA* gene. Reproduced from (Payne *et al.,* 2005) with permission from the American Society of Microbiology.

Agent Program (Butler, 2012). Consequently these classifications have resulted in increased research into the virulence and survival mechanisms of the bacterium.

1.0.1 Genome

The *B. pseudomallei* genome consists of 2 chromosomes, the larger 4.7 Mb chromosome 1 and smaller 3.17 Mb chromosome 2. The genome shares a core set of genes with other members of the *Burkholderia* genus and 87% of the genome of the K96243 strain of *B. pseudomallei* is conserved throughout all strains with 14% variable between different isolates (Sim*, et al.*, 2008). There are currently over 70 different strains of *B. pseudomallei* isolated from melioidosis patients or the environment that have been categorised into the 3 different clades: animal (A), clinical (C) and environmental (E) based on the accessory genome (Sim*, et al.*, 2008). The variability between strains is associated with multiple genomic islands (GI) that undergo substantial horizontal gene transfer and can dramatically alter the gene repertoire of *B. pseudomallei* (Tumapa, et al., 2008). It is likely that these genomic islands are associated with virulence and the potential for infection (figure 1.1). The 5 reference strains of *B. pseudomallei* K96243, 1710b, 1106a, 668 and 305 contain 71 genomic islands between them with each strain having a distinct selection of GIs (Tuanyok*, et al.*, 2008). The genomic positions of these GIs are not random and appear to be associated with tRNA gene loci, which are believed to be involved in integration of the GI (Tuanyok*, et al.*, 2008). The 16 GIs associated with the K96243 genome are uncommon in the other 4 strains. Instead distinct GIs were found at both the same and at additional genetic locations in the other strains. Genotyping of several *B. pseudomallei* colonies from different tissue types in a patient during acute

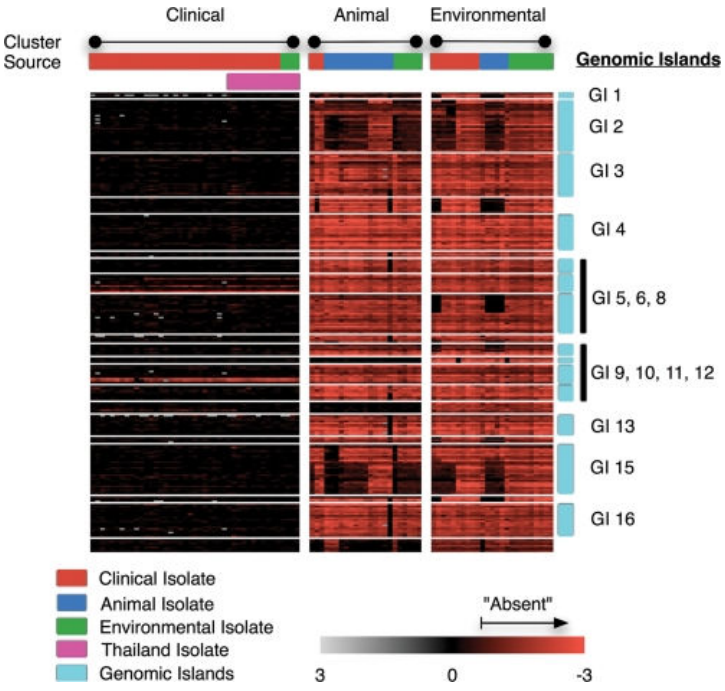

Figure 1.1. Heat map showing the absence (red) or presence (black) of GI genes in Clinical, Animal and Environmental isolates which were categorised by accessory genome clustering. Strains are also colour coded according to their original source of isolation, where red = clinical, blue = animal, and green = environmental. Locations of the 14 GIs are shown on the right. Genomic islands are enriched in clinical isolates. Reproduced from (Sim, *et al.*, 2008).

melioidosis can result in substantial genetic diversity showing the micro-organism's ability to quickly evolve and adapt within the host (Price*, et al.*, 2010).

1.0.2 Virulence factors

1.0.2.1 Secretion systems

Many potential virulence factors have been identified in *B. pseudomallei*. The micro-organism contains 3 type III secretion systems (TTSS) that act as syringes transporting effector proteins into the host. Inactivation of TTSS1 did not have an effect on virulence in a hamster model of infection and may have a role in interaction with plants in the soil (Attree & Attree, 2001). The TTSS3, (a Inv/Mxi-Spa– like type system) named the *Burkholderia* secretion apparatus (Bsa), has been shown to play a key role in intracellular survival of *B. pseudomallei* (Stevens*, et al.*, 2002). The TTSS3 proteins BipA, BipC and BipD react with convalescent sera from melioidosis patients showing functional expression of the secretion apparatus proteins *in vivo* (Stevens*, et al.*, 2002).

The *B. pseudomallei* K96243 genome encodes 6 type VI (T6SS) clusters although their function in virulence is unclear. Inactivation of 1 gene from one of these clusters (*tssH-5*) had no effect on intracellular invasion and replication in macrophages (Schell*, et al.*, 2008).

1.0.2.2 Adhesion

The *B. pseudomallei* K96243 genome encodes multiple type IV pilin associated loci, which may have involvement in bacterial virulence. Deletion of the *pilA* type IV structural gene from 1 of these loci resulted in reduced adherence and virulence in epithelial cells, nematode infection models and BALB/c mice via the intranasal route

(Essex-Lopresti, *et al.*, 2005). Inactivation of either *boaA* or *boaB* putative autotransporter adhesins also reduced attachment to epithelial cells compared to wild type *B. pseudomallei*. A double deletion of these genes also had a defect in intracellular growth although it is unclear what role these genes have in bacterial intracellular replication (Balder, *et al.*, 2010).

1.0.2.3 Flagella

The *fliC* gene is needed for the synthesis of the flagellin protein. Inactivation of this gene in *B. pseudomallei* KHW showed attenuation following intranasal or intraperitoneal infection into BALB/c mice (Chua, *et al.*, 2003). Inactivation of the gene in *B. pseudomallei* 1026-b prevented adhesion to *Acanthamoeba astronyxis* cells but did not result in attenuation in Syrian hamsters or a diabetic rat model of infection (DeShazer, *et al.*, 1997, Inglis, *et al.*, 2003).

1.0.2.4 Quorum sensing

Quorum sensing systems are involved in cell to cell communication between bacterial populations. Multiple signalling signals have been detected in *B. pseudomallei* culture supernatant (Ulrich, *et al.*, 2004). Mutation of any of the 3 *luxI* or 5 *luxR* homologous genes, which code part of the sensing apparatus in *B. pseudomallei,* results in increased time to death in mice and hamster models (Ulrich, *et al.*, 2004, Valade, *et al.*, 2004).

1.0.2.5 Polysacharides

Other potential virulence factors include lipopolysaccharide (LPS), capsular polysaccharide (CPS) and two other O-antigen polysaccharide clusters (type III O-PS

and type IV O-PS). *B. pseudomallei* LPS is a poor activator of macrophages compared to *E. coli* LPS (Utaisincharoen, *et al.*, 2000). Mutation of LPS biosynthesis genes in *B. pseudomallei* can also lead to reduced virulence in animal models and increased bacteriocidal activity by polymyxin-B or human sera (DeShazer, *et al.*, 1998, Burtnick & Woods, 1999).

The *B. pseudomallei* genome contains 4 operons encoding proteins needed for CPS biosynthesis. Disruption of the capsule operon gene *wcbB,* which encodes mannosyltransferase, results in significant attenuation of virulence in mice and hamster models (Atkins, *et al.*, 2002a, Reckseidler-Zenteno, *et al.*, 2005, Cuccui, *et al.*, 2007). In the presence of purified capsule the virulence of the *wcbB* mutant could be significantly increased (Reckseidler-Zenteno, *et al.*, 2005).

Inactivation of type III or type IV O-PS genes in *B. pseudomallei* and then challenging mice with these mutants could increase the time to death compared to challenge with wild type *B. pseudomallei* (Sarkar-Tyson, *et al.*, 2007).

1.0.2.6 Secreted factors

*B. pseudomalle*i also produces many secreted proteins that may have a role in virulence. The *Burkholderia* lethal factor 1 was recently characterised acting as a cytotoxin that leads to alteration in the cytoskeleton in the eukaryotic host causing cell death in cell models and mice. Specifically the toxin promotes deamidation of glutamine-339 of the translation initiation factor eIF4A, abolishing its helicase activity and inhibiting translation (Cruz-Migoni, *et al.*, 2011).

The bacteria also produce siderophores for iron acquisition called malleobactin. This siderophore can remove iron from transferrin, lactoferrin or EDTA (Yang, *et al.*, 1993).

Secreted proteins such as haemolysins, phospholipase C and proteases may also form part of the virulence factor repertoire (Ashdown & Koehler, 1990, Yang*, et al.*, 1993, Korbsrisate*, et al.*, 2007).

1.0.3 Antibiotic resistance and phenotypic tolerance

B. pseudomallei is intrinsically resistant to many antibiotics. Antibiotic resistance can also develop during treatment with antibiotics, albeit at a frequency of less than 1%. Resistance has been mapped to a point mutation in the β-lactamase gene *penA* (Sarovich, *et al*., 2012). Relapse is also a major problem in *B. pseudomallei* infection. One reason for this is the evolution of antibiotic resistance during infection. A study comparing whole genome sequences from primary and relapse infections from 6 months to 6 years in Thai patients revealed genome changes, many associated with deletions in a TetR family transcription factor. This transcription factor is often associated with antibiotic resistance and strains with mutations had increased MIC to a range of antibiotics (Hayden*, et al.*, 2012).

In addition to antibiotic resistance, a reservoir of cells can reside inside the host to cause chronic and recurrent infection. In mouse models *B. pseudomallei* cells have been found to persist primarily in the GI tract, most commonly in the stomach, during chronic infection (Goodyear*, et al.*, 2012). This reservoir of persistent bacterial cells could also have involvement in chronic and recurring human melioidosis months or years post infection. Persister cells are characterised as bacterial cells that are genetically identical to the population but are in a state of reversible dormancy and tolerant rather than resistant to antibiotic treatment (Lewis, 2010). As most antibiotics target actively growing cells, those in a dormant and non-dividing state can survive

antibiotic treatment. Following removal of the antibiotic, cells may re-awaken to cause recurrent infection in the host.

1.1 Melioidosis

1.1.1 Risk factors

There is a positive association between melioidosis and environmental contamination with *B. pseudomallei.* The disease is endemic in parts of Thailand, Northern Australia, Malaysia, Singapore, Vietnam and Myanmar (Burma). Possible endemic areas include Southern India, Southern China, Hong Kong, Taiwan, Brunei, Laos and Cambodia (figure 1.2). Sporadic cases and occasional clusters have been reported in large areas of Asia, the Americas (notably Brazil), the Caribbean, the Pacific, Africa and the Middle East (Wiersinga*, et al.*, 2006).

Incidences of the disease are more common in the rainy season, especially amongst rice paddy workers who come into increased contact with the organism during this period. Paddy workers rarely wear protective clothing and damage to the skin can result in infection by the bacterium. Heavy rain and wind can aerosolise the bacterium and this form of extreme weather is associated with a higher rate of pneumonia in patients presenting with melioidosis (Currie & Jacups, 2003). Near-drowning is also a known risk factor for melioidosis, as a cluster of melioidosis cases were reported in southern Thailand following the tsunami in 2004 (Chierakul*, et al.*, 2005).

The disease is most prevalent in adults between 40 and 60 years old and >80% have at least 1 other underlying disease or condition. These include diabetes mellitus, renal failure, cirrhosis, thalassaemia or alcoholism. Adults that are immunosupressed by diseases or drug treatment are also more susceptible to melioidosis

(Suputtamongkol, *et al.*, 1999). Children only account for 1 in 5 melioidosis patients in north east Thailand (Wiersinga, *et al.*, 2006).

1.1.2 Clinical features

Most frequently the disease manifests as a septicaemia and is characterised by abscess formation (Vatcharapreechasakul, *et al.*, 1992, Wong, *et al.*, 1995). In Thailand the mortality rate is 51%, with septic shock being the main cause of death within 48 hours (White, 2003). The lung is the most commonly infected organ, with symptoms including coughing and fever due to an abscess or pneumonia. Other commonly infected organs include the liver, spleen, skeletal muscle and prostate (White, 2003). The bacteria do not cause clinical disease in all infected individuals and can persist within the host and re-activate to cause disease at a later date. One of the longest documented cases of persistence was reported in a Vietnam war veteran who developed symptoms 18 years post infection (Koponen, *et al.*, 1991). More recently an 82 year old man, who was a prisoner of war in Japan during World War 2, presented clinical manifestations of melioidosis 62 years after initial exposure (Ngauy, *et al.*, 2005).

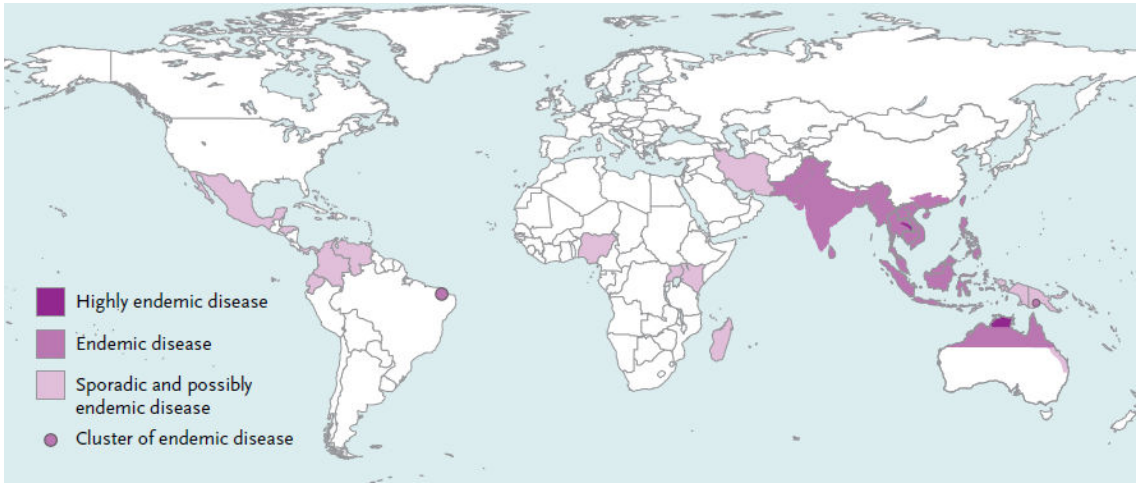

Figure 1.2. World distribution of highly endemic, endemic and sporadic cases of melioidosis based on current data. Reproduced with permission from (Wiersinga, *et al.*, 2012), Copyright Massachusetts Medical Society.

1.1.3 Diagnosis

Abscess formation is often detected in the lungs using chest radiographs or by ultrasound examination in the liver and spleen (Dhiensiri*, et al.*, 1988, Wibulpolprasert & Dhiensiri, 1999). *B. pseudomallei* can be cultured from infected sites, blood or throat swabs, and latex agglutination tests using poly or monoclonal antibodies against lipopolysacharide or exopolysacharide can be used for bacterial identification (Smith*, et al.*, 1993, Walsh & Wuthiekanun, 1996, Wuthiekanun*, et al.*, 2001).

1.1.4 Treatment

The first line of treatment for melioidosis has been the third generation cephalosporin antibiotic ceftazidime for over two decades (White*, et al.*, 1989). This drug is injected intravenously for at least 10 days until there is clear improvement in patient health before oral drugs can be taken. Other cephalosporin antibiotics are often used but are less effective at combating the bacteria (Chaowagul*, et al.*, 1999). Members of the carbapenem class of antibiotic (such as imipenem and meropenem) can also be used to treat melioidosis and are used in northern Australia (Simpson*, et al.*, 1999).

Oral treatment is with a combination of 4 different drugs: chloramphenicol, doxycycline, trimethoprim and sulfamethoxazole for 20 weeks (Rajchanuvong*, et al.*, 1995). Despite the long treatment time relapse infection rates are around 10% and this can increase to 30% if treatment is undertaken for 8 weeks or less (Chaowagul*, et al.*, 1993, Currie*, et al.*, 2000).

1.1.5 Intracellular survival of *B. pseudomallei*

B. pseudomallei has the ability to invade and survive in many cell types in the human host, including epithelial cells and phagocytic cells such as macrophages (Pruksachartvuthi, *et al.*, 1990, Harley, *et al.*, 1998, Ahmed, *et al.*, 1999). The *Burkholderia* secretion apparatus (Bsa) plays a crucial role in invasion, release from phagosomes and intracelluar proliferation (Stevens, *et al.*, 2002). Following bacterial uptake into the host cell, *B. pseudomallei* is released from the endosome into the cytoplasm by lysing the endosome membrane. Once in the cytoplasm the bacteria are able to survive host defences such as the inducible nitric oxide synthase (iNOS) and antimicrobial peptides including protamines and defensins (Pruksachartvuthi, *et al.*, 1990, Harley, *et al.*, 1998). In addition, *B. pseudomallei* induce the formation of actin-based membrane protrusions, within the host cell using the bacterial BimA protein. *B. pseudomallei* can spread to neighbouring host cells via the protrusions and multiply intracellularly (Kespichayawattana, *et al.*, 2000, Stevens, *et al.*, 2002). In some instances *B. pseudomallei* can induce apoptosis of phagocytic or non-phagocytic cells. In addition it has the unique ability to induce cell fusion of host cells to create giant multinucleated cells types (Kespichayawattana, *et al.*, 2000). Transcriptome profiling reveals that following infection of *B. pseudomallei* into the human macrophage 22% of the genome shows significant transcriptional adaptation. Metabolism, cell envelope, motility, replication, regulatory pathways and ion transport systems are down regulated, as are many catabolic and housekeeping genes, suggesting a lower energy requirement. In contrast many genes involved in anaerobic metabolism are up regulated (Chieng, *et al.*, 2012). Figure 1.3 shows *B. pseudomallei* invasion and the associated host immune response.

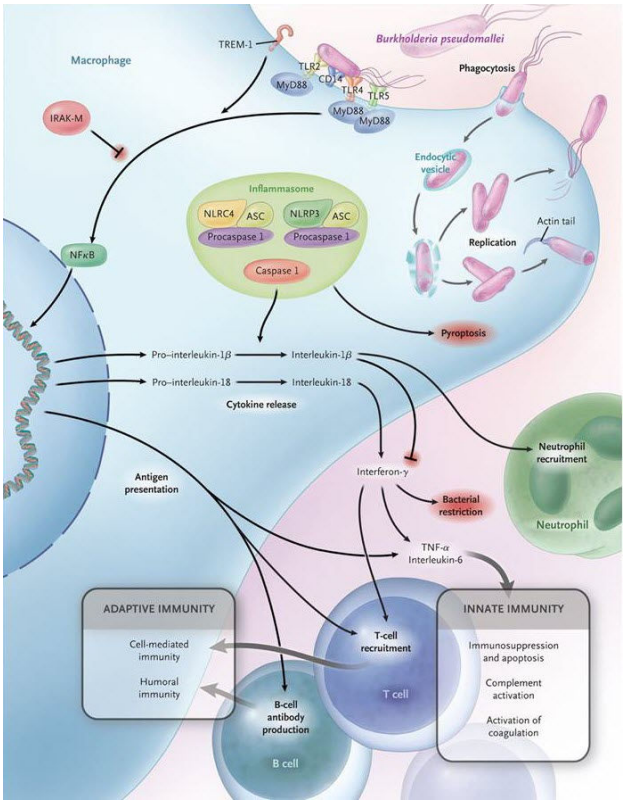

Figure 1.3 *Burkholderia pseudomallei* infection and host response. *B. pseudomallei* can invade macrophages and while some bacteria are destroyed after phagocytosis a proportion of the organisms escape from endocytic vacuoles. The bacteria can then infect other cells through actin-based membrane protrusions. Toll-like receptors (TLR) on host cells detect invading *B. pseudomallei*, leading to nuclear factor-κB (NF-κB) induced activation of the immune response through the release of proinflammatory cytokines. This results in neutrophil recruitment towards the site of infection, and the complement and coagulation cascade becoming activated. As infection progresses, the adaptive immune response leads to T-cell recruitment in response to interferon-γ production, which gives rise to a cell-mediated immune response and the production of antibodies by B cells. Reproduced with permission from (Wiersinga*, et al.*, 2012), Copyright Massachusetts Medical Society.

1.1.6 Immune response

Interferon (IFN) γ, tumour necrosis factor and the interleukins IL-12 and IL-18 have essential roles in human resistance to *B. pseudomallei* infections (Wiersinga*, et al.*, 2007, Wiersinga & van der Poll, 2009). Mouse studies with strains depleted of CD4+ and CD8+ T-cells show the importance of both innate and adaptive immunity against the bacteria (Haque*, et al.*, 2006, Haque*, et al.*, 2006). Activated neutrophils also have a key role in infection control. These immune cells are targeted to the site of infection and depletion results in 1000 fold increase in pulmonary bacterial loads after 4 days compared to controls (Easton*, et al.*, 2007).

The toll-like receptor and other pattern recognition receptors are the first receptors to recognise *B .pseudomallei* and mice lacking myD88, the key TLR adaptor protein demonstrate highly accelerated death (Akira*, et al.*, 2006, Wiersinga*, et al.*, 2008).

The pro-inflammatory cytokines TNFα, IL-1, IL-6, and IL-12 are all up regulated in melioidosis and are capable of activating the coagulation system. The extent of coagulation activation appears to correlate with the mortality of melioidosis patients (Wiersinga*, et al.*, 2008).

1.1.7 Vaccines

There is currently no human vaccine available that can protect against *B. pseudomallei* and melioidosis (Patel*, et al.*, 2011). Many therapeutic and preventative vaccine candidates have been identified and tested with limited success.

1.1.7.1 Live attenuated vaccines

Several live attenuated mutants of *B. pseudomallei* have been tested as vaccines. Immunisation with some mutants can extend the time to death of mice, but fails to offer complete protection following infection. For example a *bipD* mutant strain of *B. pseudomallei,* which has a dysfunctional Bsa type III secretion system provided partial protection against subsequent challenge with wild type *B. pseudomallei* (Stevens*, et al.*, 2004). However, immunisation with the BipD protein offered no subsequent protection (Stevens*, et al.*, 2004). Two mutant strains of *B. pseudomallei purN* or *purM* that are defective in purine biosynthesis offer protective immunity in BALB/C mice during acute melioidosis but no protection is provided during the chronic phase of infection (Breitbach*, et al.*, 2008). Interruption of the *ilvI* gene in *B. pseudomallei,* which encodes part of an enzyme required for branch amino acid synthesis, renders bacteria auxotrophic against these amino acids. Immunisation of BALB/C mice with the *ilvI* (2D2) strain and then subsequent infection with *B. pseudomallei* 576 results in high attenuation for up to 30 days (Atkins*, et al.*, 2002b). More recently vaccination with a *B. pseudomallei* Δ*relA* Δ*spoT* offered partial protection against infection with wild type *B. pseudomallei* 576. This protection resulted in greater survival in mice after 40 days compared to the protection given by 2D2 strain (Muller*, et al.*, 2012). An attenuated acapsular mutant could offer no protection in mice (Atkins*, et al.*, 2002a).

1.1.7.2 Subunit vaccines

Antibodies, DNA and proteins have been tested as potential subunit vaccines. Immunisation of BALB/C mice by the intravenous route with monoclonal antibodies

against LPS and CPS showed significant delayed time to death after infection with *B. pseudomallei* (Jones*, et al.*, 2002). Mice vaccinated with LPS or CPS show increased time to death. Mice vaccinated against LPS developed IgM and IgG3 responses and mice vaccinated with CPS had an IgG2b response (Nelson*, et al.*, 2004). Immunisation with the purified outer membrane proteins Omp3 and Omp 7 of the OmpA family in combination with adjuvant significantly enhanced survival of BALB/C mice (Hara*, et al.*, 2009). This was also observed when using a DNA vaccine encoding the *fliC* gene, which encodes a flagella filament protein (Chen*, et al.*, 2006).

1.2 Persister cells

Persister cells were first identified by Bigger back in the 1940s. Treatment of *Staphylococcus* infections with penicillin could not completely sterilise cultures. Inoculating the surviving bacteria into fresh media and adding fresh antibiotic resulted in the same frequency of surviving bacteria. This showed that these bacteria were not a resistant sub population but were an antibiotic tolerant persistent population (Bigger, 1944) (figure 1.4). More recently many groups have shown that treatment of different bacterial species with concentrations of different antibiotics above the MIC give populations of these tolerant persister cells. For example *E. coli* can form persisters at a frequency between 10^{-6} and 10^{-5} (Joers*, et al.*, 2010), while *B. thailandensis* can form persisters at frequencies of 10^{-2} in response to ceftazidime treatment (Hemsley *et al* unpublished data).

Persister cells are generated in mid-exponential phase and reach a peak at stationary phase (Keren*, et al.*, 2004). This suggests a molecular mechanism for persister cell formation during growth. Screening of transposon insertion libraries for

mutants with reduced ability to form persisters proved negative. Instead multiple genes appeared to reduce persister frequencies by up to 10-fold suggesting redundancy in persister cell formation mechanisms (Hu & Coates, 2005, Hansen*, et al.*, 2008). Such genes implicated in persistence include DksA, DnaKJ, HupAB and IhfAB, which are all global regulators, YgfA which can inhibit nucleotide synthesis, and YigB, which may act by blocking metabolism.

Candidate persister genes have also been identified using transcriptomic profiling of persister cells (Shah*, et al.*, 2006). The profile revealed down regulation of biosynthesis genes but up regulation of a series of Toxin-antitoxin (TA) modules including RelBE, MazEF, DinJYafQ and YgiU. Another study also revealed that a mutant allele of a TA toxin *hipA7* was also implicated in persistence that was dependent on the stringent response regulator pp(G)pp (Korch*, et al.*, 2003).

The TisB TA toxin has also been implicated in persister formation. Treatment of cultures with the fluoroquinolone antibiotic ciprofloxacin causes DNA damage and induces the SOS response increasing levels of TisB toxin, which in turn increases persister cell numbers (Dörr*, et al.*, 2010). Based on this result, Wu *et al* 2012 hypothesised that other stress responses may also induce persister cell formation. Induction of the oxidative stress response using paraquat (PQ) did indeed increase persister cell numbers following flouroquinolone antibiotic treatment, which subsequently increased tolerance to other antibiotics. PQ induces SoxRS,

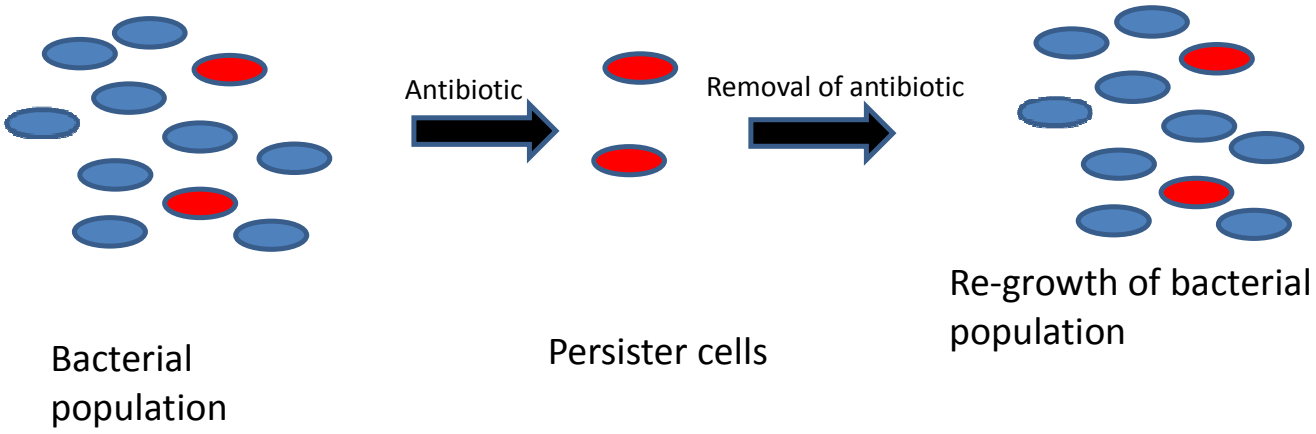

Figure 1.4 In a normal bacterial population there are normal growing cells (blue) and bacterial persister cells (red). The persister cells account for a small fraction of the population. If the bacteria are treated with antibiotic, actively growing cells will be killed, while the perister cells will survive as they are tolerant to the antibiotic. On removal of the antibiotic the persister cells can revert to a growth phenotype to re-populate. This new population of cells contains both normally growing cells and persisters. The persistent state may act as an insurance policy to ensure survival of the population as a whole after exposure to a stress.

which induces expression of the AcrAB-TolC multidrug-resistant (MDR) pump. This pump removes antibiotic from the cell to give a greater population of persister cells (Wu*, et al.*, 2012).

Reactive oxygen has also been shown to be important in the eradication of persisters. Maintenance of high concentrations of reactive oxidative species can eliminate persisters of *Mycobacterium smegmatis* (Grant, *et al.,* 2012).

There is also evidence that persisters can be generated via indole. Incubation of *E. coli* cultures with indole before antibiotic treatment was able to increase persister frequencies. Inactivating the gene responsible for indole production reduced these frequencies (Vega*, et al.*, 2012). A proposed mechanism for the indole response, suggests indole is sensed by a membrane or periplasmic component which then increases persistence by inducing OxyR (oxidative stress) and the phage shock response. These were significantly expressed in microarray data following indole incubation (Vega*, et al.*, 2012). Again this shows an importance for oxidative stress in persister cell formation.

In *Pseudomonas aeruginosa* persister numbers can also be increased in response to quorum sensing signals. Addition of pyocyanin, paraquat and acyl-homoserine lactone 3-OC12-HS significantly increases persister numbers of logarithmic phase cultures (Moker*, et al.*, 2010). Adding spent media from a stationary phase culture of wild type *P. aeruginosas* PA14 was also able to increase persister frequencies when added to early logarithmic cultures.

1.2.1 Eradication of persister cells

Since persister cells have been implicated in chronic diseases such as melioiodosis and tuberculosis, many groups are investigating methods for their eradication,

summarised in figure 1.5. One potential method is to cause these cells to re-awaken so they are then sensitive to antibiotics or bactericidal chemicals. Kim *et al* used a chemical library to indentify chemicals that could kill persisters. They found that the chemical 3-[4-(4-methoxyphenyl)piperazin-1-yl]piperidin-4-yl biphenyl-4-carboxylate (C10) was able to selectively kill persister cells of *E. coli* and *P. aeruginosas* in combination with flouroquiolones by reverting persisters back to antibiotic sensitivity (Kim, *et al.*, 2011). Another group demonstrated that the chemical Z-4-bromo-5-(bromomethylene)-3-methylfuran-2(5H)-one (BF8) can also restore the susceptibility of isolated *P. aeurginosa* persister cells to ciprofloxacin and tobramycin antibiotics and reduce persister frequencies during growth (Pan, *et al.*, 2012). BF8 is an inhibitor of quorum sensing in gram negative bacteria but inhibition of quorum sensing does not appear to be the method of persister re-activation by this chemical in *P. aeruginosa* and other mechanisms for re-activation seem likely.

Persister killing does not necessarily need to rely on persister wake up. Specific metabolites can stimulate persister killing of both Gram positive and Gram negative bacteria with aminoglycoside antibiotics in both aerobic and anaerobic conditions (Allison, *et al.*, 2011). The aminoglycoside gentamicin could significantly increase killing of persisters by up to 3 logs when specific metabolites were added. These metabolites were those that enter the upper stages of glycolysis (glucose, fructose and mannitol) in addition to pyruvate. The effect of this increased killing was also shown to be aminoglycoside specific. Killing of *E. coli* cells by ampicillin or ofloxacilin in the presence of mannitol was not increased compared to the antibiotic only controls. This provided evidence that the sugars were not re-initiating growth of the persister but involved another mechanism. This mechanism involves activation of the proton motive force by the specific metabolites which allows uptake of the

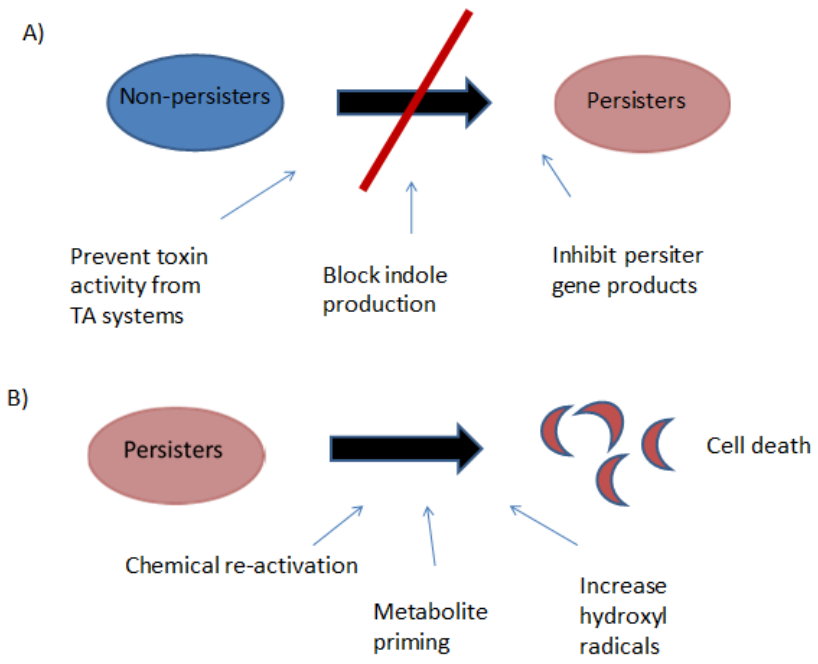

Figure 1.5 Potential methods for the eradication of persister cells. A) Approaches for blocking cells from entering into a persistent state. This includes preventing persister signalling molecules and TA toxins from inducing growth arrest. B) Approaches for killing persister cells. Chemical re-activation and metabolite priming can revert persister cells back to actively growing cells. These cells can then be killed by antibiotic treatment. Increasing hydroxyl radicals via reactive oxygen species may directly kill persisters by damaging internal machinery.

aminoglycoside antibiotic and persister killing. The manitol-gentamicin combination was also used to treat mice with catheters containing uropathogenic *E. coli* and the presence of the manitol was able to reduce the biofilm viability by 1.5 orders of magnitude (Allison*, et al.*, 2011).

1.3 Toxin-antitoxin (TA) modules

1.3.1 Background

Toxin-antitoxin (TA) modules are found throughout the prokaryotic world and consist of a gene pair that codes for both a toxin and antitoxin. They were first identified as plasmid borne killer systems. If the plasmid on which the TA modules are encoded, is either lost or not transferred to the daughter cell, the daughter cell will die, known as postsegregational killing (PSK). This effect is due to the unstable antitoxin not being replenished after both toxin and antitoxin transfer to the new cell. The TA module genes are coded by the plasmid, therefore loss or non-transfer of plasmid DNA provides no replenishment of the antitoxin and leads to eventual toxicity by the more stable toxin (Hayes, 2003).

More recently TA systems have been identified on the chromosomes of prokaryotic species. One proposed function includes the formation of persister cells as described in 1.2. Other possible roles of TA systems include nutritional stress response regulators, programmed-cell death, providing protection from phages or acting as anti-addiction molecules that allow bacteria to avoid plasmid addiction or stabilisation of genomic regions. Alternatively, TA modules may be selfish gene elements (Pandey & Gerdes, 2004, Melderen & De-Bast, 2009). TA systems show strong interpendence, with the antitoxin being indispensable in both plasmid and chromosomally encoded TA loci. This could suggest that TA systems are just selfish

gene elements with no physiological function. More likely it appears that the other physiological functions caused by these TA systems in bacteria are by products of their selfish nature to retain themselves within host genomes. TA systems contribute to the maintenance of plasmids, proviruses and genomic islands. They are also encoded on defence islands to protect the bacteria from foreign DNA invasion. This shows that there are interconnected functions for these TA systems both defending against foreign invasion while maintaining their own genomic location. The HicBA TA system is expanded substantially within antivirus defence systems (Makarova*, et al.*, 2011).

1.3.2 Toxin-antitoxin structure

TA modules are categorised into 4 groups (type I, II, III or V) based on the gene products produced (figure 1.6). The toxin gene, in all TA systems identified to date, codes for a relatively stable protein which is usually 95-135 amino acids in length and specific TA toxins have been shown to interact with cellular activities to cause either a bactericidal or bacteriostatic state in the cell by a defined or proposed mechanism, if unbound from antitoxin. The antitoxin, on the other hand, can be either a small RNA molecule or a small protein molecule that under normal cellular conditions prevents activity of the toxin protein (Hayes, 2003).

Protein antitoxins and/or TA complexes have been demonstrated to provide a negative feedback loop regulating their own expression (Hayes & Low, 2009). Antitoxin and/or TA complex can bind to the operator region within the promoter region to prevent transcription of toxin and antitoxin mRNA. The RelBE TA system

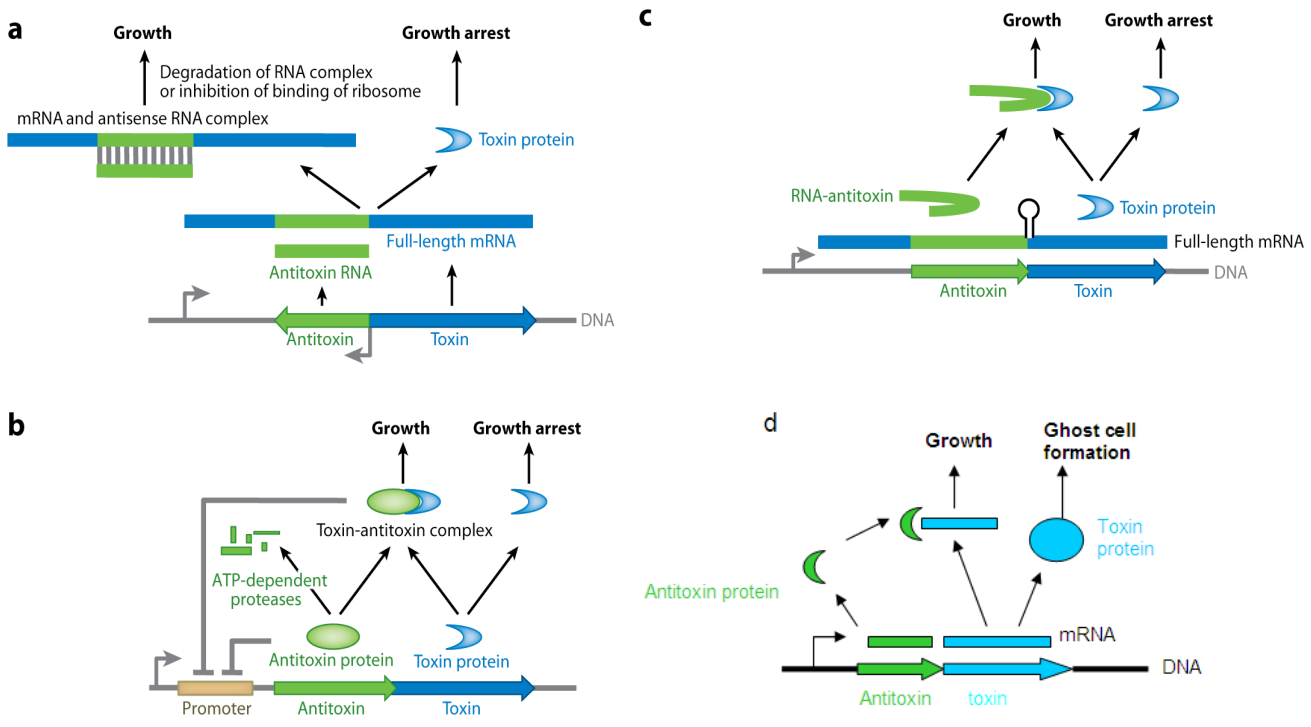

Figure 1.6 Regulation of TA systems. a) Type I TA systems. Toxin and RNA-antitoxin (antisense RNA) are transcribed separately. RNA-antitoxin binds to mRNA that encode toxin to form a duplex inhibiting toxin translation. b) Type II TA systems. Antitoxin and toxin mRNAs are synthesized from the same promoter and both are translated into protein.The antitoxin gene usually precedes the toxin gene. Antitoxin forms a heterodimeric polypeptide complex with toxin to inhibit toxicity of toxin and to autoregulate the TA module. Antitoxins are subjected to cleavage under stress conditions by an ATP-dependent protease. Antitoxin itself can also autoregulate the TA systems, but more weakly than the TA complex. Toxin, released from the TA complex then attacks its cellular target. This toxin activity leads to bacterial cell growth or cell death. c) Type III TA systems. RNA-antitoxin binds to toxin protein and inhibits the toxicity. d) TypeV TA systems. Antitoxin protein binds and degrades toxin mRNA to prevent translation of toxin protein. A-C reproduced from (Yamaguchi, *et al.*, 2011).

acts in this way. In the absence of the RelE toxin, RelB will dimerise and bind to the operator causing repression of transcription. If RelE is present such that dimerised RelB is at greater levels than RelE, then a complex of the two proteins will bind co-operatively to repress transcription. If the RelE toxin is at greater levels than the RelB antitoxin dimer then the excess RelE will destabilise the RelE-RelB-operator complex inducing strong transcription from the promoter (Overgaard*, et al.*, 2008, Overgaard*, et al.*, 2009). This shows transcription is very sensitive to the relative levels of toxin and antitoxin known as conditional co-operativity.

1.3.2.1 Type I

Type I TA modules are those with an antisense RNA antitoxin. The antitoxin RNA is transcribed from the toxin gene in reverse orientation and binds to the mRNA of the associated toxin to form a double RNA complex which is presumed to be targeted for degradation (Gerdes K & Wagner, 2007, Fozo EM*, et al.*, 2008). This complementary activity establishes regulatory control of the toxin by preventing its translation and subsequent inhibition or interaction of the toxin with its target. If this RNA antitoxin is absent or degraded, the toxin is translated by the ribosome becoming active within the cell.

Examples of Type I systems include RdlD-LdrA (Kawano*, et al.*, 2002), SymR-SymE (Kawano*, et al.*, 2007) and IstR-TisB (Unoson & Wagner, 2008). The toxins of type I systems are usually small hydrophobic proteins that cause damage to bacterial cell membranes by affecting ATP synthesis. It is thought that this occurs by the α-helical toxin forming a pore in the membrane that destroys the membrane potential (Gerdes*, et al.*, 2005, Fozo EM*, et al.*, 2008). For example the SprA1 toxin

from a *Staphylococcus aureus* toxin-antitoxin system causes cell death of the bacteria because the long bent alpha helical structure of the peptide switches to a 7nm long continuous helix on association with its membrane target (Sayed*, et al.*, 2012).

1.3.2.2 Type II

In type II systems the antitoxin gene is usually located upstream of the toxin gene and together they make up an operon, which is self-regulated. These TA gene pairs often overlap by 1 or 4bp suggesting coupled transcription. Expression of the toxin and antitoxin genes encode 2 protein products that interact to form a functionally inactive TA complex under normal cellular conditions (Hayes & Low, 2009). The antitoxins of type II TA modules are proteins that are usually 65-85 amino acids in length. They are relatively unstable proteins that are degraded by different cellular proteases such as Lon, ClpA and ClpX due to their loose structures and their lower thermodynamic stability (Buts*, et al.*, 2005). Under certain stress induced conditions degradation may be increased, allowing the toxin to become active. Under normal cellular conditions protein antitoxins sequester the toxin through complex formation causing structural alterations. They do this by blocking the toxin's intrinsic enzymatic activity by binding to the active site preventing activity or by causing allosteric changes in the structure (Buts*, et al.*, 2005).

Most type II TA loci analysed consist of a toxin and antitoxin gene from the same family. For instance the *mazF* toxin is located with the *mazE* antitoxin. However there are examples of TA loci containing mixed families. For instance the *yhaV* gene in *E. coli* is partnered with *prlF*. The YhaV toxin is an endoribonuclease and member of the RelE superfamily, whereas the PrlF antitoxin is homologous to the MazE family. These 2 proteins have been shown to interact and the PrlF antitoxin is able to

counteract the toxic activity of YhaV (Schmidt, *et al.*, 2007). *Mycobacterium tuberculosis* also has hybrid Toxin-antitoxin loci within its genome. Some of the chromosomally encoded *mazF* genes are partnered with *vapB* and *mazE* genes can be partnered with *vapC* (Zhu, et al., 2010).

Other groups have shown that non-cognate toxin and antitoxins are also able to cross talk. The YefM antitoxin from the YefM-YoeB TA system in *E. coli* was able to partially reduce the toxicity of the Txe toxin from the Axe-Txe system in *Enterococcus faecium.* Equally the Axe antitoxin from this *E. faecium* was able to prevent the toxicity of the YoeB toxin (Grady & Hayes, 2003). In *M. tuberculosis* different combinations of VapB and MazE antitoxins were able to bind to non-cognate VapC and MazF toxins (Zhu, *et al.*, 2010).

1.3.2.3 Type III

Type III systems also have RNA antitoxins but they bind directly to the toxin protein rather than to the mRNA (Yamaguchi, *et al.*, 2011). The RNA is encoded by short tandem repeats upstream of the toxin gene. Recent bioinformatic searching has identified many type III systems distributed throughout bacteria but currently only one system has been characterised, the ToxI-ToxN system (Blower, *et al.*, 2012). This system was identified on a plasmid from the plant pathogen *Erwinia carotovora* subspecies *atrosepticum* (*Pectobacterium atrosepticum*) and the ToxN toxin causes endoribonuclease activity when expressed in *E. coli* (Fineran, *et al.*, 2009). This TA system was also able to elicit phage protection against a variety of phages and in different host micro-organisms, suggesting it may have an evolutionary role in bacterial protection against phage infection. The crystal structure of the complex

reveals that three ToxI RNA molecules bind to three ToxN monomers to generate an inactive trimeric complex (Blower*, et al.*, 2011).

1.3.2.4 Type V

The most recent class of toxin-antitoxin to be discovered has been named type V. Thus far, only 1 TA family has been characterised for this class named GhoST. The GhoT toxin is a membrane specific peptide that causes ghost cell formation by damaging the membrane but not killing the cells. Expression of the toxin results in an increase in persistence (Wang*, et al.*, 2012). The GhoS antitoxin masks the toxic nature of the toxin by degrading the GhoT mRNA. More specifically it has a preference for U and A codons, as these are prevalent in the cleavage site within the mRNA transcript. The structure of the GhoS antitoxin revealed it to be a monomer related to the CRISPR-associated-2 RNase (Wang*, et al.*, 2012).

1.3.3 Targets of Type II TA toxins

1.3.3.1 DNA replication

Of the ten currently categorised type II families (Table 1.0), two of these inhibit DNA replication by actively targeting DNA gyrase (CcdB and ParE). The toxins do not share structural sequence homology and may therefore target the gyrase enzyme in different ways. The CcdB toxin binds to the A subunit of the DNA gyrase molecule stabilising a gyrase:DNA adduct (Dao-Thi*, et al.*, 2005). ParE was first identified on the broad host range plasmid RK2. As with CcdB the toxin is thought to stabilise gyrase:DNA complexes but a CcdB resistant gyrase was not resistant to ParE. This suggests they have different binding targets. The ParE toxin also requires ATP for functionality whereas the CcdB toxin does not (Roberts*, et al.*, 1994, Jiang*, et al.*, 2002).

1.3.3.2 Ribosome dependent mRNA interferases

The RelBE family is perhaps the best studied ribosome dependent mRNA interferase. The RelE toxin binds to 16s rRNA in the 30s subunit of the ribosome and the current understanding is that the toxin either stimulates endoribonuclease activity of the ribosome or endoribonuclease activity of itself through a conformational change in its structure upon ribosome binding. The resulting toxic activity, whatever the mechanism, is degradation of mRNA at the ribosome A site. RNA is cleaved preferably between the second and third base in the termination codon to effectively shut off protein synthesis (Christensen & Gerdes, 2003, Pedersen*, et al.*, 2003).

The YoeB toxin (a RelE homologue) is another ribosome dependent mRNA interferase that binds to the 50s subunit rather than 30s subunit, blocking translation initiation rather than translation elongation exhibited by RelE. This ribosome binding may result in a conformational change in the toxin to activate it. The active YoeB toxin causes degradation of the mRNA downstream of the initiation codon, although the activity is fairly weak (Kamada & Hanaoka, 2005, Zhang & Inouye, 2009).

The *higBA* locus was first identified on the Rst-1 plasmid of *Proteus vulgaris* (Budde*, et al.*, 2006). Since then similar chromosomal loci have been identified in many bacterial species including *Vibrio cholerae, Streptococcus pneumoniae, E. coli* CFT073, and *E. coli* O157:H7 (Pandey & Gerdes, 2004). Experiments have shown that overexpressing HigB from either of the 2 modules found in *V. cholerae* or from Rst1 causes the inhibition of protein synthesis through translation dependent mRNA cleavage (Budde*, et al.*, 2006). It has also been demonstrated that cloning the 2 *higBA* loci from *V. cholerae* into *E. coli* plasmids can stabilise them (Christensen-Dalsgaard & Gerdes, 2006).

Table 1.0 The 10 Type II toxin-antitoxin families identified and characterised to date. The cellular targets for the toxins include DNA gyrase, ribosomes, RNA and UNAG.

Toxin- antitoxin (TA) family	Toxin	Cellular target
CcdAB	CcdB	DNA gyrase
HigBA	HigB	mRNA
Phd/Doc	Doc	Ribosome
VapBC	VapC	RNA
ParDE	ParE	DNA gyrase
HipBA	HipA	EF-TU
RelBE	RelE	mRNA
MazEF	MazF	mRNA
ω-ε-ζ	ζ	Uridine diphosphate-N-acetylglucosamine (UNAG)

Unlike other characterised TA module families (with the exception of HicAB) the gene order is reversed in *higBA* loci. Taking the *E. coli* gene pair as an example, the toxin lies upstream of the antitoxin and they overlap by 1bp. Although this TA module has this different locus makeup, regulation is similar to that of other TA systems with antitoxin or complex binding to the operator region blocking transcription (Hurley & Woychik, 2009).

Until recently it was unknown how the HigB toxin functioned, but work by Hurley and colleagues has shown it acts by cleaving A-rich sequences in mRNA. More specifically it is a complex of HigB and ribosome that actively targets mRNA for cleavage. The HigB toxin binds to the ribosome at the 50s region of the 70s subunit and it is only when this association exists that the toxin is able to exhibit ribonuclease activity. The HigB toxin can cut in frame and out of frame AAA sequences 100% of the time, and also has the ability to cut AA and A sequences but with much less efficiency (Hurley & Woychik, 2009). This study revealed that HigB cleavage can occur throughout the length of the mRNA suggesting the HigB toxin binds to actively translating ribosomes. It was also hypothesised that HigB may also bind to ribosomes as the 50s and 70s subunits are assembled.

The interaction of the toxin with the ribosome appears to cause an allosteric change within the HigB structure that activates its endoribonuclease activity. The large scale cleavage of mRNA causes subsequent depletion in translation and thus protein synthesis inhibition.

1.3.3.3 Ribosome independent interferases

The most well studied TA family of this group is the MazEF family. The *E. coli* MazF

toxin cleaves mRNA at ACA sequences to prevent translation and hence protein synthesis of ACA containing transcripts (Zhang, *et al.*, 2003). Homologues have been found in many species of bacteria and archaea and those homologous that have been phenotypically characterised also cleave at ACA regions via 3, 5 or 7 base pair recognition sites.

Interestingly MazF also has the ability to degrade its own mRNA suggesting that MazF expression could also be negatively regulated by its own gene product. In solution, in the absence of MazE, MazF protein exists in a dimeric state. On addition of MazE a stable 1:2 MazE:MazF TA complex is established (Engelberg-Kulka, *et al.*, 2005).

Although many examples of MazEF homologues have been identified, screening of the *Myxococcus xanthus* genome identified a single *mazF* toxin that was not coupled to a *mazE* antitoxin gene (Nariya & Inouye, 2008). This MazF toxin is involved in cell death during fruiting body formation and acts as an mRNA interferase like other MazF toxins. Surprisingly its regulation is negatively controlled by MrpC, an essential developmental transcription factor, which also acts as an antitoxin binding and forming a TA complex, which is coded for elsewhere in the genome. This example highlights the functional diversity of TA systems and the difficulty in identifying functional TA genes on a strict set of parameters, assuming they must be part of a 2 gene locus.

Experimental studies have revealed that MazF is activated by a variety of mechanisms. These include ppGpp, the signal produced by RelA protein following amino acid starvation, certain antibiotics and by the toxic protein Doc (Zhang, *et al.*, 2003). More recently, evidence has come to light that activation of MazF toxin to cause cell death is also dependent on the densisty of the cell population; more

specifically relying on the action of the quorum like communication factor Extracellular death factor (EDF) (Kolodkin-Gal*, et al.*, 2007). EDF is produced during logarithmic growth, which correlates with results that MazF related cell death only occurs during this period of growth and is absent from stationary phase, in which MazF related cell death does not occur. The EDF communication factor is a pentapeptide and is an autoinducer of MazF activity (figure 1.7). In essence this allows the cells within a population to sense each other and under conditions of stress a sub-population undergoes cell death. This possibly provides nutrients for the rest of the population or could allow the release of substrates for biofilm production and subsequent protection.

Recent research has shown that *mazEF* can mediate 2 different cell death pathways, 1 of which is dependent on reactive oxygen species and another which is independent. As MazF is an endoribonuclease, which cleaves mRNA creating truncated proteins, enzymes that are involved in the removal of ROS also become inactive which results in a build-up of ROS (Kolodkin-Gal*,, et al.*, 2008). When *mazEF* is activated by antibiotics or some form of stress that inhibits transcription or translation it is suggested that it is ROS and not MazF that cause cell death. The ROS-independent pathway takes place when MazF is activated by agents causing DNA damage. In this circumstance it is suggested that the endoribonucleolytic action of MazF triggers a downstream cascade leading to cell death.

Other research by the same group indicate that upon induction of MazF ribonuclease activity, not all mRNAs are cleaved leading to the selectivity of some specific proteins (Amitai*, et al.*, 2009). Some of these proteins are involved in causing cell death but others permit the survival of a small subpopulation of cells under the stressful condition that could be a persister population.

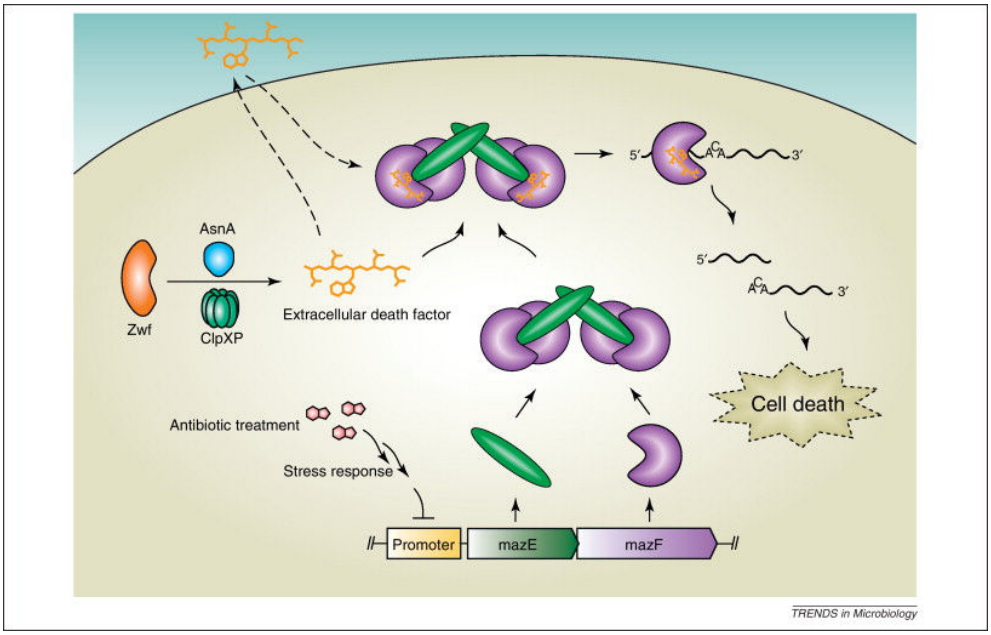

Figure 1.7 A possible model for *mazEF*-dependent cell death induced by the extracellular death factor (EDF). Production of the EDF pentapeptide (NNWNN) requires the Zwf protein, (glucose-6-phosphotate dehydrogenase) which acts as an EDF precursor, in addition to the the protease ClpXP and the AsnA protein. EDF can freely diffuse in and out of the cell being found in the extracellular media. Treatment with an antibiotic triggers the stress response, which inhibits transcription of *mazEF*. EDF can bind either to free MazF or to the MazEF complex and enhance MazF ribounuclease activity *in vitro*. MazF cleaves single-stranded mRNA in a sequence-specific manner, leading to cell death. Reproduced with permision from (Williams & Hergenrother, 2012), Elsevier liscense agreement.

1.3.3.4 Ribosome inhibition

The Doc toxin from the Doc-Phd TA system has been shown to block translation and protein synthesis by binding to the 30S region of the ribosome. This toxin does not result in mRNA degradation but blocks translation elongation by binding to the same 16s rRNA region in the ribosome as the antibiotic hygromycin B, as a strain resistant to this antibiotic is also resistant to Doc toxin activity (Liu, *et al.*, 2008).

The Doc toxin protein causes growth arrest by acting as an inhibitor of translation through binding to the 30s subunits of the ribosome (Garcia-pino, *et al.*, 2008). Studies by Llu and colleagues demonstrate that the mechanism of action by Doc toxin is different from all other characterised TA toxins as it directly targets translation elongation, mirroring the effects of translation elongation defects. It is thought that Doc protein binds to the 30s subunit of ribosomes and prevents translation by causing them to stall. These ribosomes with bound toxin accumulate along the length of mRNA undergoing protein synthesis, causing ribosomes to lose their ability to dissociate from mRNA and thus they cannot translate other mRNA molecules in the mRNA pool (Liu, *et al.*, 2008). This subsequently causes a loss of protein synthesis.

1.3.3.5 Cell division

CbtA inhibits cell division by targeting the cytoskeletal proteins FtsZ, a highly conserved GTPase involved in cell division, and MreB, an actin-like protein required for maintaining the shape of cells, cell division, chromosome segregation and cell polarity. Binding of the toxin to the 2 proteins results in altered shape of *E. coli* cells in addition to cell division inhibition (Tan, *et al.*, 2011).

1.3.3.6 Other targets

The pneumococcal zeta toxin PezT, from the ω-ε-ζ TA family, can impair cell wall synthesis and triggers autolysis in *E. coli* cells when expressed. The toxin works by phosphorylating the cell wall precursor uridine diphosphate N-acetylglucosamine (UNAG). This phosphorylated UNAG can then inhibit the MarA protein which catalyses the first step in peptidoglycan synthesis (Mutschler*, et al.*, 2011).

The HipA toxin targets transcription factor elongation factor TU (EF-Tu) in a similar manner to the zeta toxin described above, i.e. via a phosphorylation mechanism. The HipA toxin can autophosphorylate itself which in turn allows for phosphorylation of EF-Tu. EF-Tu has an essential role in translation by catalysing aminoacyl-transfer RNA binding to the ribosome. As GTP is hydrolysed to GDP, EF-Tu undergoes a conformational change and can no longer bind to ribosomes. It is thought that HipA may phosphorylate the residue Thr382 within EF-Tu, which would favour a state that cannot bind ribosome due to repulsion with Glu117 residue. This would prevent aminoacyl-tRNA binding to the ribosome, as EF-Tu would be absent, preventing translation and protein synthesis (Schumacher*, et al.*, 2009).

1.4 Structural relationships of toxins and antitoxin proteins

1.4.1 Antitoxins

Antitoxins usually consist of a toxin binding domain and a DNA binding domain for transcriptional regulation of the TA operon (Yamaguchi*, et al.*, 2011). This domain is a helix-turn-helix (HTH) domain or a ribbon-helix-helix (RHH) that binds to palindromic sequences in the promoter regions in double stranded DNA (Madl*, et al.*, 2006, Mattison*, et al.*, 2006, Khoo*, et al.*, 2007, Oberer*, et al.*, 2007, Brown*, et al.*, 2009). Co-operative binding of TA complex to the promoter is usually greater than

antitoxin binding alone so production of the TA complex is preferential over antitoxin alone (Garcia-Pino, *et al.*, 2010).

The RHH domain of the MqsR antitoxin is different from other antitoxins as it requires binding by a zinc ion to stabilise the interaction. This antitoxin is also different as it can bind to different promoters in addition to its own. This suggests a wider regulatory role for this antitoxin (Brown, *et al.*, 2009). Some antitoxins, such as Phd, have neither a distinct RHH nor HTH domain and the domain used for dimerization of the antitoxin is also used for DNA binding (Smith & Magnuson, 2004, Kedzierska, *et al.*, 2007).

The toxin binding domain in antitoxins is believed to be specific for neutralisation of the toxin protein. Binding of the antitoxin domain to the toxin is through both hydrophobic and electrostatic interactions with the electrostatic interactions giving rise to the specificity of the antitoxin to the cognate toxin. For instance the C-terminal domains of MazE and RelB antitoxins from *E. coli* are very similar, yet MazF and RelE toxins do not show structural similarity suggesting neutralisation must be very specific (Kamada & Hanaoka, 2005, Li, *et al.*, 2009). In contrast the RelB antitoxins from *E. coli* and *M. tuberculosis* have different C-terminal regions despite the RelE toxins being very similar (Arbing, *et al.*, 2010).

Two distinct methods for neutralisation of the toxin by the antitoxin have been discovered. In most cases this involves direct interaction of the antitoxin with the active site of the toxin to prevent toxicity. In other cases the antitoxin binds elsewhere to cause a conformational change in the toxin structure to prevent substrate binding. An example of this is the HipB antitoxin. It is thought that cross contacts and a number of interactions between the HipB dimer and the N and C domains of HipA cause HipA to undergo an open and inactive conformation (Schumacher, *et al.*, 2009).

As mentioned before, type II antitoxins often have loose disordered structures that are susceptible to degradation by proteases (Lehnherr & Yarmolinsky, 1995, Donegan*, et al.*, 2010). Upon binding of the antitoxin to the toxin this disordered domain is often ordered into a secondary structure that causes conformational change in the toxin to remove the toxin from its substrate (Oberer*, et al.*, 2007).

1.4.2 Toxins

Toxins of type II and III systems can be classified into 6 different subgroups based on their structural similarity. Often, proteins of the same structural class share little sequence similarity. Members of the first subgroup, the Kid family (figure 1.8a-d), are primarily mRNA interferases with the exception of CcdB. The proteins have compact globular folds with twisted anti-parallel beta-sheet cores, masked by alpha-helices (Blower*, et al.*, 2011). The RelE family is a second distinct family of toxins that includes RelE toxin and the MqsR toxin (figure 1.8e-h). These toxins have structural similarity to the endoribonuclease RNase T1(Neubauer*, et al.*, 2009). The other 4 toxin groups have fewer members and include the HipA toxin family with its sequence relatedness to eukaryotic ser/thr kinase, the phosphylltransferase zeta toxin family, the entirely alpha-helical Doc toxin and the VapC toxin family that shares sequence similarity with the highly conserved PIN domains that are found in metal-dependent ribonucleases in the eukaryotic RNA exosome (Blower*, et al.*, 2011).

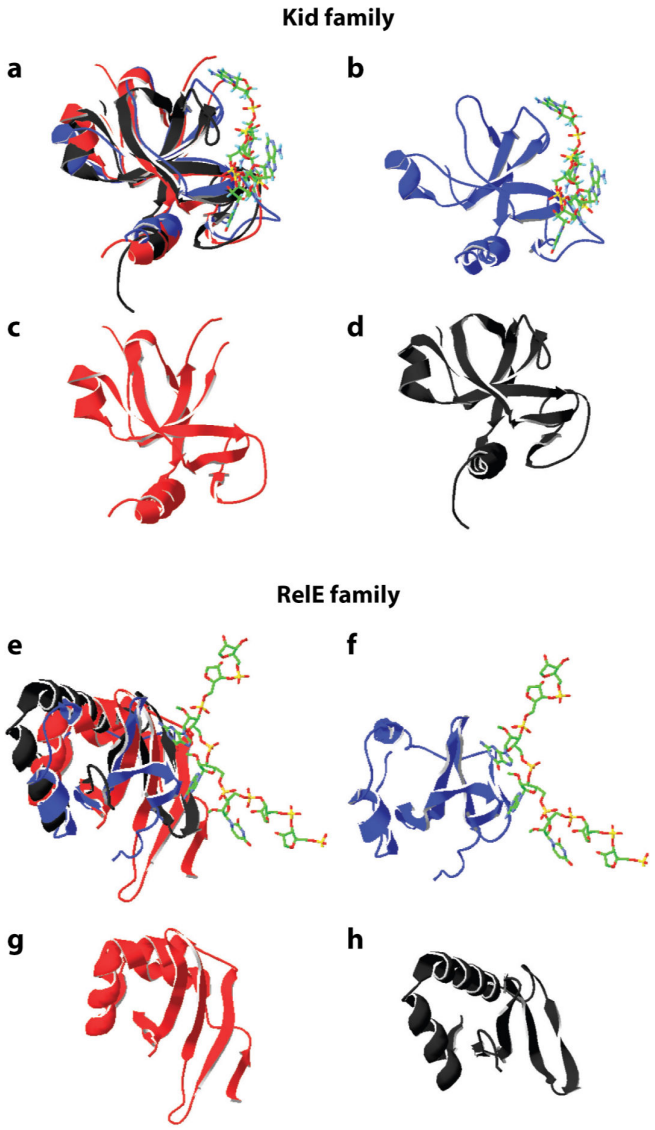

Figure 1.8 Structures of 2 toxin families. a)-d) Structures from the Kid family. a) Structural alignment of Kid monomer with 5 dU-RNA (rAdUrArCrA) (PDB ID: 2C06), MazF monomer (1UB4), and YdcE monomer (1NE8). b) Kid monomer with 5 dU-RNA. c) MazF monomer. d) YdcE monomer. e)-h) Structures from the RelE family. e) Structural alignment of MqsR monomer (PDB ID: 3HI2), RelE monomer (3KIQ) with 2′-O-methylated RNA, and YoeB monomer (2A6Q). f) RelE monomer. g) MqsR monomer. h) YoeB monomer. Homologues of the Kid family or RelE family have highly conserved structures. Reproduced from (Yamaguchi, *et al.*, 2011).

1.5 Species distribution of TA systems

Work by Gerdes and co-workers have shown that toxin-antitoxin systems are present in nearly all free-living prokaryotes (Pandey & Gerdes, 2004). This work used BLASTP and TBLASTN to search 126 completely sequenced prokaryotic genomes for members of 7 known TA module families. One important conclusion that was drawn from this study was based on the distribution and abundance of TA loci in bacteria. Pandey and Gerdes showed that of those bacterial species that appeared to lack TA modules, the majority were obligate host associated parasites or that they lived in close contact with other organisms. This lead to the conclusion that bacteria living in constant environments have none or few TA loci, whereas almost all free-living bacteria that live in changing environments have multiple TA loci. A good highlighted example of this is Mycobacteria. BLAST results showed that *M. tuberculosis* had 36 and 38 TA loci depending on the strain. *Mycobacterium leprae* on the other hand had no identifiable TA systems. If their lifestyles are taken into consideration the differences in identified TA backs up the conclusion drawn by Pandley and Gerdes. *M. leprae* is an obligate intracellular organism, whereas *M. tuberculosis* has both an intracellular and extracellular growth phase i.e. it has stages of being a free living bacterium. It should also be noted that *M. leprae* does have toxin pseudogenes that are closely related to toxins in *M. tuberculosis* suggesting *M. leprae* is undergoing genomic decay and is evolving from *M. tuberculosis*. This evidence seems to disprove the theory that TA modules are selfish genes and suggests they do provide some functional role in bacteria that live in changing environments.

This genomic analysis also revealed that the number of TA modules in the genome is not directly correlated to its size. In fact there is evidence to suggest that the number of TA loci may be linked to growth rate in free living prokaryotes. For

example *Nitrosomas europea* has 43 TA loci and is an obligate chemolithotrophic soil organism, whereas *M. tuberculosis* is a human pathogen, showing that numbers of TA are not linked to their free living environment. However both organisms are associated with low growth rates. On the other hand *Mycobacterium smegmatis* is a fast growing close relative of *M. tuberculosis* and has only 2 TA loci that fall into the 7 TA families used in the study.

In enteric bacteria such as *E. coli* and *Salmonella enterica* serovar Typhimurium TA systems are often situated downstream of *relA* genes. The *relA* genes code for a transcription factor and in many bacteria have been shown to be involved in stringent response, which is an important stress response (Gaynor*, et al.*, 2005). It is therefore possible that the *relA* gene may also be important in controlling transcription of downstream TA modules under conditions of stress.

Perhaps one of the most significant identifications of a TA system in bacteria is the MazEF module on plasmids encoding vancomycin-resistance in *Enterococci*. This TA module was found on plasmids in 100% of vancomycin resistant strains and in over 90% of cases the genes encoding the resistance were on the same plasmid as the TA module and thus physically linked (Moritz & Hergenrother, 2006). This suggests that TA systems play a role in plasmid stability in this bacterial species and hence the selective pressure for antibiotic resistance. Development of a drug to induce toxic activity of the MazF toxin by suppression or removal of MazE would kill the bacterial cells and could potentially be an important factor in the removal of vancomycin resistant strains.

1.5.1 TA distribution in *Burkholderia*

An unusual distribution of TA modules is reported to exist in the *Burkholderia* genus. Many of the species in this genus are found free living in soil, with some having the ability to become opportunistic human pathogens such as *Burkholderia pseudomallei* and *Burkholderia cenocepacia* (Chantratita*, et al.*, 2008). Based on Pandey and Gerdes observations, it may be expected that this genus would contain multiple TA modules within their genomes. This theory holds true for many members of the *Burkhoderia cepacia* complex *(Bc*c*)* with species having between 5 and 9 TA modules which are members of the 7 highlighted TA families from the Pandey and Gerdes study. 1 *B. cenocepacia* subtype J2315, which is a member of the Bcc, only has 1 of these TA modules. *B. pseudomallei* appeared to have none of the 7 type II TA families identified at the time of this study in its genome despite primarily being free living soil bacteria. *B. pseudomallei* contained only 1 identified TA module and this is the *hipBA* locus thought to be involved with persistence.

Due to the differences in TA numbers amongst the *Burkholderia* genus and based on Pandey and Gerdes observation that free living bacteria tend to harbour more TA, it seems likely that there are in fact more families of TA modules that are yet to be identified. This thought process has lead to the generation of software that scans genomes for existing and novel TA genes. Recently a wider bioinformatic search looking for new families based on properties of existing families was carried out on all 750 fully sequenced prokaryotic genomes. Such characteristics that were included in search parameters were gene size, locus arrangement, DNA binding properties, conserved partner gene and homology (Sevin E & Barloy-Hubler, 2007, Makarova*, et al.*, 2009).

1.6 Aims of this study

- Identify candidate type II Toxin-antitoxin systems in *B. pseudomallei.*
- Express candidate toxin and antitoxin genes in *E. coli* screening for growth arrest and growth resuscitation phenotypes.
- Deletion of confirmed TA gene loci from *B. pseudomallei* screening for loss of persistence/ survival phenotypes against a series of antibiotics and stress conditions
- Structural determination of TA proteins and complexes
- Determine cellular targets and mode of action for identified TA toxins
- Determine the regulatory nature of the *B. pseudomallei* TA systems.

Chapter 2

Materials and Methods

2.0 Bacterial strains and plasmids

All bacterial strains and plasmids used in this study are described in Table 2.0.

2.1 Culture Media

Bacterial cultures were routinely cultured at 37 ^{o}C in autoclaved Luria-Bertani (LB) broth or on LB agar plates. Antibiotics for plasmid selection were purchased from Sigma-Aldrich and were added at the following final concentrations: Ampicillin 100 μg/ml, tetracycline 15 μg/ml, chloramphenicol 35 μg/ml or 50 μg/ml, kanamycin 50 μg/ml or 250 μg/ml, trimethoprim 50 μg/ml or 300 μg/ml. Antibiotics were filtered sterilised using 0.2 μm filters before adding to culture media.

2.2 Bacterial storage

2.2.1 Freezer stocks

Bacterial strains were stored at -80 ^{o}C in O-ring sealed 2 ml Eppendorf tubes. 700 μl of overnight bacterial cultures were added to 300 μl of 50% glycerol before storage.

2.2.2 Fridge storage

Bacterial strains were often stored on LB agar or LB agar selective plates at 4 ^{o}C. *E. coli* strains grown on plates were stored for periods of weeks. *Burkholderia* strains grown on plates were stored in the fridge for a maximum of 1 week.

Table 2.0 Bacterial strains used or created in this study

Bacterial Strain	Genotype/ comments	Source
E. coli K-12 MG1655	F^- λ^- ilvG- rfb-50 rph-1	Lab strain collection
E. coli DH5α λ*pir*	ΔlacU169(ΦlacZΔM15), recA1, endA1, hsdR17, thi-1, gyrA96, relA1, λpir phage lysogen	Lab strain collection
E. coli S17-1 λpir	TpR SmR recA, thi, pro, hsdR-M^+RP4: 2-Tc:Mu: Km Tn7 λpir	Lab strain collection
E. coli DH5a (pRK2013)	ΔlacU169(ΦlacZΔM15), recA1, endA1, hsdR17, thi-1, gyrA96, relA1, pRK2013 (KmR oriColE1 RK2-Mob^+ RK2-Tra^+	Lab strain collection
E. coli Top10	F- mcrA Δ(mrr-hsdRMS-mcrBC) φ80lacZΔM15 ΔlacX74 nupG recA1 araD139 Δ(ara-leu)7697 galE15 galK16 rpsL(Str^R) endA1 λ^-	Invitrogen
E. coli Rosetta(DE3)pLysS	F^- ompT $hsdS_B(R_B^- m_B^-)$ gal dcm λ(DE3 [lacI lacUV5-T7 gene 1 ind1 sam7 nin5]) pLysSRARE (Cam^R)	Novagen
E. coli XL-10 Gold	endA1 glnV44 recA1 thi-1 gyrA96 relA1 lac Hte Δ(mcrA)183 Δ(mcrCB-hsdSMR-mrr)173 tet^R F'[proAB $lacI^qZ$ΔM15 Tn10(Tet^R Amy Cm^R)	Stratagene
E. coli Δ*hipBA:*	*E. coli* MG1655 derivative Δ*hipBA: Cm*^{R}	This study
B. thailandensis E264	Environmental isolate	Lab strain collection
B. pseudomallei K96243	Clinical isolate	Lab strain collection
B. pseudomallei K96243 *ΔhipBA*	K96243 derivative. Unmarked deletion *ΔhipBA*	Lab strain collection
B. pseudomallei K96243 *ΔBPSS0390-0391*	K96243 derivative. Unmarked deletion *ΔBPSS0390-0391*	This study

2.3 Bioinformatic screening

2.3.1 RASTA bacteria

The online software tool RASTA bacteria (http://genoweb1.irisa.fr/duals/RASTA-Bacteria/) was used to screen the input *E. coli* MG1655 K-12 and *Burkholderia pseudomallei* genomes for candidate toxin-antitoxin genes. The software generated a list of all open reading frames from both chromosome 1 and 2 with percentage likelihood scores, which were used to narrow down candidate genes for further study. Percentage scores were generated using specific parameters outlined by the creators of the software (Sevin & Barloy-Hubler, 2007). The encoded protein sequences of the candidate TA genes, generated by the software, were inputted, using FASTA format, into the BLASTp search facility on http://www.ncbi.nlm.nih.gov/ to determine any protein homology to other characterised TA systems.

2.3.2 Other data sources

Candidate TA genes that were documented on the toxin-antitoxin database (http://bioinfo-mml.sjtu.edu.cn/TADB/index.php) and data produced by the Makarova *et al* bioinformatic study were also considered for this study. Only paired genes from the Makarova *et al.* study were used and the corresponding GI numbers were searched on the NCBI website for the corresponding gene name. Candidate genes were generated in these studies as documented by the authors (Makarova*, et al.*, 2009, Shao*, et al.*, 2011)

2.4 Molecular Biology

2.4.1 Polymerase chain reaction (PCR)

PCR reactions were carried out in a BioRad thermocycler as follows:

Step 1- 95 °C for 5 minutes

Step 2- 95 °C for 45 seconds

Step 3- 50-68 °C (approx. 5 °C below melting temp of primers) for 30 seconds

Step 4 72 °C for 30 seconds per kb

35 cycles

Step 5 72 °C for 10 minutes

All PCR reactions were carried out using either Hot start taq (Qiagen), HiFi taq (Qiagen) or Failsafe (Cambio) polymerase enzymes. Appropriate buffers and concentrations were used as indicated in the manufacturer's instructions. For *E. coli hipA* cloning, *E. coli* MG1655 genomic DNA was used as template DNA. For cloning of *B. pseudomallei* genes, K96243 genomic DNA was used as a template. PCR was also used to confirm insertional inactivated and gene deletion mutants. In this instance, template DNA was acquired by boiling bacterial cells in water rather than isolation by DNA extraction kits. For each bacterial colony to be PCR screened, 50 µl nuclease free water was added to a 1 ml Eppendorf tube and a small loopful of bacteria from the colony was added and re-suspended. For *E. coli* and *B. thailandensis* samples, the tubes were heated at 100 °C for 10 minutes and then centrifuged at 13,500 rpm for 1 minute. 5 µl of cell lysate was added as template to the subsequent PCR reaction. For *B. pseudomallei* the same procedure was followed except samples were boiled for 1 hour before centrifugation and O-ring sealed tubes were used.

2.4.2 Gel electrophoresis

PCR products for size determination or DNA fragments for cloning purposes were separated using gel electrophoresis. 1% (w/v) agarose dissolved in 1 x Tris-acetate-EDTA (TAE) buffer was used to make the gels for electrophoresis and Syber green safe stain from Invitrogen was added for band visualisation. Fermentas 1 kb and 100 bp ladders were used as size markers and Qiagen 5x loading dye was added to ladders and samples before loading onto agarose gels. For gel extraction purposes electrophoresis was run at 90V for approximately 35 minutes for high resolution band separation. For size determination of PCR products 120V was used for approximately 25 minutes. Band sizes were visualised under UV light using a BioRad gel visualizer.

2.4.3 PCR purification

PCR reactions that proved positive were PCR purified by the Qiagen PCR clean up kit. DNA from individual PCR reactions were pooled and purified as per manufacturer's instructions.

2.4.4 Determining DNA concentration

DNA concentrations were determined using a Nanodrop from Thermo scientific. The equipment was washed and blanked with water and 2 µl of DNA sample was loaded for concentration determination.

2.4.5 Digest of DNA using restriction enzymes

Approximately 1µg of plasmid or linear DNA was digested in 50 µl reaction volumes using 1 µl of each restriction enzyme (NEB or Promega). Appropriate reaction buffer was added and Bovine serum albumin (BSA) where recommended at 1:10 dilutions

according to the manufacturer's recommendations. Final volume was made up with nuclease free water. DNA digests were incubated at 37 ^{o}C in a water bath for 2 hours before running the entire sample on an agarose gel using gel electrophoresis as described above.

2.4.6 Extraction of digested DNA fragments and plasmids

Digested DNA fragments and plasmids for cloning were cut from the agorose gel following gel electrophoresis using a razor blade. Extracted bands were added to 1.5 ml Eppendorf tubes and the Qiagen gel extraction kit was used to purify the digested DNA. Agarose/DNA mix was melted in a heat block at 50 ^{o}C and DNA was eluted from spin columns using nuclease free water.

2.4.7 Ligation of digested vector to insert DNA

Ligation reactions were set up in 15 µl reaction volumes when using T4 DNA ligase (NEB) or 20 µl volumes when using quick ligase (NEB). Buffers were added at a 1:10 dilution. 150 ng of vector was added to the reaction mix and the amount of insert added was determined by the following formula:

$$150 \text{ X } \frac{\text{Size of insert (kb)}}{\text{size of vector (kb)}} \text{ x } 3$$

The remaining reaction volume was nuclease free water. T4 DNA ligase reactions were incubated at 15 ^{o}C in a PCR machine for 15 hours. Quick ligase reactions were incubated at room temperature for 5 minutes.

2.4.8 Gateway cloning

PCR products for cloning into expression vectors were first cloned into gateway vectors. The gateway vectors used were either pGEM-T-Easy (Promega) or TOPO PCR 2.1 (Invitrogen). Cloning was carried out as instructed by manufacturers. In summary, this involved incubating the PCR product with the gateway vector and T4 ligase at room temperature before transformation of the resulting ligated plasmid/PCR product into calcium competent cells. Blue/white screening was used to detect positive colonies by plating onto X-galactose containing plates. White colonies were screened for presence of insert either by colony PCR or carrying out a miniprep and subsequent restriction digests of cultured bacteria from the colonies of interest.

2.4.9 Plasmid extraction

Plasmid DNA was extracted from bacteria using the Qiagen miniprep kit as per manufacturer's instructions. In summary the method involved lysing bacterial cells and precipitating and removing protein and chromosomal DNA. Plasmid DNA was eluted in nuclease free water.

2.4.10 Chromosomal DNA extraction

Chromsomal genomic DNA was extracted from bacteria using the Promega DNA extraction kit as per manufacturer's instructions.

2.4.11 Sequencing of PCR products and plasmid DNA

DNA was sequenced by Source Bioscience using gene specific or plasmid specific primers. For sequencing, plasmid DNA was sent at 100 ng/µl and PCR products at 1

ng/µl per 100 bp. DNA sequences were downloaded and aligned with the consensus sequence using BioEdit software. Vector maps were generated in Clone manager.

2.5 Competent cells

2.5.1 Electrocompetent cells

Overnight cultures (ONCs) of bacteria grown in LB were diluted 1:100 into 40 ml volumes of fresh LB in 50 ml falcon tubes. These tubes were incubated at 37 ^{o}C 200 rpm until the OD_{590}nm reached 0.5-0.8. Cultures were then incubated on ice for 10 minutes before centrifugation at 3,200 x g at 4 ^{o}C for 10 minutes. The supernatant was discarded and cells were washed in 40 ml ice cold sterile water before repeating centrifugation as described above and the supernatant discarded. Cells were then washed in 25 ml of sterile water and re-centrifuged discarding the supernatant. Finally cells were washed in 5 ml of ice cold sterile 10% glycerol. Cells were centrifuged for a final time and supernatant discarded before adding 500 µl of 10% glycerol. Cells were then aliquoted into 100 µl volumes into eppendorf tubes on ice and stored at -80 ^{o}C or used directly for electroporation.

2.5.2 Calcium Chloride competent cells

ONCs were diluted 1:100 into 40 ml volumes of LB in 50 ml falcon tubes. These tubes were incubated at 37^{o}C, 200 rpm until the OD_{590}nm reached 0.5-0.8. Cultures were then incubated on ice for 10 minutes before centrifugation at 3200 x g at 4 ^{o}C for 10 minutes. The supernatant was discarded and cells were washed in 40 ml sterile ice cold 0.1 M calcium chloride and incubated on ice for 30 minutes. Cells were then centrifuged as before and supernatant discarded. Cells were then resuspended in 600 µl of 0.1 M calcium chloride and 300 µl of ice cold 50% glycerol. Cells were then

aliquoted into 200 µl volumes into Eppendorf tubes on ice and stored at -80 ^{o}C or used directly for transformation.

2.6 Electroporation

Electrocompetent cells were thawed on ice for 10 minutes before approximately 50ng of plasmid DNA was added to 100 µl of competent cells and chilled on ice for 20 minutes. The bacteria/plasmid mix was then added to a BioRad electroporation cuvette and pulsed with 2 kV of electricity. 900 µl of LB was then added to the cuvette before decanting into an Eppendorf tube. The electroporated culture was then incubated for 1 hour at 37 ^{o}C, 200 rpm. After this time, a 100 µl sample was plated onto selective plates (neat) and the remainder of the sample was concentrated by centrifugation at 17,000 x g for 2 minutes. The cell pellet was re-suspended in 100 µl of LB. This was plated onto a selective LB agar plate (concentrated sample). Plates were incubated at 37 ^{o}C overnight.

2.7 Transformation

Calcium competent cells were thawed on ice for 10 minutes before approximately 50 ng of plasmid DNA was added to 50 µl of competent cells and chilled on ice for 20 minutes. The bacteria/plasmid mix was then heat shocked at 42 ^{o}C for 45 seconds in a water bath before returning to ice for 2 minutes. 900 µl of LB was then added to the Eppendorf tube and then incubated for 1 hour at 37 ^{o}C, 200 rpm. After this time, a 100 µl sample was plated onto selective plates (neat) and the remainder of the sample was concentrated by centrifugation at 17,000 x g for 2 minutes and the cell pellet was resuspended in 100 µl of LB and plated on a selective plate (concentrated sample). Plates were incubated at 37 ^{o}C overnight.

2.8 Wanner mutagenesis

The *E. coli hipBA* locus was knocked out using the Wanner mutagenesis method as described (Datsenko & Wanner, 2000). In summary a PCR product was generated that contained homology to upstream and downstream regions of the *hipBA* locus, FRT regions and a chloramphenicol resistence cassette. The plasmid pKD3 was used as template DNA. The PCR product was electroporated into the MG1655 strain of *E. coli*, which contained a pKD46 plasmid expressing the arabinose inducible λ Red recombinase plasmid for homologous recombination of the PCR product with the *hipBA* locus. Cultures were grown at 30 ^{o}C to maintain the pKD46 plasmid during recombination and shifted to 37 ^{o}C to remove the plasmid after successful recombination. Deletion of *hipBA* was confirmed by PCR using flanking region primers. Confirmation of pKD46 removal was by plating on LB ampicillin plates, since the plasmid encodes ampicillin resistance. Confirmation of homologous recombination was by plating on LB chloramphenicol plates since the knockout PCR product coded for chloramphenicol resistance.

2.9 Conjugation

E. coli strains DH5α or S17λ were used as donor strains for plasmid exchange into *B. thailandensis* and *B. pseudomallei.* When DH5α was used as a donor, an *E. coli* helper strain containing the pKR2013 plasmid was also used. Donor, recipient and helper strains were grown in LB media with appropriate antibiotic selection overnight at 37 ^{o}C, 200 rpm. The next day 1 ml aliquots were centrifuged at 17,000 x g in 1.5 ml Eppendorf tubes to isolate bacterial cells. The supernatant was removed and the cell pellets of the donor and helper stains were resuspended in 200 µl of LB without antibiotic. 100 µl of donor and helper (where applicable) were then added to the cell

pellet of the recipient strain and re-suspended to make a conjugation mix. 100 µl of the mixed bacterial culture was then added to an LB plate and left as a pool for plasmid exchange. 100 µl of donor, recipient and helper strain were also plated as controls. Plates were incubated at 37 ^{o}C in an upright position overnight in a static incubator. The next day the lawns of bacteria on the test and control plates were scraped off of the plate using a loop and resuspended in 1 ml volumes of PBS in Eppendorf tubes. 100 µl volumes were then plated onto selective plates containing gentamicin to kill the donor and recipient *E. coli* strains and an appropriate antibiotic for selection of recipients that had received the plasmid. These plates were incubated for 2-3 days at 37 ^{o}C for colonies to grow. Colonies were then re-streaked onto selective plates to confirm that they were conjugants.

2.10 Toxicity assays with *E. coli* harbouring cloned toxin genes

E. coli strains carrying pBAD cloned putative toxins were inoculated into 5 ml of LB containing 100 µg/ml ampicillin and grown overnight at 37^{o}C, 200 rpm. Cultures were then diluted 1:100 into 40 ml fresh LB in a 200 ml conical flask and supplemented with fresh antibiotic. Cultures were grown at 37^{o}C in a shaking incubator at 200 rpm until reaching an OD_{590}nm of ~0.1. 10 ml volumes of culture were aliquoted into universal tubes and supplemented with 0.2% (w/v) glucose to repress expression from the pBAD promoter or supplemented with 0.2% (w/v) arabinose to induce gene expression. Cultures were returned to the 37 ^{o}C incubator and grown for a further 3 hours taking samples every hour measuring the OD_{590}nm and determining CFU counts. Alternatively the CFU was determined after 0 and 2 hours and the fold change in CFU counts was calculated. OD_{590}nm was measured using a spectrophotometer blanked with LB. CFU was determined by serial diluting

cultures in LB in a 96 well plate and spot plating onto LB-ampicillin 100 µg/ml plates. Plates were grown at 37 ^{o}C overnight in a static incubator.

2.10.1 Expression at different cell densities

Once the *E. coli* cultures reached the early exponential phase (OD_{590}nm ~ 0.1), a 10 ml volume (neat), a 1 ml volume (1:10) and a 100 µl volume (1:100) were aliquoted into universal tubes. The 1:10 and 1:100 samples were made up to 10 ml volumes with LB. Fresh ampicillin was added to the cultures. 0.2% (w/v) arabinose was used to induce expression.

2.10.2 Preparing *E. coli* cultures at high or low cell densities

Once the cultures reached the early exponential phase (OD_{590}nm ~ 0.1), a 10 ml volume (high cell density containing ~ 10^7 CFU/ml) or a 100 µl volume (low cell density containing ~ 10^5 CFU/ml) were aliquoted into universal tubes. Low density samples were made up to 10 ml volumes with LB. Where appropriate cells were pelleted by centrifugation at 3,200 x g for 10 minutes and re-suspended in either fresh LB or spent media (described below). Fresh ampicillin was added to cultures. 0.2% (w/v) arabinose was used to induce toxin gene expression.

2.10.3 Preparing stationary phase spent media

2 x 20 ml volumes of LB were inoculated with appropriate *E. coli* or *B. thailandensis* strains and supplemented with 100 µg/ml ampicillin where necessary, then grown overnight to stationary phase at 37 ^{o}C, 200 rpm. The cultures were centrifuged at 3,200 x g for 10minutes and the supernatant was combined and filter sterilised using a

0.2µm filter into a fresh tube to provide spent media. Fresh ampicillin was added to the spent media.

2.10.4 Preparing Log phase spent media

Overnight cultures of appropriate *E. coli* strains were diluted 1:100 in 30 ml LB, supplemented with ampicillin and grown to an OD_{590}nm ~0.3. A 10 ml aliquot of culture was then centrifuged at 3,200 x g for 10 minutes and the SUPERNATANT filter sterilised with a 0.2 µm filter into a fresh universal tube to give log phase spent media. Fresh ampicillin was added to the media.

2.10.5 Acid treatment of spent media

Stationary spent media was prepared as previously described. 1 M HCl was then added to the spent media until reaching a pH of 2. The pH was measured using a calibrated pH meter. The spent media was stored at a pH of 2 at room temperature (RT) for 1 hour and then neutralised by adding 1M NaOH until reaching the original pH of the spent media pre-treatment (approximately 6.5). The media was filter sterilised before use. Fresh ampicillin was added to the media.

2.10.6 Heat treatment of spent media

Stationary spent media was prepared as previously described. The spent media was aliquoted into 1 ml fractions in 1.5 ml Eppendorf tubes and heat treated at 100 ^{o}C for 1 hour in a heat block. Media was allowed to cool to RT before combining the fractions and filter sterilising before use. Fresh ampicillin was added to the media.

2.10.7 Fractionation of the spent media

Stationary phase spent media was prepared as previously described. The spent media was then fractionated into < 3 kDa or > 3 kDa fractions using a 3kDa spin column (Millipore) by centrifuging for 40 minutes at 3,200 xg for complete separation. The volume of the > 3 kDa fraction following centrifugation was approximately 500 µl in volume and was made up to 15 ml with fresh LB. Both fractions were filter sterilised and fresh ampicillin was added before use.

2.11 Co-expression assays

E. coli harbouring pBAD cloned toxin and pME6032 cloned antitoxin were inoculated into 5 ml LB supplemented with 15 µg/ml tetracycline and 100 µg/ml ampicillin and grown overnight at 37 ^{o}C, 200 rpm. The following day the culture was diluted 1:100 in 50 ml of fresh LB and supplemented with fresh ampicillin and tetracycline at the same concentration. Cultures were grown at 37 ^{o}C, 200 rpm in 200 ml conical flasks until reaching an OD_{590}nm of ~0.1. Cultures were then aliquoted into 4 x 10 ml volumes in universal tubes supplemented with 0.2% (w/v) glucose or 0.2% glucose (w/v) and 25 mM IPTG or 0.2% (w/v) arabinose or 0.2% (w/v) arabinose and 25 mM IPTG. Cultures were returned to the incubator and samples were taken after 2 hours for measurement of OD_{590}nm by spectrophotometry and CFU determination by serial dilutions in 96 well plates. Cells were spot plated onto LB ampicillin tetracycline plates and incubated overnight at 37 ^{o}C.

2.12 Resuscitation assay

Overnight cultures of *E. coli* harbouring pBAD cloned toxin and pME6032 cloned antitoxin were diluted 1:100 in 60 ml fresh LB supplemented with ampicillin and

tetracycline. Cultures were grown at 37 ^{o}C, 200 rpm in conical flasks until reaching an OD_{590}nm of ~0.1. 2 x 25 ml volumes were then aliquoted and supplemented with either 0.2% (w/v) glucose or 0.2% (w/v) arabinose to repress or induce toxin expression respectively. The cultures were then returned to the incubator for a further 2 hours. These cultures were aliquoted into 2 x 10 ml volumes and 1 aliquot was supplemented with 25 mM IPTG for antitoxin expression (for experiments without a wash step) and grown for a further 2 hours. Where experiments required a wash step, after the initial 2 hour incubation, arabinose induced cultures were centrifuged for 10 minutes at 3,200 x g and washed in LB to remove arabinose. Cultures were then re-suspended in LB and aliquoted into 2 x 10 ml volumes. To 1 aliquot 0.2% (w/v) arabinose was added and to the other 25 mM IPTG. Both had fresh ampicillin added and were incubated for a further 2 hours. The OD and CFU were determined as with Co-expression assay at 0, 2 and 4 hours.

2.13 Live/dead staining

Overnight cultures of *E. coli* MG1655 pBAD-BPSS0390 or *E. coli* MG1655 Δ*hipBA* pBAD-BPSS1584 were diluted 1:100 in 30 ml fresh LB media and supplemented with ampicillin. Cultures were grown at 37 ^{o}C, 200 rpm in conical flasks until reaching an OD_{590}nm of 0.1. Cultures were aliquoted into 2 x 10 ml volumes and supplemented with either 0.2% (w/v) glucose or 0.2% (w/v) arabinose to repress or induce gene expression respectively. Cultures were returned to the incubator for 3 hours before diluting/standardising to an OD_{590}nm of 0.5 and carrying out the LIVE/DEAD Baclight protocol as indicated in the Invirogen manual. Fluorescent bacteria were visualised using a CETI inverted fluorescence microscope using green and red filters at a 40 x objective. ProgRes CF software and a Jenoptik camera were used for image

capture. Alternatively a fluorescence plate reader was used to detect fluoresce units. For microscope imaging, samples were washed and stored in 0.85% NaCl and dead controls were treated with 70% isopropanol. Samples and controls were visualised on separate slides under both fluorescent channels on the microscope. With the florescence plate reader, dead controls were mixed sequentially with test samples under both toxin induced and repressed conditions. Samples were prepared in a 96-well plate.

2.14 Minimum inhibitory concentration (MIC) determination

Overnight cultures of *E. coli* were diluted to an OD_{590}nm of 0.5 in 1.5 ml Eppendorf tubes in LB, to give approximately 10^8 CFU/ml. Antibiotic stock solutions of ciprofloxacin or ceftazidme were diluted in LB to a concentration double that of the desired start concentration to be tested. 100 µl of the antibiotic solution was added to the first well of a 96 well plate and subsequent 10-fold dilutions were performed along the row by diluting 10 µl into 90µl of LB. 100 µl of diluted bacterial culture was added to each well to give a 50:50 mix of antibiotic to bacterial culture. 96-well plates were incubated at 37 ^{o}C overnight before measuring the OD_{590}nm using a BioRad plate reader. The minimum concentration of antibiotic that prevented the bacterial cells from growing (indicated by OD increase) was considered to be the MIC.

2.15 Persister assays

2.15.1 Stationary phase cultures

Overnight cultures of *B. pseudomallei* strains were grown in universal tubes in 5 ml volumes of LB. The next day cultures were diluted to approximately $2x10^8$ cells in LB. 500 µl of the diluted cultures were then mixed with 500 µl of LB containing 200 x

MIC of ciprofloxacin or ceftazidime in a 24 well plate. This gave a mix of 10^8 bacterial cells and 100 x MIC antibiotic in each well. Cultures were incubated for 24 hours at 37 ^oC in a static incubator. A sample was taken and serial diluted to determine the input CFU before mixing the diluted cells with antibiotic. Cultures were plated onto LB plates. Following 24 hours incubation cultures were removed from the well by pipetting and added to 1.5 ml O-ring sealed Eppendorf tubes. The cultures were then centrifuged for 7 minutes at 13,000 rpm and the supernatnat discarded. 1 ml of fresh LB was then added and cell pellets were re-suspended to wash before repeating the centrifugation and wash step. A sample of culture was serial diluted in a 96 well plate by adding 10 µl of culture to 90 µl of LB. These samples were plated onto LB plates and incubated overnight at 37 ^oC in a static incubator to give a 24 hour time point. Persister frequencies were determined by dividing 24 hour CFU counts by the input CFU.

2.15.2 *E. coli* cultures expressing BPSS0390

Overnight cultures of *E. coli* strains harbouring pBAD cloned toxin and pME6032 cloned antitoxin were grown in 5 ml LB supplemented with 100 µg/ml ampicillin and 15 µg/ml tetracycline for plasmid selection. The next day cultures were diluted 1:100 in 30 ml fresh LB supplemented with antibiotic in 100 ml conical flasks and grown at 37 ^oC, 200 rpm until the OD_{590}nm of the culture reached ~ 0.1. Cultures were then aliquoted into 2 x 10 ml volumes in universal tubes and supplemented with either 0.2% (w/v) glucose or 0.2% (w/v) arabinose to repress or induce expression of the toxin. These cultures were incubated for 3 hours at 37 ^oC, 200 rpm. Cultures were then standardised to $2x10^8$ cells in LB and 500 µl of culture was mixed with 500 µl of 200 x MIC of antibiotic in a 24 well plate. Plates were incubated for 24 hours at 37 ^oC.

After 24 hours the cultures were washed as described in 2.15.1. T0 and T24 samples were plated onto LB ampicillin tetracycline plates containing 1 mM IPTG to induce antitoxin expression from the pME6032 vector. The persister frequency was calculated as CFU counts after 24 hours/ CFU counts at T0.

2.15.3 *E. coli* expressing BPSS0390 at different cell densities

As with 2.15.2 except the following changes. Once cultures reached OD_{590}nm~0.1, a 5 ml, 500µl or 50µl volume of culture was aliquoted into a universal tube. Culture volumes were made up to 5 ml with LB and supplemented with fresh ampicillin and tetracycline. Expression of BPSS0390 was then induced with 0.2% (w/v) arabinose and the cultures were grown for 3 hours at 37 ^{o}C, 200 rpm. After the 3 hours samples were mixed 1:1 with ciprofloxacin and the persister assay performed.

2.16 Deletion of *B. pseudomallei* K96243 TA loci

To create the Δ*BPSS0390-0391* mutant in *B. pseudomallei* the pDM4 sucrose selection method was utilised. 600bp fragments upstream and downstream of the BPSS0390-0391 locus were PCR amplified from *B. pseudomallei* K9643 genomic DNA. The upstream fragment was amplified using primers 1 and 2, while the downstream fragment was amplified with primers 3 and 4 (figure 2.0). Primers 2 and 3 were designed to contain the start codon and the first 12 bp of the BPSS0390 gene followed by the last 12bp and the stop codon of the BPSS0391 gene in addition to a *Not*I restriction site. Primers 1 and 4 had a specific restriction site for cloning the combined fragment into the pDM4 vector *Xma*I and *Sac*I respectively. Upstream and downstream PCR fragments were first cloned into the gateway vector pGEM before digesting with appropriate restriction enzymes. The 2 PCR products were then fused

together to create a 1.2 kb fragment using primers 1 and 4 in a PCR reaction. This combined fragment was then cloned into pDM4 and transformed into *E. coli* DH5α λpir and plated onto LB agar plates containing 35 μg/ml chloramphenicol. Transformants were checked for the pDM4 constructs containing the 1.2 kbp deletion cassette by PCR and restriction digestion of isolated plasmid DNA. Plasmid DNA was also sent for sequencing and plasmids with the correct sequence were transformed into *E. coli* S17 λpir by heat shock.

A conjugation was then set up using transformed S17λ cells containing the cloned pDM4-deletion cassette and *B. pseudomallei* K96243 as a recipient strain. Conjugates were plated onto gentamicin 100 μg/ml chloramphenicol 50 μg/ml LB agar plates to kill *E. coli* and any *B. pseudomallei* that did not take up the pDM4 plasmid. Colonies that grew were re-streaked onto chloramphenicol 50 μg/ml plates and PCR screened using a pDM4 specific primer and a primer upstream of the TA locus to confirm the plasmid had integrated into the chromosome. PCR confirmed integrants were grown overnight in LB supplemented with chloramphenicol 50 μg/ml for subsequent sucrose selection to remove the integrated plasmid. Overnight cultures of integrants were diluted to an OD_{590}nm 0.4 and serial diluted to the 10^{-6} dilution. The 10^{-4}, 10^{-5} and 10^{-6} dilutions were plated onto LB agar plates containing 10% (w/v) sucrose and incubated for 3-4 days at 2 5 ^{o}C. Colonies that grew on the sucrose plates were re-streaked onto both chloramphenicol 50 μg/ml plates and LB plates. Those colonies that grew only on LB were assumed to have lost the plasmid through recombination and were PCR screened using primers upstream and downstream of the TA locus to determine if the loci had been deleted or whether colonies had reverted to wild type. PCR products that were of the size expected following a deletion event (800 bp) were PCR purified and sent for sequencing to confirm the deletion.

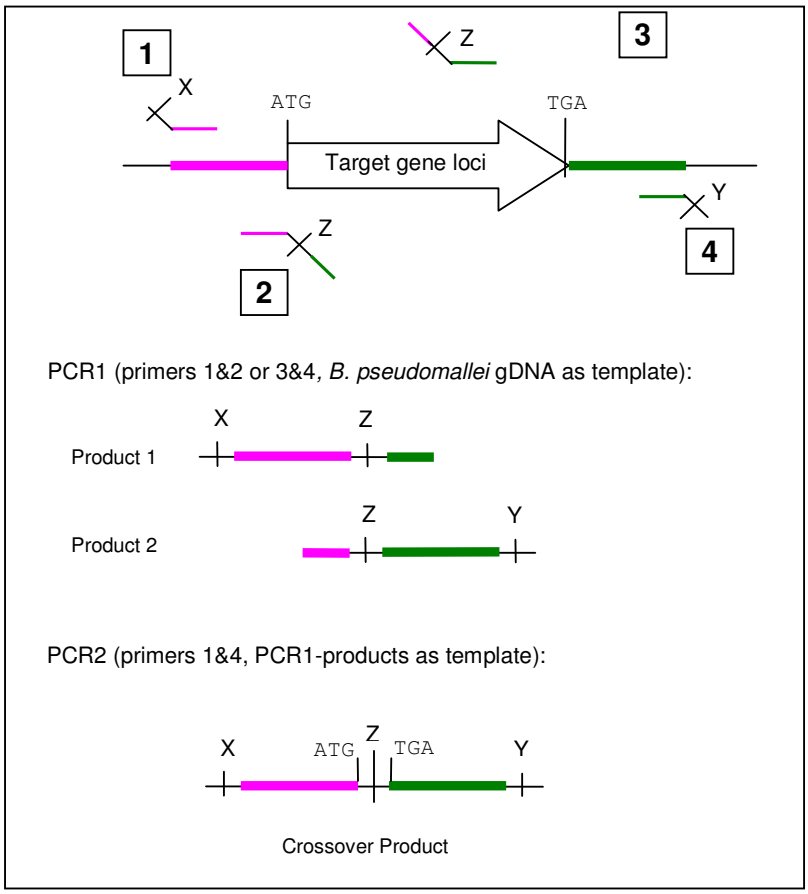

Figure 2.0 Schematic representation of how the deletion cassette was created. X, y and z show restriction enzyme sequences. Numbers 1-4 are primer numbers.

2.17 Expression of TA toxins in *Burkholderia*

For expression of BPSS0390 and BPSS1584 in *Burkholderia*, the pBHR and pSCrhaB3 plasmids were utilised, as they could be maintained and replicate within this genus. Details of specific cloning procedures are indicated in relevant results chapters.

2.17.1 Expression in *B. thailandensis*

Overnight cultures of *B. thailandensis* E264 or CDC301 harbouring empty plasmid or plasmid cloned toxins were diluted 1:100 in 30 ml fresh LB supplemented with the appropriate antibiotic for plasmid selection. Cultures were grown to OD_{590}nm ~0.1 and then aliquoted into 2 x 15 ml volumes supplementing with 0.2% (w/v) glucose or 0.2% (w/v) arabinose for pBHR plasmid and 0.2% (w/v) glucose or 0.2% (w/v) rhamnose for pScrhaB3 plasmids. Cultures were grown for 3-5 hours at 37 ^{o}C, 200 rpm and the OD was measured and CFU count determined at indicated time points by plating onto LB agar supplemented with antibiotic. Plates were incubated for 48 hours before counting.

2.17.2 Expression in *B. pseudomallei*

5 ml volumes of LB supplemented with trimethoprim 100 μg/ml and 0.2% (w/v) glucose were inoculated with *B. pseudomallei* K96243 harbouring pSCrhaB3 constructs and grown at 37 ^{o}C, 200 rpm. The next day cultures were diluted 1:100 into 2 x 5 ml volumes of fresh LB supplemented with Tp 100 and 0.2% (w/v) glucose or 0.2% (w/v) rhamnose to repress or induce expression of BPSS0390 respectively and returned to the incubator. OD_{590}nm and CFU were determined at indicated time points

as previously described. Cells were plated onto Tp100 0.2% (w/v) glucose LB agar plates for CFU counts. Plates were incubated for at least 24 hours before counting.

2.17.3 Expression in *B. pseudomallei ΔBPSS0390-0391*

5 ml ONCs of *B. pseudomallei ΔBPSS0390-0391* K96243 harbouring pSCrhaB3 constructs supplemented with Tp 100 and 0.2% (w/v) glucose to minimise leaky expression were grown at 37 ^{o}C, 200 rpm. The next day cultures were diluted 1:50 into 2 x 5 ml volumes of fresh LB supplemented with Tp 100 and cultures were grown to OD_{590}nm~ 0.1 and then 0.2% (w/v) glucose or 0.2% (w/v) rhamnose was added to each culture to repress or induce expression respectively. Cultures were then returned to the incubator and OD_{590}nm and CFU were determined at indicated time points. Cells were plated onto Tp 100 0.2% (w/v) glucose LB agar plates for CFU counts. Plates were incubated for 24 hours before counting.

2.17.4 Isolation of *B. pseudomallei* K96243 Δ*BPSS0390-0391* spent media

Overnight cultures of *B. pseudomallei* Δ*BPSS0390-0391* K96243 pSCrhaB3-BPSS0390 supplemented with trimethoprim were centrifuged for 10 minutes at 3,200 xg. The supernatant was filter sterilised using 0.2 µm filters to isolate spent media.

2.17.5 Expression in spent media

Overnight cultures of *B. pseudomallei* Δ*BPSS0390-0391* K96243 pscrhaB3-BPSS0390 were diluted 1:50 in 2 x 5 ml volumes of LB**.** Cultures were then grown to an OD_{590}nm 0.1. 2 x high density cultures (neat culture) and 2 x low density cultures (1;100 dilution of neat culture in LB) were centrifuged at 3,200 x g for 10 minutes and the supernatant discarded. Cultures were then re-suspended in fresh LB or spent

media. 0.2% (w/v) rhamnose was then added to all the samples and incubated for 24 hours at 37 ^{o}C, 200 rpm. T0 samples and T24 samples were taken and CFU was determined by serial diluting and plating onto LB agar Tp 100 0.2% (w/v) glucose. CFU fold change was then calculated as CFU counts post rhamnose induction of BPSS0390 expression divided by CFU counts pre BPSS0390 expression.

Where *E. coli* spent media was used the same procedure was carried out as above, except rather than re-suspending in filter sterilised spent media from *B. pseudomallei*, spent media from an overnight culture of *E. coli* MG1655 pBAD-BPSS0390 was used.

2.18 Hydrogen Peroxide stress experiment

Overnight cultures of *B. pseudomallei* K96243 and the *B. pseudomallei* K96243 *ΔBPSS0390-0391* mutant were diluted in 1 ml of LB to an OD_{590}nm 0.2 (approximately 2 x 10^8 cells). 10µl samples were serial diluted and plated onto LB plates for T0 CFU enumeration. Cells were then centrifuged at 13,400 rpm for 7 minutes to pellet. The supernatant was removed by pipetting and the cells were re-suspended in 1 ml of 15 mM hydrogen peroxide, which had been diluted in LB from a 1 M stock. Cells were incubated for 10 minutes at RT before repeating the centrifugation step. The supernatant was removed and cells were re-suspended in fresh LB. This step was repeated to remove residual hydrogen peroxide. 10 µl samples were aliquoted and serial diluted and plated on LB agar. Plates were incubated at 37 ^{o}C until colonies were visible. Survival frequency was calculated as CFU counts post hydrogen peroxide divided by CFU counts pre-treatment.

2.19 Heat stress experiment

Overnight cultures of *B. pseudomallei* K96243 and *B. pseudomallei* K96243 *ΔhipBA* were diluted to an OD_{590}nm of 1.0 or 0.2 in 3 ml volumes. 1 ml aliquots of each sample were then added to 2 ml Eppendorf tubes and incubated at 65 ^{o}C for 2 hours in a pre heated heat block. 10 µl samples were taken pre and post heat treatment, serial diluted and plated onto LB agar plates. Survival frequency was calculated as CFU counts post heat treatment/ pre treatment. Plates were incubated at 37 ^{o}C for 24 hours.

2.20 pH stress experiments

Overnight cultures of *B. pseudomallei* K96243 or *B. pseudomallei ΔhipBA* were diluted to 10^8 CFU/ml in 1 ml of LB. Cells were then pelleted by centrifugation for 7 minutes at 13,000 rpm, the supernatant was discarded and the pellet re-suspended in 1 ml of LB that had been adjusted to either a pH of 3.5 or pH 2.5 using 1M HCl. Cells were incubated for 24 hours at 37^{o}C in a static incubator. After this incubation period cells were centrifuged for 7 minutes at 13,000 rpm and the cell pellet was re-suspended in LB. This process was repeated twice to remove all residual acidified LB. Serial dilutions of the cells were then prepared and cells were plated onto LB agar for CFU determination. Survival was calculated as CFU counts post pH stress divided by CFU counts pre stress.

2.21 Cadmium sulphate stress

2.21.1 Cadmium in LB broth

Overnight cultures of *B. pseudomallei* K96243 and *B. pseudomallei* K96243 *ΔBPSS0390-0391* were diluted to 2 x 10^8 CFU/ml in LB before mixing a 1:1 ratio of cells with various cadmium concentrations diluted in LB and incubating in 24 well

plates at 37°C for 24 hours. After incubation, cells were pelleted by centrifugation at 13,000 rpm for 7 minutes and the supernatant discarded. The cell pellet was re-suspended in 1 ml of fresh LB to wash. This centrifugation and wash step was repeated twice. After washing, cells were serial diluted and plated onto LB agar for CFU determination. Survival was calculated as CFU counts post cadmium stress divided by CFU counts pre stress.

2.21.2 Cadmium in LB agar

The *B. pseudomallei* strains were diluted in LB to a concentration of 10^8 CFU/ml before serial diluting and spot plating onto LB agar containing various concentrations of cadmium sulphate. Cultures were also plated onto an LB agar plates as a negative control. Plates were incubated up to 48 hours until colonies were visible and at a size where they could be counted. Survival was calculated as CFU counts on the cadmium plate divided by CFU counts on LB agar only.

2.22 Site directed mutagenesis

Primers for site directed mutagenesis were designed on the Agilent website and synthesised by Eurofins MWG. Primers contained the base pair(s) substitution needed to encode the amino acid change. Site directed mutagenesis was carried out on the his tagged BPSS0390 toxin DNA as per manufacturer's instructions using the Quick-change lightning kit. In summary, this involved the synthesis of forward and reverse mutant plasmid DNA strands using the designed primers, pBAD/his-BPSS0390 as a template and a pfu-based polymerase blend. *Dpn*I was then used to digest the parental non-mutant methylated DNA before transformation of the mutant plasmid into XL10-gold ultracompetent cells by heat shock in the presence of β-mercaptoethanol.

Transformants were plated onto LB ampicillin plates and grown overnight at 37 ^{o}C. Colonies were then picked and plasmid DNA was re-isolated using the Qiagen miniprep kit as previously described and sent for sequencing to confirm that the appropriate nucleotides were mutated.

2.23 Protein gels

For detection of protein, Novex 4-12% SDS-PAGE gels (Invitrogen) were used. A total of 20 µl of protein preparation were loaded into each well of the gel. Protein samples containing 4 x loading dye were boiled at 95 ^{o}C for 5 minutes in a heat block before loading. 5 µl of a protein ladder was loaded for size comparison. For the majority of gels the BioRad precision plus dual xtra standards marker was used. Gels were run in 1 x MES or MOPS buffer at 180 V for 45minutes or until the protein reached the bottom of the gel. After the gel was run it was washed in de-ionised water before staining with simply blue protein stain (Invitrogen). The protein gel was incubated with approximately 20 ml of Simply Blue stain and microwaved in 30 second intervals until protein bands were visible. Following staining the gel was washed with de-ionised water 3 times and then incubated on a rocker in 100 ml de-ionised water overnight to de-stain the gel.

2.24 Western Blots

Protein samples were boiled, loaded and run on SDS-PAGE gels as previously described. After gel electrophoresis the gel was removed from its cast and washed twice in approximately 20 ml of deionised water. The gel was then placed onto a nitrocellulose membrane using the iblot dry blotting system (Invitogen). Alternatively the nitrocellulose membrane was removed and a Polyvinylidenfluoride (PVDF)

membrane (Millipore) was used in its place. The protein was blotted onto the appropriate membrane for 5-7 minutes using 20-23 V. The membrane was then transferred to 30 ml of a 3% (w/v) BSA solution dissolved in TBST (Tris buffer saline 1% Tween) which was used as a blocking agent. The membrane was incubated in this solution overnight at 4 ^{o}C. The next day the solution was removed. The anti-xpress epitope antibody (Invirogen) was diluted 1:5000 in 15 ml of 3% (w/v) BSA dissolved in TBST and added to the membrane, incubating for 1 hour at room temperature on a rocker. Following this incubation step, the BSA and antibody mix was discarded and then 20 ml of TBST was added to wash and incubated on a rocker for 10 minutes before discarding. This washing process was repeated 3 times. A secondary anti-goat anti-mouse-horseradish peroxidise (HRP) conjugated antibody was then diluted 1:10000 in 10 ml of fresh 3% (w/v) BSA dissolved in TBST and incubated with the membrane for a further hour. The wash steps in TBST were repeated as described above. Following this, 500 µl of both reagents in the super signal west femto chemiluminescent substrate kit (Thermo scientific) were mixed and added to the membrane before wrapping the membrane in cling film. Protein on the membrane was detected using chemiluminescence with the gel imaging system (BioRad).

2.25 Large scale protein expression

2.25.1 Zym-5052 media

An overnight culture of *E. coli* Rosetta (DE3) harbouring pET26-b constructs were grown in a 5 ml volume of LB supplemented with 50 µg/ml kanamycin. The next day cultures were diluted 1:100 in 4 x 100 ml aliquots of ZYM-5052 autoinduction media (Studier, 2005) supplemented with fresh kanamycin. 500 ml conical flasks were used to grow the cultures and they were incubated at 300 rpm at 37 ^{o}C until reaching mid

log phase. The temperature was reduced to 20 ^{o}C and growth continued for a further 24 hours before the cultures were processed.

2.25.2 ^{15}N labelled N-5052 media

As with 2.25.1, an overnight culture supplemented with kanamycin was grown in LB. The next day cells were harvested by centrifugation at 4000 rpm for 10 minutes. The supernatant was discarded and the cell pellet re-suspended in N-5052 media (Studier, 2005) containing ^{15}N labelled ammonium chloride. This step was repeated to remove residual LB media. The cultures were then diluted 1:100 in 4 x 100 ml aliquots of the labelled N-5052 media in 500 ml conical flasks supplemented with kanamycin. Cultures were grown at 300 rpm, 37 ^{o}C until reaching mid log phase and then at 20 ^{o}C for a further 24 hours before processing.

2.25.3 ^{15}N and ^{13}C N-5052 media

A culture of *E. coli* Rosetta (DE3) pET26-b-H24A was grown overnight in LB supplemented with kanamycin. The next day the cultures were diluted 1:100 in 2L of fresh LB aliqouted into 5 x 400 ml volumes each in a 2 L flask. These cultures were grown to an OD_{590}nm of approximately 0.8-0.9 before spinning the cultures at 3000 x g for 10 minutes in sterile 250 ml tubes to collect the cell pellets. The cell pellets were then re-suspended in a total volume of 500 ml double labelled N-5052 media (Studier, 2005) and grown at 37^{o}C for a further hour. After this time had elapsed 0.5 mM IPTG was added to induce expression of the cloned H24A and the temperature was reduced to 20 ^{o}C for maximal expression and grown for a further 24 hours.

2.26 Protein extraction

2.26.1 Large scale overexpression

Cultures overexpressing protein to be purified were harvested by centrifugation at 12000 x g for 10 minutes. The supernatant was then discarded and cell pellets were either frozen for downstream processing days later or processed directly on the same day. 10 ml of Bugbuster was used to lyse every 100 ml of culture along with 10 µl of benzonase and 10 µl of lysozyme (Novagen). Cell pellets were re-suspended in the lysis mix by vortexing and then incubated on a rocker for 30 minutes until the cell mix appeared translucent. If the cell lysis mix was still viscous, more Bugbuster, benzonase and lysozyme were added and the culture was incubated for a further 30 minutes. Following lysis, cell debris was harvested by centrifuged at 16000 x g for 20 minutes. The supernatant containing the expressed protein was collected for subsequent purification.

2.26.2 Small scale protein expression

To check for expression of his tagged proteins, 1 ml of cells at cell density of OD_{590}nm 1.0 were harvested. The cells were centrifuged for 2 minutes at 17,000 x g in a 1.5 ml Eppendorf tube before discarding the supernatant. 100 µl of Bugbuster was added along with 1 µl of benzonase and 1 µl of lysozyme and cells were re-suspended and incubated on a rocker for 30 minutes. The lysed cultures were then centrifuged for 1 minute at 17,000 xg to separate the soluble and insoluble material. The soluble fraction was pipetted into a fresh Eppendorf tube and 30 µl of 4 x loading dye was added to the soluble fraction. 130 µl of loading dye was added to the insoluble pellet and re-suspended. The samples were then heat treated at approximately 95 ^{o}C for 5 minutes before running 20 µl samples on a protein gel.

2.27 Protein purification of histidine tagged protein

2.27.1 Affinity chromatography

Cell lysate containing his tagged protein was purified using Nickel affinity based column systems. Either the his gravi trap (GE healthcare) or the his purification column (Novagen) were used. The manufacturer's protocols were followed. In summary this involved equilibrating the columns with binding buffer before applying the protein. The column was then washed to remove non-bound protein and any unspecific binding. Bound protein was eluted from the column with an imadizole based buffer.

2.27.2 De-salting columns

Protein was de-salted by running through a PD-10 desalting column (GE Healthcare). The PD-10 columns were first equilibrated with 25 ml TBS buffer (20 mM Tris.Hcl 150 mM NaCl) or PBS (20 mM phosphate 150 mM NaCl) before adding a maximum of 2.5 ml of protein sample to the column as indicated in manufacturer's instructions. Protein was eluted in 3.5 ml of TBS or PBS. This procedure was repeated until all protein was de-salted.

2.27.3 Enterokinase digest

The protein was incubated with enterokinase to remove the 3 kDa his tag from the protein. Approximately 0.16ng of enterokinase was added for every 25 μg of protein and incubated at 23 ^{o}C for 16 hours.

2.27.4 Concentrating protein

Protein was concentrated using an Amicon Ultra-15 Centrifugal Filter Unit with Ultracel-3kDa membrane by centrifugation at 3,200 x g, 4 ^{o}C.

2.27.5 Size exclusion chromatography

A Superdex 75 16/60 hr column (GE healthcare) was used for size exclusion gel chromatography to exclude any impurities from the protein preparation. The column was equilibrated with PBS before the sample was added. The fractions were collected into 1 ml volumes. Appropriate fractions containing the purified protein were combined as indicated by the computer software.

2.27.6 Determining protein concentration

Protein concentration was then determined by the Nanodrop. The Nanodrop reading was divided by the extension coefficient of the protein to determine the true concentration.

2.28 Circular Dichoism

Circular Dichroism (CD) spectroscopy experiments were carried out at the Biomolecular Spectroscopy Centre, King's College London. Protein was stored and diluted in PBS buffer to a standardised concentration of 0.3 mg/ml for experimentation. UV absorption and CD spectra were acquired on the Applied Photophysics Chirascan Plus spectrometer (Leatherhead, UK). 10 mm and 0.5 mm rectangular cells were employed in the regions 400-230nm and 260-190nm respectively. The instrument was flushed continuously with pure evaporated nitrogen throughout the experiment. The following parameters were employed: 1 nm spectral bandwidth, 1nm stepsize and a 1.5 s instrument time-per-point. All spectra were

buffer baseline subtracted and measured at 23 ^{o}C. The far-UV CD data was normalised for concentration and pathlength and expressed in terms of Δε per residue (MWt =113). The CD spectra were smoothed using the *Savitzky–Golay* method with a window factor of 2. Protein secondary structure content was calculated based on the principle component regression method.

2.29 Crystallisation of protein

For initial crystallisation trials a 96 well plate containing 96 buffer/salt conditions was used along with purified protein at a concentration of 10 mg/ml. A vapour diffusion method was employed, using a robot to aliquot and mix 1 µl of a buffer with 1 µl of the sample protein in small wells adjacent to each of the main buffer wells. This was done for each buffer condition. The test plate was sealed with oil and incubated in a fridge at 4 ^{o}C for crystal growth. The plate was checked periodically for 1 week using a light microscope to screen for crystals. The condition of the resulting buffer and protein mix was scored using a crystal scoring system.

2.30 Electrophoretic mobility shift assay (EMSA)

H24A, BPSS0391 and his tagged BPSS0391 protein that had been purified by affinity and size exclusion chromatography were used in Electrophoretic mobility shift assay (EMSA) experiments. Indicated amounts of protein were added to a reaction mix containing 500 ng of either a random PCR product (BPSL2333 DNA) or a 600 bp DNA fragment upstream of the BPSS0390 gene, which was assumed to contain the promoter region of the BPSS0390-0391 locus. The total reaction volume was 20 µl made up to final volume with nuclease free water. BSA and water only were used as controls for the experiment. Reactions were incubated at room temperature for 10

minutes before mixing with loading dye and adding to a 1% (w/v) agarose gel containing sybersafe DNA stain. The DNA gel was run as described for electrophoresis and visualised under UV light. A 1kbp DNA ladder was also run on the gel for size comparison.

2.31 RNase assay

Purified H24A protein that had been cut to remove the his tag and purified BPSS0390 from co-expression with BPSS0391 was used in the RNase experiments. Protein at 1 mg/ml was incubated with 1 µg of MS2 RNA for 10 minutes in a 20 µl final volume reaction at room temperature. The reaction was made up to volume with nuclease free water. Samples were then added to a 1% agarose gel as described above, mixing with loading dye. Gloves and gel casting equipment were treated with RNase Zap prior to loading samples. Water only, BSA (5 mg/ml) and RNaseH (0.5-2 U/µl) were used as controls for the experiment.

2.32 Pull down assays

Purified his tagged H24A protein was used as bait protein in the pull down assay and total cell lysate from *E. coli* DH5α pME6032-BPSS0391 was used as prey. This strain was grown to early log phase before inducing expression of the BPSS0391 gene with 25 mM IPTG for 3 hours. The cells were then lysed by addition of Bugbuster, lysozyme and benzonase to release protein and the cell lysate was isolated by removing cell debris through centrifugation.The ProFound Pull-Down PolyHis Protein:Protein Interaction Kit (Thermo Scientific) was used for this assay. The manufacturers' protocol was followed. In summary, his tagged H24A bait protein was added and bound to immobilised nickel chelate resin in a column. Any unbound

protein was washed away with wash buffer before incubating the bead-to bait mix with prey cell lysate for 16 hours at 4 ^{o}C. The column was then washed with wash buffer to remove unbound prey. Any prey-bait complexes that had formed were then eluted by competitively displacing the his tag to nickel interaction with imidazole. Eluted protein was prepared and visualised on a SDS-PAGE gel as previously described.

2.33 Stabilisation experiments

A 450µl master mix was set up containing 0.133 mg/ml of protein, 0.96 mL of 5000X Sypro Orange and de-ionised water. 15 µl of reaction mix was then added to each well in a 48 well PCR plate. In parallel a 96-well plate containing the test compounds was centrifuged for 5 minutes at 1,500 x g. Using a multichannel pipette, 5 µL of compound library solutions were added to the corresponding wells of the 48 well plate containing the reaction mix. The plate was then sealed and centrifuged for 2 minutes at 300 x g before loading the samples onto a qPCR machine. Samples were heated between 25 ^{o}C and 99 ^{o}C over 50 minutes measuring fluorescence emitted from the dye. Computer software was then used to calculate the melting temperature (Tm) of the protein using two methods, Boltzmann and the derivative.

2.34 NMR spectroscopy

The concentration of the final NMR sample (500 ul in 2x3 mm Wilmad NMR tubes) was typically 1 mM dissolved in PBS buffer with 10% D_2O.

All NMR experiments were acquired at 25 °C on a cryoprobe equipped Varian VNMRS 600MHz spectrometer. Standard triple resonance experiments were used to assign the backbone (HNCA,HNCOCA, HNCACB, HNCO) and sidechains (15N-

TOCSY, HCCONH, CCONH, HCCH-TOCSY). ^{15}N- edited and ^{13}C-edited NOESY datasets were acquired with 100ms mixing times to generate distance restraints for structure calculations. All the NMR data was processed using NMRPipe spectral processing and analysis system, and the assignment and NOE data were analysed using CCPN Analysis Version 2.2

Chapter 3

Identification of type II toxin-antitoxin systems in *Burkholderia pseudomallei*

3.0 Introduction

Toxin-antitoxin (TA) modules are found throughout the prokaryotic world and are believed to have involvement in metabolic regulation and persistence during conditions of stress, which may link them to chronic bacterial disease (Yamaguchi*, et al.*, 2011). Pathogenic members of the *Burkholderia* genus including *B. cenocepacia* and *B. multivorans* contain multiple TA loci, as does *M. tuberculosis,* which like *B. pseudomallei* is associated with chronic persistent disease (Pandey & Gerdes, 2005). It is hypothesised that TA modules are present in the *B. pseudomallei* genome.

Type II TA systems are the most widely studied of the 3 categories of TA systems and consist of a locus containing 2 genes that code for 2 protein products. All currently annotated type II TA modules are grouped into 10 distinct families based on amino acid sequence similarity of the toxin and the antitoxin (Jorgensen*, et al.*, 2008). There are also examples of hybrid associations with a toxin from 1 family partnering with an antitoxin from another (Grady & Hayes, 2003, Schmidt*, et al.*, 2007). Recent bioinformatic studies have also identified novel putative families of TA systems that may add to the current library of type II systems (Makarova*, et al.*, 2009, Leplae*, et al.*, 2011). Software such as RASTA-bacteria has been developed to aid in identification of previous TA families and novel families based on gene size, location with a partner gene and domain homology (Sevin E & Barloy-Hubler, 2007).

To investigate the phenotypic properties of TA systems, various expression systems have been developed. In some cases both the putative toxin and the antitoxin have been cloned into the same plasmid and expression is driven from a single promoter (Sevillano*, et al.*, 2012). Other groups have established expression systems that involve cloning putative toxin and antitoxin genes into 2 different plasmids, both driven by different promoters for independent or co-expression of the genes (Gupta,

2009, Christensen-Dalsgaard*, et al.*, 2010, Heaton*, et al.*, 2012). Expression of functionally active TA toxins in these and other expression systems predominantly results in either reversible or non reversible growth inhibition that can also be associated with a reduction in the number of culturable cells. In some cases expression of toxins is associated with cell death, as is the case with MazF (Amitai*, et al.*, 2004).

To identify type II TA systems in *B. pseudomallei,* bioinformatic resources were utilised and an expression system developed similar to those used in the studies with 2 different inducible promoters for independent expression of putative toxins and antitoxins.

3.0.1 Aim

Identify type II Toxin-antitoxin systems in *B. pseudomallei.*

3.1 Bioinformatic screening

3.1.1 RASTA-bacteria

3.1.1.1 Validation

To identify candidate TA genes in *B. pseudomallei*, the prediction software RASTA bacteria was used. This scores ORFs based on sequence annotation, presence of conserved domains with known TA families, size of the encoded protein and presence of a coupled partner gene. The developers of this software suggest that genes that score over 55% should be considered for further study. To validate the software, the *E. coli* K-12 genome was selected for analysis and the data output from RASTA-bacteria was compared to already known and characterised TA systems from this micro-organism (Table 3.0). RASTA-bacteria successfully scored 20 of the 24 currently annotated *E. coli K-12* TA genes as being likely candidates. The software was subsequently used for predictions of *B. pseudomallei* TA genes.

3.1.1.2 Screening publicly available *B. pseudomallei* genomes

The sequenced genomes of *B. pseudomallei* strains K96243, 1106a, 1710b and 668 were analysed with the RASTA-bacteria software. Table 3.1 shows some clinical data regarding the strains. The output data from RASTA-bacteria for K96243 suggested 61 ORFs could be potential TA genes (scoring over 55%). For *B. pseudomallei* 1106a 73 ORFs were predicted, for *B. pseudomallei* 1710b 41 ORFS were predicted, and lastly for *B. pseudomallei* 668 88 ORFs were scored as possible TA genes (genes listed in appendix). 3 of the 4 strains are isolated from Thailand. The patients with 1106a and 668 survived, while those with K96243 and 1710b died.

Table 3.0. Testing the validity of RASTA-bacteria at predicting toxin-antitoxin genes. The genes listed in the left of the table are known *E. coli* K-12 TA genes indicated by (Gerdes & Maisonneuve, 2012).

In column 2 are the predicted RASTA-bacteria scores. The software successfully predicted these genes as likely candidates and identified the correct partner gene.

Gene Name	**RASTA score (%)**	**Predicted partner gene**
mazE	94	*mazF*
chpS	93.6	*chpB*
relE	93.5	*relB*
relB	92.8	*relE*
mazF	88.7	*mazE*
chpB	88	*chpS*
dinJ	80.7	*yafQ*
yefM	80.4	*yoeB*
yafN	78.6	*yafO*
hipB	74.5	*hipA*
ygjM	72.4	*ygjN*
yafQ	68.2	*dinJ*
sohA	71.9	*yhaV*
yoeB	68	*yefM*
ygiT	70.6	*mqsR*
mqsR	66.7	*ygiT (mqsA)*
hipA	65	*hipB*
ygiN	64.6	*ygiM*
yafO	64	*yafN*
yhaV	60.8	*sohA (prlF)*

Table 3.1 Clinical information, country of origin and the number of RASTA-bacteria predicted toxin-antitoxin open reading frames scoring over 55% for 4 fully sequenced *B. pseudomallei* strains. Clinical data from (Tuanyok*, et al.*, 2008).

Strain	**Country of origin**	**Clinical information**	**Number of predicted TA from RASTA**
K96243	Thailand	Isolated in 1996 in Khon Kaen, Thailand from a 34 year old female diabetic patient with a clinical history of short incubation, septicemic infection, and rapid progression to death.	61
1106a	Thailand	Isolated in 1993 in Ubon Ratchathani, Thailand from pus aspirated from liver abscess from a 23-year old female rice farmer. The patient survived.	73
1710b	Thailand	Isolated in 1999 in Ubon Ratchathani, Thailand from blood collected from a 55 year old male patient with known primary melioidosis in 1996. This second episode represented relapse with the same strain. The patient died	41
668	Australia	Isolated in 1995 in Darwin, Australia from the blood of a 53 year old male patient with severe melioidosis encephalomyelitis. The patient survived.	88

3.1.2 TA predictions and comparisons with other data sources.

Toxin-antitoxin predictions were also utilised from a bioinformatic study carried out by Makarova *et al* and the toxin-antitoxin database for the 4 fully sequenced publicly available *B. pseudomallei* strains. Makarova *et al* searched for pairs of genes that were located together in an operon and that were significantly non-uniformly distributed amongst prokaryotic genomes (Makarova*, et al.*, 2009). The toxin-antitoxin database is a resource listing both predicted and experimentally validated TA loci (Shao*, et al.*, 2011). Genes identified in these 2 studies were compared against the TA genes predicted using RASTA. Those genes which appeared in at least 2 of the 3 studies (appearance in RASTA-bacteria was equivalent to a score over 55%) were considered as potential candidate genes for further study. Those genes and corresponding orthologs that met the criteria are listed in Table 3.2. *B. pseudomallei* 1106a had 5 TA gene candidates that met the criteria, with 3 of these genes having orthologs in *B. pseudomallei* 668 and *B. pseudomallei* 1710b. The *B. pseudomallei* 1170b genome contained 7 gene candidates with 5 orthologs of the genes in *B. pseudomallei* K96243 and 2 orthologs of the genes in *B. pseudomallei* 668 and *B. pseudomallei* 1710b. *B. pseudomallei* 668 contained 3 predicted TA genes and orthologs for all of these genes were present in *B. pseudomallei* 1710b and *B. pseudomallei* 1106a. 18 TA genes were predicted for *B. pseudomallei* K96243. 1 of these genes, BPSS1583, was present in all the strains. BPSS1584, BPSL2333 and BPSL2334 had orthologs in *B. pseudomallei* 1710b only.

Gene name	**Putative toxin (t) or antitoxin (a) or unknown (u)**	***B. pseudomallei* K96243 ortholog**	***B. pseudomallei* 1107b ortholog**	***B .pseudomallei* 668 ortholog**	***B. pseudomallei* 1106a ortholog**
BURPS1106A_0095 (1)	a	-	+	+	N/A
BURPS1106A_0096 (1)	t	-	-	-	N/A
BURPS1106A_3174 (2)	a	-	+	+	N/A
BURPS1106A_3175(2)	t	-	+	+	N/A
BURPS1710b_3191(3)	a	-	N/A	+	+
BURPS1710b_3192 (3)	t	-	N/A	+	+
BURPS1710b_2785 (4)	t	+	N/A	-	-
BURPS1710b_2786 (4)	a	+	N/A	-	-
BURPS1710b_0117	u	+	N/A	+	+
BURPS1710b_A0634(5)	a	+	N/A	+	+
BURPS1710b_A0635(5)	t	+	N/A	-	-
BURPS668_3137 (6)	a	-	+	N/A	+
BURPS668_3138 (6)	t	-	+	N/A	+
BURPS668_A2236	u	+	+	N/A	+
BPSL0174 (7)	a	N/A	-	-	-
BPSL0175 (7)	*t*	N/A	-	-	-
BPSL0558 (8)	a	N/A	-	-	-
BPSL0559 (8)	t	N/A	-	-	-
BPSL2333 (9)	t	N/A	+	-	-
BPSL2334 (9)	a	N/A	+	-	-
BPSS0390 (10)	t	N/A	-	-	-
BPSS0391 (10)	a	N/A	-	-	-
BPSS0394 (11)	a	N/A	-	-	-
BPSS0395 (11)	t	N/A	-	-	-
BPSS1060 (12)	a	N/A	-	-	-
BPSS1061 (12)	t	N/A	-	-	-
BPSS1583(13)	a	N/A	+	+	+
BPSS1584(13)	t	N/A	+	-	-
BPSS1816(14)	t	N/A	-	-	-
BPSS1817(14)	a	N/A	-	-	-
BPSS1820 (15)	t	N/A	-	-	-
BPSS1821(15)	a	N/A	-	-	-

Table 3.2 A list of predicted TA genes in *B. pseudomallei* 1106a, 1710b, 668 or K96243 and the presence or absence of orthologs. Genes and orthologs in the table appeared in at least 2 of the 3 bioinformatic resources, which include RASTA-bacteria (score over 55%), the toxin-antitoxin database and the data produced by (Makarova*, et al.*, 2009). (+) indicates ortholog present. (-) indicates no ortholog. Numbers in brackets correspond to a predicted toxin-antitoxin gene pair.

3.1.3 Distribution of candidate *B. pseudomallei* K9243 TA genes in assembled or partially assembled *B. pseudomallei* strains

Table 3.3 shows how the predicted candidate K96243 TA genes were distributed in all *B. pseudomallei* strains available for analysis on the Prokaryotic Genome Analysis Tool website http://tools.nwrce.org/pgat/. There was a mixed distribution of the *B. pseudomallei* K96243 TA genes amongst other strains. Notably, orthologs of BPSS1584-BPSS1583 were present in 27 out of the 29 *B. pseudomallei* strains, whereas orthologs of BPSS0390-0391 were present in 3 strains.

Looking at the fully assembled genomes only, *B. pseudomallei* 1106a contained orthologs of 4 of the 8 predicted TA loci and also possessed BPSL2334 but not the associated BPSL2333 gene. *B. pseudomallei* 1710b possessed 4 of the 8 loci and a further 2 of the loci contained only 1 of the 2 genes (BPSS0391- predicted antitoxin and BPSS0395-predicted toxin). *B. pseudomallei* 668 contained 3 of the 8 loci and again a further 2 loci contained only 1 of the 2 genes (BPSL2334-predicted antitoxin and BPSS0394-predicted antitoxin).

Table 3.3 Heat map showing the distribution of predicted *B. pseudomallei* K96243 TA genes in fully assembled or partially assembled *B. pseudomallei* genomes. Paired genes are predicted TA modules. Strains highlighted in purple are fully assembled strains. Green indicates the presence of an orthologous gene, green with a border indicates an orthologous pseudogene, red indicates that there is no ortholog and yellow indicates no match in a strain that is not fully assembled.

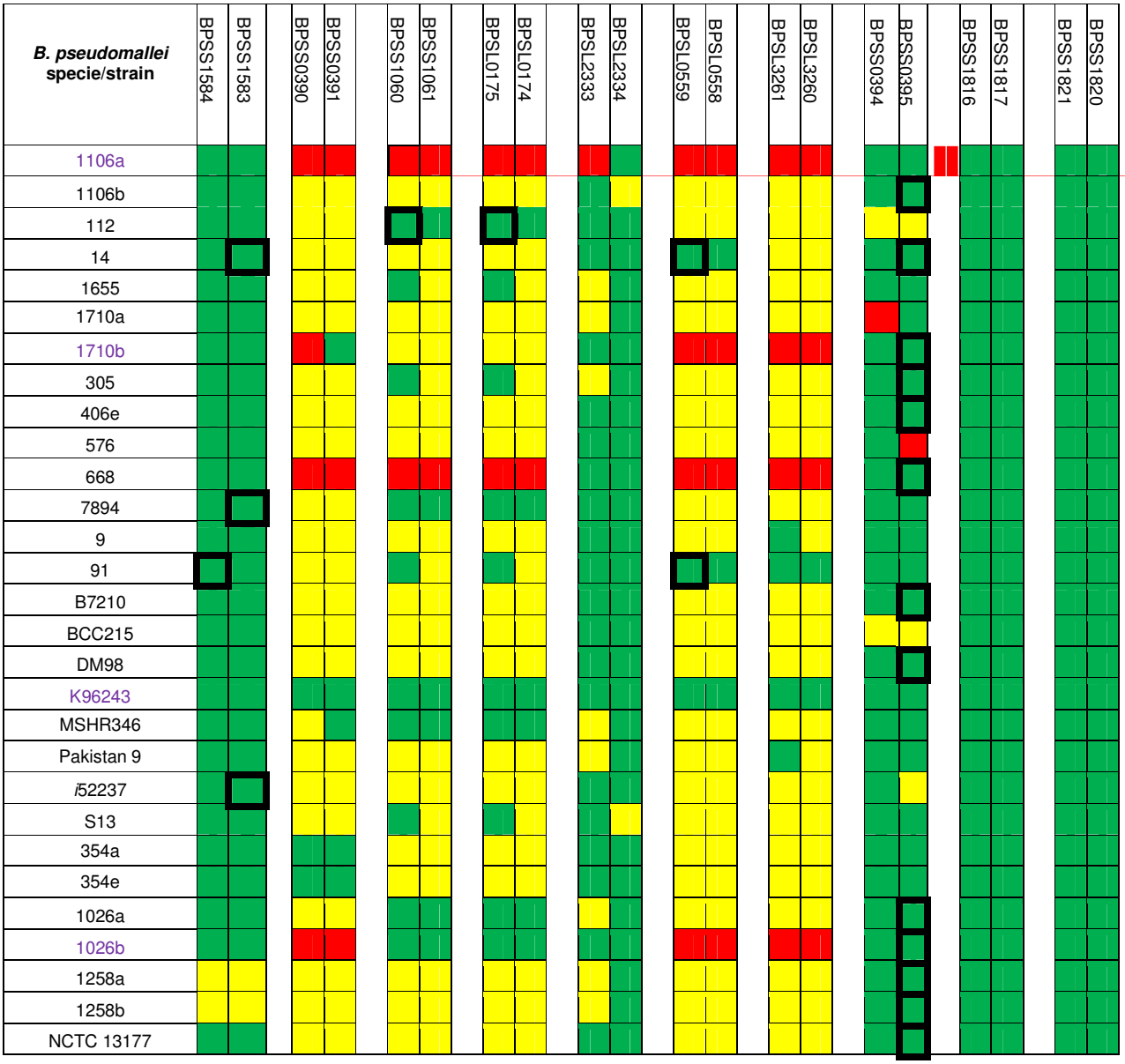

3.1.4 Genomic location of candidate *B. pseudomallei* K96243 TA genes

Many of the candidate TA genes are located on genomic islands, indels and phage elements. Of the 8 putative TA loci, 5 are located on genomic islands: BPSL0558-0559, BPSL0174-0175, BPSL3260-3261 BPSS1060-161 and BPSS0390-0391 (GI 3, GI 2, GI 11, GI 15 and GI 13 respectively), while the BPSS0395 gene is located on indel 11. BPSL0174-0175, BPSS1060-1061 and BPSS0390-0391 are also putative/ hypothetical phage related proteins. BPSS1060, BPSS0391, BPSL0559 and BPSL3260 are also present in *B. pseudomallei* strains associated with the clinical AGC clade. The genomic islands on which these genes are located are enriched in clinical strains of *B. pseudomallei* (Sim*, et al.*, 2008). 4 of the putative loci are located on chromosome 1 and 4 of the loci are located on chromosome 2 (figure 3.0).

3.1.5 Distribution of *B. pseudomallei* K96243 putative TA in *B. mallei* and *B. thailandensis*

A heat map was generated comparing predicted *B. pseudomallei* K96243 TA loci in *B. mallei* and *B. thailandensis* strains (table 3.4) .BPSL0558-559, BPSL3260-3261 and BPSS0394-395 were absent from all of the fully assembled sequences and all non fully assembled *B. mallei* and *B. thailandensis* strains with the exception of BPSS0394-0395 which was present in *B. thailandensis* E264. BPSL2333-2334 was absent from *B. mallei* but was present in 3 of the 4 *B. thailandensis* strains. BPSS1060-BPSS1061 was found in the majority of *B. mallei* and *B. thailandensis* strains with the exception of *B. thailandensis* E264 and *B. mallei* SAVP1. *B. mallei* ATCC 23344 and NCTC 10247 were also missing the BPSS1060 ortholog but contained a BPSS1061 ortholog. Only *B. thailandensis* E264 contained the BPSS0390-0391 locus, while *B. thailandensis* TXDOH contained BPSS0391, with

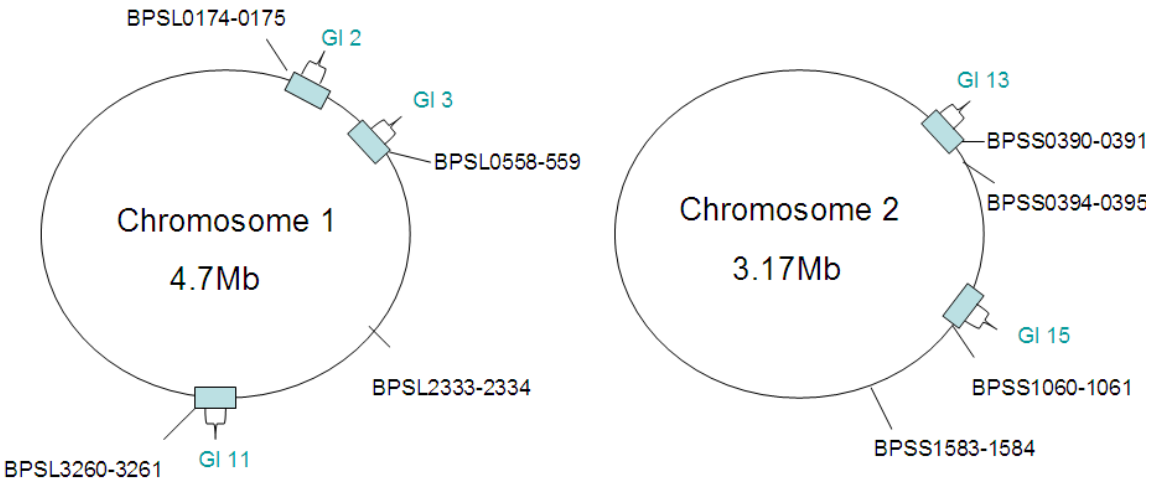

Figure 3.0 Genome location of the 8 putative TA loci and the genomic islands (GI) in which they are located in *B. pseudomallei* K96243.

both genes being completely absent from *B. mallei*. Lastly, it can be seen that the BPSS1583-1584 locus was present in all *B. mallei* strains except SAVP1. In *B. thailandensis* BPSS1583 orthologs were found in all the strains, however BPSS1584 was found only in the MSMB43 strain. In general more of the predicted *B. pseudomallei* TA gene loci appear to be conserved in *B. thailandensis* than *B. mallei.*

3.1.6 BLAST searching *B. pseudomallei* K96243 TA candidates

BLAST searching the amino acid sequences of the predicted *B. pseudomallei* K96243 TA candidate gene products against all accessible genomes on the NCBI website revealed some of the genes had sequence identity to members of previously reported TA families. Table 3.5 shows that BPSL0175, BPSS1060 and BPSL2333 had identity to the RNase toxin RelE, while BPSL2334 had sequence identity to the RelB antitoxin. BPSS1584 was annotated as HipA in the *B. pseudomallei* K96243 genome and subsequently shared identity with other HipA toxin members with BPSS1583 sharing sequence identity with HipB proteins. BPSL0559 also had sequence identity to a HipA toxin domain containing protein. BPSS0390 and BPSS0391 shared sequence identity to the HicAB system, while BPSL3260 had sequence identity to HigA. These data supported these candidate genes as likely members of TA systems and helped warrant further phenotypic validation.

Table 3.4. Heat map showing the distribution of the predicted *B. pseudomallei* K96243 TA genes in available *B. mallei* and *B. thailandensis* genome sequences. Paired genes are predicted TA modules. Strains in purple are those that have been fully assembled. Green indicates that an orthologous gene is present in that species, green with a thick border indicates a pseudogene, red shows there is no ortholog present and yellow shows no ortholog match but the genome for that strain is not fully assembled.

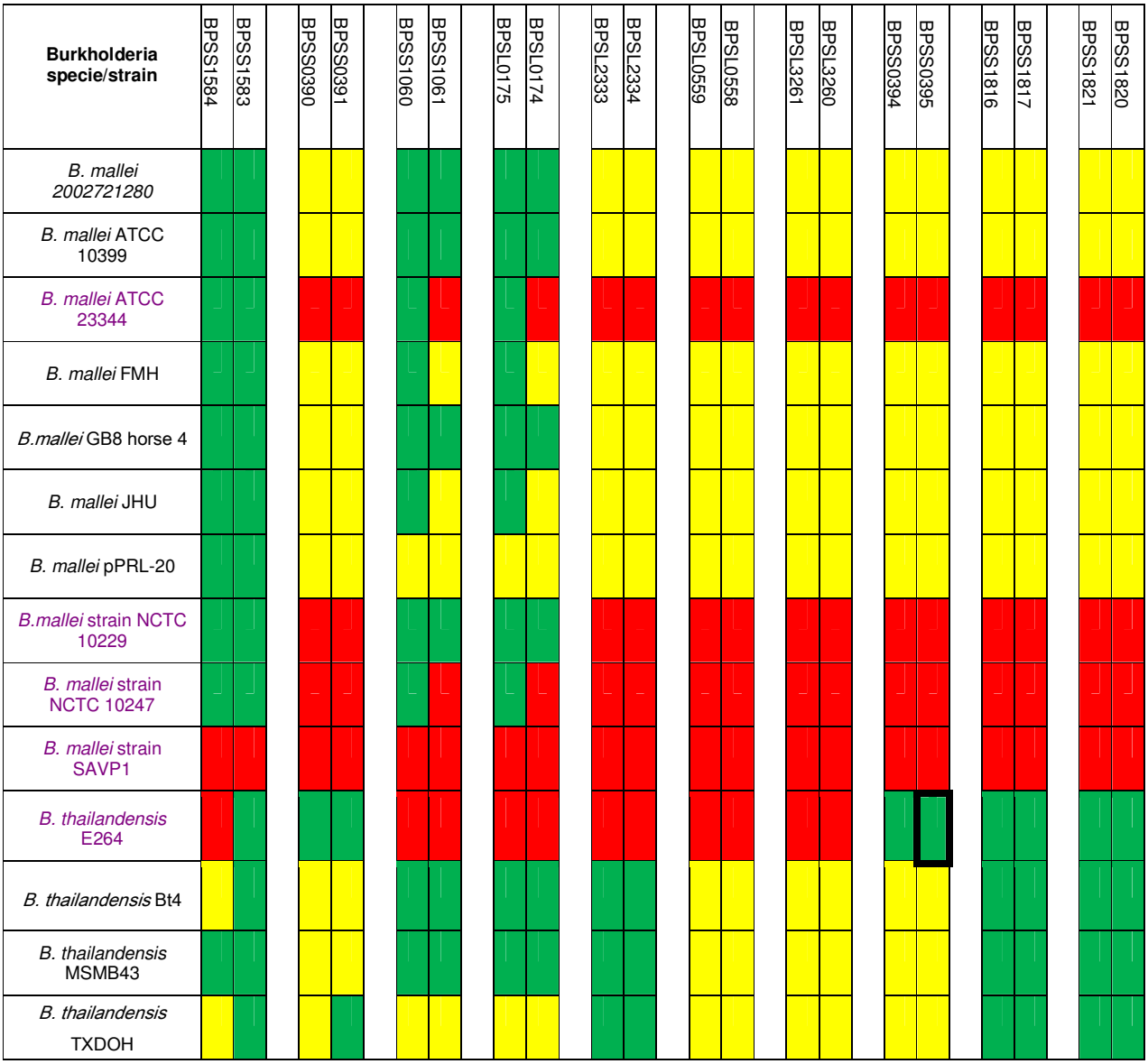

Table 3.5. A list of the putative *B. pseudomallei* K96243 TA genes and identity with previously reported toxin-antitoxin gene products. Homology was identified by BLASTp search. (-) indicates no homology.

Gene name	**Homology to known TA families**
BPSL0175	RelE toxin- 54% identity *Klebsiella pneumonia*
BPSL0174	-
BPSS1060	RelE toxin- 53% identity *Klebsiella pneumonia*
BPSS1061	-
BPSL0559	HipA toxin domain containing protein- 73% identity *Thiomonas intermedia* K12
BPSL0558	-
BPSL2333	RelE toxin- 62% identity *Variovorax paradoxus* S110
BPSL2334	RelB antitoxin- 40% identity *Escherichia coli* SMS-3-5
BPSS0390	HicA toxin-78% *Acinetobacter baumannii* ATCC 17978
BPSS0391	HicB antitoxin- 43% *Neisseria subflava* NJ9703
BPSS1584	HipA toxin- 100% *Burkholderia mallei* ATCC 23344
BPSS1583	HipB antitoxin domain containing protein- 92% *Burkholderia mallei* ATCC 23344
BPSS0395	-
BPSS0394	-
BPSL3261	-
BPSL3260	HigA antitoxin family protein- 51% *Bartonella taylorii* 8TBB

3.2 Microarray data

3.2.1 Growth phase data

To assess if any of the TA candidate genes were up-regulated during growth, they were searched against a microarray data set kindly provided by Patrick Tan at the Genome Institute of Singapore. The data listed up-regulated genes at 9 different growth phases categorised as early 1, early 2, log 1, log 2, log 3, log 4, stationary 1, stationary 2 and stationary 3 based on the predominant patterns of gene expression (Rodrigues, *et al.*, 2006). The predicted TA genes were searched for in all 9 growth phases. The data reveals that the BPSS1060 (RelE toxin family) gene was up-regulated during early log phase (log phase 1 in data set) and the BPSL2334 gene (RelB antitoxin family) was up-regulated in late log phase (log phase 4 in data set). The data also revealed up-regulation of BPSS1584 (HipA toxin family) during early stationary phase (stationary phase 1 in the data set). None of the other TA candidate genes showed up-regulation in any of the growth phases.

3.2.2 BALB/C mouse infection data.

The candidate TA genes were also searched for in a microarray data set generated by Claudia Hemsley. This data set compared up and down regulated genes from *B. pseudomallei* K96243 isolated from lungs of BALB/C mice 3 days after infection with 1000 CFU (acute melioidosis model) compared to growth of *B. pseudomallei* K96243 grown in LB. In this study BPSS1061 (RelB antitoxin family) was down regulated 0.5 fold in the mouse infection compared to LB. None of the other candidate TA genes were up or down regulated in this data set.

3.2.3 Hamster infection

Tuanyok *et al* previously infected hamsters by intraperitoneal and intranasal routes of infection. Transcriptional levels of *B. pseudomallei* expressed genes in infected organs including liver, lung, and spleen were compared to those from bacteria grown *in vitro* to generate microarray datasets (Tuanyok*, et al.*, 2006). Screening for the TA candidate genes in these data sets showed that none were significantly up or down regulated.

3.2.4 NaCl treatment

The candidate genes were also searched for in a microarray data set comparing gene regulation when *B. pseudomallei* was grown in standard LB (170 mM NaCl) compared to LB supplemented with high NaCl (320 mM) for 3 or 6 hours (Pumirat*, et al.*, 2010). None of the toxin-antitoxin genes were significantly up or down regulated under NaCl stress.

3.2.5 Macrophage infection

A data set comparing the gene expression profiles of *B. pseudomallei* K96243 following infection of human macrophage-like U937 cells compared to *in vitro* growth (Chieng, *et al.*, 2012), showed that BPSL0174 (RelB antitoxin family) was down regulated.

3.2.6 Growth in iron

Looking for the candidate TA genes in a microarray data set (Tuanyok, *et al.*, 2005) comparing gene expression of *B. pseudomallei* K96243 in response to growth in low

iron compared to high iron (200μM ferric chloride) revealed both the BPSS1584 (HipA toxin family) and BPSL2334 genes to be up regulated by 0.22 log.

3.3 Expression of putative *B. pseudomallei* toxin genes in *E. coli*

3.3.1 Expression of $hipA_{E.coli}$ in MG1655

For phenotypic characterisation studies, an expression system was developed for expressing candidate *B. pseudomallei* K96243 toxins in *E. coli* MG1655. The *E. coli* MG1655 *hipA* gene was first cloned into the pBAD/his vector under the control of the arabinose inducible promoter as a positive control for this expression system. Both a poly-histidine tagged and non-poly-histidine tagged version of the gene was cloned into the pBAD vector via *Sac*I and *EcoR*I restriction sites or *Nco*I and *EcoR*I sites respectively (figure 3.1). Constructs were checked by sequencing. Firstly, the non tagged pBAD-*hipA* construct was transformed into *E. coli* MG1655. To test the functionality of the cloned gene, cultures were grown in LB supplemented with ampicillin and when the culture had reached the early log phase (OD_{590}nm approximately 0.2) either 0.2% (w/v) glucose (to repress expression) or 0.2% (w/v) arabinose (to induce expression) was added to the culture. The optical density (OD_{590}nm) was then measured every hour for 3 hours to assess the affect of expression on cell density. Figure 3.2 shows the result of *hipA* expression. The graph shows that after 3 hours in either glucose or arabinose, cultures reach a similar optical density. It was hypothesised that the lack of phenotype could either be due to an expression issue or endogenous HipB sequestering the expressed HipA protein.

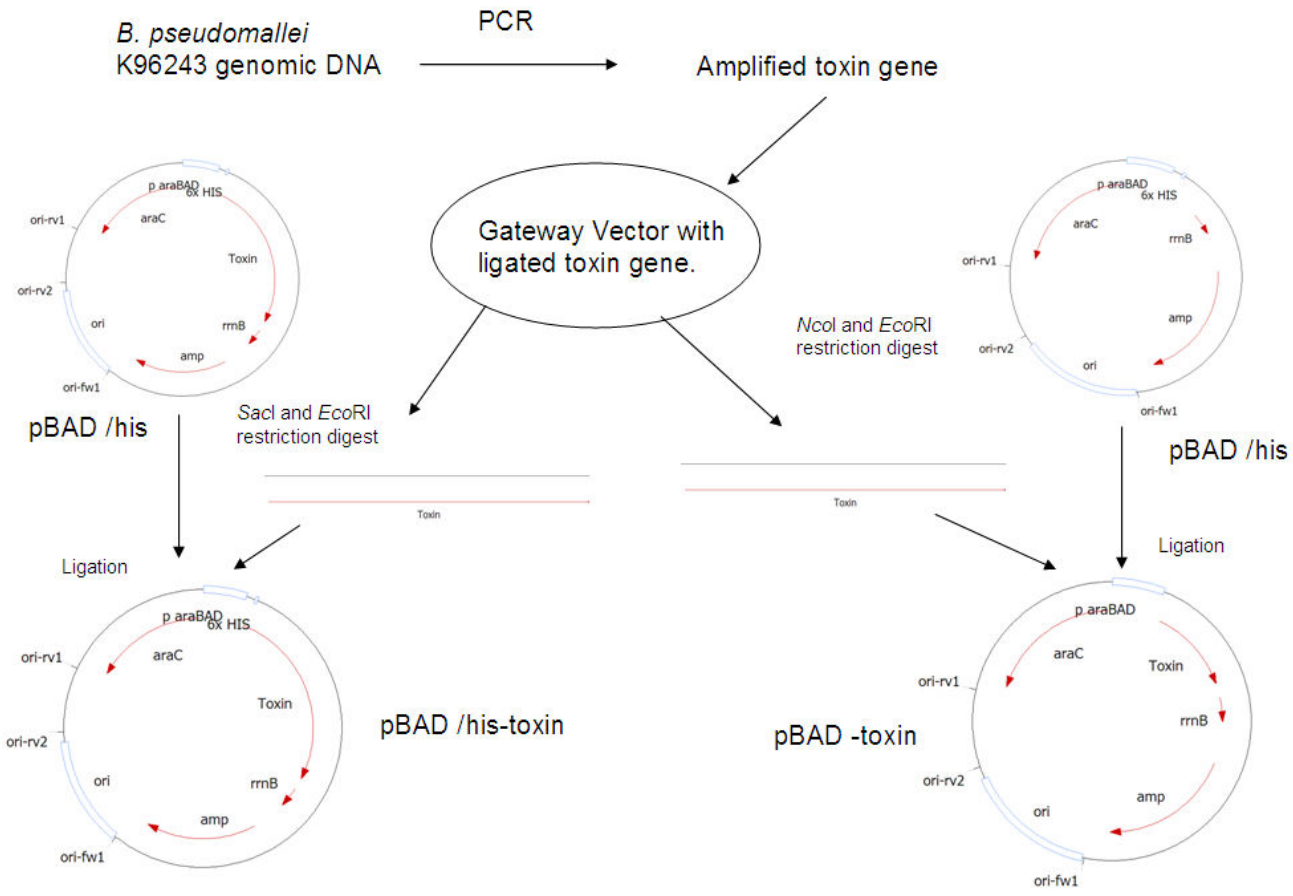

Figure 3.1 Generation of the pBAD expression constructs with cloned toxin. *B. pseudomallei* K96243 DNA (or *E. coli* MG1655 for *E. coli hipA* cloning) was used as template DNA for PCR. Amplified PCR products using primers containing either *Sac*I or *Nco*I (forward primers) or *Eco*R1 (reverse primers) were cloned into TOPO or PGEM-T-Easy gateway vectors. The toxin genes were then restriction digested from the gateway vector using the appropriate restriction enzymes and cloned into restriction digested pBAD/his vector to create pBAD/his-toxin or pBAD-toxin constructs.

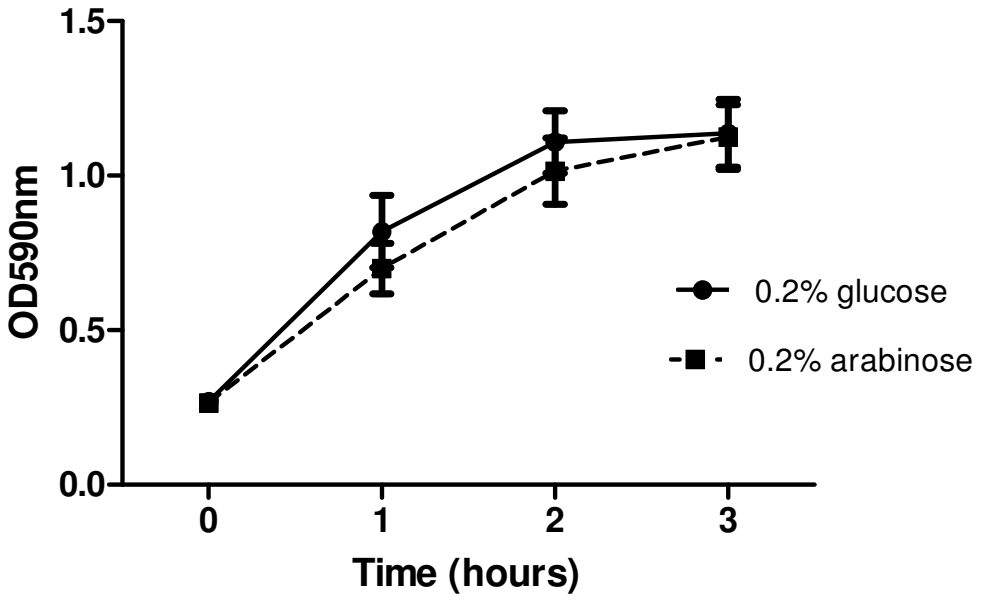

Figure 3.2 Expression of the *E. coli hipA* gene from the arabinose inducible pBAD plasmid in *E. coli* MG1655. Cultures were grown to early log phase (OD_{590}nm ~0.2) before inducing expression with 0.2% (w/v) arabinose or repressing expression with 0.2% (w/v) glucose. The OD was measured every hour for 3 hours. The data is the average of 3 biological replicates and error bars show SEM.

3.3.2 Expression of *hipA and hipA*-his tag in *E .coli* MG1655 *ΔhipBA*

3.3.2.1 Creating Δ*hipBA::Cm*^{R}

To address the lack of phenotype when expressing *hipA* in MG1655, a *ΔhipBA::Cm*^{R} mutant of *E. coli* MG1655 was constructed using the Wanner mutagenesis method (figure 3.3). A PCR generated knockout cassette was electroporated into *E. coli* MG1655 for recombination and insertional inactivation of the *hipBA* locus.

Inactivation of *hipBA* was confirmed by PCR with flanking region primers and plating onto LB agar plates supplemented with 50 μg/ml chloramphenicol.

Figure 3.4 shows the resulting DNA agarose gel confirming the deletion as the 2.3kbp HipBA locus had been replaced with a subsequent 1.5kbp fragment, which corresponded to the size of the antibiotic resistance cassette.

3.3.2.2 Expression of the pBAD-his-*hipA* and pBAD-*hipA* constructs in *E. coli* MG1655 Δ*hipBA::Cm*^{R}

Following creation of the Δ*hipBA::Cm*^{R} mutant the pBAD/his-*hipA* and pBAD-*hipA* constructs were independently transformed into calcium competent *E. coli ΔhipBA::Cm*^{R} cells by heat shock transformation at 42^{o}C and plated onto LB agar plates containing ampicillin for plasmid selection. Approximately 50-100 transformants were obtained for each strain. Selected colonies were grown in LB in the presence of ampicillin and expression was repressed or induced as described for *hipA* expression in MG1655.

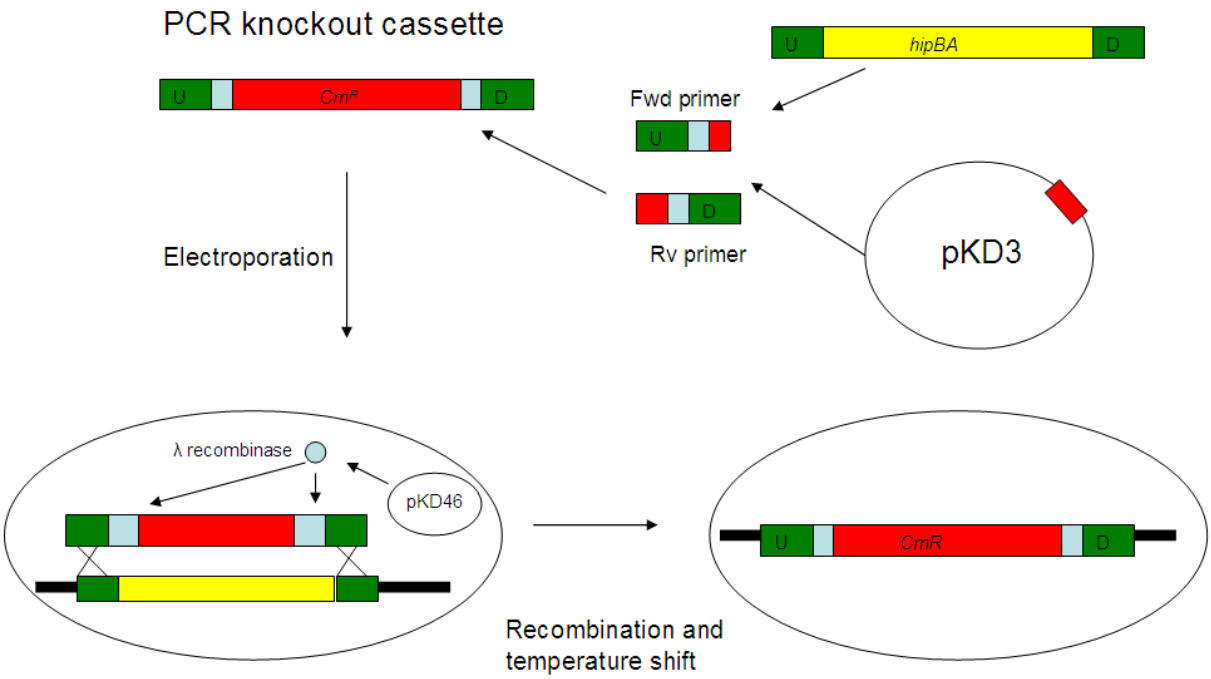

Figure 3.3 Schematic for the Wanner mutagenesis method used for insertional inactivation of the *hipBA* locus. A knockout cassette was created by PCR that contained homology to upstream and downstream regions of the *hipBA* locus, flippase recognition sites and the chloramphenicol resistance gene. The pKD3 plasmid was used as template DNA to amplify the chloramphenicol resistance cassette. The knockout cassette was electroporated into *E. coli* MG1655 cells harbouring the arabinose inducible pKD46 plasmid encoding a λ recombinase for recombination. Cells were grown at 30^0C with 5 mM IPTG for recombination before shifting to 37 ^{o}C to remove the pKD46 plasmid.

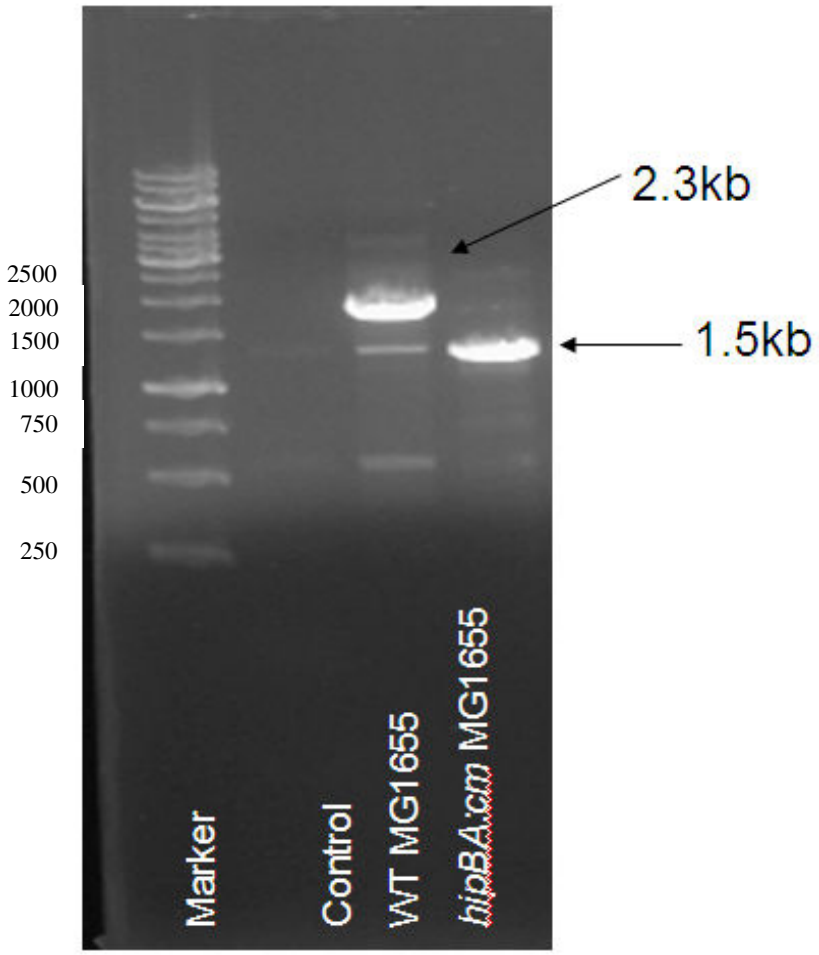

Figure 3.4 0.5% (w/v) agarose gel stained with ethidium bromide to reveal the presence of amplified PCR products. The marker is a 1kbp ladder from Fermentas and 5 µl of each sample was mixed with 1 µl of 6x loading dye before loading to the gel. The control well was a PCR with no template DNA, while the MG1655 lane was a sample of the resulting PCR containing genomic MG1655 DNA and the *hipBA:cm* lane was a sample of the resulting PCR containing isolated genomic DNA from a predicted *ΔhipBA:cm*^{R} mutant culture. The wild type band gives the predicted 2.3kbp fragment, while the mutant gives the predicted 1.5kbp fragment. The gel was run at 100mV for 30 minutes in TAE buffer.

Figure 3.5 shows the resulting growth profile for the 2 strains. 1 hour after induction of *hipA* there was a marked reduction in the rate of increase in optical density compared to the glucose repressed control (figure 3.5A). When expression of the N-terminally tagged *hipA* gene was induced or repressed there was no difference in optical density of the culture (figure 3.5B). This could indicate that the histidine tag interferes with the activity of the HipA toxin.

3.3.3 Expression of the 8 putative *B. pseudomallei* K96243 toxin genes in MG1655

The 8 candidate *B. pseudomallei* K96243 toxin genes were next cloned into the pBAD/his vector (figure 3.1). To decipher which of the genes of the putative TA loci was the toxin component, homology to other genes of known TA families (indicated in Table 3.6) was considered. For the BPSS0394-0395 locus, as there was no sequence homology for either gene, the BPSS0395 gene was considered the toxin since it was downstream of BPSS0394, which is the usual genetic layout of TA systems. The amplified genes were cloned via the *Nco*I and *Eco*RI restriction sites of pBAD/his to generate tag-less cloned gene constructs and then transformed into *E. coli* MG1655 for expression. Cultures were grown to early log phase before switching on expression of the cloned *B. pseudomallei* gene with 0.2% (w/v) arabinose or switching off with 0.2% (w/v) glucose.

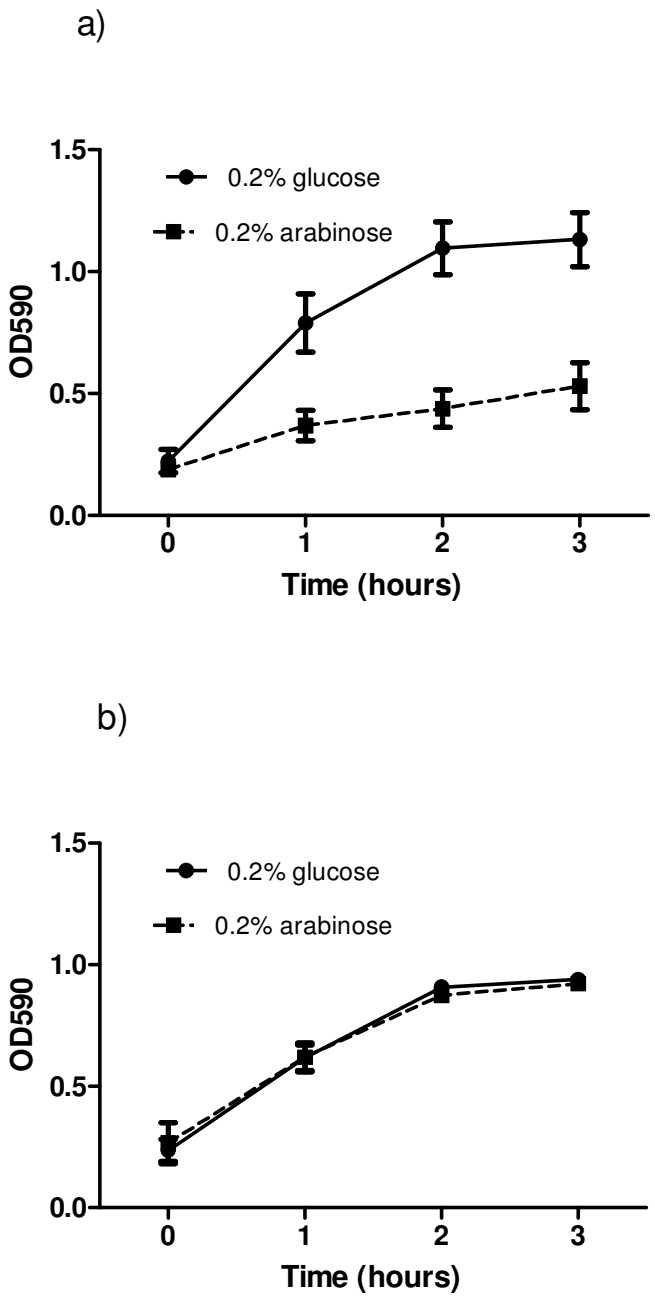

Figure 3.5 Expression of *E. coli hipA* in *E. coli ΔhipBA* and the effect on optical density of the culture. a) Expression of the non tagged version of the protein. b.) Expression of an N-terminal polyhis tagged version of the protein. Cultures were grown to early log phase (OD_{590}nm ~0.2) before inducing expression with 0.2% (w/v) arabinose or repressing expression with 0.2% (w/v) glucose. The OD was measured every hour for 3 hours. The data is the average of 3 biological replicates and error bars show SEM.

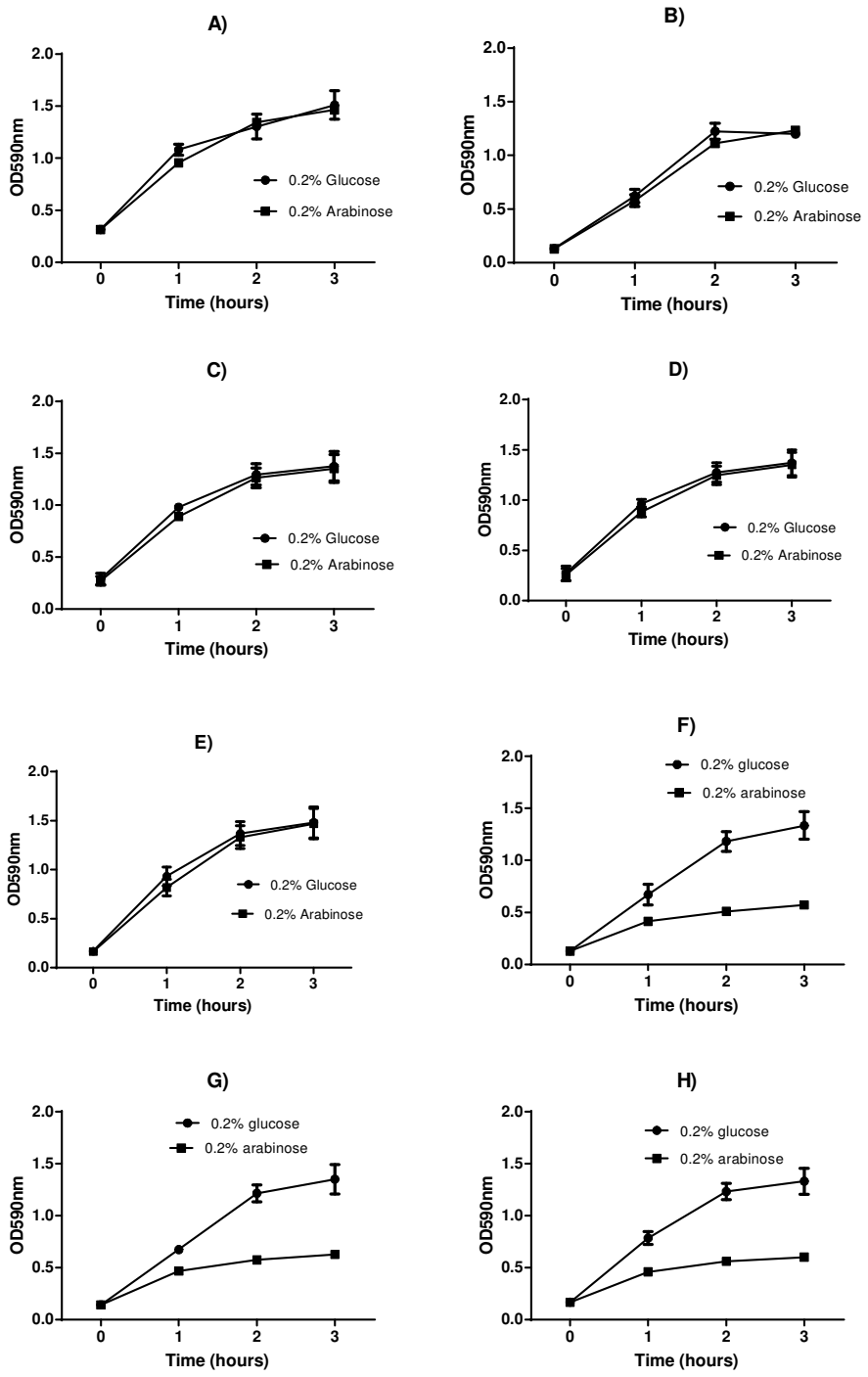

Figure 3.6 The OD_{590}nm growth profiles of the 8 putative TA toxins cloned into the pBAD vector and expressed in *E. coli* MG1655 A) BPSS1584 B) BPSS0395 C) BPSS0559 D) BPSL2333 E) BPSL3261 F) BPSS1060 G) BPSS0390 H) BPSL0175. Cultures were grown to early log phase (OD_{590}nm ~0.2) before inducing expression with 0.2% (w/v) arabionse or repressing expression with 0.2% (w/v) glucose. The optical density was measured every hour for 3 hours. The data shown is the average of 3 biological repeats. Error bars show SEM.

The optical density of the cultures was measured every hour for 3 hours and the resulting growth profile for each of the *E. coli* harbouring different toxin-encoding genes is shown in figure 3.6. When glucose was added to the strains they all grew in a similar manner. In contrast the addition of arabinose resulted in a reduced growth rate of *E. coli* harbouring BPSS1060, BPSS0390 or BPSL0175 (figures 3.5 F, G and H respectively). Expression of BPSS1584, BPSS0395, BPSL0559, BPSL2333 and BPSL3261 had no effect on bacterial growth.

3.3.4 Monitoring CFU following induction of BPSS1060, BPSL0175 and BPSS0390

As expression of BPSS1060, BPSL0175 or BPSS0390 all had an effect on OD compared to the corresponding glucose-repressed control, the number of colony forming units (CFU) was measured following expression to determine if the reduced rate of OD increase was due to a difference in cell numbers. The experimental procedures were followed as described above, except that rather than taking OD measurements, samples were removed and serially diluted in a 96-well plate in LB and relevant dilutions were plated onto LB amp plates for CFU determination the following day. Figure 3.7 shows the CFU profiles following expression of the 3 genes. Addition of glucose to repress expression allowed for continued growth depicted by the increase in CFU for all 3 of the genes. Addition of arabinose to induce expression of the cloned gene resulted in 2 distinct phenotypes. Following induction of BPSS1060 and BPSL0175 expression (fig 3.7A and B respectively) the CFU continued to increase for the first hour and then remained constant for the following 2 hours of the experiment. However, following induction of BPSS0390 expression (fig 3.7C) the CFU count decreased by approximately 10,000 fold over the 3 hour period,

with an approximately 10 fold decrease in the first and third hours and 100 fold in the second hour.

3.3.5 Colony size following BPSS1060, BPSL0175 and BPSS0390 expression

In addition to affecting optical density and CFU numbers when expressing the BPSS1060, BPSL0175 and BPSS0390 toxins in *E. coli*, the size of the colonies on agar plates were smaller following overnight incubation at 37 ^{o}C compared to uninduced controls. Figure 3.8 shows plates inoculated with *E. coli* pBAD-BPSS0390 or *E. coli* pBAD-BPSL0175. When BPSS0390 expression was repressed in MG1655 for 2 hours, plated and then incubated overnight for 16 hours, colonies were large (Fig 3.7A). In comparison, if BPSS0390 or BPLS0175 were expressed for 2 hours, plated and incubated overnight for 16 hours then the colonies appeared smaller and of variable size (Fig 3.8B and C). This indicates that toxin induction either caused cells to become very slow growing, forming smaller colonies on agar, or alternatively, cells had entered into a dormant state and on plating cells re-awaken at different rates to give different sized colonies.

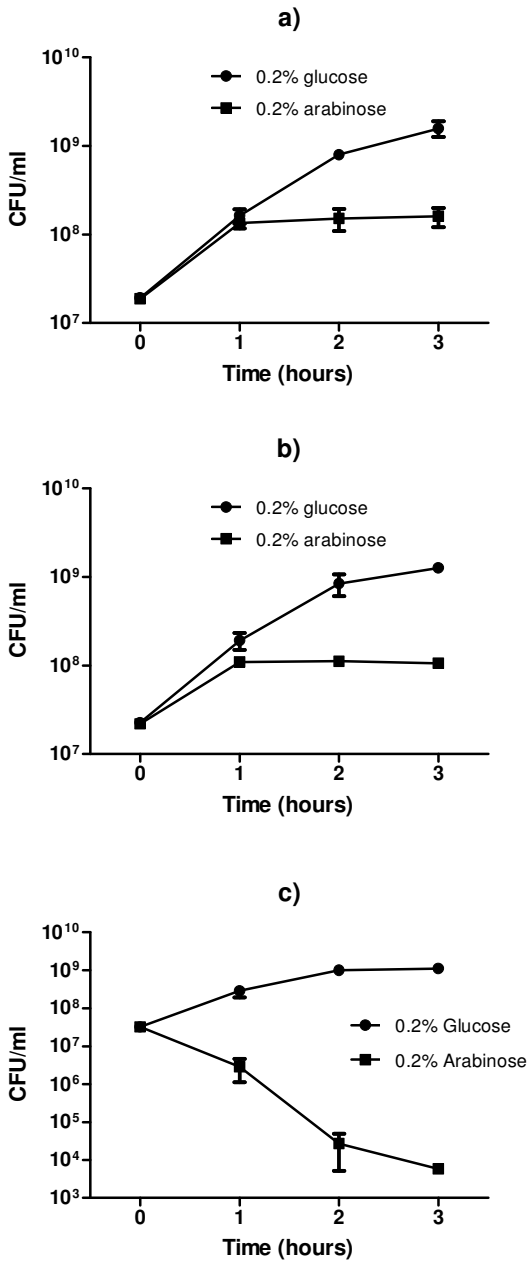

Figure 3.7 Effect of toxin expression on culturability. Enumeration of *E. coli* MG1655 harbouring plasmid-cloned BPSS1060 (A), BPSL0175 (B) or BPSS0390 (C) monitoring culturable cells (CFU). Toxin expression was repressed or induced by adding 0.2% (w/v) glucose or arabinose respectively to cultures at T0. Data is the average of 3 biological repeats and error bars show the SEM.

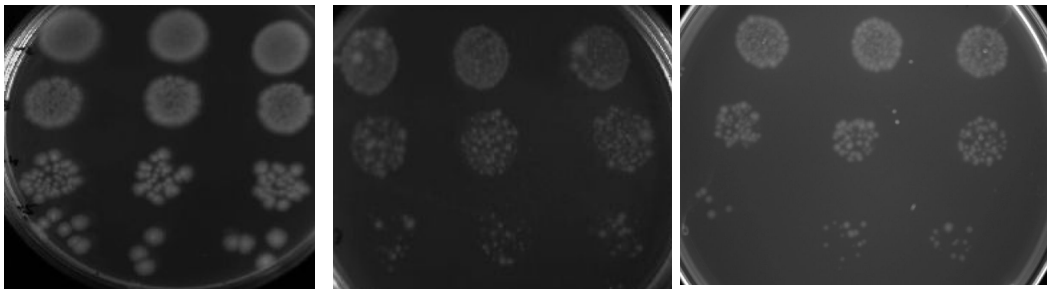

Figure 3.8 Size of *E. coli* MG1655 pBAD-BPSSS0390 or BPSL0175 colonies following repression or expression of toxin, with 0.2% (w/v) glucose or 0.2% (w/v) arabinose respectively for 2 hours. Cultures were plated on LB agar 100 μg/ml ampicillin plates and incubation at 37 ^{o}C for 16 hours. A) Repression of BPSS0390 toxin B) Expression of BPSS0390 toxin. C) Expression of BPLS0175 toxin.

3.3.6 Screening for homologs of the putative K6343 TA genes in *E. coli* MG1655

It was hypothesised that the failure of 5 of the 8 putative TA toxins (BPSS1584, BPSL0559, BPSL2333, BPSL3261 and BPSS0395) to give a growth restricted phenotype may be due to the presence of chromosomally encoded antitoxins sequestering the activity of the ectopically expressed toxin protein. The protein sequences for BPSL2333-2334, BPSL0559-0558, BPSL3260-3261, BPSS0394-0395 and BPSS1583-1584 were BLASTp searched against the *E. coli* MG1655 predicted proteome to identify any homologous proteins that may account for the lack of phenotype. The search did not identify any significant matches for 4 of the TA loci but a significant match was found for the BPSS1583 and BPSS1584 genes. The *E .coli* MG1655 *hipBA* locus encodes proteins with sequence homology of 40% and 33% to BPSS1584 and BPSS1583 respectively. As a result of this search it was decided to re-test the toxic nature of BPSS1584 in an *E. coli ΔhipBA* strain.

3.3.7 Expression of BPSS1584 in *E. coli* MG1655 Δ*hipBA*

To test for a growth inhibition phenotype the pBAD-BPSS1584 construct was transformed into *E. coli* Δ*hipBA* and the OD_{590}nm was measured and the CFU count determined following subsequent expression or repression of the toxin. Fig 3.9A shows that with this strain the OD was affected by expression of the toxin (similar to *E. coli hipA* expression in *E. coli* Δ*hipBA,* fig 3.5A) i.e. the increase in the OD was reduced compared to the glucose repressed control. When looking at CFU (Fig 3.9B) the phenotype observed was similar to that seen when BPSS0390 was expressed. Over the 3 hour experiment cell numbers dropped by approximately 10,000 fold compared to the input while the glucose repressed control increased in CFU over the same duration.

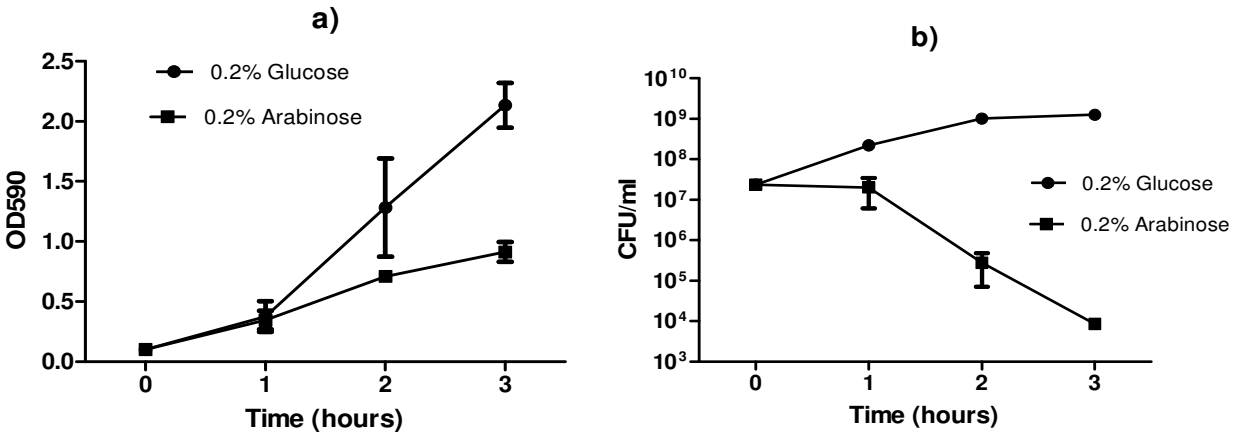

Figure 3.9 Effect of BPSS1584 expression on *E. coli* MG1655 *ΔhipBA* growth and culturabilty. a.) OD_{590}nm growth profile following induction or repression of the cloned toxin gene with 0.2% (w/v) arabinose or glucose respectively over 3 hours. b.) Monitoring the number of culturable cells (CFU) every hour for 3 hours following induction or repression.

3.4 Expression of partner antitoxin genes.

3.4.1 Co-expression of toxin and antitoxin partner gene

Type II TA systems identified to date involve a toxin and antitoxin that bind together to form an inactive complex. Next, the cognate antitoxins for BPSL0175, BPSS0390 and BPSS1584 were cloned into the IPTG inducible vector pME6032 (figure 3.10). As BPSS1060-1061 and BPSL0175-0174 loci are paralogs with 98% identity, it was assumed that if BPSL0174 demonstrated an antitoxin phenotype then so too would BPSS1061 and therefore it was not cloned.

The 3 antitoxin genes were PCR amplified and cloned into the pME6032 vector via the *Sac*I and *Nco*I restriction sites. The sequences of the cloned inserts were determined by sequencing before transforming into a calcium competent strain of *E. coli* MG1655 containing the corresponding pBAD-toxin constructs. PME6032-BPSS1583 was transformed into calcium competent *E. coli* MG1655 *ΔhipBA* containing pBAD-BPSS1584 rather than wild type *E. coli* MG1655. Transformants were selected by plating on LB plates supplemented with ampicillin and tetracycline.

To test the ability of the cognate antitoxins to sequester the activity of the toxins, cultures were grown to early log phase before addition of 0.2% (w/v) glucose to repress expression of the toxin or 0.2% (w/v) glucose and 25 mM IPTG to repress toxin expression but allow antitoxin expression, or 0.2% (w/v) arabinose for toxin expression, or 0.2% (w/v) arabinose and 25 mM IPTG for toxin and antitoxin expression. For all strains, expression of only the putative antitoxin had no effect on CFU, as numbers were comparable to the glucose only control (figure 3.11A-C). Induction of BPSL0175 expression allowed for an increase in CFU by approximately 5 fold over the 2 hours but this was significantly less of an increase than the glucose

control. However, co-expression of the BPSL0175 toxin with the BPSL0174 gene was able to significantly restore growth to numbers comparable to the glucose control ($p<0.01$ student's t-test) (fig 3.11A).

BPSS0390 expression also reduced the CFU over the 2 hour period by approximately 500 fold (fig 3.11B). Co-expression of the BPSS0390 toxin with the BPSS0391 antitoxin permitted growth to similar levels as the glucose control. The difference in the CFU change between co-expression of BPSS0390 and BPSS0391 with BPSS0390 expression alone was significant ($p<0.05$ student's t-test). A similar reduction in CFU was observed when expressing the BPSS1584 gene in the Δ*hipBA* background. Although co-expression with BPSS1583 was able to significantly block toxicity of BPSS1584 preventing the reduction in CFU ($p<0.05$, student's t-test), the CFU fold change was also significantly reduced compared to glucose repressed conditions ($p<0.001$, student's t-test) (Fig 3.11C). In summary, co-expression of BPSS1584 and BPSS1583 prevented the reduction in CFU but was not able to restore cell growth.

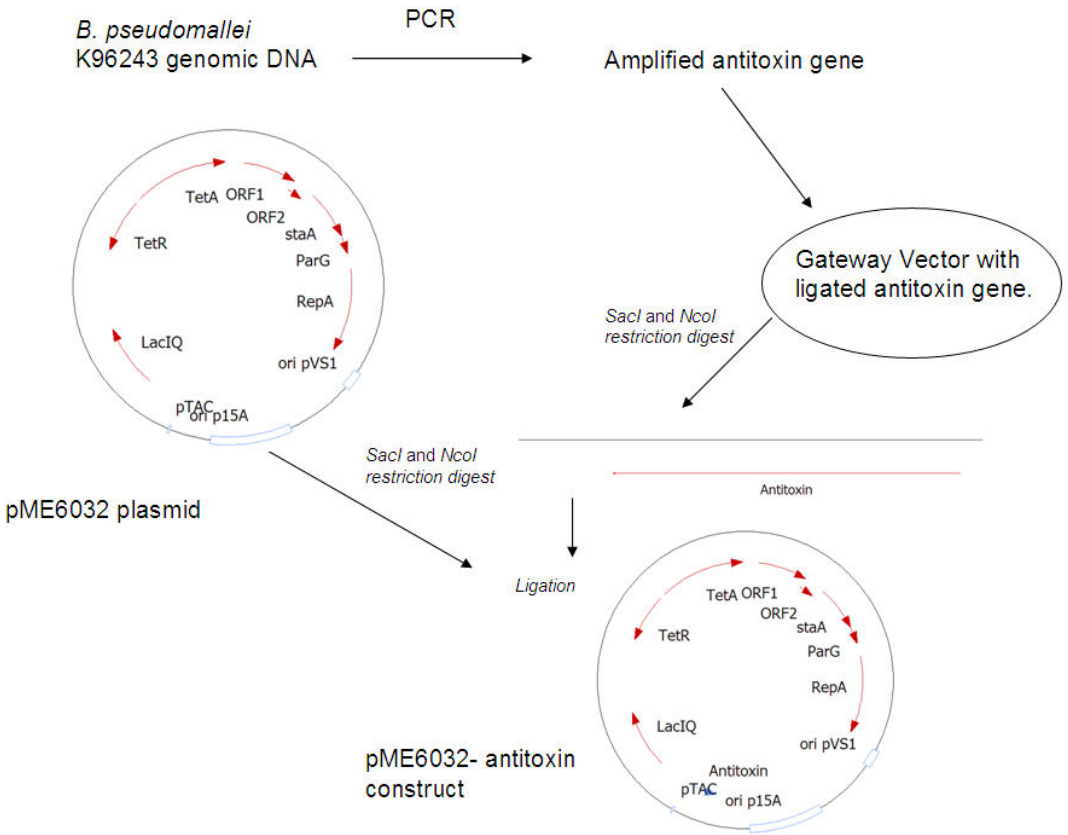

Figure 3.10 Generation of the pME6032 expression constructs with cloned antitoxin. *B. pseudomallei* K96243 DNA was used as template DNA for PCR. PCR products amplified using primers containing a *Sac*I restriction site (forward primers) or *Nco*I restriction site (reverse primers) were cloned into TOPO or PGEM-T-Easy gateway vectors. The antitoxin genes were then restriction digested from the gateway vector using the appropriate restriction enzymes and cloned into restriction digested pME6032 vector to create pME6032-antitoxin constructs.

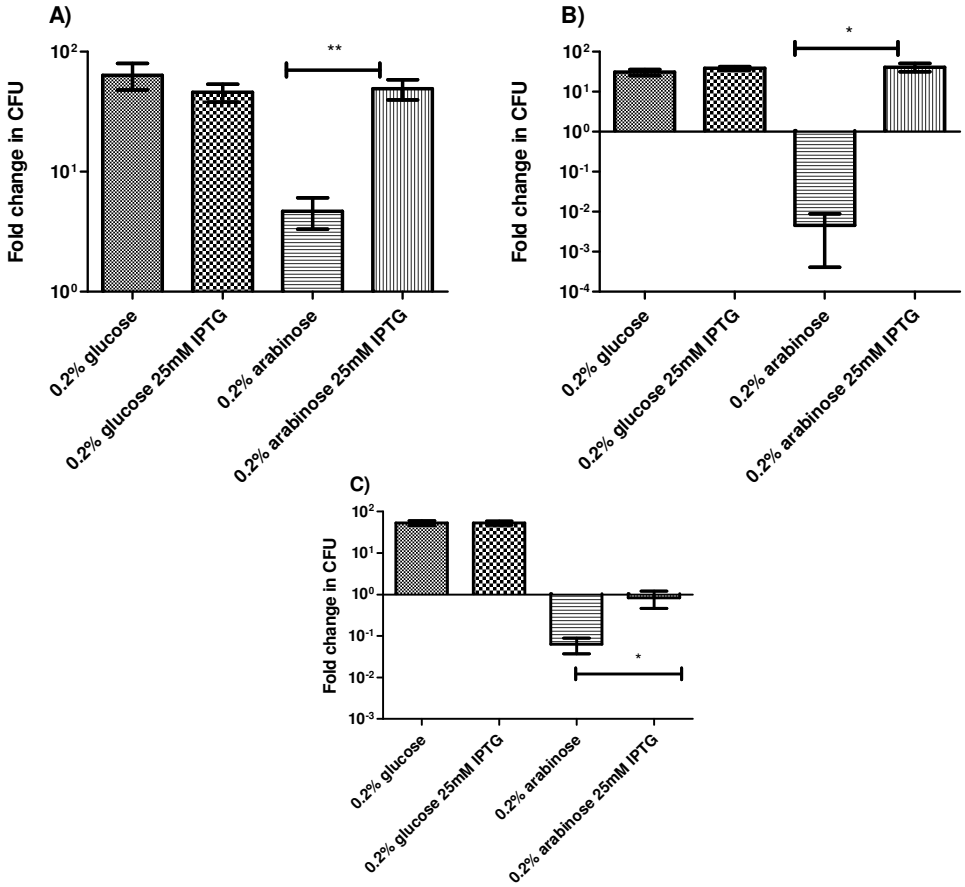

Figure 3.11 Co-expression of cognate toxin and antitoxin pairs. Change in the number of culturable cells (CFU) of *E. coli* MG1655 harbouring A) plasmid-cloned toxin (BPSL0175) and the cognate plasmid-cloned antitoxin (BPSL0174); B) plasmid-cloned toxin (BPSS0390) and the cognate plasmid-cloned antitoxin (BPSS0391); C) *E. coli* MG1655 *ΔhipBA* harbouring plasmid-cloned toxin (BPSS1584) and the cognate plasmid-cloned antitoxin (BPSS1583). The results shown are the fold change in number of culturable bacteria 2 hours after inducing expression of toxin, antitoxin, or both with 0.2% (w/v) arabinose, 25 mM IPTG or 0.2% (w/v) arabinose and 25 mM IPTG, respectively. 0.2% (w/v) glucose was added to control cultures. Data shown are the mean of 3 biological repeats and error bars show SEM. *= $p<0.05$ for an unpaired 2-tailed student's t-test. **= $p<0.01$.

3.4.2 Co-expression of different toxin and antitoxin families

3.4.2.1 Co-expression of BPSS0390 and BPSL0174

Next it was determined whether the rescue phenotype achieved by co-expressing the cognate antitoxin was toxin-specific, or whether an antitoxin from a different family can also rescue toxicity. To test this, the pME6032-BPSL0174 construct was transformed into *E. coli* MG1655 containing pBAD-BPSS0390 for co-expression of BPSS0390 (HicA) with BPSL0174 (RelB). Toxin expression was induced with 0.2% (w/v) arabinose and antitoxin expression was induced with 25 mM IPTG. Repression of BPSS0390 and BPSL0174 or expression of BPSL0174 only resulted in an increase in CFU (Figure 3.12). BPSS0390 expression alone resulted in approximately 500 fold reduction in CFU. Surprisingly, co-expression of BPSL0174 with BPSS0390 was able to rescue the toxic phenotype and the CFU fold change was similar to the controls.

3.4.3 Resuscitation of growth by antitoxin expression following a period of toxin expression

As all of the putative cognate antitoxins had the ability to significantly block the activity of their toxin partner when co-expressed, it was next determined whether antitoxin expression could rescue growth after a period of toxin-induced growth arrest. Expression of BPSS0390 by the addition of arabinose reduced the number of CFU by approximately 1000 fold over the first 2 hours and the CFU count continued to decrease slightly over the next 2 hours. However, if after 2 hours IPTG was added to induce BPSS0391 expression, the number of culturable bacteria was restored to a level similar to the start of the experiment over a subsequent 2 hour period (figure

3.13A). If glucose alone was added or IPTG post a period of glucose repression then normal cell growth occurred in all of the experiments (fig 3.13A-D).

Next a similar experiment was performed with BPSL0175 and BPSL0174 (fig 3.13B). BPSL0175 expression for 2 hours had an inhibitory effect on cell growth. However, addition of IPTG to induce BPSL0174 expression was unable to reactivate growth over the next 2 hours. It was hypothesised that perhaps washing away the arabinose to no longer induce expression of BPSL0175 toxin before the addition of IPTG for BPSL0174 induction may enhance recovery of growth. Figure 3.13C shows that under these conditions cell numbers did indeed increase following BPSL0174 expression.

The adapted method that involved a wash step was then utilised to test the ability of BPSS1583 to recover culturability of BPSS1584 expressing cells (figure 3.13D). When cells were washed to remove arabinose before adding IPTG, cells were able to re-grow to levels of approximately 10 fold higher than that at the start of the experiment. Interestingly, between 2 and 4 hours of BPSS1584 expression only, CFU also increased to levels comparable with the start of the experiment.

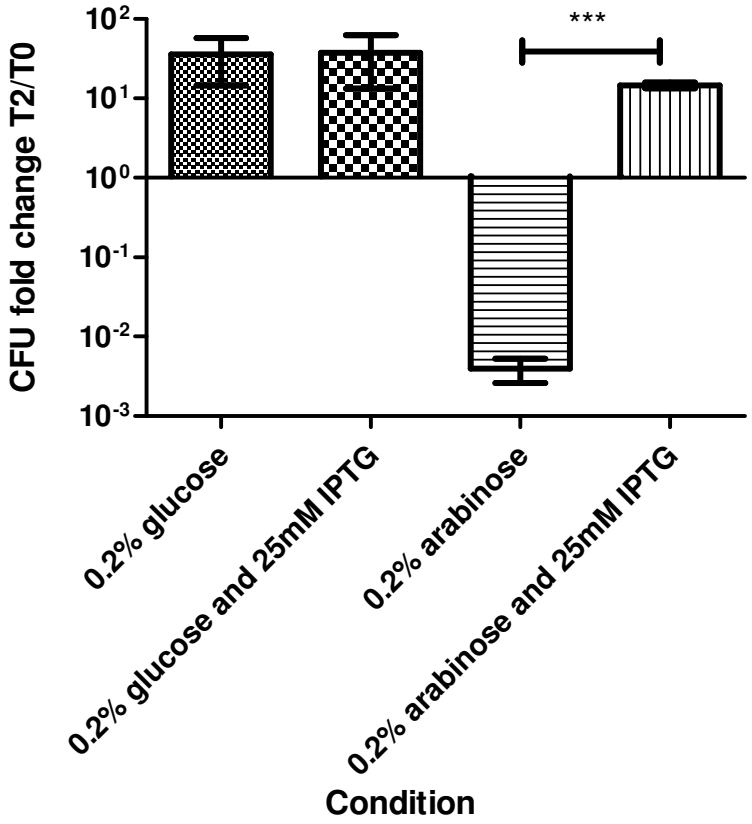

Figure 3.12 Co-expression of *E. coli* MG1655 harbouring pBAD cloned BPSS0390 and pME6032 cloned BPSL0174. The results shown are the fold change in number of culturable bacteria 2 hours after inducing expression of toxin, antitoxin, or both with 0.2% (w/v) arabinose, 25 mM IPTG or 0.2% (w/v) arabinose and 25 mM IPTG, respectively. 0.2% (w/v) glucose was added to control cultures. Data shown are the mean of 3 biological repeats. Error bars show SEM. ***=$p<0.001$ for an unpaired 2-tailed student's t-test.

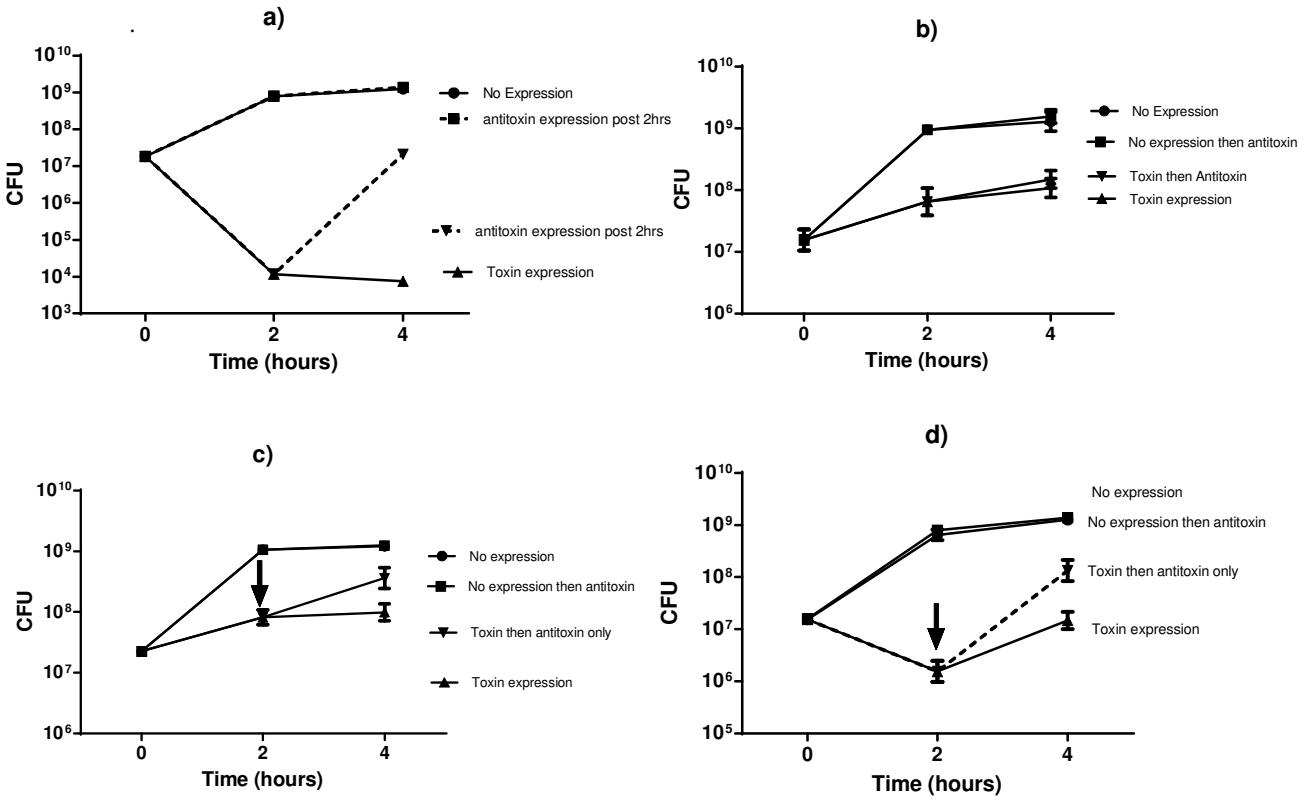

Figure 3.13 Resuscitation by antitoxin. *E. coli* MG1655 culturable cells (CFU) were enumerated at the time shown. A) BPSS0390 (toxin) expression was induced with 0.2% (w/v) arabinose and 2 hours later BPSS0391 (antitoxin) expression was induced with 25 mM IPTG. B) BPSL0175 (toxin) expression was induced with 0.2% (w/v) arabinose and 2 hours later BPSL0174 (antitoxin) expression was induced with 25 mM IPTG. C) BPSL0175 (toxin) expression was induced with 0.2% (w/v) arabinose and 2 hours later the cells were washed, re-suspended in fresh medium and BPSL0174 (antitoxin) expression was induced with 25 mM IPTG. D) BPSS1584 (toxin) expression was induced with 0.2% (w/v) arabinose and 2 hours later the cells were washed in fresh medium and BPSS1583 (antitoxin) expression was induced with 25 mM IPTG. Arrows indicate wash steps. 0.2% (w/v) glucose only (for repression) and 0.2% (w/v) glucose for 2 hours followed by 25 mM IPTG for 2 hours (repression followed by antitoxin expression) were set up as controls for all experiments The data shown are the average of 3 biological repeats and error bars show SEM.

3.5 Discussion

A range of methods have been proposed for the identification of TA systems. Some groups have identified candidate TA systems using programmes such as RASTA (Sevin & Barloy-Hubler, 2007, Goulard*, et al.*, 2010). However, Ramage *et al* have reported some limitations with the ability of this software to identify TA loci (Ramage*, et al.*, 2009). The software also had limitations in this study and although RASTA successfully predicted TA genes characterised in *E. coli,* it failed to predict the BPSS1060-1061 and BPSL0175-174 loci in *B. pseudomallei* K96243 as being significant candidates for subsequent expression despite proving functionally active in the experimental validation. As all of the bioinformatic screens are only predictions, confirmation that these TA systems are functional requires experimental validation. One approach might be to assess the phenotype of TA system deletion mutants. However, a number of workers have now reported that the inactivation of individual TA systems in *E. coli* does not provide an obvious phenotype (Shah*, et al.*, 2006, Tsilibaris*, et al.*, 2007) possibly because of redundancy of TA systems (Tsilibaris*, et al.*, 2007). Indeed, there is now evidence that the inactivation of multiple TA systems is required to reveal clear phenotypes (Maisonneuve*, et al.*, 2011).

An alternative approach to confirm the functionality of TA systems is to over-express the candidate toxins. However, over-expression in the native host may not reveal a clear phenotype unless the genes encoding cognate antitoxin(s) are also inactivated because they would otherwise mask the phenotype (Budde*, et al.*, 2006). An alternative option is to express the toxin in *E. coli*. Even in this host the results indicate that a homologue of the cognate antitoxin can mask the phenotype. This problem was resolved by inactivating the *E. coli* antitoxin homologue of BPSS1583. Korch and Hill (Korch & Hill, 2006) were able to express native *E. coli hipA* from

an arabinose inducible pBAD vector in a strain with endogenous *hipB* but this appears to be due to the potency of the native toxin. Expression of *E. coli* HipA in Δ*hipBA* caused filamentation and cell death and in this instance the endogenous *hipB* was needed to partially sequester activity (Korch*, et al.*, 2003). My data also showed that tagging the toxins can interfere with their toxic activity.

Nevertheless, my expression system proved successful in validating the functionality of several so far uncharacterised *B. pseudomallei* TA systems. The results indicate 2 phenotypes in *E. coli* expressing the *B. pseudomallei* toxins. Toxins of the RelE family (BPSL0175 and BPSS1060) caused the apparent cessation of growth, with no change in the number of culturable cells. The induction of expression of others (BPSS0390, HicA homologue, and BPSS1584, HipA homologue) resulted in a rapid decline in the number of cells which were culturable on agar and formed colonies.

The system I have developed for the independent or co-expression of predicted toxin and antitoxin genes has applications for the screening of genes from other micro-organisms. Although other groups have developed systems to screen the phenotype predicted TA loci, they rely on expression of both genes from the same promoter (Sevillano*, et al.*, 2012), which does not allow for independent gene expression. Alternatively, Gupta *et al.* (Gupta, 2009) have reported the independent expression of toxin and antitoxin in *E. coli* which involved tetracycline addition to induce antitoxin expression. One aim of this study was to develop a method that relied on non-antibiotic inducers for expression of candidate toxin and antitoxin genes, avoiding the possibility that the added antibiotic would modulate the number of persister cells.

It was also shown that the toxin-induced stasis or non culturability of bacteria could be reversed following expression of the cognate antitoxin. The results are similar to those reported by Jorgensen *et al*. who showed similar reduction in the culturability of *E. coli* when HicA was over-expressed and the ability of HicB to rescue cells (Jorgensen*, et al.*, 2008). This phenotype has also been observed with the RelBE system and with a MazEF homologue ChpAK/AI (Penderson*, et al.*, 2002). In this study they showed that cells were in a state of dormancy following toxin induction and after 3 hours, growth could be resumed by antitoxin expression through the recovery of translation and/or replication. Amitai *et al*. also observed this resuscitation phenotype with the MazEF system. However, they observed a point of no return, whereby after 8 hours of MazF expression, MazE was no longer able to restore growth (Amitai*, et al.*, 2004). The study of the HigBA system showed similar results: HigA could rescue HigB toxicity, but the longer HigA was expressed, the lower the ability of HigB to counteract toxicity (Budde*, et al.*, 2006).

Overall, the expression system could validate that 4 of 8 of the candidate toxins of *B. pseudomallei* possessed activity in *E. coli*. It is possible that the remaining 4 genes do not encode toxins or that expression of the toxins was not induced under the conditions we tested. No correlation between the RASTA-bacteria score and the identification of genes encoding functional toxins could be found. The functionality of the other predicted TA systems which were not tested in the expression system remains to be elucidated.

The distribution of the predicted TA genes in the different *Burkholderia pseudomallei* strains revealed different patterns of conservation. The BPSS1583-1584 locus for instance, was present in nearly all the strains compared to BPSS0390-391 which was present in only 3. Other predicted TA loci had a mixed distribution. It is

possible that the most highly conserved TA loci have important function and are subsequently retained in the genetic pool. Perhaps the sparsely spread BPSS0390-0391 loci has been recently acquired to provide some adaptation or the loci has been widely lost from many *B. pseudomallei* stains. The varying distribution of TA loci may also be dependent on where the strains were isolated. Different strains may require a different repertoire of TA to deal with the local environment. What the data does show is that TA systems are highly mobile in terms of genetic loss or gain.

The lack of the predicted TA loci in *B. mallei* is indicative of obligate host dependent bacteria (Pandey & Gerdes, 2005). *B. thailandensis* on the other hand has more of the predicted TA, presumably due to its environmental lifestyle.

It is also interesting to note the correlation between the putative TA systems identified in our study with genomic islands. Sim *et al*. have previously shown that genomic islands are associated with clinical strains of *B. pseudomallei* and the genes encoded on them may be involved with human host adaptation and survival (Sim*, et al.*, 2008). In their study they identified the genes BPSS0391, BPSS1060, BPSL0559 and BPSL3260 amongst others in *B. pseudomallei* strains associated with a clinical clade. This provides further evidence that TA systems may have involvement in human disease as the genes are positively selected for in these strains.

Chapter 4

Characterisation of BPSL0175 (RelE2) toxin activity

4.0 Introduction

The BPSL0175 protein and the paralogous protein BPSS1060 have up to 54% sequence homology to RelE proteins previously identified in other species. The RelBE locus was first identified on the chromosome of *E. coli* K-12, with the *relE* gene encoding a toxin and *relB* encoding an antitoxin gene (Gotfredsen & Gerdes, 1998). Overexpression of the RelE toxin in *E. coli* caused growth cessation, a reduction in colony forming units and inhibition of translation through ribosome binding (Galvani, *et al.*, 2001). It was originally thought the reduction in CFU was the result of cell death but subsequent experimentation showed that cells could be resuscitated by RelB expression (Pedersen, *et al.*, 2002).

The RelE toxin inhibits translation through degradation of mRNA at the ribosomal A site *in vitro* and *in vivo.* Specifically, this involves cleavage of codons between the second and third base. RelE binds to the 30S subunit of the ribosome which stimulates either endogenous ribonuclease activity by the ribosome or ribonuclease activity of the RelE toxin through a conformational change on binding (Pedersen, *et al.*, 2003). The crystal structure of the RelE: ribosome complex reveals the toxin binds to 16 srRNA and not to a ribosomal protein (Neubauer, *et al.*, 2009). On binding the RelE toxin is able to inhibit translation. The Lon protease, in response to nutrient stress, can degrade the RelB antitoxin, which allows release and activation of the RelE toxin (Christensen & Gerdes, 2003).

The activity of the RelE toxin has been shown to be cell density dependent in *E. coli* MG1655 (Tashiro, *et al.*, 2012). Cell dormancy was enhanced at higher cell densities compared to low cell densities. *E. coli* cells expressing RelE form more persister cells following treatment with a range of antibiotics compared to non RelE expressing cells. Moreover higher cell densities of RelE expressing *E. coli* form more

persisters than those at lower cell densities. Further analysis revealed that amino acid starvation and a currently unidentified heat-liable extracellular factor were responsible for the density dependent phenotype.

4.0.1 Aims

- Determine if the growth inhibition affect of BPSL0175 (RelE2) expression is cell density dependent
- Determine if the age of media has an effect on growth inhibition

4.1 Expression of BPSL0175 at different cell densities

Since Tashiro *et al* demonstrated that RelE induced growth inhibition was cell density dependent in *E. coli*, it was hypothesised that this could also be true for the BPSL0175 (RelE2) homolog. To test this, overnight cultures of *E. coli* MG1655 pBAD-BPSL0175 were diluted and grown in fresh LB media until reaching early-mid log phase (OD_{590}nm ~0.3). Neat (~10^8 CFU/ml), 1 in10 (~ 10^7 CFU/ml) or 1 in 100 (~ 10^6 CFU/ml) diluted cultures were then supplemented with 0.2% (w/v) arabinose to induce expression of BPSL0175 and incubated at 37 ^oC, 200 rpm for a further 3 hours. CFU numbers were determined every hour. Figure 4.0 shows the resulting growth profile. In the undiluted starting cultures, CFU counts remained relatively constant throughout the experiment. In contrast, CFU numbers continued to increase when the cells had been diluted 1 in 100. At the 1 in 10 dilution, cell numbers increased for the first 2 hours but once the culture reached a cell density of approximately 10^8 CFU/ml, cell numbers remained constant thereafter. By 3 hours the CFU for all dilutions was approximately the same.

4.2 Expression of BPSL0175 in spent media

4.2.1 Empty pBAD and LacZ controls

Control cutltures were grown in spent media to determine if growth was altered compared to growth in fresh LB. *E. coli* MG1655 pBAD/his or *E. coli* Top10 pBAD/his-LacZ were grown overnight in LB and then centrifuged. The supernatant was filter sterilised to provide spent media. In parallel *E. coli* MG1655 pBAD/his or *E. coli* Top10 pBAD/his-LacZ were grown to early exponential phase (OD_{590}nm~ 0.2)

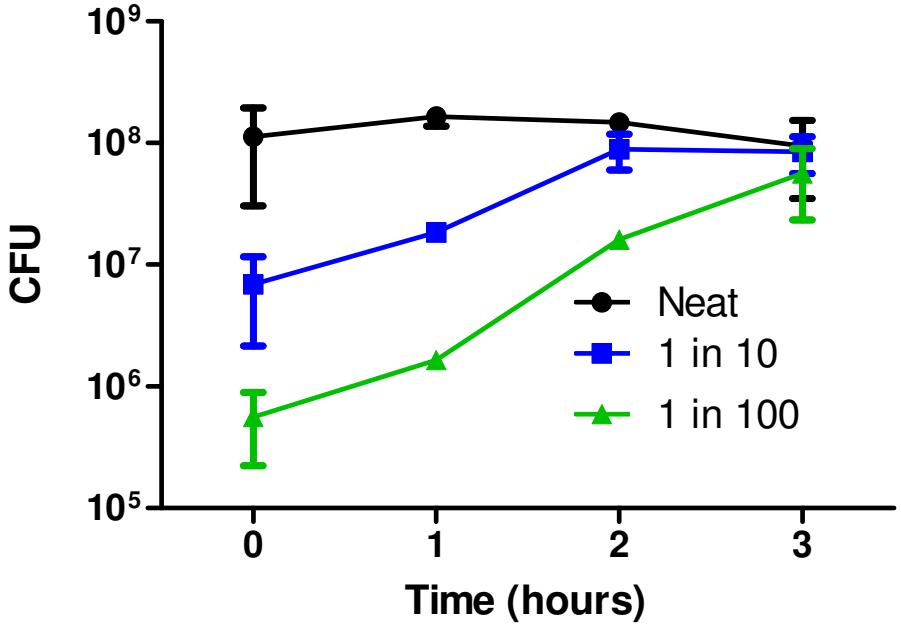

Figure 4.0 Growth profile monitoring the CFU of *E. coli* MG1655 pBAD-BPSL0175 at different cell densities. Cultures were grown to early-mid log phase before inducing neat, 1 in 10 or 1 in 100 cultures with 0.2% (w/v) arabinose for BPSL0175 expression. Cultures were diluted in LB. CFU was measured every hour for 3 hours by plating onto LB agar plates supplemented with ampicillin. Data is an average of 3 biological repeats and error bars are SEM.

before harvesting high cell density (10^7 CFU/ml) or low cell density (10^5 CFU/ml) cultures. The cultures were re-suspended in fresh LB or in the relevant filter sterilised spent media and supplemented with 0.2% (w/v) arabinose to induce expression from the arabinose inducible pBAD promoter for 2 hours. When *E. coli* MG1655/ pBAD was grown in spent media or in fresh LB there was no significant difference in the fold change in CFU counts at either high or low cell densities (Fig 4.1A). This was also true for *E. coli* Top10 pBAD/his lacZ (Fig 4.1B).

4.2.2 BPSL0175 expression

E. coli MG1655 pBAD-BPSL0175 was grown in LB overnight then centrifuged and the supernatant filter sterilised to provide spent media. In parallel *E. coli* MG1655 pBAD-BPSL0175 cultures were grown to early log phase before pelleting high (10^7 CFU/ml) or low (10^5 CFU/ml) cell density cultures. These cultures were re-suspended in fresh LB or spent media and supplemented with 0.2% (w/v) arabinose to induce BPSL0175 expression for 2 hours at 37 ^{o}C. Figure 4.2 shows the resulting fold change in CFU. At high densities (10^7 CFU/ml), *E. coli* grown in spent medium or LB increased in CFU. Growth in spent media was 5 fold less in CFU counts compared to fresh LB and this difference was significant ($p<0.01$ student t-test). At low cell densities there was no change in CFU numbers when *E. coli* was grown in spent media. In contrast there was nearly a 100 fold increase in CFU counts when grown in fresh LB media. The difference was significant ($p<0.01$ student's t-test).

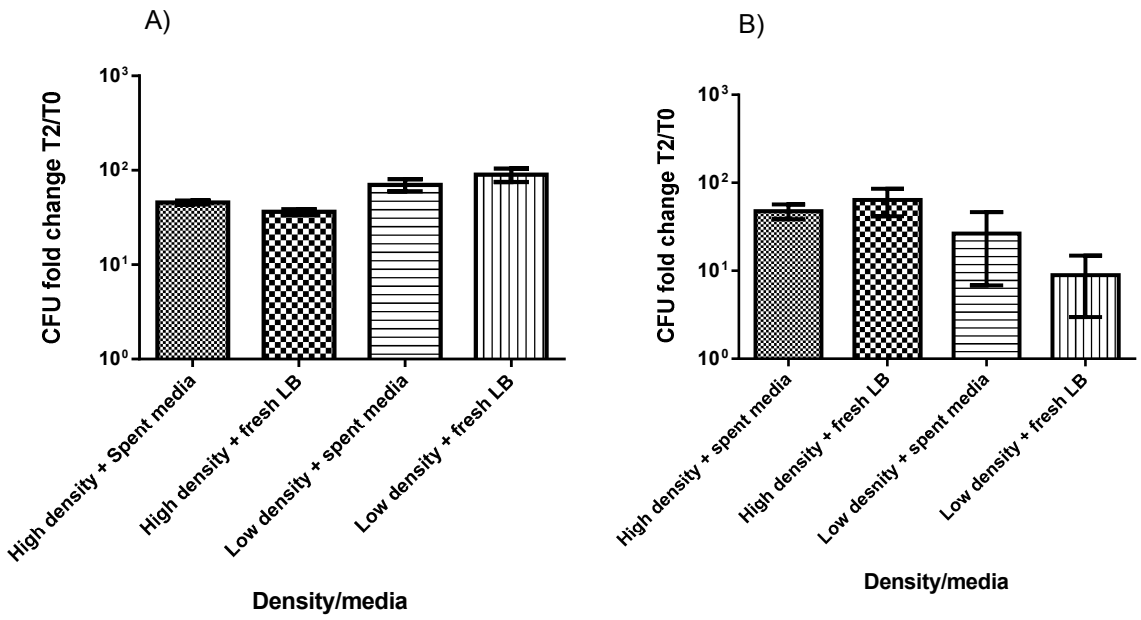

Figure 4.1 The effect of spent media or LB on *E. coli* growth at 2 different cell densities. A) *E. coli* MG1655 pBAD/his grown at high (10^7 CFU/ml) or low (10^5 CFU/ml) cell densities B) *E. coli* Top10 pBAD/his-LacZ grown at high (10^7 CFU/ml) or low (10^5 CFU/ml) cell densities. CFU fold change was calculated as CFU counts at T2/ CFU counts at T0. LacZ expression was induced for 2 hours with 0.2% (w/v) arabinose. Data is the average of 3 biological repeats. Error bars represent SEM.

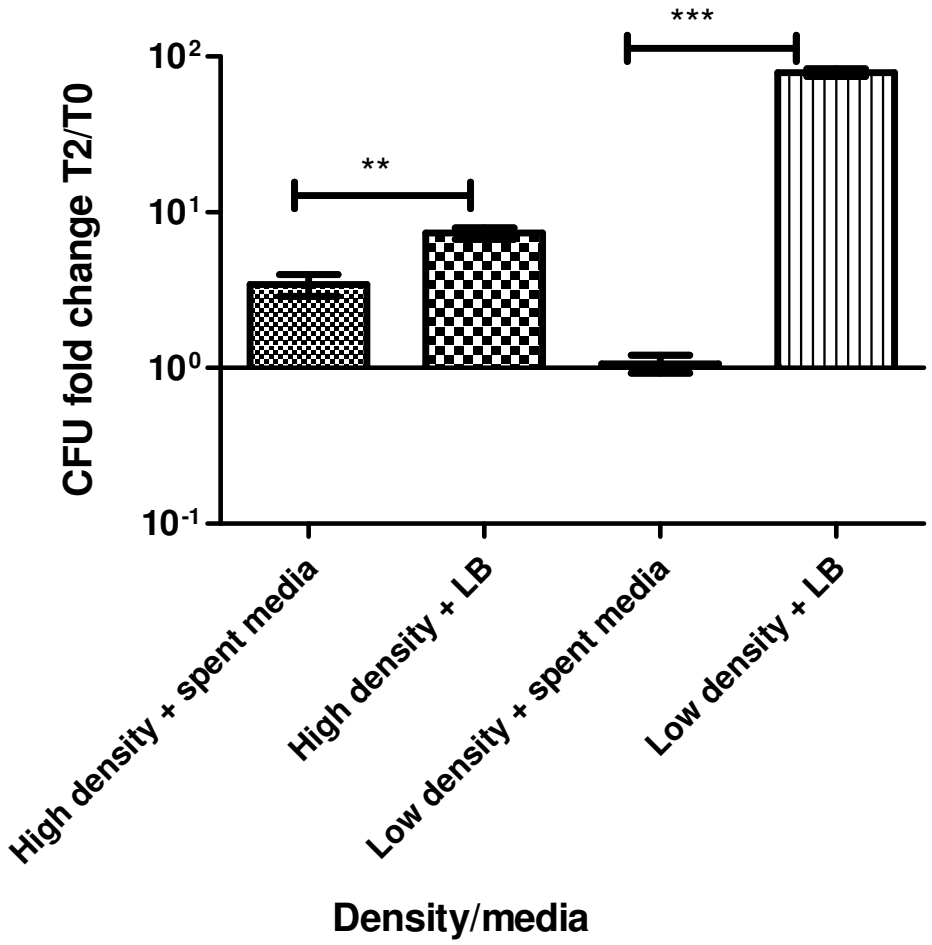

Figure 4.2 The effect of spent media or fresh LB on the CFU change of *E. coli* MG1655 pBAD-BPSL0175 grown at 2 different densities high (10^7) or low (10^5) CFU/ml. Once cultures had reached early log phase, high or low cell densities were re-suspended in spent media or fresh LB and BPSL0175 expression was induced with 0.2% (w/v) arabinose for 2 hours. CFU fold change was calculated as CFU numbers at T2 divided by CFU numbers at T0. Data is the average of 3 biological repeats and error bars represent SEM. **=$p<0.01$, ***=$p<0.001$, student's t-test.

4.3 Discussion

Cell density had a profound impact on the magnitude of the toxin-induced response. Tashiro *et al.* have previously shown a population effect when expressing RelE in *E. coli* (Tashiro*, et al.*, 2012). They attribute this to an unidentified dormancy factor that is heat labile and accumulates during stationary phase. My data shows that the *B. pseudomallei* RelE homolog BPSL0175 has cell density dependent activity and that spent culture media from stationary phase increases the activity of the BPSL0175 toxin compared to fresh media. This supports the idea of a signalling factor or co-factor that aids in growth inhibition and cellular dormancy mediated by the RelBE TA system at least in *E. coli*. The MazF toxin has also been shown to have population-density regulated activity involving a small peptide named the extracellular death factor (Kolodkin-Gal*, et al.*, 2008). This factor is at highest levels during mid-log phase rather than stationary phase and is needed for the cell death activity via the MazF toxin (Kolodkin-Gal*, et al.*, 2007, Kolodkin-Gal I & H, 2008). These studies reveal that cellular dormancy and the action of TA toxins involve communication between members of the bacterial population, perhaps as an insurance policy or act of altruism to protect the population as a whole from stress. One could argue that reduced cell numbers in spent media compared to fresh LB could be due to nutrient limitation. The control experiments, using either empty plasmid or plasmid cloned lacZ show that for both strains there is no significant difference between the changes in CFU numbers in either spent media or LB at either density. This suggests that the difference in the *E. coli* MG1655 strain expressing BPSL0175 must be due to something other than nutrient depletion. Further investigation is needed into the molecular basis for the cell density dependence effect for this TA system which includes isolation of any potential exported signalling factor. In future chapters where

BPSS1584 and BPSS0390 have been characterised, more studies on the density dependent effect have been carried out to try and elucidate the molecular basis for this phenotype.

Chapter 5

Characterisation of the BPSS1583-BPSS1584 (HipBA) system

5.0 Introduction

The BPSS1584 and BPSS1583 genes encode proteins which share sequence homology to members of the HipA and HipB families respectively, including the HipA (40% sequence identity) and HipB (33% sequence identity) proteins from *E. coli* MG1655. The HipBA locus is associated with persistence in *E. coli* and a number of expression studies have been undertaken to elucidate its specific functionality (Korch & Hill, 2006).

A possible role in persistence was first determined through studies on the *hipA7* allele of the *hipA* gene in *E. coli*. This mutant allele increased persister frequencies following penicillin treatment from 10^{-6} to 10^{-2} (Black*, et al.*, 1991). This high persistence phenotype requires the (p)ppGpp alarmone, which regulates the stringent response. Knocking out the *relA spoT* genes, which synthesises the alarmone eliminates persistence in the *hipA7* strain (Korch*, et al.*, 2003). It is believed that strains carrying the *hipA7* allele generate a sub-population of slow growing cells during stationary phase that enter a dormant tolerant state. Expression of the *hipA7* gene is not toxic to growth. In comparison, expression of *hipA* is toxic to growth. Sequencing of the *hipA7* gene revealed it had 2 point mutations G22S and D291A compared to the wild type *hipA*. Introducing these mutations independently into *hipA* showed that both were needed for both the non-toxic and increased persistence phenotypes. The G22C mutation abolished the growth inhibition phenotype of HipA when expressed in *E. coli* but persister frequencies remained the same. The D291A mutation retained the toxicity of *hipA* but increased persistence to levels of *hipA7* when expressed (Korch*, et al.*, 2003).

Expression of wild type *hipA* in *E. coli* causes growth inhibition and a reduction in CFU by inhibiting protein, RNA and DNA synthesis inducing a dormant

state rather than cell death (Korch & Hill, 2006). Expression of the toxin in a *hipB*+ background also increases persister frequencies following ampicillin treatment (Korch & Hill, 2006). Expression of *hipB* is able to resuscitate growth of *hipA*-induced cells and restore culturabilty.

Transcription of the *hipBA* locus is auto regulated by the HipB protein. The protein can cooperatively bind 4 operators with the consensus sequence $TATCCN_8GGATA$ located in the *hipBA* promoter region (Black*, et al.*, 1994). The gene sequences of *hipA* and *hipB* overlap suggesting they are co-transcribed (Black*, et al.*, 1994). Sequence comparison of the HipA protein showed that it is a member of the phosphatidylinositol 3/4-kinase superfamily and in the presence of ATP the HipA protein could be autophosphroylated (Correia*, et al.*, 2006). The HipA protein has a eukaryotic serine/threonine kinase-like fold and is able to phosphorylate and inactivate the translation factor EF-Tu. Phosphorylated EF-Tu results in growth inhibition, since the transcription factor can no longer bind aminoacyl-tRNA for protein synthesis. To inactivate the HipA protein, a dimer of 2 HipB proteins binds 2 HipA proteins to sequester the proteins and cause conformational change (Schumacher*, et al.*, 2009). Structural studies revealed that the high persistent phenotype observed in the *hipA7* mutant is probably due to a weak interaction between the HipA and HipB proteins.

For the HipA protein to be active it must be released from the HipB protein. Recent studies have confirmed this requires the Lon protease, which recognises the unstructured C-terminus of the HipB protein (Hansen*, et al.*). Moreover the activity of the HipA protein is dependent on toxin levels being above a threshold that is dependent on the level of HipB antitoxin (Rotem*, et al.*, 2010). Fluctuations above and below the threshold result in the co-existence of dormant and growing cells and

cells above the threshold are believed to be the persisters that survive antibiotic treatment as long as they stay dormant.

Stress and survival studies on an *E. coli K-12* Δ*hipBA* mutant have shown that this TA system may have involvement in long term survival as Δ*hipBA* had a prolonged life span when cultivated in M9 media compared to the wild type, although both survive similarly in anaerobic conditions. Under conditions of hydrogen peroxide stress, the Δ*hipBA* strain showed greater survival than wild type (Kawano*, et al.*, 2009). One theory is that the HipA toxin causes initial bacteriostasis but can then induce cell death after stationary phase. Another study showed that there was no difference in persister frequencies between wild type *E. coli and* Δ*hipBA* strains at various points during stationary phase following ampicillin treatment. Persister frequencies increase for both wild type and Δ*hipBA* during stationary phase to levels similar to the *hipA7* mutant showing the age of media can influence persister frequency (Luidalepp*, et al.*, 2011).

5.0.1 Aims

- Determine if BPSS1584 expression in Δ*hipBA* causes cell death or dormancy and whether this effect is cell density dependent
- Determine if such an effect is media dependent and if so isolate/characterise any factor in the media responsible for such a phenotype
- Determine if a *B. pseudomallei* K96343 Δ*hipBA* mutant has a survival/fitness disadvantage when treated with a variety of stresses or a reduction in persister frequencies.

5.1 Phenotypic characterisation following BPSS1584 toxin expression

5.1.1Live/Dead screening following BPSS1584 expression in *ΔhipBA*

5.1.1.1 Fluorescence microscope imaging

It was hypothesised that CFU reduction following BPSS1584 (*hipA)* expression was not the result of cell death but of cellular dormancy and the establishment of a viable but non culturable state. To test this theory a LIVE/DEAD staining approach was used.

E. coli MG1655 *ΔhipBA* pBAD-BPSS1584 was grown to the early log phase before adding 0.2% (w/v) glucose or 0.2% (w/v) arabinose for repression or induction of BPSS1584 expression respectively. Cultures were incubated for a further 2 hours before standardising to an OD_{590}nm of 0.5. 10 µl samples of *E. coli* with BPSS1584 repressed or expressed were stained using Invitrogen LIVE/DEAD stain and then applied to microscope slides for visualisation under the 2 fluorescence filters on the microscope. Figure 5.0 shows representative images of cells under the red filter and overlaying images of cells under both fluorescent filters. When BPSS1584 was either repressed or expressed for 2 hours >99% of *E. coli* cells fluoresced green suggesting they were alive.

5.1.1.2 Fluorescece plate reader

Fluorescence was also measured using a fluorescence plate reader. *E. coli* Δ*hipBA* MG1655 pBAD-BPSS1584 was grown to early exponential phase and then BPSS1584 was repressed or expressed for 2 hours by addition of 0.2% (w/v) glucose or 0.2% (w/v) arabinose respectively. Half of the *E. coli* cells under either BPSS1584 repressive or expressive conditions were washed and stored in 0.85% NaCl and the other half were stored in 70% isopropanol to kill the cells. NaCl and isopropanol-treated cells were stained with LIVE/DEAD stain and different ratios of test bacteria

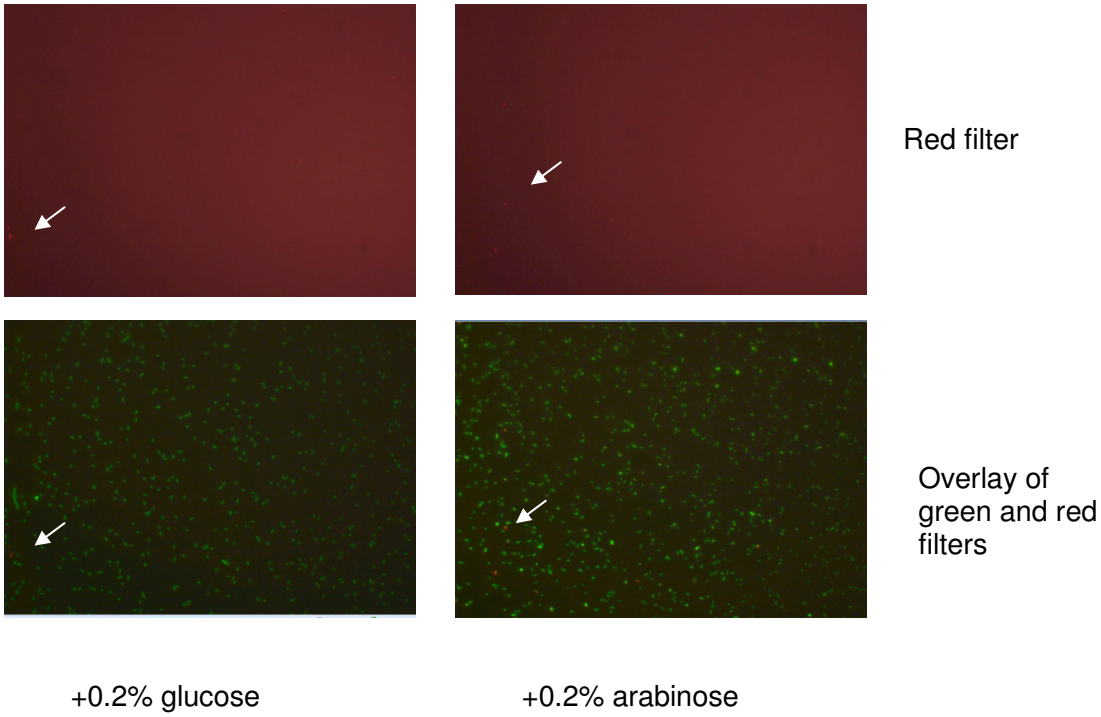

Figure 5.0 Fluorescent imaging following Live/Dead staining of 2 hour BPSS1584 repressed (0.2% (w/v) glucose) or BPSS1584 expressed (0.2% (w/v) arabinose) *E. coli* MG1655 *ΔhipBA* pBAD BPSS1584 cultures. Cultures were standardised to an OD_{590}nm of 0.5 before following the Invitrogen Live/Dead protocol and visualising under a fluorescence microscope. Live cells fluoresce green and dead cells fluoresce red. The top panels show fluorescent cells under the red filter and the bottom panels show overlaying images of cells under both green and red filters. Arrow shows a dead cell.

(0.85% NaCl treated) were mixed with dead bacteria (isopropanol treated) in a 96 well plate format before measuring fluorescence under the different channels. As the percentage of test bacteria to dead bacteria was increased the ratio of green:red fluorescence increased when BPSS1584 expression was repressed or induced (fig 5.1A). There was no significant difference in the rate of increase between BPSS1584 repressed or expressed cultures following a linear regression analysis ($p=0.68$). Conversely, as the percentage of test bacteria to dead bacteria was increased, the ratio of red:green fluorescence decreased when BPSS1584 expression was repressed or induced (fig 5.1B). There was no significant difference in the rate of decrease between BPSS1584 repressed or expressed cultures following a linear regression analysis ($p=0.47$). This suggested that BPSS1584 expressed cultures did not have a significantly greater ratio of dead cells:live cells compared to BPSS1584 repressed cultures. Expression of BPSL1584 was not significantly killing *E. coli* cells.

5.1.2 Expression of BPSS1584 at different cell densities

E. coli ΔhipBA cells carrying the pBAD-BPSS1584 construct were grown to early-mid log phase before inducing expression of BPSS1584 in neat, 1 in 10 or 1 in 100 diluted cultures with 0.2% (w/v) arabinose. The CFU count was determined every hour for 3 hours. Figure 5.2 shows the resulting profile. At ~10^7 CFU/ ml, the CFU count started to drop after 1 hour and there was a dramatic reduction by approximately 500 fold by 2 hours. At the 1 in 10 dilution, cultures continued to grow and CFU increased for the first 2 hours. Between 2 and 3 hours after the culture had reached approximately 5 x 10^6 CFU/ml, the CFU count dropped by approximately 1000 fold to ~10^4 CFU/ml. The 1 in 100 dilution grew for the first 2 hours

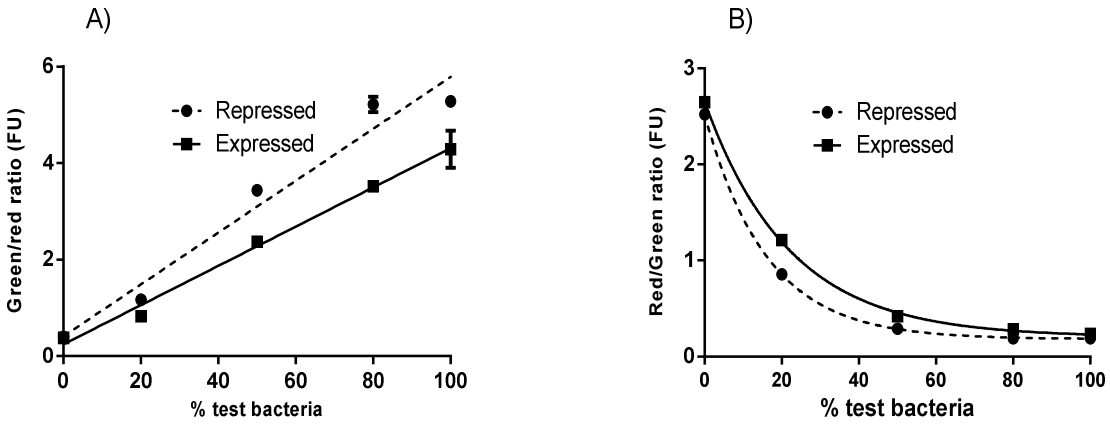

Figure 5.1 Ratio of fluorescence units, after mixing various amounts of test and dead *E. coli* cells. *E. coli* MG655 *ΔhipBA* pBAD-BPSS1584 were grown to early exponential phase and then supplemented with 0.2% (w/v) glucose or 0.2% (w/v) arabinose to repress or induce expression of BPSS1584 for 2 hours. Cultures were then standardised to OD_{590}nm 0.5, resuspended in 0.85% NaCl (test) or 70% isopropanol (dead) and stained using the Live/Dead kit (Invitogen). Different percentages of test and dead bacteria were mixed and added to a 96 well plate in triplicate. The fluorescence was recorded using a plate reader. Live cells fluoresced green and dead fluoresced red. A) Green:red fluorescent unit ratio of BPSS1584 repressed or expressed cultures. B) Red:green fluorescent unit ratio of BPSS1584 repressed or expressed cultures.

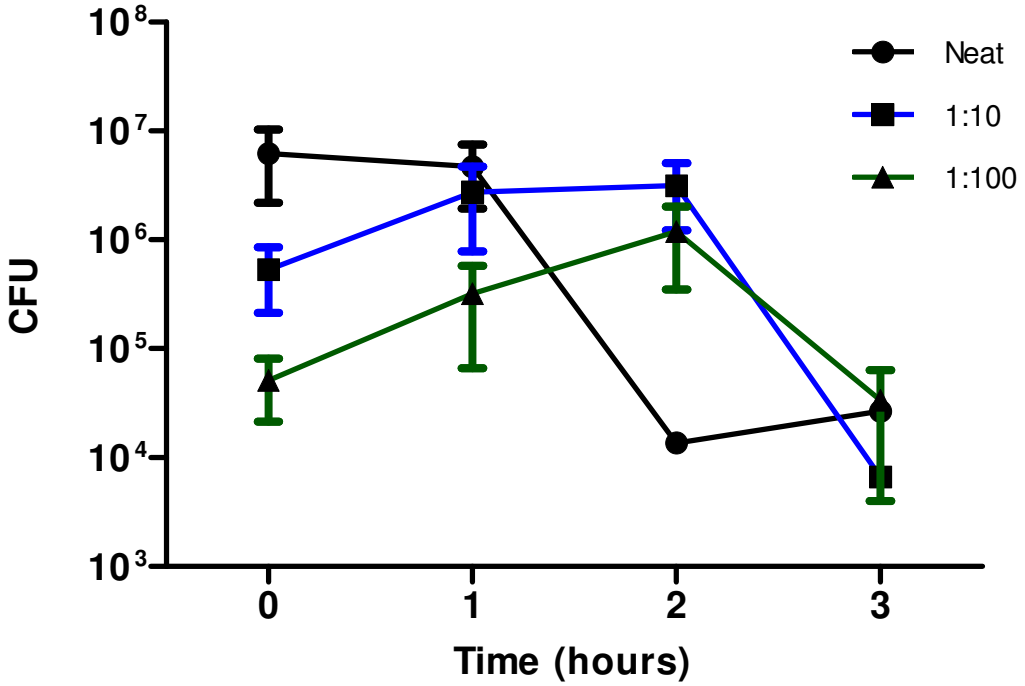

Figure 5.2 Overnight cultures of *E. coli* MG1655 *ΔhipBA* pBAD-BPSS1584 were diluted 1:100 in fresh LB and grown to early log phase before inducing expression of BPSS1584 in a neat, 1:10 diluted and 1:100 diluted culture with 0.2% (w/v) arabinose for 3 hours. Samples were taken every hour for CFU count determination. Data shown is the average of 3 biological repeats. Error bars show SEM.

and between the hours of 2 and 3, after the culture had reached approximately 1 x 10^6 CFU/ml, the CFU then dropped by approximately 50 fold.

5.1.3 Expression of BPSS1584 in spent media

E. coli MG1655 Δ*hipBA* pBAD-BPSS1584 grown overnight in LB was harvested by centrifugation and the supernatant was filter sterilised to provide spent medium. In parallel *E. coli* MG1655 Δ*hipBA* pBAD-BPSS1584 was grown to early exponential phase and high density (~10^7 CFU/ml) or low cell density (~10^5 CFU/ml) cultures were harvested and re-suspended in LB or in spent medium. BPSS1584 expression was then induced with 0.2% (w/v) arabinose for 2 hours. At high cell densities, there was a 100 fold reduction in CFU counts in spent medium compared to a 20 fold reduction in fresh LB (figure 5.3). This difference was significant ($p<0.001$, student's t-test). At low cell densities BPSS1584 expression resulted in a 100 fold increase in CFU counts in fresh LB. In contrast, *E. coli* cells grown in spent medium had a 10 fold decrease in CFU numbers. This difference was significant ($p<0.01$, student's t-test). Controls for this experiment using *E.coli* MG1655/ pBAD were carried out previously (chapter 4, section 4.2.1).

5.1.4 Expression of BPSS1584 in fractionated spent media

E. coli MG1655 Δ*hipBA* pBAD-BPSS1584 was grown overnight in LB and then centrifuged. The supernatant was filter sterilised to provide spent medium. The spent medium was added to a 3kDa cut-off membrane filtration column and fractionated into <3-kDa and >3kDa fractions by centrifuged for approximately 40 minutes for complete size fractionation. In parallel *E. coli* MG1655 Δ*hipBA* pBAD-BPSS1584 was grown to early exponential phase before harvesting cells into high (10^7 CFU/ml) or low (10^5 CFU/ml

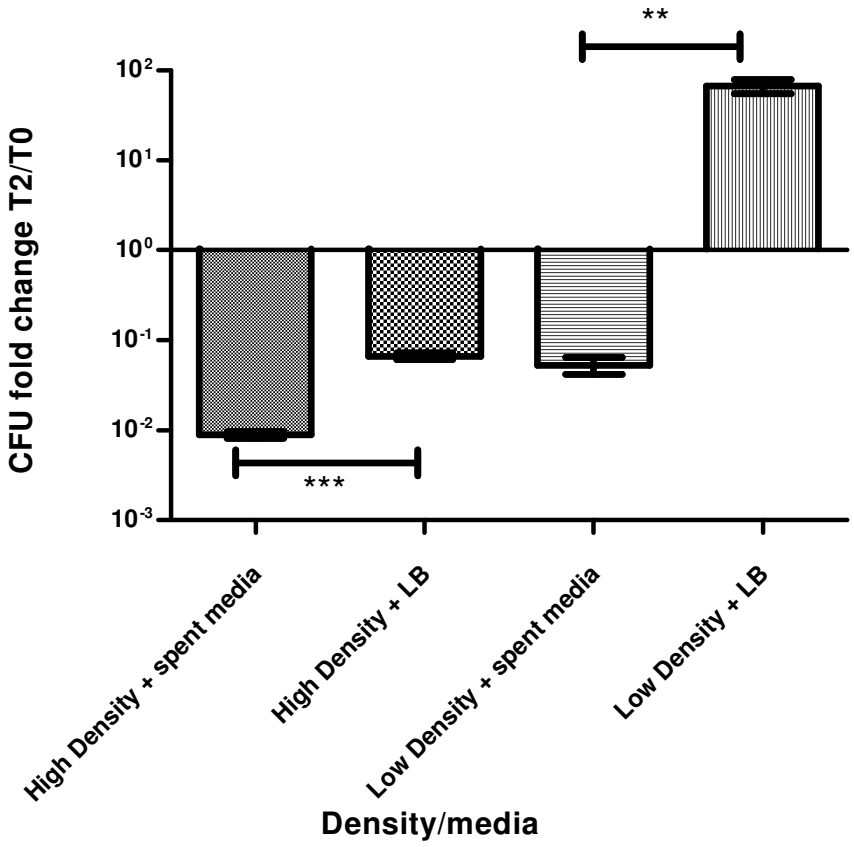

Figure 5.3 The effect of BPSS1584 expression on CFU change when *E. coli* MG1655 *ΔhipBA* pBAD-BPSS1584 at 2 different cell densities, high (10^7) or low (10^5) CFU/ml were re-suspended and grown in spent medium or fresh LB for 2 hours. Spent medium was harvested from overnight cultures of *E. coli* MG1655 *ΔhipBA* pBAD-BPSS1584 grown in LB and filter sterilised. BPSS1584 expression was induced with 0.2% (w/v) arabinose once cultures had reached early exponential phase. CFU fold change was calculated as CFU at 2 hours divided by CFU at 0 hours. Data is representative of 3 biological repeats and error bars represent SEM. **=p<0.01. ***=p<0.001, student's t-test.

) cell densities. Cells were re-suspended in either fractionated spent medium or LB or un-fractionated spent media. BPSS1584 expression was then induced for 2 hours with 0.2% (w/v) arabinose. *E. coli* re-suspended in <3kDa fractionated media at high densities showed a 1000 fold reduction in CFU numbers similar to the spent media control (figure 5.4A). *E. coli* grown in >3kDa fractionated media showed a 100 fold reduction in CFU numbers similar to the reduction in fresh LB. The difference in fold change in CFU numbers in < or > 3kDa fractionated media was significant ($p<0.01$, student's t-test).

At low densities *E. coli* grown in fractionated media <3kDa showed a 50 fold reduction in CFU numbers similar to the spent media control (figure 5.4B). *E. coli* re-suspended in fractionated media >3kDa showed a 100 fold increase in CFU numbers similar to fresh LB following BPSS1584 expression. The difference in fold change in CFU in < or > 3kDa fractionated media at low density was significant ($p<0.001$, student's t-test)

5.1.5 Expression of BPSS1584 in acid treated spent media

E. coli MG1655 Δ*hipBA* pBAD-BPSS1584 was grown overnight in LB and then harvested to isolate spent medium. The spent medium was treated with 1M HCl and adjusted to pH 2 for 1 hour and then neutralised back to pH 6.5 using 1M NaOH before filter sterilising. In parallel *E. coli* MG1655 Δ*hipBA* pBAD-BPSS1584 was grown to early exponential phase and cells were separated into high (10^7 CFU/ml) or low (10^5 CFU/ml) cell densities. Cells were then re-suspended into acid treated spent media or untreated spent media as a control and BPSS1584 expression was induced with 0.2% (w/v) arabinose for 2 hours. *E. coli* cells expressing BPSS1584 grown in acid treated or untreated media had a 100 to 1000 fold reduction in CFU numbers

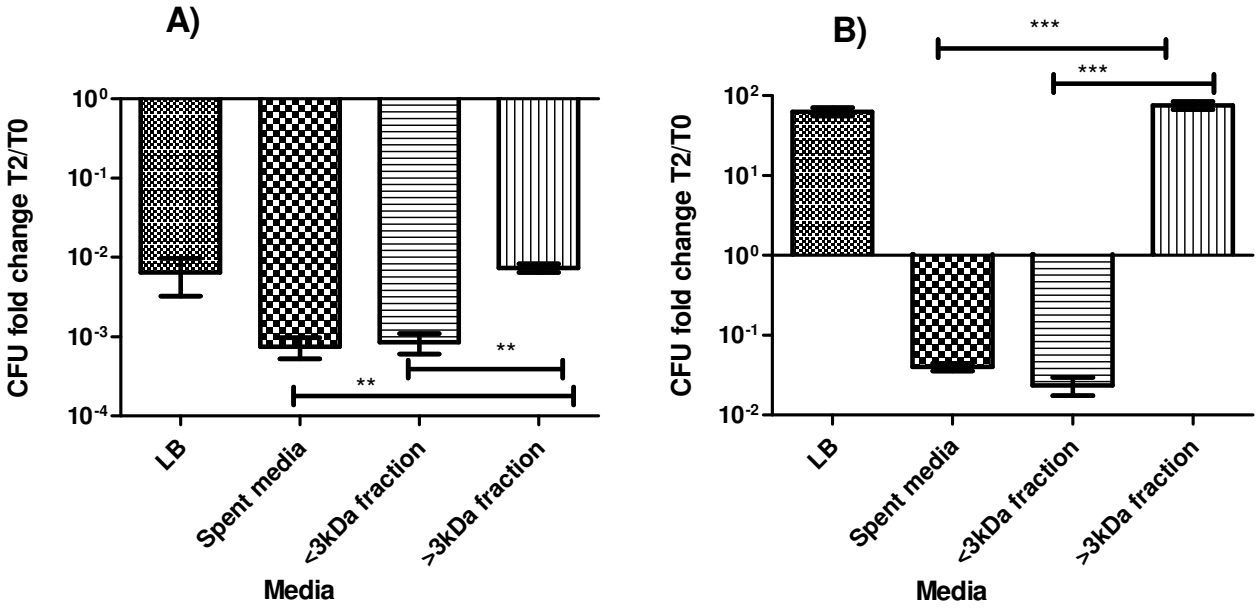

Figure 5.4 The effect of BPSS1584 expression on CFU change when *E. coli* MG1655 *ΔhipBA* pBAD-BPSS1584 was grown at 2 different cell densities A) high (10^7 CFU/ml) or B) low (10^5 CFU/ml) in fractionated spent media. Spent media was isolated from an overnight culture of *E. coli* MG1655 *ΔhipBA* pBAD-BPSS1584 by centrifugation and filter sterilising. The spent media was fractionated using a 3kDa size exclusion column to isolate the 2 different fractions. High and low density early exponential cultures were re-suspended in the fractionated media or LB or unfractionated media before inducing expression of BPSS1584 with 0.2% (w/v) arabinose. CFU fold change was calculated as CFU numbers at T2 divided by CFU numbers at T0. **=$p<0.01$. ***=$p<0.001$, student's t-test.

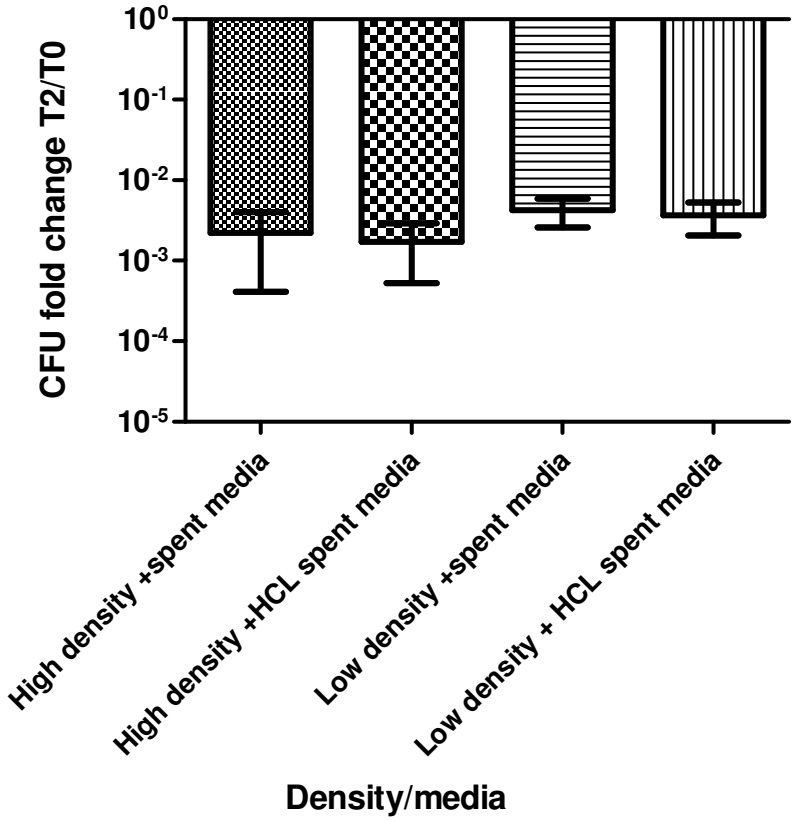

Figure 5.5 The effect of BPSS1584 expression on the CFU of early exponential phase *E. coli* MG1655 Δ*hipBA* pBAD-BPSS1584 grown at 2 different cell densities – high (10^7 CFU/ml) or low (10^5 CFU/ml) –in spent media that was HCl treated. Spent media was isolated from an overnight culture of *E. coli* MG1655 pBAD-BPSS1584 by centrifugation. The spent media was acidified for 1 hour by addition of 1M HCl and neutralised to pH6.5 with 1M NaOH. BPSS1584 expression was induced with 0.2% (w/v) arabinose for 2 hours. CFU fold change was calculated as CFU numbers at T2 divided by CFU numbers at T0. Data is the average of 3 biological repeats. Error bars represent SEM.

at both high and low cell densities (figure 5.5). The fold changes in CFU counts in acid treated or untreated media were not significantly different at either cell density.

5.2 Expression of BPSS1584 in *B. pseudomallei* K96243

5.2.1 Generation of an expression construct

A *B. pseudomallei* K96243 *ΔBPSS1584-1583 (hipBA)* mutant, made by Claudia Hemsley prior to the start of this work, was selected as the *B. pseudomallei* expression host along with the E264 strain of *B. thailandensis* which naturally lacks a *hipA* ortholog. pBAD/his does not replicate in *Burkholderia,* as it does not have a compatible origin of replication. Therefore the BPSS1584 gene was cloned into the pBHR broad host-range plasmid, along with the arabinose inducible promoter from pBAD. Using the pBAD-BPSS1584 DNA as a template and plasmid specific primers, the promoter region and BPSS1584 gene were PCR amplified and cloned via the *Sac*I and *Ale*I restriction sites into pBHR to create the construct pBHRparaBPSS1584BAD (figure 5.6). The plasmid was first transformed into *E. coli* MG1655 *ΔhipBA*. *E. coli* MG1655 Δ*hipBA* pBHRparaBPSS1584BAD was grown to early exponential phase and then supplemented with 0.2% (w/v) glucose or 0.2% (w/v) arabinose to repress or induce expression of BPSS1584 for 3 hours. Following induction of BPSS1584 expression the growth rate was reduced in comparison to the glucose repressed control (figure 5.7A). This confirmed that the expression vector was functioning in *E. coli*. Next the vector was transformed into *E. coli S17λ* and this strain was used as a donor to conjugate the plasmid construct into *B. thailandensis* E264 or *B. pseudomallei* K96243 Δ*hipBA*. Conjugants were selected on LB agar plates containing kanamycin for plasmid selection and gentamicin to kill the *E. coli* donor strain. Colonies that grew on the plates were checked by PCR and a PCR positive

colony was picked for experimentation. Figure 5.7B shows a growth profile of *B. thailandensis* E264 expressing BPSS1584. Overnight cultures of *B. thailandensis* E264 pBHR-paraBPSS1584BAD were diluted 1:100 and grown to early log phase before inducing expression of BPSS1584 with 0.2% (w/v) arabinose or repressing expression of BPSS1584 with 0.2% (w/v) glucose for 3 hours. Cultures were supplemented with kanamycin for plasmid selection. Under either BPSS1584 repressed conditions (glucose) or expressed conditions (arabinose) the growth profiles were similar. This suggested that the gene was not being expressed, the experimental time frame was too short or the toxin had no effect in this species. Attempts to conjugate the plasmid construct into the *B. pseudomallei* Δ*hipBA* strain were unsuccessful.

5.3 Characterisation of the *B. pseudomallei* K96243 *ΔhipBA* mutant

5.3.1 Transciptomics data

The BPSS1583 and BPSS1584 genes were searched for in a transcriptomics data set (provided by Catherine Ong at the Genome Institute of Singapore) to determine if the genes were up or down regulation in *B. pseudomallei* in response to different stress conditions. Table 5.0 lists the stress conditions which affected BPSS1583 and BPSS1584 regulation. BPSS1583 was up regulated in response to acid, cadmium, heat and oxidative stress, while BPSS1584 was up regulated in response to heat and ceftazidime. The data set suggests that the genes can be regulated independently, as the stress conditions in which regulation was altered differed between the 2 genes. The only stress condition which was common to both and resulted in up regulation is heat. Both genes were down regulated in a quorum sensing mutant and under anaerobic growth conditions.

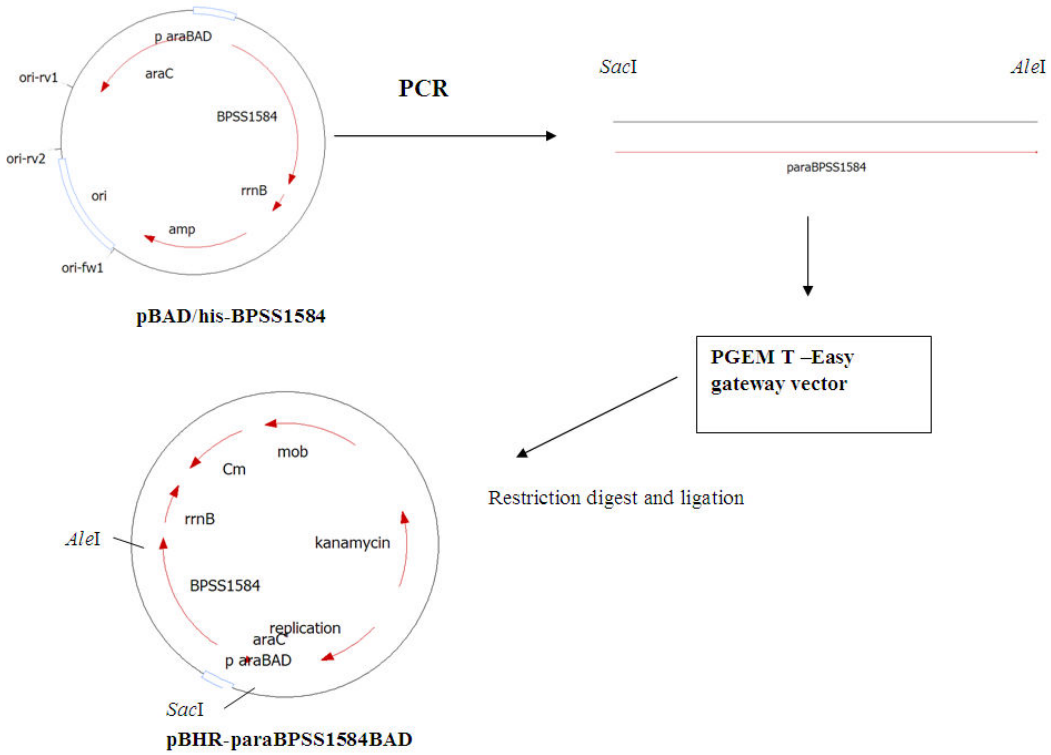

Figure 5.6 Methodology for creation of the pBHR-paraBPSS1584BAD plasmid. The BPSS1584 gene and pBAD promoter were PCR amplified from the pBAD -BPSS1584 plasmid with a forward primer containing a *Sac*I restriction site and reverse primer containing an *Ale*I restriction site. The resulting PCR product was checked for size and amplification by gel electrophoresis before adding to the gateway vector PGEM-T-Easy. The PGEM plasmid containing paraBPSS1584 and the pBHR plasmid were digested with *Sac*I and *Ale*I. The digested paraBPSS1584 DNA was ligated into the pBHR plasmid to create pBHR-paraBPSS1584.

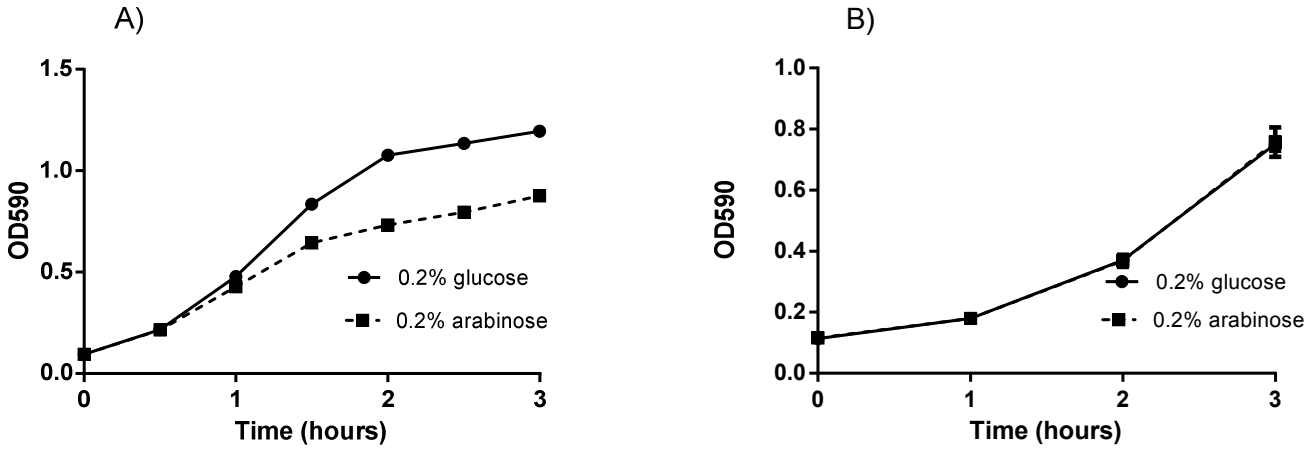

Figure 5.7 Growth profiles measuring the optical density at 590nm of pBHR-paraBPSS1584BAD containing bacterial strains. A) *E. coli ΔhipBA* and B) *B. thailandensis* E264. Cultures were grown to early exponential phase before expression of BPSS1584 was induced with 0.2% (w/v) arabinose and repressed with 0.2% (w/v) glucose. Time points were taken every 30 minutes (*E. coli)* or every hour (*B. thailandensis)* for 3 hours to measure optical density at 590nm.

Table 5.0 Stress conditions in which BPSS1583 or BPSS1584 were up or down regulated in *B. pseudomallei* K96243. Up or down regulation was assessed by comparing BPSS1583 or BPSS1584 mRNA levels in stressed bacteria vs. normal LB grown bacteria. *Comparison of mRNA in LB grown *B. pseudomallei* K96243 vs quorum sensing mutant.

Gene name	**Up/down regulated**	**Stress condition**
BPSS1583	Up	Acid (pH 4)
		Cadmium (200μM)
		In Vitro infection RAW 264.7
		Nutrient deprivation
		Oxidative stress (100 mM H_20_2)
		Heat (42 ^oC)
	Down	Anaerobic
		Quorum sensing mutant*
BPSS1584	Up	Ceftazidime (2 ug/ml ceftazidime (1X MIC))
		Heat (42 ^oC)
	Down	Quorum sensing mutant*
		Anaerobic

5.3.2 Heat stress assay

B. pseudomallei K96243 or *B. pseudomallei* K96243 Δ*hipBA* grown overnight in LB were diluted to high (10^9 CFU/ml) or low (2 x 10^8 CFU/ml) cell densities. Cultures were then heat stressed in a heat block at 65 ^oC for 2 hours before plating onto LB agar plates. At low densities the *B. pseudomallei* K96243 Δ*hipBA* mutant had a greater fold change in CFU numbers compared to the wild type strain but the difference was not significant (figure 5.8A). At high cell densities there was a 1000 fold reduction in CFU for both wild type and Δ*hipBA* strains (figure 5.8B).

5.3.3 Persister assay with ciprofloxacin and ceftazidime

B. pseudomallei K96243 or *B. pseudomallei* K96243 Δ*hipBA* were grown overnight in LB and 10^8 bacterial cells were incubated with 100 x the minimum inhibitory concentration (MIC) of ceftazidime or ciprofloxacin for 24 hours. Following treatment, cells were washed and plated onto LB agar plates. On average the *B. pseudomallei* K96243 Δ*hipBA* mutant appeared to form more persister cells than the wild type *B. pseudomallei* K96243 strain for both ciprofloxacin (fig 5.9A) and ceftazidime (fig 5.9B), although the difference was not significant.

5.3.4 Acid stress

A final stress that was tested on *B. pseudomallei* K96243 and the *B. pseudomallei* K96243 Δ*hipBA* mutant was acid stress. *B. pseudomallei* K96243 or *B. pseudomallei* K96243 Δ*hipBA* were grown overnight to stationary phase before re-suspending 10^8 bacterial cells in LB that had been adjusted to either a pH of 3.5 (fig 5.10 A) or pH 2.5 (fig 5.10 B) using 1M HCl. In pH 3.5 conditions both the wild type and the Δ*hipBA* strain were able to grow with over a 10 fold increase in CFU numbers after 24 hours. There was no significant difference between the CFU increases.

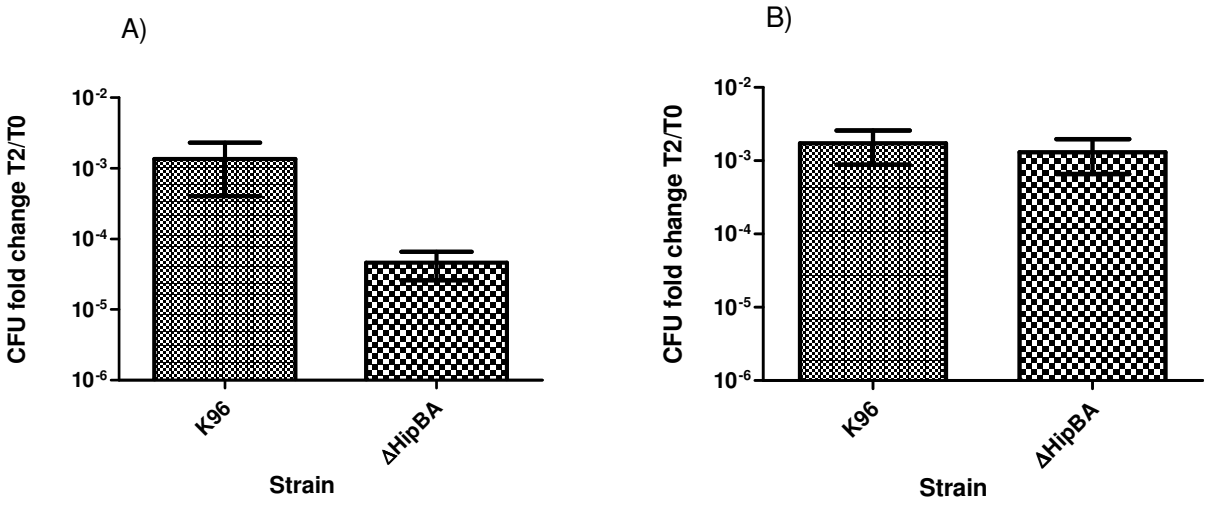

Figure 5.8 Fold change in CFU numbers of *B. pseudomallei* K96243 and *B. pseudomallei* K96243 *ΔhipBA* heat treated for 2 hours at 65^0C. Overnight cultures were diluted in LB to A) 2 x 10^8 CFU/ml (low cell density) or B) 10^9 CFU/ml (high cell density). Heat treatment was carried out in a heat block. Data shown are the average of 3 biological repeats. Error bars represent SEM

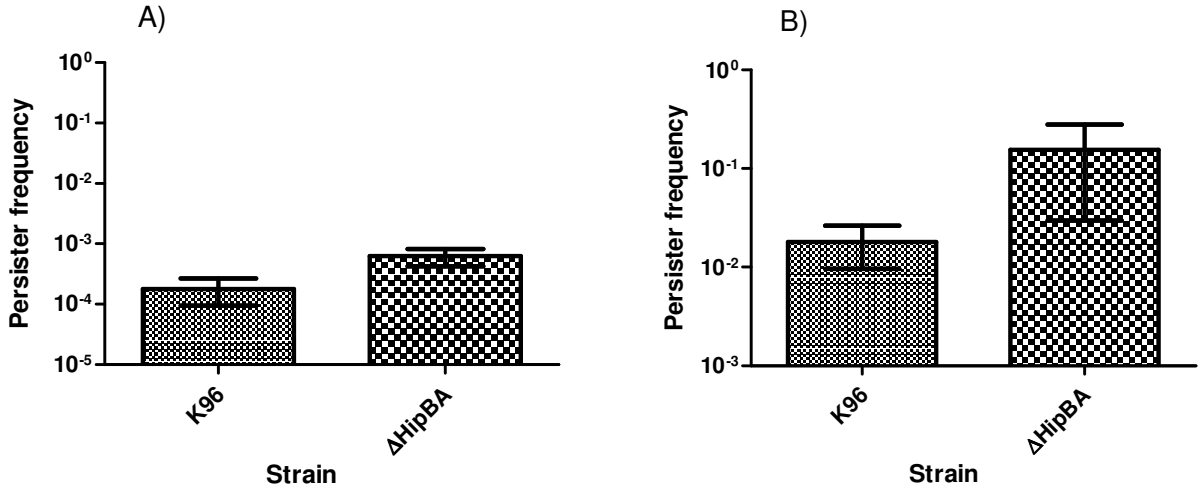

Figure 5.9 Persister frequency of *B. pseudomallei* K96243 or *B. pseudomallei* K96243 *ΔhipBA* treated with 100 x MIC (200 µg/µl) of antibiotic for 24 hours. Overnight cultures grown in LB were diluted to an OD_{590}nm 0.2 (approx 2x 10^8 CFU/ml) before mixing 1:1 with A) ciprofloxacin or B) ceftazidime. After 24 hours incubation at 37 ^oC, cells were washed twice in fresh LB to remove antibiotic and plated onto LB agar plates. Data shown is the average of 3 biological repeats. Error bars show SEM.

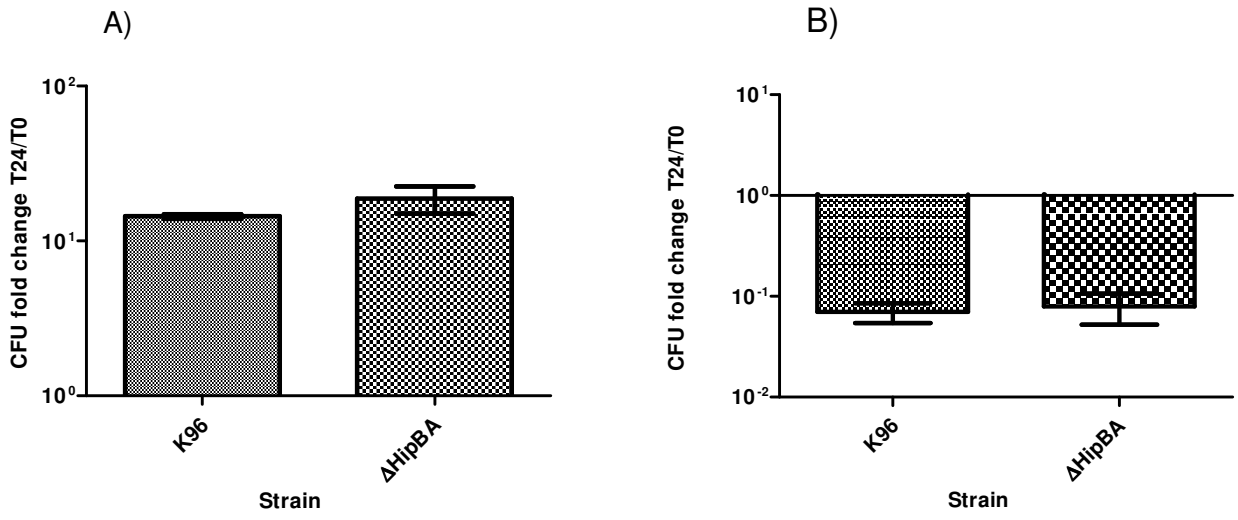

Figure 5.10 CFU fold change of *B. pseudomallei* K96243 or *B. pseudomallei ΔhipBA* subjected to pH stress at either pH 3.5 A) or pH 2.5 B). Approximately 10^8 stationary phase cells were re-suspended in pH adjusted LB using HCl for 24 hours. Cells were then washed and plated. CFU fold change was calculated as CFU post stress divided by time zero. Cells were plated on LB agar plates and incubated at 37 ^{o}C. Data shown are the average of 3 biological repeats and error bars show SEM.

At pH 2.5 there was over a 10 fold decrease in CFU counts for both the wild type and Δ*hipBA* strain but there was no significant difference.

5.4 Discussion

Expression of BPSS1584 (*hipA*) in *E. coli ΔhipBA* decreased CFU counts, however Live/Dead staining showed that the inability of the majority of the population to form colonies when plated onto agar was not the result of death. This implied that the cells had entered into a dormant state, which could be similar to a viable but non culturable state. The results of this experiment are similar to observations made by Korch and Hill (Korch & Hill, 2006). They observed that >95% of *hipA* induced *E. coli* cells were live following Live/Dead staining and that 1.8% of these were still able to form colonies when plating (Korch & Hill, 2006). They concluded that cells were not being killed but entering dormancy that could be resuscitated by *hipB* expression.

The activity of the *B. pseudomallei hipA* toxin in *E. coli ΔhipBA* was cell density dependent and required cell numbers to be approximately 10^7 CFU/ml before a reduction in culturability of the cell population was observed. This could indicate a quorum sensing like factor may be involved in switching cells into a state of dormancy. A study by Spoering and Lewis suggested that quorum sensing may play an important role in the development of persistence in *Pseudomonas* and recently a Competence Stimulating Peptide (CSP) pheromone has been shown to be involved in stress induced persistence in S*treptococcus mutans* (Spoering & Lewis, 2001, Leung & Lévesque, 2012).

Activity of the BPSS1584 (HipA) toxin was enhanced in spent media compared to fresh LB and this was particularly evident at lower cell densities. Moreover spent media that was size excluded to contain only components smaller

than 3kDa was responsible for the enhanced phenotype providing further evidence for a quorum sensing like factor that accumulates during stationary phase. Acid treatment of the spent media had no effect on its enhancing ability to reduce CFU following *hipA* expression. If such a quorum sensing factor in the spent media was a protein, high acid could denature the protein to inactivate it. Having said this some proteins do not lose their structure in acid conditions and neutralising the media following acid treatment could have allowed for re-folding of the protein (Fink*, et al.*, 1994). It is possible that such a quorum like factor is a small peptide or compound based on other signalling systems but a small protein cannot be completely ruled out.

In addition to expression of *B. pseudomallei hipA* in *E. coli*, attempts were also made to express the gene in *B. thailandensis* E264 and in *B. pseudomallei* K96243 *ΔhipBA* to confirm the toxin was active in *Burkholderia.* A growth inhibition phenotype was not observed when expressing the gene in *B. thailandensis* E264. Although this strain does not posses a *hipA* homologue it carries a chromosomal *hipB* gene and the encoded protein shares 74% sequence identity with the *B. pseudomallei* HipB protein. It is possible that endogenous HipB protein is able to sequester the recombinant HipA protein preventing its biological activity. Conversely attempts to express *hipA* in *B. pseudomallei* K96243 Δ*hipBA* failed. It is possible that leaky expression from the pBAD promoter was sufficient to prevent the formation of transformed colonies. In other bacteria attempts at cloning the *hipA* gene close to strong promoters and transforming the gene into strains absent of *hipB* have proven unsuccessful (Moyed & Broderick, 1986, Black*, et al.*, 1991). Even when transformants containing cloned *hipA* do arise, growth in media can result in cell death in Δ*hipBA* strains (Korch*, et al.*, 2003).

It was hypothesised that the BPSS1583 and BPSS1584 genes may be responsible for increased persistence and survival under stress conditions. A series of stress conditions were tested on the wild type *B. pseudomallei* K96243 strain and the *B. pseudomallei* K96243 *ΔhipBA* strain where gene expression of *hipB* and/or *hipA* was up regulated in the transcriptomics data. A temperature of 65 ^{o}C was used to heat stress cells. This temperature was greater than the 42 ^{o}C used to create the transcriptomics data set as *B. pseudomallei* can readily grow at 42 ^{o}C (Chen*, et al.*, 2003). The next stress condition tested on *B. pseudomallei* K96243 and the *B. pseudomallei* K96243 Δ*hipBA* mutant was antibiotic. In *E. coli* the HipA toxin has been shown to have involvement in persistence (Korch & Hill, 2006) and BPSS1584 was upregulated in response to ceftazidime treatment. It was hypothesised that the *B. pseudomallei* K96243 Δ*hipBA* mutant may form fewer persisters when incubated with antibiotic which could have clinical significance. In addition to ceftazidime, another class of antibiotic (ciprofloxacin) was tested to determine if any difference in persister frequencies was antibiotic specific. There was no significant difference in persistence or survival when stressing with heat, antibiotic or acid. However, when cells were heat treated there was a trend for the wild type to survive better that the mutant, yet when cells were treated with antibiotic or acid stressed there was a trend for the *B. pseudomallei* K96243 Δ*hipBA* mutant to survive better than wild type *B. pseudomallei* K96243. This could indicate that the *hipBA* locus responds differently to different stresses. The mutant surviving better than the wild type does partially link in with the Δ*hipBA* mutant of *E. coli* surviving hydrogen peroxide stress better than the wild type (Kawano*, et al.*, 2009). There were variations between the biological repeats in my study that may be explained by the age of the media, as this can mask persister phenotypes (Luidalepp*, et al.*, 2011). It is also possible that there is functional

redundancy between TA systems and knocking out one single TA loci may not give a signficant phenotype. Progressive deletions of TA systems may be needed to observe a phenotype in *B. pseudomallei,* as demonstrated in *E. coli* (Maisonneuve*, et al.*, 2011).

Chapter 6

Characterisation of the BPSS0390-BPSS0391 (HicBA) system

6.0 Introduction

BLAST searching the BPSS0390 and BPSS0391 protein sequences in chapter 3 against the NCBI database revealed sequence identity to HicA and HicB proteins respectively. The HicA and HicB proteins constitute a toxin-antitoxin system that is relatively under-studied in comparison to many of the other type II TA systems. The gene structure of the *hicBA* loci is unusual with the *hicA* toxin preceding the *hicB* antitoxin. This structure is uncommon amongst the different TA families and only *higBA* also has this reversed gene layout (Pandey & Gerdes, 2005). HicA proteins are small proteins that consist of a double stranded RNA binding fold and HicB proteins have a DNA binding domain that is linked to a degraded RNase H fold (Makarova*, et al.*, 2006). A study by Jorgensen *et al* identified 119 *hicBA* families distributed amongst different bacterial and archaeal species (Jorgensen*, et al.*, 2008). The 2 bacterial species with the greatest number of predicted *hicAB* loci were *Treponema denticola* and *Photorhabdus luminescens* with 9 and 8 loci respectively. *T. denticola* is an obligate anaerobe that lives in the oral cavity of humans and is commonly associated with periodontal disease (Seshadri*, et al.*, 2004), while *P. luminescens* lives in the gut of an entomopathogenic nematode that is released and kills when the nematode infects insects (Waterfield*, et al.*, 2009).

Overexpression of the *E. coli hicA* gene in *E. coli* MG1655 was previously shown to cause growth arrest, while expression in a Δ*hicBA* background caused growth arrest and a reduction of CFU (Jorgensen*, et al.*, 2008). Expression of *hicB* was able to neutralize the *hicA* induced bacteriostasis. The *E. coli* HicA toxin functions by degrading mRNA and tmRNA to prevent translation. Specifically the HicA toxin could degrade the 3 test mRNAs *ompA, dksA* and *rpoD* in addition to tmRNA by inducing multiple cleavage sites but no obvious consensus sequence was

detectable (Jorgensen, *et al.*, 2008). The *hicAB* locus is transcribed in response to amino acid and carbon starvation and dependent on the Lon protease. This protease degrades the unstable HicB antitoxin, which acts as an auto-repressor of the locus, subsequently allowing transcription of the genes in response to starvation (Jorgensen, *et al.*, 2008).

The *hicB* gene has also been associated with the *E. coli* sigma factor σ^E, which responds to stress in the cell membrane and periplasmic space (Erickson & Gross, 1989). Insertions in the *hicB* gene could render the σ^E non-essential and deletions of the *hicB* gene resulted in significant downregulation of extracytoplasmic stress response, though the σ^E and ClpX dependent response and causes a severe reduction in outer membrane vesicle formation (Button, *et al.*, 2007). This could suggest an additional regulatory role for this antitoxin.

6.0.1 Aims

- Determine if BPSS0390 expression in *E. coli* MG1655 and *B. pseudomallei* causes cell death or dormancy and whether this is cell density dependent and/or age of media dependent.
- Determine if a *B. pseudomallei* K96343 Δ*BPSS0390-0391* mutant has a survival/fitness disadvantage when treated with a variety of stresses or a reduction in persister frequencies.

6.1 Phenotypic characterisation following BPSS0390 toxin expression in *E. coli* MG1655

6.1.1 Live/Dead screening following BPSS0390 expression

E. coli MG1655 containing pBAD-cloned BPSS0390 was grown to early log phase before adding 0.2% (w/v) glucose or 0.2% (w/v) arabinose for repression or induction of expression respectively. Cultures were incubated for a further 3 hours before standardising to an OD_{590}nm 0.5 and then using the Invitrogen LIVE/DEAD kit to stain the cells. Figure 6.0 shows representative microscope images of cells under the red filter and overlaying images of cells under both green and red fluorescent filters. These images show that the majority of the cells were alive when BPSS0390 was either repressed or expressed. This indicated that BPSS0390 expression was not resulting in significant *E. coli* death.

6.1.2 Expression of BPSS0390 at different cell densities

The effect of BPSS0390 expression at different cell densities was next investigated. *E. coli* MG1655 cultures with pBAD-cloned BPSS0390 were grown to early log phase before inducing neat, 1 in 10 or 1 in 100 diluted cultures with 0.2% (w/v) arabinose for 3 hours, taking CFU counts every hour. At the neat density, expression of BPSS0390 resulted in a decline in cell numbers by approximately 1000 fold over the experiment (figure 6.1.). At the 1 in 10 dilution the CFU increased by approximately 1 log for the first hour reaching over 10^7 CFU/ ml but then declined slightly from hour 1 to 2. CFU numbers dropped approximately 100 fold from hour 2 to 3. At the 1 in 100 dilution the CFU increased every hour and reached over 10^7 CFU/ ml.

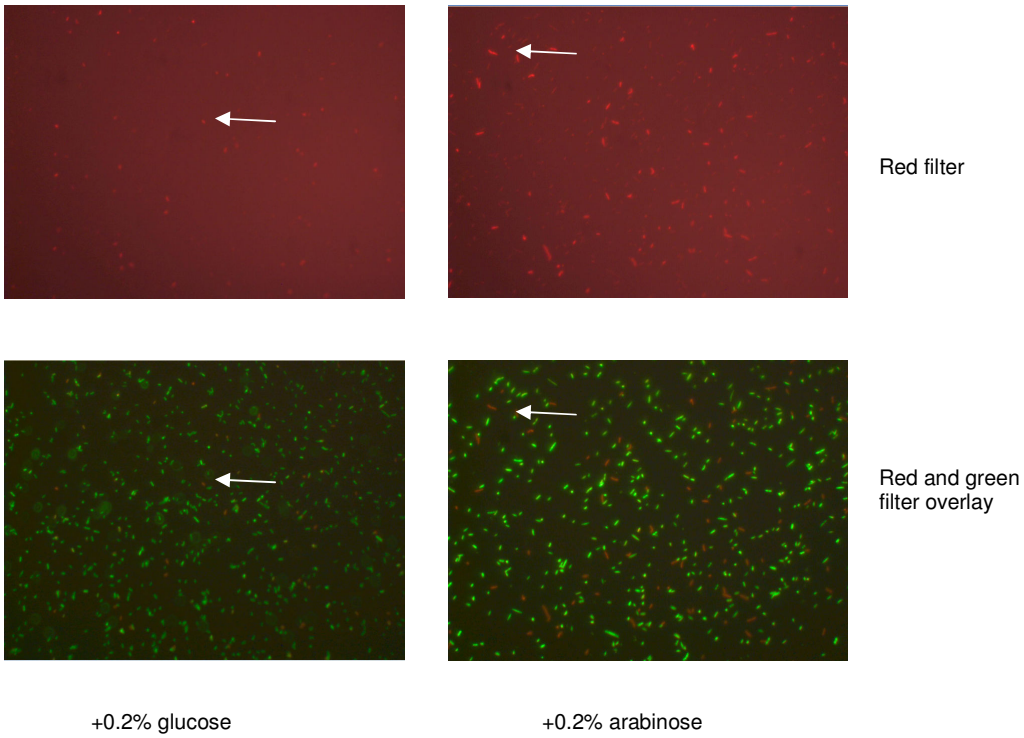

Figure 6.0 Fluorescent imaging following live/dead staining of 3 hour BPSS0390 repressed (0.2% (w/v) glucose) or BPSS0390 expressed (0.2% (w/v) arabinose*) E. coli* MG1655 pBAD BPSS0390 cultures. Cultures were standardised to an OD_{590}nm of 0.5 before following the Invitrogen LIVE/DEAD protocol and visualising under a fluorescence microscope under both the green and red filters. Live cells fluoresce green and dead fluoresce red. The top panels show cells under the red filter and the bottom panels show overlaying images of cells under both green and red filters. The white arrow shows a dead cell.

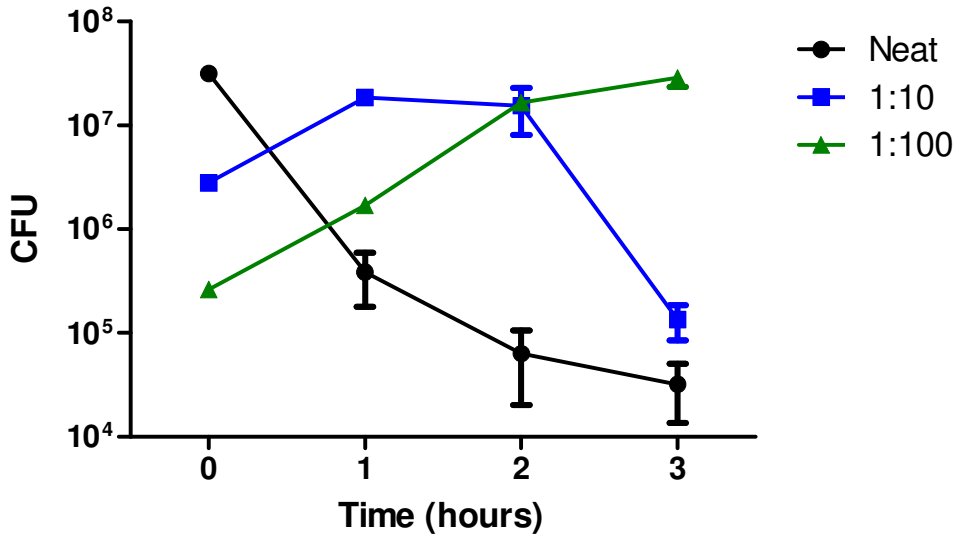

Figure 6.1 Growth profile of BPSS0390 expressing *E. coli* MG1655 pBAD-BPSS0390 at 3 different cell densities over 3 hours. Cultures were grown to early log phase before inducing a neat culture (black line), 1 in 10 (blue) and 1 in 100 (green) with 0.2% (w/v) arabinose. Samples were taken every hour and plated onto LB agar plates supplemented with ampicillin for CFU determination. Data shows the average of 3 biological replicates and error bars show SEM.

6.1.3 Expression of BPSS0390 in spent media

6.1.3.1 Expression in exponential phase media

E. coli MG1655 pBAD-BPSS0390 was grown to early log phase in LB, centrifuged and filter sterilised to provide exponential phase medium. 10^7 (high) or 10^5 (low) CFU/ml of early log phase cultures of *E. coli* MG1655 pBAD-BPSS0390 were re-suspended in the exponential phase medium. Expression of BPSS0390 was then induced with 0.2% (w/v) arabinose for 2 hours. Figure 6.2 shows the resulting change in CFU numbers. At high density there was a reduction in CFU counts to approximately 10^{-3} but in fresh LB the reduction in CFU counts was significantly less at around 5 x 10^{-3}($p<0.05$, student's t-test). At low densities in either fresh LB or exponential medium the CFU count increased. The CFU increase was significantly less in exponential media (approximately 50 fold compared to 100 fold) ($p<0.05$, student's t-test).

6.1.3.2 Comparing BPSS0390 expression at low density in different aged media

E. coli MG1655 pBAD-BPSS0390 cultures grown overnight in LB to stationary phase or grown to early exponential phase were centrifuged and filter sterilised to provide stationary phase spent medium and exponential phase medium respectively. 10^5 CFU/ml early exponential phase *E. coli* cells were then re-suspended in fresh LB, exponential phase medium or stationary phase medium and BPSS0390 expression was induced with 0.2% (w/v) arabinose for 2 hours. In fresh LB or early exponential media the fold change in CFU numbers increased following expression of BPSS0390 (figure 6.3). However, in stationary phase media there was a reduction in CFU numbers with an approximate 10^{-3} fold reduction. The CFU change in each media condition was significantly different ($p<0.05$ or $p<0.01$, student's t-test).

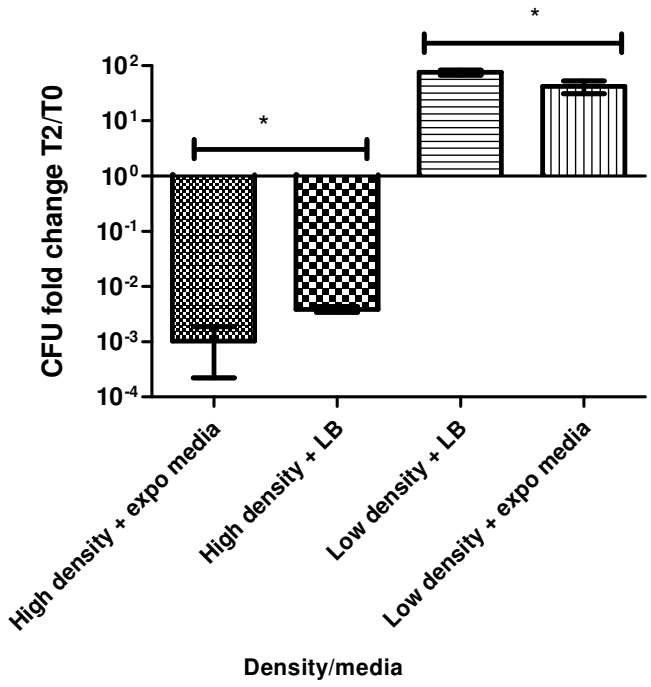

Figure 6.2 Fold change in CFU counts following expression of BPSS0390 in *E. coli* MG1655 grown in exponential phase media or fresh LB at 2 cell densities for 2 hours. The *E. coli* MG1655 pBAD-BPSS0390 strain was grown to exponential phase and then high density (10^7 CFU/ml) or low density (10^5 CFU/ml) cultures were re-suspended in either exponential phase growth media or fresh media before inducing expression of BPSS0390 with 0.2% (w/v) arabinose. Data shown is the average of 3 biological repeats. Error bars show SEM. *= $p<0.05$ student's t-test.

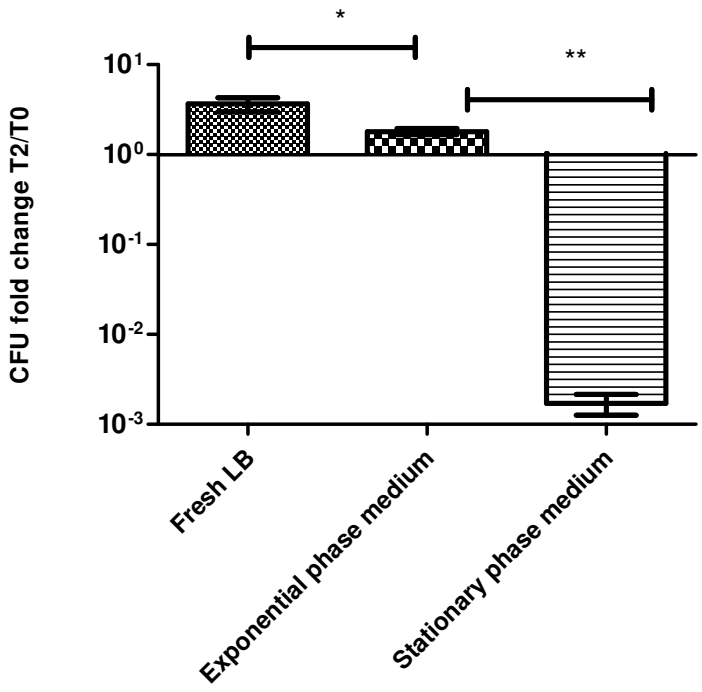

Figure 6.3 CFU fold change following expression of BPSS0390 in *E. coli* MG1655 pBAD-BPSS0390 grown in fresh LB, exponential phase medium or stationary phase media for 2 hours. Exponential and stationary phase media was isolated from *E. coli* MG1655 pBAD-BPSS0390 cultures grown to early exponential phase or grown overnight to stationary phase respectively. 0.2% (w/v) arabinose was used to induce expression of pBAD cloned BPSS0390. A cell density of approximately 10^5 CFU/ml (low density) *E. coli* MG1655 pBAD-BPSS0390 early exponential phase cells were used in this experiment. Error bar show SEM. *=$p<0.05$, **=$p<0.01$ student's t-test.

This suggested that medium from different growth phases of *E. coli* had significant effects on the activity of BPSS0390 toxin.

6.1.4 Expression of BPSS0390 in fractionated media

E. coli MG1655 pBAD-BPSS0390 was grown overnight in LB, centrifuged and filter sterilised to provide spent medium. Spent medium was fractionated using a 3kDa cut off spin column. In parallel *E. coli* MG1655 pBAD-BPSS0390 was grown to early exponential phase and cells harvested by centrifugation into high (10^7) or low (10^5) CFU/ml cell densities. The >3kDa or <3kDa spent medium fractions were then added to high or low density cultures and cells were re-suspended. BPSS0390 expression was induced for 2 hours by adding 0.2% (w/v) arabinose. The < 3-kDa fraction had an enhancing effect on the CFU reduction phenotype similar to the spent media control at both cell densities (Figure 6.4). *E. coli* cells expressing BPSS0390 grown in the >3kDa fraction had a CFU fold change similar to LB only. The difference in CFU fold change, when *E. coli* was grown in either <3kDa or >3kDa fractionated media was significant at both cell densities ($P<0.05$ or $P<0.01$, student's t-test).

6.1.5 Heat treatment of spent media pre BPSS0390 expression

E. coli MG1655 pBAD-BPSS0390 was grown overnight in LB, centrifuged and filter sterilised to isolate spent medium. This spent medium was then heat treated at 100^0C for 1 hour. In parallel *E. coli* MG1655 pBAD-BPSS0390 was grown to early exponential phase and cells were harvested into 10^7 (high) or 10^5 (low) CFU/ml density cultures. The cultures were then re-suspended in the heat treated media and BPSS0390 expression was induced with 0.2% (w/v) arabinose for 2 hours. Figure 6.5 shows the resulting CFU fold change. At high density the CFU fold change of *E. coli*

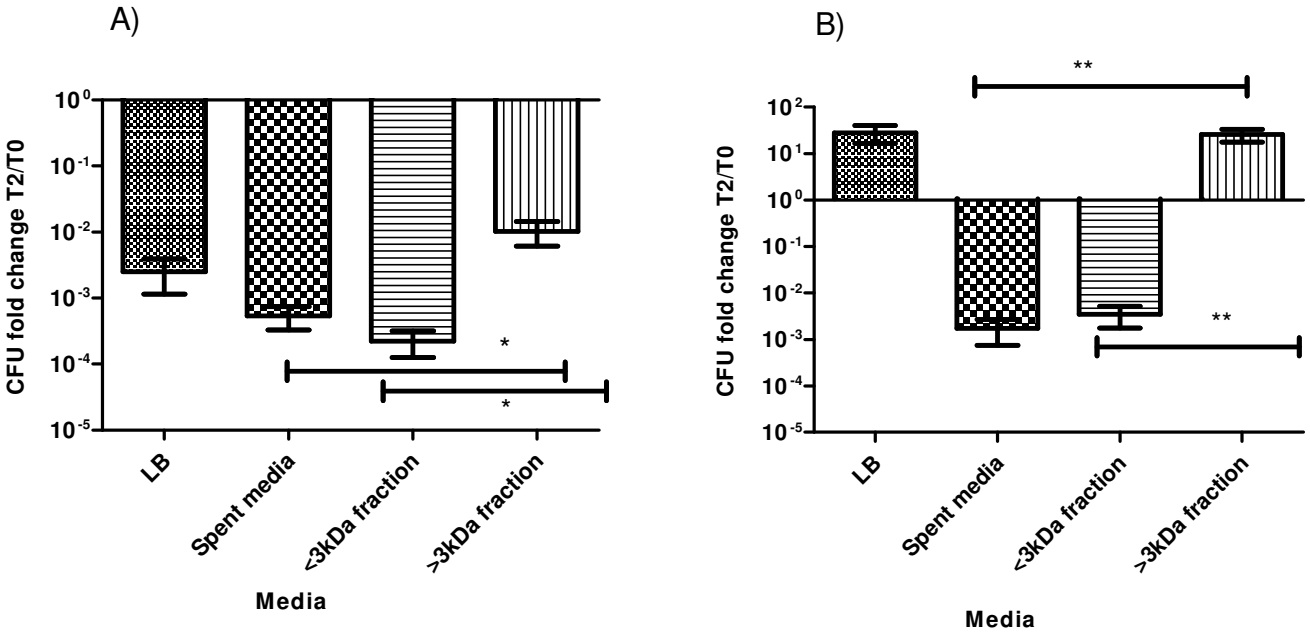

Figure 6.4 CFU fold change of *E. coli* cells expressing BPSS0390 in fractionated media at different cell densities A) high density (10^7) B) low density (10^5) for 2 hours. Stationary phase spent media was taken from a culture of *E. coli* MG1655 pBAD-BPSS0390 grown overnight to stationary phase. The spent media was fractionated into <3kDa and >3kDa fractions by centrifugation in a 3kDa spin column. Cultures were then filter sterilised and incubated with the relevant cell pellets. Unfractionated spent media and LB were also used as controls for comparison. Data shown is the average of 3 biological repeats. Error bars indicate SEM. *=p<0.05, **=p<0.01 student's t-test.

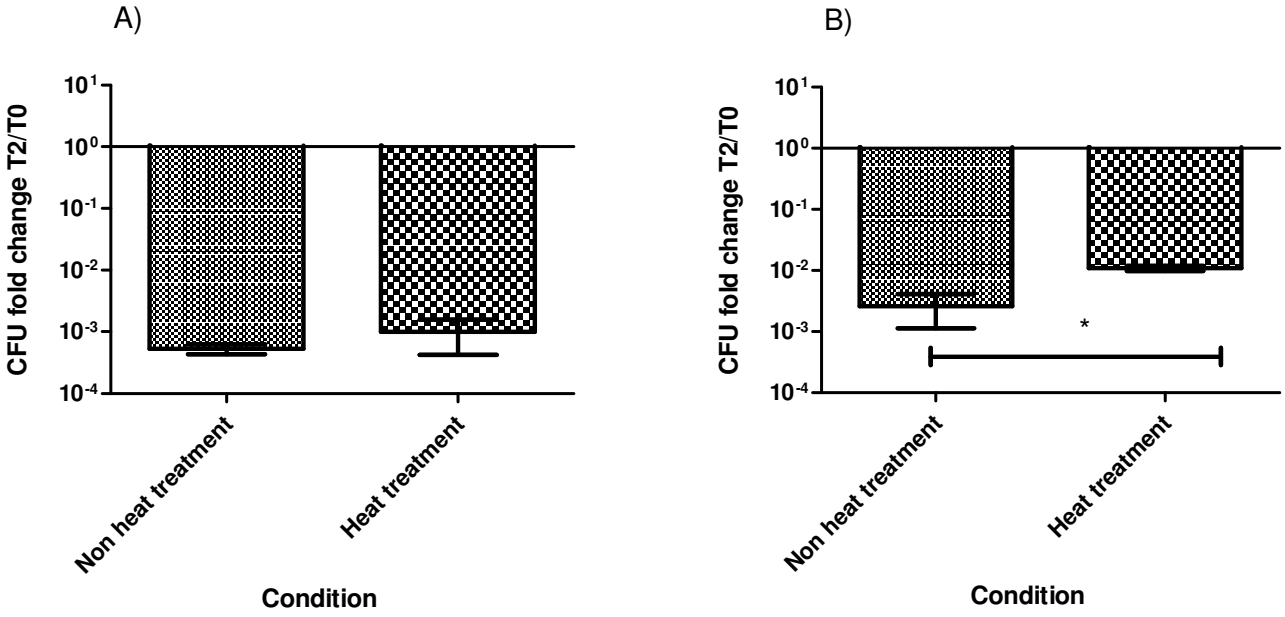

Figure 6.5 CFU fold change of *E. coli* MG1655 pBAD-BPSS0390 cultures expressing BPSS0390 grown in heat or non-heat treated spent media at different cell densities for 2 hours A) high density (10^7) B) low density (10^5). Spent media was taken from an overnight culture of the strain and either non- treated or boiled at 100 ^oC for 1 hour before allowing to cool, filter sterilising and then adding it to the appropriate cell pellets. Data shown is the average of 3 biological repeats. Error bars indicate SEM. *=$p<0.05$ student's t-test.

following BPSS0390 expression was similar in both heat treated spent media and non heat treated spent media (~10^{-3} fold change) (Fig 6.5A). However at low cell density the CFU fold reduction of *E. coli* cells following BPSS0390 expression was significantly less when the spent media had been heat treated compared to a non heat treated control (5x 10^{-3} compared to 10^{-2}) ($P<0.05$, student's t-test) (figure 6.5B). This suggested that the heat had partially affected the media in some way, possibly degrading or partially degrading an extracellular factor.

6.1.6 Acid treatment of spent media before BPSS0390 expression in *E. coli*

Spent media isolated from a stationary phase *E. coli* MG1655 pBAD-BPSS0390 culture was adjusted to pH 2 and then neutralised after l hour. *E. coli* MG1655 pBAD-BPSS0390 was grown to early exponential phase and harvested into high (10^7) or low (10^5) CFU/ml cell densities. High or low densities were then re-suspended in acid treated spent media and BPSS0390 expression was induced for 2 hours with 0.2% (w/v) arabinose. Figure 6.6 shows the CFU fold change. At both high and low densities the averaged difference between CFU numbers in acid treated media and untreated control was not significant. However, many of the individual biological repeats were significantly different, with *E. coli* MG1655 expressing BPSS0390 having less of a CFU fold reduction when grown in acid treated spent media.

6.1.7 Expression of BPSS0390 in *E. coli* with *B. thailandensis* spent media

B. thailandensis E264 was grown overnight in LB, centrifuged and filter sterilised to provide spent culture medium. In parallel *E. coli* MG1655 pBAD-BPSS0390 was grown to early exponential phase and the cells harvested by centrifugation. These pelleted cells were re-suspended in LB or in *B. thailandensis* E264 spent medium to final cell densities of 10^7 or 10^5 CFU/ml.

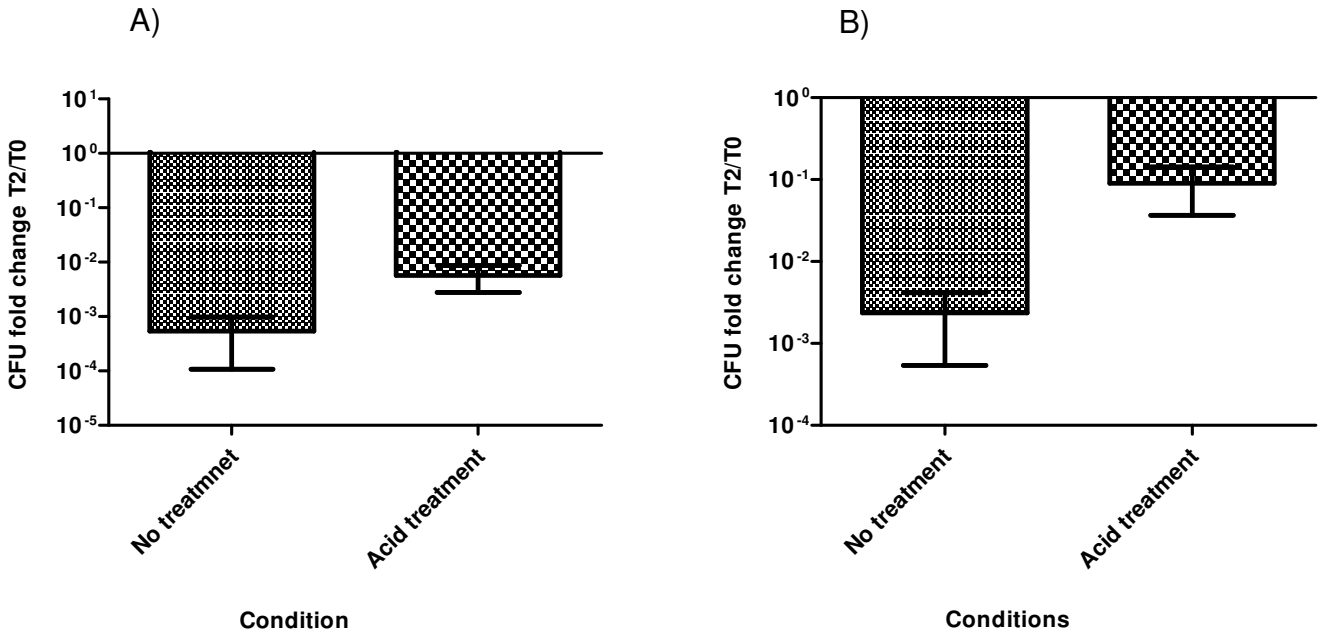

Figure 6.6 CFU fold change of *E. coli* MG1655 pBAD-BPSS0390 cultures expressing BPSS0390 grown in acid or non-acid treated spent media at different cell densities for 2 hours A) high density (10^7) B) low density (10^5). Spent media was taken from an overnight culture of the strain and non-treated or acid treated with 1M HCl to adjust the pH to 2 for 1 hour before neutralising back to pH 6.5 with 1M NaOH and filter sterilising. Exponential phase cultures at high or low densities were then re-suspended in the spent media. BPSS0390 expression was induced with 0.2% (w/v) arabinose. Data shown is the average of 3 biological repeats. Error bars show SEM.

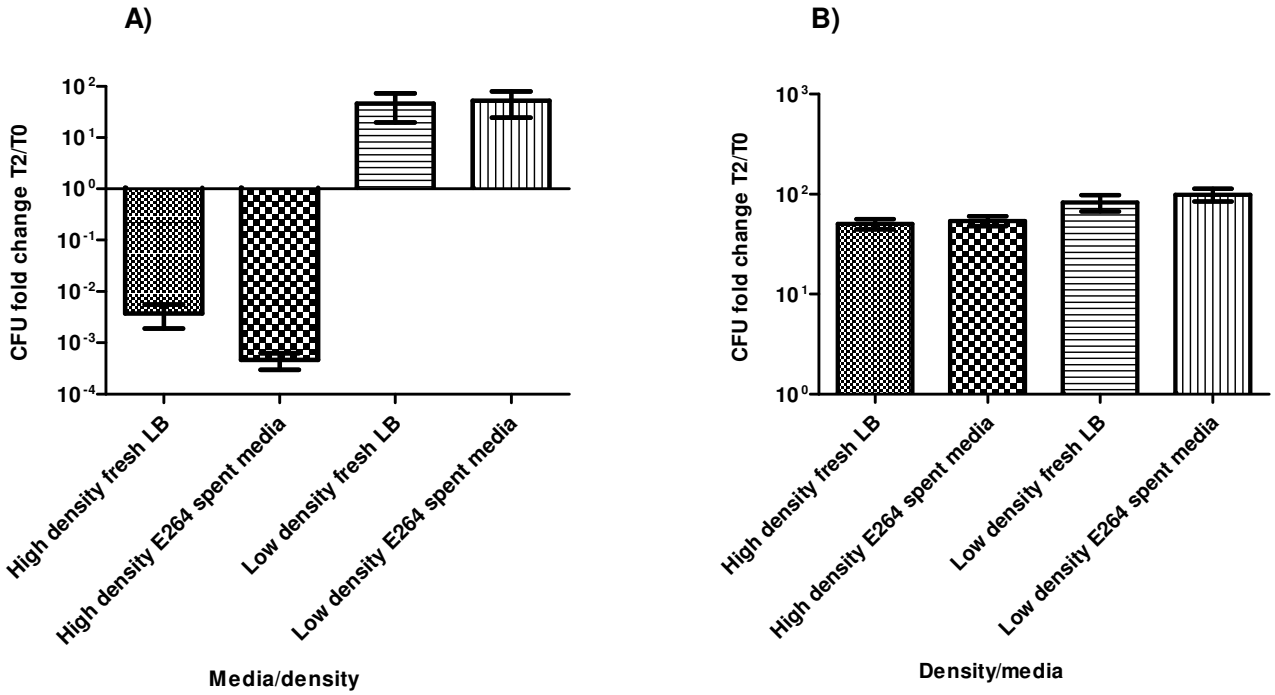

Figure 6.7 CFU fold change following induction of BPSS0390 expression by 0.2% (w/v) arabinose in *E. coli* MG1655 pBAD-BPSS0390 A) or addition of 0.2% (w/v) arabinose to *E. coli* pBAD B) for 2 hours at high (10^7 CFU/ml) or low (10^5 CFU/ml) cell densities in fresh media or *B. thailandensis* E264 spent media. Spent media was isolated from an overnight culture of E264 and added to the high or low density early exponential phase cultures of *E. coli* post filter sterilisation. Data shown are the average of 3 biological repeats and error bars show SEM.

0.2% (w/v) arabinose was added and the cultures incubated at 37 ^{o}C for 2 hours when cells were enumerated after plating suitable dilutions onto LB agar. There was no significant difference in the number of culturable *E. coli* MG1655 pBAD-BPSS0390 cells after re-suspension and growth in LB or in *B. thailandensis* E264 spent medium (figure 6.7)

6.1.8 Antibiotic treatment of *E. coli* MG1655 expressing BPSSS0390

6.1.8.1 Ciprofloxacin

A range of ciprofloxacin concentrations were incubated with 10^8 CFU/ml of *E. coli* MG1655 pBAD-BPSS0390 pME6032-BPSS0391 and the minimum inhibitory concentration (MIC) was calculated as 0.32 μg/ml (data not shown). Next *E. coli* MG1655/pBAD-BPSS0390/pME6032-BPSS0391 was grown to early log phase before inducing or repressing expression of BPSS0390 with 0.2% (w/v) arabinose or 0.2% (w/v) glucose respectively for 3 hours. The cultures were then standardised to an OD_{590}nm 0.5 before incubating with ciprofloxacin at 100 x MIC for 24 hours. Following incubation, cells were washed twice in LB to remove antibiotic and plated. Both time 0 and 24 hour cultures were plated onto LB agar plates supplemented with 1mM IPTG to induce BPSS0391 expression and resuscitate non-culturable cells. When BPSS0390 was repressed the persister frequency was approximately 10^{-6} following incubation with ciprofloxacin (Figure 6.8). However, when BPSS0390 expression was induced the persister frequency was significantly increased to approximately 10^{-3} ($p<0.05$).

6.1.8.2 Ciprofloxacin at different cell densities

It was hypothesised that the increase in persistence phenotype following BPSS0390 expression may be density dependent. *E. coli* MG1655 pBAD-BPSS0390 pME6032-

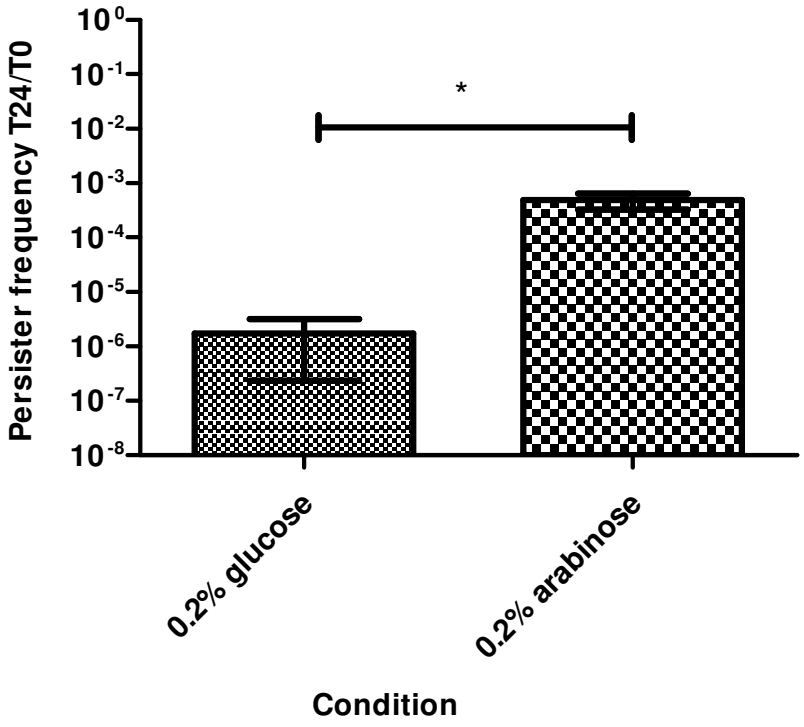

Figure 6.8 Persister frequency following 24 hour ciprofloxacin treatment of BPSS0390 repressed or expressed *E. coli* MG1655 pBAD-BPSS0390 pME6032-BPSS0391 cultures. Cultures were grown to early log phase before repressing or inducing expression of BPSS0390 for 3 hours with 0.2% (w/v) glucose or 0.2% (w/v) arabinose respectively. Cultures were then standardised to OD_{590}nm 0.5 before 100 x MIC (32 μg/ml) ciprofloxacin treatment for 24 hours. After incubation with antibiotic cultures were washed twice in LB and plated. T0 and T24 samples were plated onto LB agar supplemented with 1 mM IPTG. Persister frequencies were calculated as CFU numbers post antibiotic treatment divided by CFU numbers pre antibiotic treatment. The data shown is the average of 3 biological repeats. Error bars show SEM, *=$p<0.05$, student's t-test.

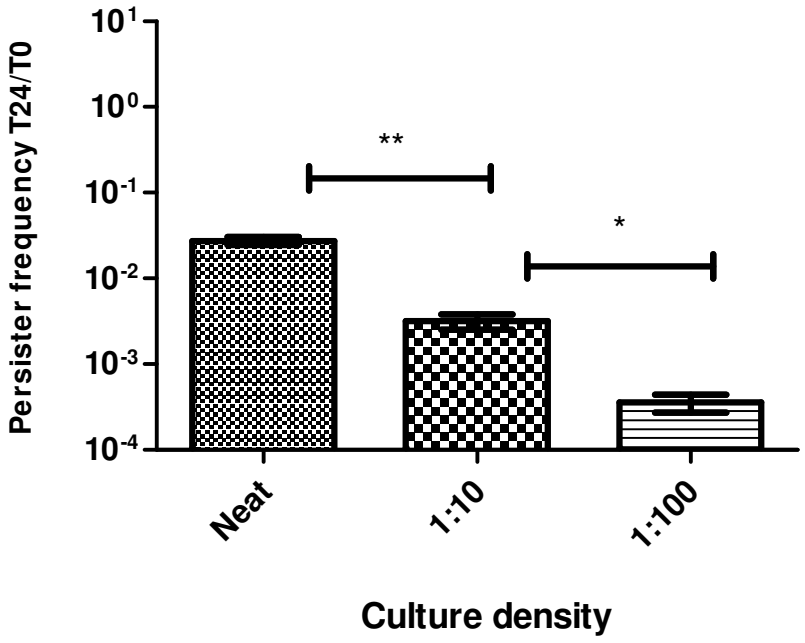

Figure 6.9 Persister frequency following 24 hours ciprofloxacin treatment of BPSS0390 expressed *E. coli* MG1655 pBAD-BPSS0390 pME6032-BPSS0391cultures at different cell densities. Cultures were grown to early log phase before taking a neat, 1 in 10 or 1 in 100 diluted culture and inducing BPSS0390 expression with 0.2% (w/v) arabinose for 3 hours. Cultures were then incubated in 24 well plates with 100 x MIC ciprofloxacin (32 μg/ml) for 24 hours. After the incubation cultures were washed twice in LB and plated onto LB agar supplemented with 1 mM IPTG for BPSS0391 expression to resuscitate non-culturable cells. T0 samples were also plated on these plates to resuscitate non-culturable cells. Data shown are a representative data set from 3 biological repeats. Error bars show SEM for this biological repeat. *=$p<0.05$, **=$p<0.01$ student's t-test.

BPSS0391 was grown to early exponential phase before taking a neat, 1 in 10 or 1 in 100 diluted culture and inducing expression of BPSS0390 with 0.2% (w/v) arabinose for 3 hours. A persister cell assay was then carried out. Figure 6.9 shows that as the cell density of the culture was diluted by 10 fold, the persister frequency decreased proportionally i.e. the 1:100 diluted culture had a persister frequency 10 fold lower than the 1:10 dilution and the 1:10 dilution had a frequency 10 fold lower than the neat culture (5×10^{-2}, $5x\ 10^{-3}$ and 5×10^{-4} respectively). The difference between each dilution was significant ($p<0.05$ or 0.01, student's t-test).

6.1.8.3 Ceftazidime

As BPSS0390 expression increased persister frequencies following ciprofloxacin treatment, it was next asked whether this was antibiotic specific. A range of ceftazidime concentrations were incubated with 10^8 CFU/ml of *E. coli* MG1655 pBAD-BPSS0390 pME6032-BPSS0391 and the minimum inhibitory concentration (MIC) was calculated as 0.2 μg/ml (data not shown). *E. coli* MG1655 pBAD-BPSS0390 pME6032-BPSS0391 was then grown to early log phase in LB before inducing or repressing expression of BPSS0390 with 0.2% (w/v) arabinose or 0.2% (w/v) glucose respectively. Ceftazidime was then incubated with cultures at 100 x MIC (20 μg/ml) using the same persister assay method as 6.1.8.1. When BPSS0390 was repressed with 0.2% (w/v) glucose, prior to 24 hour ceftazidime treatment, the resulting persister frequency was below the detectable level in this experiment i.e. $< 10^{-7}$ (figure 6.10). In contrast if BPSS0390 was expressed with 0.2% (w/v) arabinose, the resulting persister frequency following ceftazidime treatment increased to 10^{-4}. This showed that the protective effect following BPSS0390 expression was not specific to ciprofloxacin.

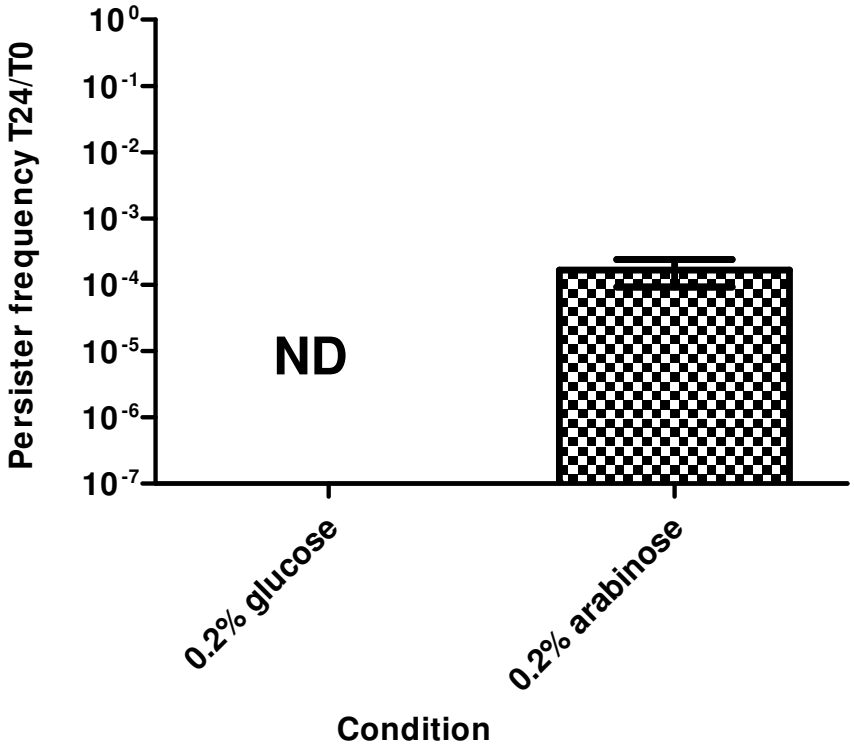

Figure 6.10 Persister frequency following 24 hour ceftazidime treatment of BPSS0390 repressed or expressed *E. coli* MG1655 pBAD-BPSS0390 pME6032-BPSS0391 cultures. Cultures were grown to early log phase before repressing or inducing expression of BPSS0390 for 3 hours with 0.2% (w/v) glucose or 0.2% (w/v) arabinose respectively. Cultures were then standardised to OD_{590}nm 0.5 before 100 x MIC (20 µg/ml) ceftazidime treatment for 24 hours. After static incubation with antibiotic, cultures were washed twice in LB and plated onto LB agar plates supplemented with 1 mM IPTG to induce BPSS0391 expression to resuscitate non-culturable cells. T0 samples were also plated onto these plates to resuscitate non-culturable cells. Persister frequency was calculated as CFU count post antibiotic treatment divided by CFU counts pre antibiotic treatment. The data shown is the average of 3 biological repeats. Error bars show SEM, "ND" indicated no detectable colonies post ceftazidime treatment.

6.2 Expression of BPSS0390 in *Burkholderia*

6.2.1 Creation and testing of the pSCrhaB3-BPSS0390 construct

The pBAD plasmid cannot replicate in *Burkholderia* therefore a plasmid (pSCrhaB3) containing a rhamnose inducible promoter and a trimethoprim resistance cassette was used for BPSS0390 expression (Cardona & Valvano, 2005). The BPSS0390 gene was digested from the pBAD-BPSS0390 construct using the *Nco*I and *Hind*III restriction enzymes and cloned into the corresponding restriction sites of pSCrhaB3 to create pSCrhaB3-BPSS0390. This plasmid was transformed into an *E. coli* DH5α strain selecting for transformants on LB trimethoprim plates. The *E. coli* DH5α/pSCrhaB3-BPSS0390 strain was used as the donor strain for conjugation into *B. thailandensis* E264, *B. pseudomallei* K96243 and *B. pseudomallei* K96243 *ΔBPSS0390-0391*.

The pSCrhaB3-BPSS0390 expression plasmid was first tested in the *E. coli* DH5α donor strain by growing cells to early log phase and inducing or repressing expression of BPSS0390 by addition of 0.2% (w/v) rhamnose or 0.2% glucose (w/v) respectively. Inducing expression of BPSS0390 from rhamnose inducible plasmid in *E. coli* DH5α caused growth inhibition assessed by OD_{590}nm but there was no subsequent reduction in CFU (data not shown).

6.2.2 Expression in *Burkholderia thailandensis* E264

A toxicity assay was carried out with *B. thailandensis* E264 harbouring pSCrhaB3-BPSS0390. The pSCrhaB3-BPSS0390 construct was conjugated into *B. thailandensis* E264 by plating a mixed culture of *E. coli* DH5α/pSCrhaB3, *E. coli* helper strain containing plasmid pRK2013 and *B. thailandensis* E264 onto LB agar containing trimethoprim for selection of the plasmid and gentamicin to kill the *E. coli* strains.

PCR was performed on a selection of colonies to confirm the presence of the pSCrhaB3-BPSS0390 plasmid. A PCR positive colony was used for further study.
Wild type *B. thailandensis* E264 cultures harbouring empty pSCrhaB3 plasmid were grown in the presence of 0.2% (w/v) glucose or 0.2% (w/v) rhamnose as controls. Under both conditions bacteria grew to similar ODs (data not shown).

In parallel *B. thailandensis* pSCrhaB3-BPSS0390 was grown to early log phase before inducing or repressing expression of BPSS0390 with 0.2% (w/v) rhamnose or 0.2% (w/v) glucose respectively for 5 hours (Figure 6.11). Under glucose repressed conditions the OD and CFU increased over the course of the experiment. Under inducing conditions the OD (figure 6.11A) and CFU/ml (figure 6.11B) profiles were different. The optical density increased by approximately 0.1 over the experiment. There was a slight increase in CFU after 1 hour but then cell numbers remained constant from hours 1 to 3 before reducing slightly from hours 3 to 5. This suggests that BPSS0390 caused growth inhibition in *B. thailandensis* E264.

6.2.3 Expression in *B. pseudomallei* K96243

The pSCrhaB3-BPSS0390 construct was next expressed in *B. pseudomallei* K96243 Conjugants were selected on LB agar plates containing gentamicin to kill *E. coli* and trimethoprim for selection of pSCrhaB3-BPSS0390. *B. pseudomallei* colonies were screened for pSCrhaB3-BPSS0390 using a PCR.

Overnight cultures of *B. pseudomallei*/pSCrhaB3-BPSS0390 were diluted 1:100 in fresh LB and supplemented with 0.2% (w/v) glucose or 0.2% (w/v) rhamnose for 8 hours to repress or induce expression of BPSS0390 respectively. CFU counts were determined every 2 hours. Figure 6.12 shows the resulting growth profile. Cultures with either glucose or rhamnose added grew similarly.

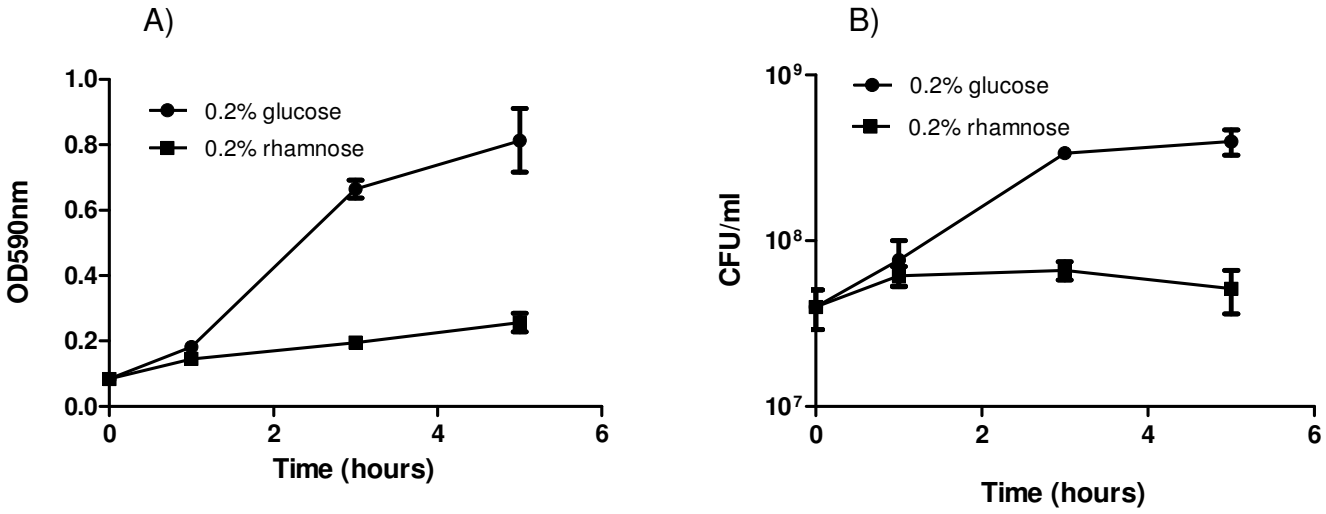

Figure 6.11 Growth profiles of *B. thailandensis* E264/pSCrhaB3-BPSS0390 with BPSS0390 expression repressed or induced with 0.2% (w/v) glucose or 0.2% (w/v) rhamnose respectively for 5 hours. Cultures were grown to early log phase before splitting the culture and repressing or inducing BPSS0390 expression. Samples were taken after 1, 3 and 5 hours and both the OD_{590}nm A) and CFU B) were determined. Data shown are the average of 3 biological repeats. Error bars show SEM.

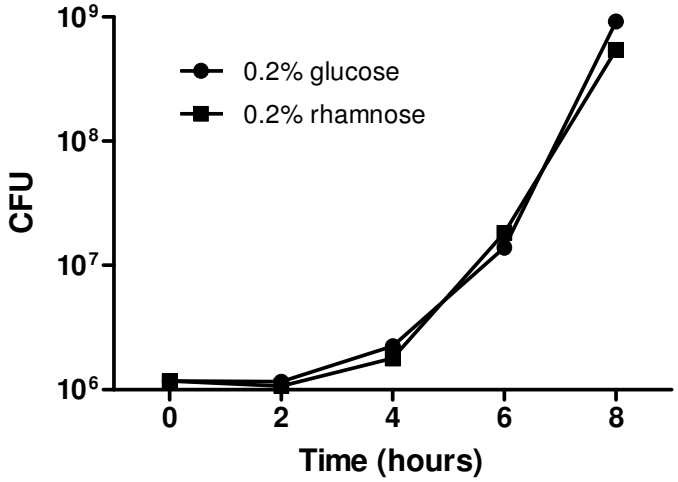

Figure 6.12 Growth profiles of *B. pseudomallei* K96243/pSCrhaB3-BPSS0390. Overnight cultures were diluted 1:100 in fresh LB before supplementing with 0.2% (w/v) glucose or 0.2% (w/v) rhamnose for repression or expression of BPSS0390 respectively. Samples were taken every 2 hours for 8 hours for CFU determination plating onto LB agar plates.

6.2.4 *B. pseudomallei* K96243 *ΔBPSS0390-0391*

6.2.4.1 Creation and confirmation of *ΔBPSS0390-0391* mutant

To determine if the lack of a growth inhibition phenotype following BPSS0390 expression in *B. pseudomallei* was due to endogenous BPSS0391 antitoxin, the BPSS0390-0391 system was deleted from *B. pseudomallei* K96243. A summary of this process is shown in figure 6.13. A PCR was set up to confirm if colonies picked after sucrose selection had reverted to wild type or had lost the BPSS0390-0391 locus following the second recombination event. Figure 6.14 shows an agarose gel with PCR amplified DNA from 6 potential mutant colonies using primers flanking the BPSS0390-0391 locus. It can be seen that 5 of the colonies (colonies 2-6) have the same banding pattern as the *B. pseudomallei* K96243 positive control i.e. they still contain the BPSS0390 and BPSS0391 genes in addition to 600bp upstream and downstream flanking regions. Colony 1 had a DNA band at approximately 800bp showing the BPSS0390-0391 locus had been deleted from this colony. This PCR product was sent for sequencing and the sequenced DNA product confirmed the deletion of the BPSS0390-0391 gene locus.

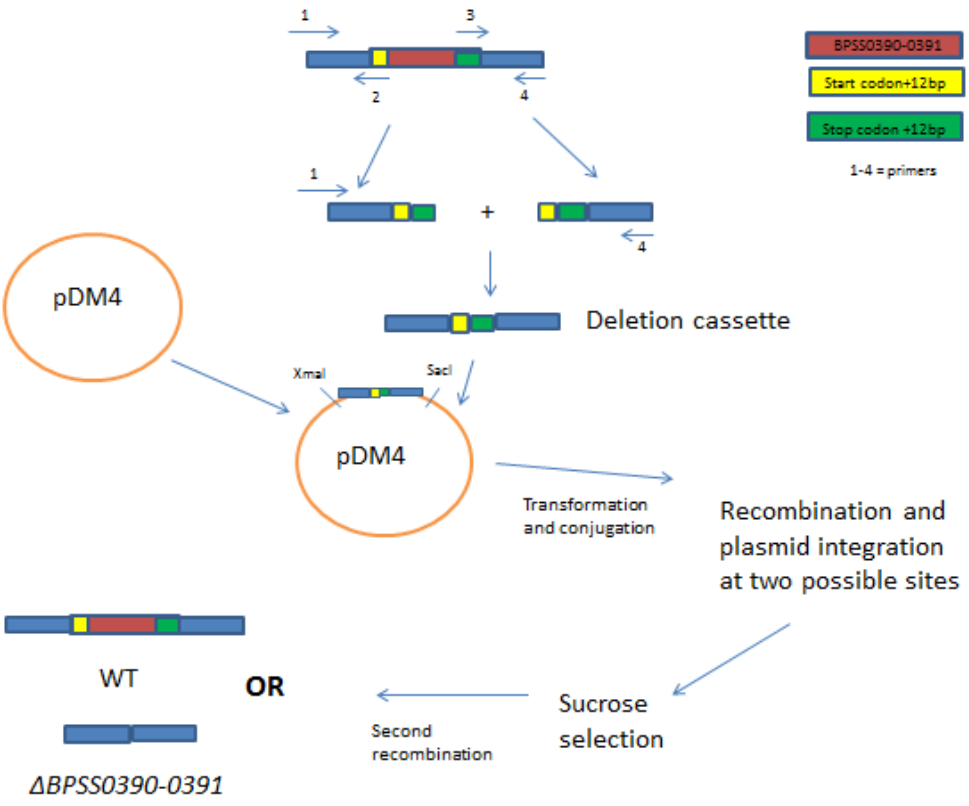

Figure 6.13 process of BPSS0390-0391 deletion using the *sacB* containing pDM4 integration plasmid. Primers were designed and used to amplify upstream and downstream regions flanking the BPSS0390-0391. Primers 2 and 3 also contained sequences specific for the start and end of the BPSS0390-0391 locus so the resulting deletion cassette could undergo homologous recombination. The upstream and downstream PCR products were then fused by PCR and cloned into PDM4 via the *Xma*I and *Sac*I restriction sites. The resulting plasmid construct was transformed into *E. coli* S17λ then conjugated into *B. pseudomallei* K96243. The plasmid then integrated into the K96243 genome by homologous recombination at 2 possible sites to create a merodiploid strain. PCR was then performed to confirm integration. Confirmed integrants were grown in LB and various dilutions were plated onto LB agar supplemented with 10% sucrose to drive *sacB* expression in pDM4, which caused a second recombination event. This recombination either caused cells to revert back to wild type or lose the BPSS0390-0391 loci.

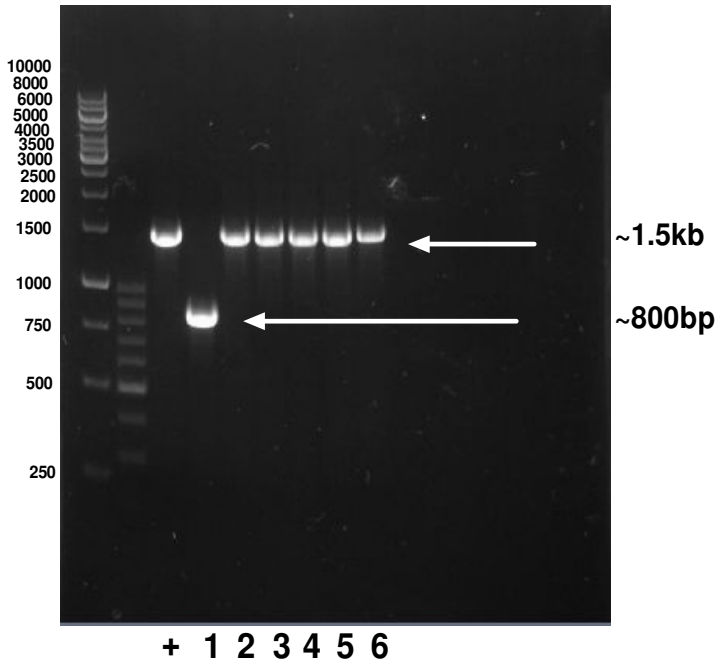

Figure 6.14 Gel image of potential *ΔBPSS0390-0391* mutants following sucrose selection. Primers used bound up and downstream of the left and right flanking regions of the BPSS0390-0391 locus. Template DNA was isolated by boiling cells in 20 µl water and then 5 µl was added to a PCR mix containing hot start taq. Following PCR 5 µl of each sample was mixed with 1 µl of 6 x loading dye and loaded onto a 1% agarose gel containing SYBR safe stain for DNA visualisation. Wild type *B. pseudomallei* DNA was used as a control (+) and 6 potential mutant colonies were screened (1-6). The gel was run at 180V for 20 minutes before visualisation under UV light.

6.2.4.2 Expression of BPSS0390 in *ΔBPSS0390-0391*

Next the pSCrhaB3-BPSS0390 plasmid was conjugated into *B. pseudomallei* K96243 Δ*BPSS0390-0391*. Mixed cultures of *E. coli* DH5α pSCrhaB3-BPSS0390, *E. coli* helper strain containing plasmid pRK2013 and *B. pseudomallei* K96243 *ΔBPSS0390-0391* were plated onto LB gentamicin and trimethoprim plates for selection of the pSCrhaB3-BPSS0390 construct and death of the *E. coli* strains. Control plates inoculated with the donor, helper or recipient had no colonies. The test plate had 5 colonies following 3 days growth. These colonies were re-streaked onto LB trimethoprim plates and grown in LB supplemented with trimethoprim and 0.2% (w/v) glucose before carrying out PCR using pSCrhaB3 specific primers. PCR amplification confirmed all 5 colonies contained the plasmid. A PCR positive colony was then grown for a subsequent toxicity assay. All of the colonies of the *B. pseudomallei ΔBPSS0390-0391* carrying the pSCrhaB3-BPSS0390 plasmid appeared to have a growth defect on plates and in broth. When colonies were re-streaked onto plates only small colonies were visible and in broth cultures could only grow to OD_{590}nm 0.6 before growth was inhibited.

B. pseudomallei ΔBPSS0390-0391 pSCrhaB3-BPSS0390 was grown overnight in LB before diluting in fresh LB and growing to an OD_{590}nm 0.1. Expression of BPSS0390 was then repressed or induced with 0.2% (w/v) glucose or 0.2% (w/v) rhamnose respectively for 8 hours. Both the OD_{590}nm and CFU/ml were determined every 2 hours. When glucose was added to the culture, the OD continued to increase until 0.6 over the 8 hours (Fig 6.15A). In contrast addition of rhamnose resulted in only a 0.05 increase in optical density over the same period. Figure 6.15B shows that when glucose was added to cultures the CFU/ml continued to increase for 6 hours and

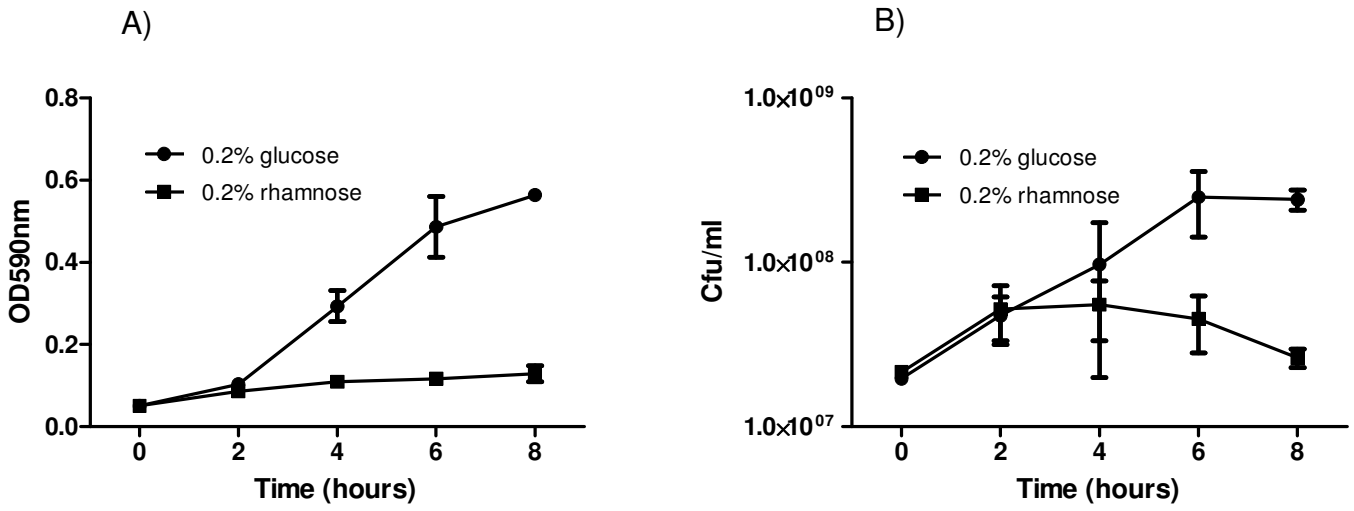

Figure 6.15 Growth profiles of *B. pseudomallei* K96243 *ΔBPSS0390-0391* /pSCrhaB3-BPSS0390 measuring either A) OD_{590}nm or B) CFU. ONCs were diluted 1 in 50 in fresh LB before growing at 37 ^{o}C until cultures reached OD_{590}nm 0.1. At this point cultures were split and BPSS0390 was either repressed or induced with 0.2% (w/v) glucose or 0.2% (w/v) rhamnose respectively for 8 hours. Samples were taken every 2 hours. Cells were plated onto LB agar supplemented with trimethoprim for CFU determination. Data shown is the average of 3 biological repeat. Error bars show SEM.

then plateaued. In contrast the addition of rhamnose resulted in the CFU count to increase by approximately 5 fold for the first 2 hours but then cell numbers stopped increasing from hours 2 to 4 and declined from hours 4 to 8 to a number similar to time 0. *B. pseudomallei* K96243 *ΔBPSS0390-0391* cultures harbouring empty pSCrhaB3 were also set up as a controls growing in the presence of 0.2% (w/v) glucose or 0.2% (w/v) rhamnose. These cultures grew to similar optical densities and cell densities in both sugar conditions (data not shown). This suggests that BPSS0390 is active in the *B. pseudomallei* K96243 *ΔBPSS0390-0391* strain.

6.2.5 Expression of BPSS0390 in *B. pseudomallei ΔBPSS0390-0391* grown in spent media

Spent media was prepared by growing *B. pseudomallei ΔBPSS0390*-0391 pSCrhaB3-BPSS0390 in LB overnight and then centrifuging and filter sterilising the extracellular fluid. In parallel an overnight culture of *B. pseudomallei ΔBPSS0390*-0391 pSCrhaB3 or *B. pseudomallei ΔBPSS0390*-0391 pSCrhaB3-BPSS0390 was diluted in fresh LB and grown to OD_{590}nm ~ 0.1. High density (10^7 CFU/ml) or low density (10^5 CFU/ml) cultures were harvested and the cell pellets were re-suspended in either fresh LB or spent media. BPSS0390 expression was then induced by addition of 0.2% (w/v) rhamnose for 24 hours.

B. pseudomallei ΔBPSS0390-0391 pSCrhaB3 had a CFU count increase over the experiment at both high and low cell densities in both fresh LB and spent media (Figure 6.16A). There was no significant difference between the CFU increases in either media.

B. pseudomallei ΔBPSS0390-0391 pSCrhaB3-BPSS0390 at high density in either spent media or fresh LB resulted in a CFU decrease. The difference between the

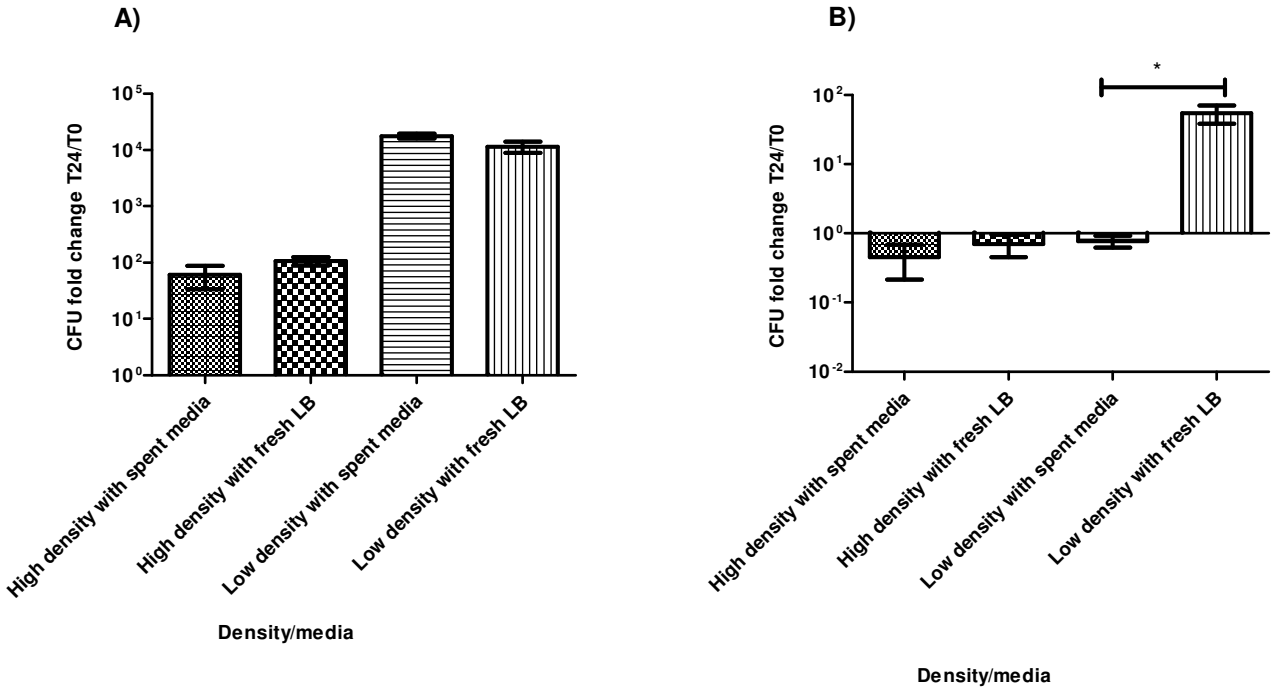

Figure 6.16 CFU fold change of A) *B. pseudomallei* K96243 ΔBPSS0390-0391/pSCrhaB3 or B) *B. pseudomallei* K96243 *ΔBPSS0390-0391*/pSCrhaB3-BPSS0390 after 24 hours growth in fresh LB or spent media at high (10^7) or low (10^5) densities in the presence of 0.2% (w/v) rhamnose for BPSS0390 expression. Cultures were grown to early log phase before adding either spent media isolated from an overnight culture of *B. pseudomallei* K96243 *ΔBPSS0390-0391*/pSCrhaB3-BPSS0390 by centrifugation and filter sterilisation or fresh LB to the high and low density cultures and inducing with rhamnose for 24 hours. Data shown are the average of 3 biological repeats. Error bars show SEM, *=$p<0.05$, student's t-test.

CFU reductions was not significant (Figure 6.16B). At low density, there was a decrease in CFU relative to time 0 in spent media. In fresh LB the CFU fold change increased by nearly 100 fold. The difference between the CFU fold changes in the different media at low density was significant ($p<0.05$).

6.2.6 Expression of BPSS0390 in *B. pseudomallei ΔBPSS0390-0391* with *E. coli* spent media

E. coli MG1655 pBAD-BPSS0390 was grown overnight in fresh LB, centrifuged and filter sterilised to isolate spent medium. In parallel overnight cultures of *B. pseudomallei ΔBPSS0390-0391* pSCrhaB3-BPSS0390 or a *B. pseudomallei ΔBPSS0390-0391* pSCrhaB3 control grown in LB supplemented with 0.2% (w/v) glucose were diluted in fresh LB media and grown to early exponential phase. High (10^7 CFU/ml) or low (10^5 CFU/ml) cell densities were re-suspended in fresh LB or in spent *E. coli* media. BPSS0390 expression was then induced by addition of 0.2% (w/v) rhamnose for 24 hours. The resulting CFU fold change for *B. pseudomallei ΔBPSS0390-0391/*pSCrhaB3 was increased when cells were grown in spent media or fresh LB at both high and low densities (Figure 6.17A).

B. pseudomallei ΔBPSS0390-0391 pSCrhaB3-BPSS0390 had a minimal CFU fold decrease when grown in spent media at high densities, whereas in LB there was no CFU fold change. The difference was not significant (Figure 6.17B).

At low cell densities the CFU decreased by approximately 10 fold in *E. coli* spent media. In comparison in fresh LB the CFU increased by approximately 100 fold. The difference in CFU fold change was significant ($p<0.01$, student's t-test).

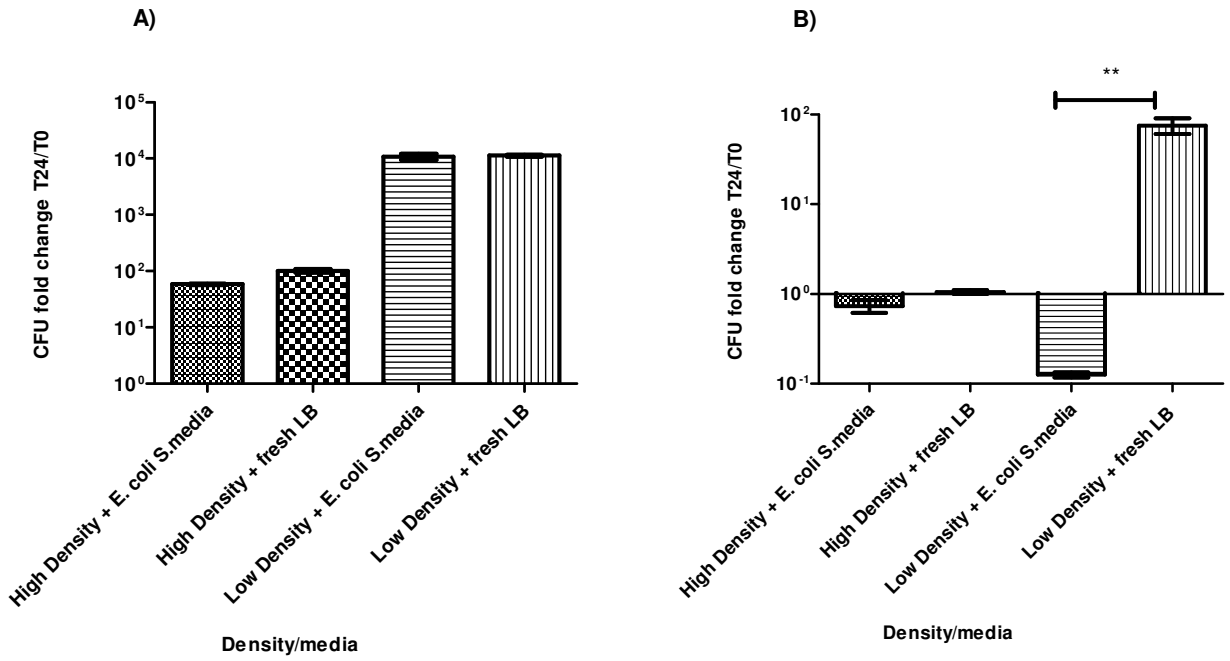

Figure 6.17 CFU fold change of A) *B. pseudomallei* K96243/pSCrhaB3 or B) *B. pseudomallei* K96243/pSCrhaB3-BPSS0390 after 24 hours growth in fresh LB or spent media from *E. coli* at high (10^7) or low (10^5) densities in the presence of 0.2% (w/v) rhamnose for BPSS0390 expression. Cultures were grown to early log phase before adding either spent media isolated from overnight cultures o*f E. coli* MG1655 pBAD-BPSS0390 or fresh LB to the high or low density cultures and inducing with 0.2% (w/v) rhamnose for 24 hours. Data shown is the average of 3 biological repeats. Error bars show SEM, **=$p<0.01$, student's t-test.

6.3 Characterisation of *B. pseudomallei* K96 Δ*BPSS0390-0391*

6.3.1 Persister assay with ciprofloxacin

Both *B. pseudomallei* K96243 and *B. pseudomallei* K96243 Δ*BPSS0390-0391* were grown in LB overnight and the next day 10^8 cells were mixed with 100 x MIC ciprofloxacin in a 24 well plate. The bacteria were then statically incubated for 24 hours at 37 ^{o}C. Cells were then washed to remove antibiotic and plated onto LB agar. Figure 6.18 shows the persister frequencies for wild type *B. pseudomallei* K96243 and the *B. pseudomallei* K96243 Δ*BPSS0390-0391* mutant. *B. pseudomallei* K96243 wild type had a persister frequency of approximately 3 x 10^{-3}, while the *B. pseudomallei* Δ*BPSS0390-0391* mutant had a persister frequency of approximately 6 x 10^{-4}. The difference between these frequencies was not significant following a student's t-test.

6.3.2 Ciprofloxacin persister assay on different aged cultures

B. pseudomallei K96243 and *B. pseudomallei* K96243 Δ*BPSS0390-0391* were grown overnight in LB. At 17 hours (early stationary) or 22 hours (late stationary) post inoculation, 10^8 cells were incubated with 100 x MIC ciprofloxacin for 24 hours. At early stationary phase there was a difference between persister frequencies but this was not significant. When looking at late stationary phase cultures the persister frequencies were similar at around 8 x 10^{-4} (figure 6.19).

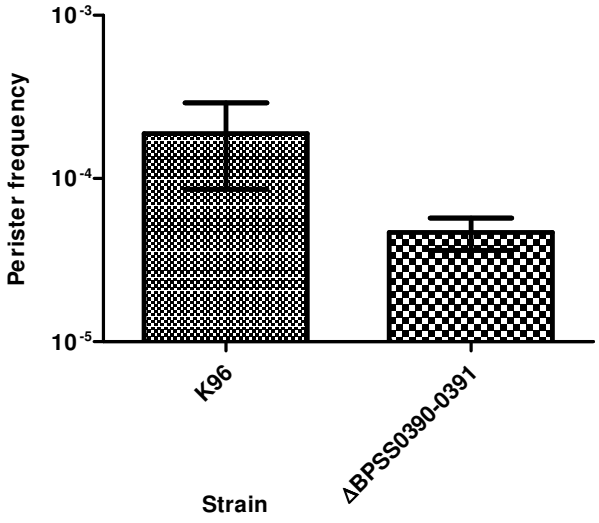

Figure 6.18 Persister frequency of *B. pseudomallei* K96243 or *B. pseudomallei* K96243 *ΔBPSS0390-0391* treated with 100 x MIC (200 μg/ml) of ciprofloxacin for 24 hours. Over night cultures of both strains were diluted to an OD_{590}nm 0.2 (2 x 10^8 CFU/ml) before mixing 1:1 with ciprofloxacin diluted in LB in a 24 well plate. Cultures were incubated statically at 37 ^oC. After incubation cultures were washed in LB twice before plating onto LB agar plates. T0 samples were also plated onto LB agar. Persister frequency was calculated as CFU numbers post antibiotic treatment divided by CFU numbers pre antibiotic treatment. The data shown is the average of 6 biological repeats. Error bars show SEM.

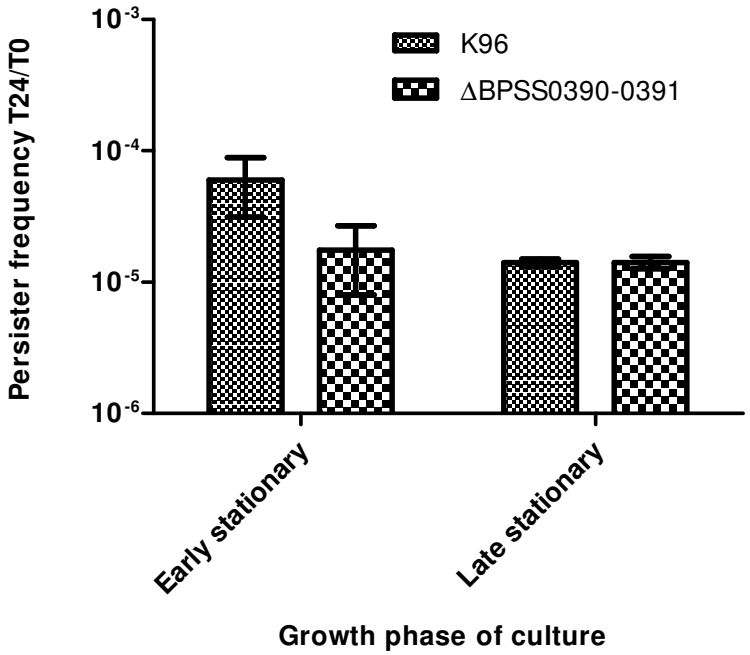

Figure 6.19 Persister frequency of *B. pseudomallei* K96243 or *B. pseudomallei* K96243 *ΔBPSS0390-0391* treated with 100 x MIC (200 μg/ml) of ciprofloxacin for 24 hours. Overnight cultures of both strains were diluted to an OD_{590}nm 0.2 (2 x 10^8 CFU/ml) before mixing 1:1 with ciprofloxacin diluted in LB in a 24 well plate. Early stationary refers to Overnight cultures 17 hours post inoculation (OD_{590}nm ~2.5) and late stationary refers to overnight cultures 22 hours post inoculation (OD_{590}nm ~3.5). Cultures treated with ciprofloxacin were incubated statically at 37°C. After incubation cultures were washed in LB twice before plating onto LB agar plates. T0 samples were also plated onto LB agar. The data shown is the average of 3 biological repeats. Error bars show SEM.

6.3.3 Transcriptomics data

The BPSS0390 and BPSS0391 genes were searched for in a transcriptomics data set (provided by Catherine Ong at the Genome Institute of Singapore) to determine if the genes were up or down regulated in *B. pseudomallei* in response to different stress conditions. Table 6.0 lists the stress conditions which affected BPSS0390 and BPSS0391 expression. The table shows that both genes were up regulated in response to more stresses than down regulated. Both genes were up regulated in response to cadmium and oxidative stress but also up regulated in an *in vitro* infection assay (mouse leukemic monocyte macrophages). BPSS0390 was also up regulated in response to lead, while BPSS0391 showed up regulation when cells were exposed to chloramphenicol. Both genes were down regulated when cold stressed and BPSS0390 also showed down regulation to osmotic stress. Interestingly a quorum sensing mutant of *B. pseudomallei* (insertion inactivation of the N-actylhomoserine lactone synthase) grown in normal LB conditions had down regulated levels of both BPSS0390 and BPSS0391 compared to wild type *B. pseudomallei* K96243.

6.3.4 Hydrogen peroxide stress

B. pseudomallei K96243 or *B. pseudomallei* K96243 Δ*BPSS0390-0391* were grown overnight in LB before centrifuging and re-suspending 10^8 bacteria in 15 mM hydrogen peroxide for 10 minutes. Following hydrogen peroxide treatment cells were centrifuged and washed in LB to remove residual hydrogen peroxide and then plated onto LB agar plates. The survival frequencies for both the wild type *B. pseudomallei* K96243 strain and the Δ*BPSS0390-0391* strain of *B. pseudomallei* were similar at approximately 10^{-3} (Figure 6.20).

Table 6.0 Stress conditions in which BPSS0390 and BPSS0391 were up or down regulated based on microarray data sets generated by comparing mRNA levels of *B. pseudomallei* K96243 grown in LB and LB containing a specific stress element. * indicates comparison of mRNA levels for mutant and wild type both grown in LB rather than a stress condition.

Gene name	**Up/down regulated**	**Stress condition**
BPSS0390	Up	Cadmium (200 μM)
		Lead (200 μM)
		In Vitro infection RAW 264.7
		Nutrient deprivation
		Oxidative stress (100 mM H_2O_2)
	Down	Osmotic (2 M Sorbitol)
		Cold stress (4^{o}C)
		Quorum sensing mutant*
BPSS0391	Up	Chloramphenicol (8 μg/ml)
		Cadmium (200 μM)
		In Vitro infection RAW 264.7
		Oxidative stress (100 mM H_2O_2)
	Down	Quorum sensing mutant*
		Cold stress (4 ^{o}C)

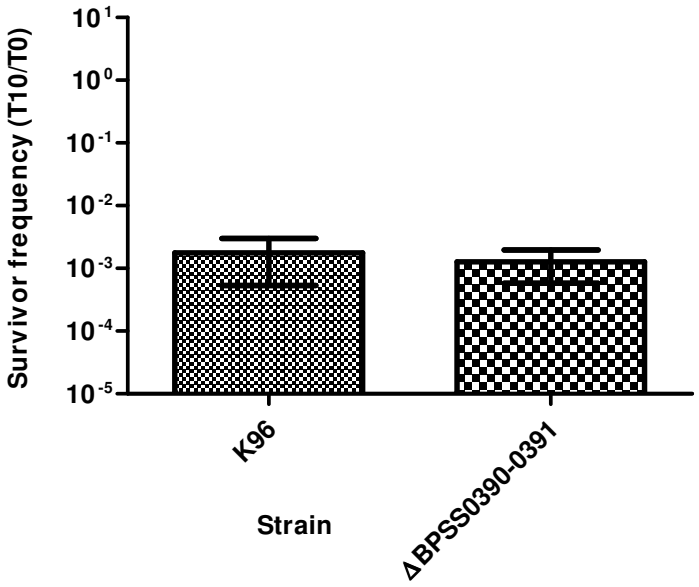

Figure 6.20 Survivor frequencies of *B. pseudomallei* K96243 or *B. pseudomallei* K96243 *ΔBPSS0390-0391* treated with 15 mM hydrogen peroxide for 10 minutes. Overnight cultures were diluted to 10^8 CFU/ml before centrifuging and re-suspending the cell pellet in hydrogen peroxide diluted in LB. After 10 minutes cells were washed twice in LB to remove the stress. Samples taken pre and post stress were plated onto LB agar plates. Survival frequencies were calculated as CFU counts after 10 minutes stress divided by time 0. The data shown is the average of 3 biological repeats and error bars show SEM.

6.3.5 Cadmium sulphate stress

10^8 bacterial cells of *B. pseudomallei* K96243 or *B. pseudomallei* K96243 *ΔBPSS0390-0391* overnight cultures grown in LB were mixed at a 1:1 ratio of cells with cadmium sulphate (200μM or 50 mM) diluted in LB and incubated in 24 well plates at 37 ^oC for 24 hours. In 200 μM cadmium sulphate the wild type *B. pseudomallei* strain and *B. pseudomallei ΔBPSS0390-0391* mutant CFU counts increased over 24 hours. In 50 mM cadmium sulphate the CFU counts decreased but gave varied survival frequencies following washing and plating (data not shown). This high concentration of cadmium (50 mM) precipitated in the wells and was also deposited with the cell pellet on washing. It was difficult to remove the cadmium and cells were still subjected to the stress on plating onto LB agar for enumeration.

To overcome this precipitation problem the heavy metal was added to LB agar and plates were made containing various concentrations of cadmium. Both wild type *B. pseudomallei* and the *B. pseudomallei* Δ*BPSS0390-0391* mutant were diluted to a working concentration of 10^8 CFU/ml and were plated onto the LB agar plates containing the different concentrations of cadmium. At 2.5 mM cadmium sulphate there was no reduction in CFU counts compared to the CFU count on LB agar only (figure 6.21). At 5 mM there was a slight decrease in CFU relative to the untreated control for either the wild type or the *B. pseudomallei* Δ*BPSS0390-0391* mutant. The difference was significant between the 2 strains showing that the mutant survives stress better than the wild type ($p< 0.01$, student's t-test). At 10 mM there were no detectable cells following 48 hours growth on the plate for either of the strains.

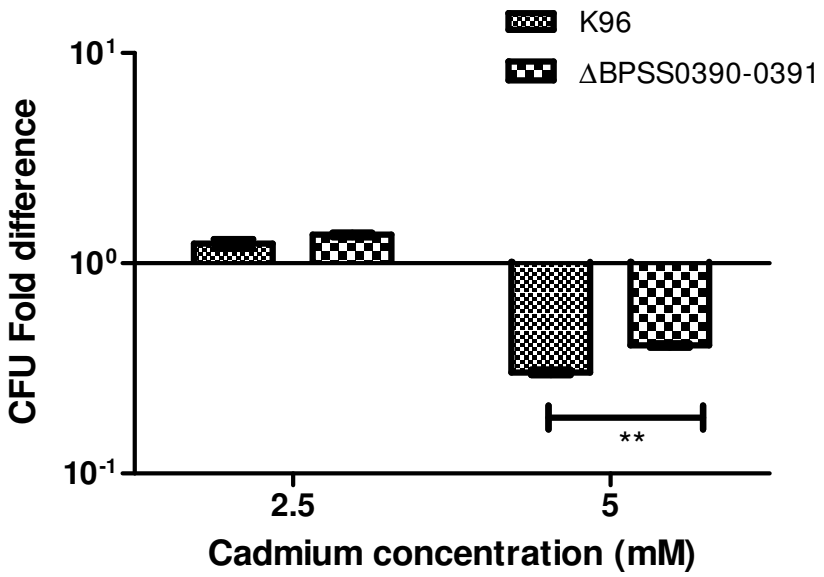

Figure 6.21 CFU fold change of *B. pseudomallei* K96243 *and B. pseudomallei* K96243 *ΔBPSS0390-0391* treated with cadmium sulphate compared to untreated controls. Overnight cultures were diluted to a cell density of 10^8 CFU/ml before plating onto LB agar plates containing 0, 2.5, 5 and 10 mM of cadmium sulphate. Plates were incubated for 48 hours at 37 ^oC for growth of colonies before counting. Data show the average of 3 biological repeats. Error bars show SEM, **=p<0.01, student's t-test.

6.4 Discussion

In chapter 3 it was shown that the BPSS0390 and BPSS0391 proteins have homology to HicA and HicB of the HicAB locus and that expression of the BPSS0390 and BPSS0301 genes displayed characteristics of the *hicA and hicB* genes from *E. coli,* i.e. a reduction in CFU following toxin expression and resuscitation of growth by the antitoxin. Live/dead staining of *E. coli* cells following expression of the BPSS0390 toxin revealed a slight increase in the amount of dead cells compared to the control culture but the amount of dead cells observed cannot explain a 10,000 fold reduction in CFU. It appears likely that the majority of the cells were entering into a state of dormancy that although non-culturable, were still viable. This observation was also seen with the BPSS1584 (HipA) toxin.

It appears that a critical cell density is necessary for reduction in CFU phenotype when expressing the *hicA* toxin in *E. coli*. The results also show that spent media had an enhancing effect on the reduction on CFU phenotype compared to fresh media. This was particularly evident when growing low density exponential phase *E. coli* cultures expressing *hicA* in spent media taken from stationary phase *E. coli* cultures. Fractionating the spent media showed that the <3kDa fraction was responsible for enhancing the phenotype of *hicA* in a similar manner to *hipA*. It was possible that enhancement of the toxin's activity by some extracellular component was restricted to expression in *E. coli* and that expression of the *hicA* toxin in *B. pseudomallei* would not involve such a component. However, spent medium from *E. coli* or *B. pseudomallei* had similar properties. The fact that spent media from both the native bacteria and the foreign *E. coli* could affect expression suggests a common extracellular compound between the species. Use of *B. thailandensis* spent media on

E. coli cells expressing *hicA* did not have the enhancing affect suggesting that this organism lacks the component needed for this enhancing effect.

As discussed in previous chapters it is possible that the extracellular component is a quorum sensing like factor. Interestingly the transcriptomic data shows that BPSS0390 and BPSS0391 genes are down regulated in the quorum sensing mutant lacking N-acylhomoserine lactone synthase. This provides further evidence for the involvement of quorum sensing in the activity of TA systems and persister cell formation. Other groups have shown that persister cell frequencies can be increased by signalling chemicals such as indole in *E. coli* and pyocyanin and acyl-homoserine lactone 3-OC12-HS in *P. aeruginosa* (Moker*, et al.*, 2010, Vega*, et al.*, 2012). The signal may be a protein as heat treatment of the spent media reduced the enhancing ability of the media when added to *hicA* expressing *E. coli.* This was particularly evident at lower cell densities. Acid treatment also had a partial affect on the spent media implying the increase in hydrogen ions may have de-stabilised a protein or interacted with a signalling chemical component to partially inactivate it. On the other hand neutralising the acid treated spent media with NaOH would have increased the salt concentration of the media and this may have affected downstream protein synthesis or activity of the HicA toxin rather than the acid directly. It would have been interesting to compare the proteome profiles of *B. pseudomallei*, *B. thailandensis* and *E. coli* spent media to decipher any commonalties or differences that could account for an extracellular protein signal.

Detection of a toxin phenotype following expression of the *hicA* toxin was not possible in wild type *B. pseudomallei* K96243. This is not surprising as it was also not possible to express *E. coli hipA* in wild type *E. coli* MG1655. Other groups have also observed this issue expressing some toxins in their native wild type host (Fiebig,

et al., 2010, Sevillano*, et al.*, 2012). It is likely that the lack of phenotype is due to endogenous chromosomally encoded antitoxin sequestering the recombinant toxin protein. Conversely, when growing the *B. pseudomallei* Δ*BPSS039-0391 (hicAB)* stain harbouring plasmid cloned *hicA,* even repression of expression by glucose prevented the strain from growing to stationary phase. This indicates that even leaky expression of the toxin was capable of causing growth arrest and this occurred once cells reached mid log phase densities. Again this suggests that there is a factor in the media that enhances the toxicity and that accumulates after the log phase. Expression of the *hicA* gene in the related organism *B. thailandensis* did cause growth arrest but there was no reduction in CFU. This could be due to the *hicB* homologue in the *B. thailandensis* partially sequestering the toxin activity preventing its full function. Another explanation is that it lacks the extracellular factor required to enhance the non-culturability phenotype.

Expression of the *hicA* toxin increased antibiotic tolerance of an *E. coli* culture to 2 different families of antibiotic, the fluoroquinolone ciprofloxacin and the cephalosporin ceftazidime. This suggests that the BPSS0390 toxin directly or indirectly shuts off both DNA replication and cell division as the antibiotics target DNA gyrase and cell wall synthesis respectively. Jorgensen *et al* showed that the HicA toxin was an RNase that could degrade mRNA and tmRNA independent of translation (Jorgensen*, et al.*, 2008). In their study they showed that while the rate of translation reduced after *hicA* expression, the rate of DNA and RNA synthesis remained constant. In their study they only looked at the synthesis of DNA and RNA 1 hour after *hicA* expression, whereas in this study the BPSS0390 toxin was expressed for 3 hours before antibiotic treatment. It is likely that as translation reduces, the proteins needed for transcription and DNA synthesis will be depleted over time

preventing replication and division thus rendering the cells dormant explaining their increased tolerance to both antibiotics.

Inducing expression of *hicA* at different cell densities in *E. coli* caused different persister frequencies following ciprofloxacin treatment. This is not surprising since the toxin only induces the dormancy phenotype once cells have reached a certain density. When *hicA* was expressed at high densities for 3 hours the cells were already at the threshold density for dormancy induction. However at the lower density after the 3 hours the cell culture density would only just have reached the threshold density meaning fewer cells will have entered into the dormant state. Thus following antibiotic treatment, the persister frequency was higher in the cultures that have more dormant cells that are antibiotic tolerant compared to cultures with fewer dormant cells.

Although most studies assaying differences between persister frequencies of a wild type strain and the corresponding toxin-antitoxin systems deletion mutant have proven unsuccessful, it was hypothesised that different TA systems may respond to different stresses and therefore a difference will only be seen if treated with the correct stress. As transcriptomics data showed up regulation of the *hicBA* locus in response to different stresses, it seemed sensible to test these stresses in addition to the ciprofloxacin antibiotic on the Δ*hicBA* mutant and compare this to wild type *B. pseudomallei* K96243. Following the experimentation there did appear to be some difference when treating with ciprofloxacin, with the mutant forming fewer persisters. However this phenotype varied between replicates and on average there was no significant difference. After consulting the literature it was apparent that the difference between replicates could be due to the age of culture used, as persister phenotypes can be masked as the cultures ages (Luidalepp*, et al.*, 2011). When

repeating the assays from 2 different aged cultures, there was more of a difference in early stationary phase cultures compared to late stationary phase but the difference was still not significant. This implies that there may be a subtle difference in persisters when removing the *hicAB* loci but persister cell production seems to be a redundant process following ciprofloxacin stress. This was also the case with hydrogen peroxide. Treatment of the 2 strains with varying concentrations of cadmium showed that at 5 mM the mutant actually survived better than the wild type, although higher concentrations prevented growth of both strains. Perhaps this is because another TA system is overcompensating for the loss of *hicAB* or that the HicA toxin or HicB antitoxins are involved in cell death in response to cadmium.

Chapter 7

Functional and structural characterisation of the BPSS0390 and BPSS0391 proteins

7.0 Introduction

Data presented in chapters 3 and 6 show that the BPSS0390-0391 (HicBA) TA system can cause functional growth restriction, CFU reduction and resuscitation phenotypes when expressed in either *E. coli* or *B. pseudomallei.* Jorgensen *et al* showed similar results when expressing *hicA* and *hicB* in *E. coli*. Although data has been presented showing the HicA toxin can degrade RNA, the catalytic regions of the toxin that can perform this degradation are unknown (Jorgensen*, et al.*, 2008). It is also not known how the HicA and HicB proteins interact, and in what ratios, to form the TA complex. The HicBA complex is also assumed to bind to its own promoter region to regulate expression but how this is achieved is unknown.

Identification of catalytic and binding residues of proteins can be achieved by site directed mutagenesis and then screening for loss of function. To determine where these residues sit in the protein(s), the structure of the protein(s) or complex may need to be solved. This can provide useful information about the substrate binding region(s) and the mechanism for catalysis based on the position and nature of neighbouring residues. To solve the structure(s) of proteins to high resolution either X-ray crystallography or NMR can be used.

X-ray crystallography has been the most widely used approach for structure determination of protein and protein complexes. The molecular sizes of proteins, determined by X-ray crystallography with modern synchrotron facilities ranges from a small protein up to the large 70S ribosomal complex (~2,500 kDa). However, the crystallization of the solution is not always straightforward. There are many unpredictable variables and multiple conditions that may need to be tried to get crystals for downstream X-ray diffraction (Jung & Lee, 2004). NMR analysis can be performed on proteins in solution similar to physiological conditions. Dynamic

processes can also be studied. The current drawback of NMR is that it is restricted to small proteins. This is due to the amount of data processing needed to analyse the various spectra produced and due to limitations in spectrophotometers. Automated analysis tools have been developed that speed up analysis, although manual analysis and correction is still currently required (Ab*, et al.*, 2006, Gronwald & Kalbitzer, 2010)

In order to isolate proteins for structural study they have to be purified. This involves adding a tag for affinity chromatography such as a histidine based tag that can bind to nickel, a chitin binding protein (CBP) that can bind chitin, a maltose binding protein (MBP) that can bind maltose, a glutathione-S-transferase (GST) that can bind glutathione or a FLAG tag that can bind specific antibody (Lichty*, et al.*, 2005). Following affinity chromatography further purification steps, such as size exclusion chromatography, are needed to increase the purity of the protein preparation to remove contaminants that may give false data readings following data capture for structure determination.

7.01 Aims

- Identify key residues in BPSS0390 and BPSS0391 that are involved in protein function
- Structural analysis of the BPSS0390 toxin
- Determine if BPSS0390 is able to bind and degrade RNA

7.1 Identification of key BPSS0390 residues

7.1.1 Conservation of residues in homologous proteins

The BPSS0390 protein sequence was BLASTp searched on the NCBI website and homologous protein sequences that had a significant E-value of less than 0.001 were downloaded and aligned against the BPSS0390 reference sequence using the BioEdit software. In total this equated to 75 different protein sequences. There were 17 residues that were at least 75% conserved between BPSS0390 and the other related toxin sequences (table 7.0). The histidine residue at position 24 in the BPSS0390 sequence was the most conserved residue, being found in 98% of the homologous sequences. This is closely followed by Glycine 22 (97%) and Glycine 14 (96%)

7.1.2 Mapping key residues on the predicted BPSS0390 structure

To generate a model of the possible BPSS0390 structure, the protein sequence was uploaded into the Swiss model software. This program generated a model based on the crystal structure of the related protein 1whzA, protein from *Thermus thermophilus* Hb8 (32% sequence identity). Figure 7.0 shows the model with 5 of the 6 most conserved residues highlighted in red. Histidine 24, Glycine 22 and Serine 23 were located on a loop that could be important in substrate binding. Proline 41 was located on a loop that lies adjacent to the other highlighted residues. Glycine 14 was located at the opposite end of the structure and appears to form part of a bridge between a predominantly beta sheeted domain and a predominantly alpha helical domain and could be a key structural residue. Based on this predicted structure and the conserved residues table, those residues highlighted in red were targeted for site directed mutagenesis.

Table 7.0 The most highly conserved residues in 75 proteins homologous to BPSS0390. The BPSS0390 sequence was BLASTp searched against the NCBI database and sequences that gave a significant E-value of <0.001 were downloaded and aligned in Bioedit software using BPSS0390 as the reference sequence. Residues that were at least 75% conserved are listed in the table.

Residue name/number (based on BPSS0390)	**Homologous proteins in which the residue is conserved (%)**
Histidine 24	98
Glycine 22	97
Glycine 14	96
Serine 23	89
Alanine 57	88
Proline 41	86
Tryptophan 15	85
Isoleucine 53	85
Proline 39	84
Aspartate 44	84
Glycine 48	82
Lysine 55	81
Alanine 58	80
Leucine 10	80
Proline 30	78
Valine 38	77
Threonine 49	77

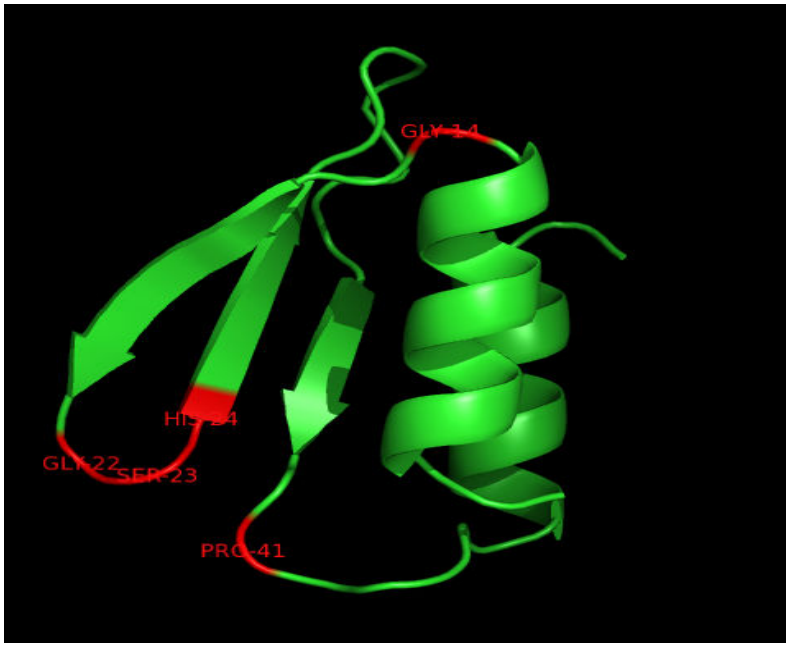

Figure 7.0 3D structural model of the BPSS0390 toxin generated by Swiss model software and visualised in Pymol software. The model was predicted based on the crystal structure of 1whzA (a protein with unknown function from *T. thermophilus* Hb8.) The highlighted red residues are 5 of the most conserved residues targeted for mutagenesis.

7.1.3 Mutagenesis of potential key residues

7.1.3.1 His tagging the BPSS0390 toxin and screening toxicity phenotype

The BPSS0390 gene was PCR amplified from *B. pseudomallei* K96243 genomic DNA and cloned into the pBAD/his vector via the *Sac*I and *Eco*R1 sites to generate a construct which encoded a 3-kDa tag upstream of the BPSS0390 gene. This would allow Western blotting to be used to assess protein expression. The pBAD/his-BPSS0390 construct was transformed into *E. coli* MG1655 cells selecting for colonies on LB agar supplemented with ampicillin. Correct cloning of the gene was confirmed by sequencing.

E. coli MG1655/pBAD/his-BPSS0390 was grown to OD_{590}nm ~ 0.1 and 0.2% (w/v) glucose or 0.2% (w/v) arabinose was added to repress or induce expression of BPSS0390 respectively for 3 hours. The optical density was measured at 590nm every hour. Addition of 0.2% (w/v) glucose resulted in continued OD increase over the 3 hours. In contrast addition of 0.2% (w/v) arabinose to induce his tagged BPSS0390 expression resulted in growth cessation (figure 7.1).

7.1.3.2 Site directed mutagenesis

Mutagenesis of the BPSS0390 toxin gene was carried out using the pBAD-N-his-BPSS0390 construct as the template DNA and primers designed using the Agilent mutagenesis primer tool along with the Agilent lightning mutagenesis kit. The substitutions made were H24A, S23A, G22C, G14C and P41A. The mutations were generated by synthesising a mutant strand of DNA using the primers that contained the mutated codon and an ultra-high fidelity DNA polymerase. *Dpn*I was used to digest methylated parental DNA and the newly generated mutant DNA strand was transformed into competent *E. coli* cells for nick repair and replication. Transformants

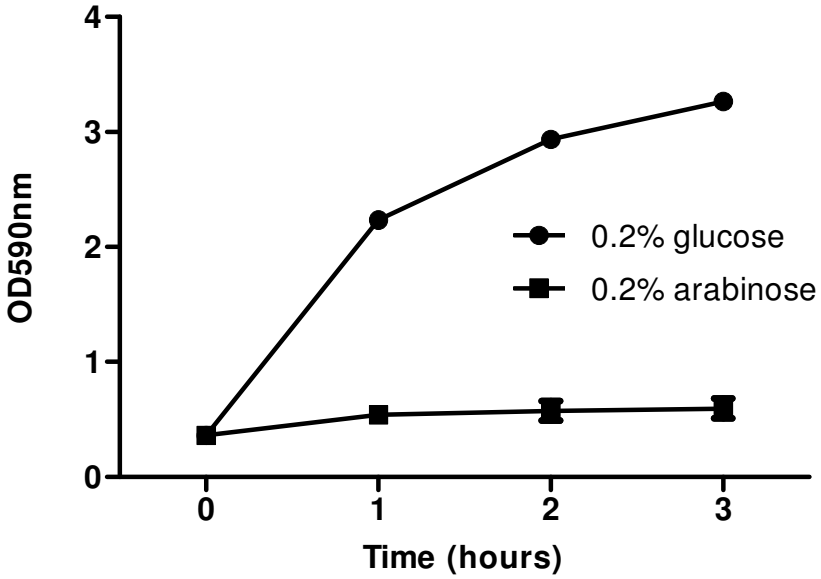

Figure 7.1 Growth of *E. coli* MG1655 /pBAD/his-BPSS0390 measuring the optical density at 590nm. Cultures were grown to early exponential phase before adding either 0.2% (w/v) glucose or 0.2% (w/v) arabinose to repress or induce expression of BPSS0390 for 3 hours. Samples were taken every hour. Data is the average of 3 biological repeats and error bars show SEM.

were selected on LB ampicillin plates. Each mutagenesis experiment gave 20+ colonies and plasmid DNA from 4 colonies from each experiment was sent for sequencing. At least 2 colonies from each experiment contained the desired mutation in the BPSS0390 gene. Plasmid constructs containing the mutations were transformed into *E. coli* MG1655.

7.1.4 Expression of BPSS0390 mutants in *E. coli* MG1655

7.1.4.1 Toxicity assay

E. coli MG1655 pBAD/his harbouring the H24A, G22C, G14C, S23A or P41A mutants were grown to early exponential phase. In parallel the control strains *E. coli* MG1655 pBAD/his and *E. coli* MG1655 pBAD/his-BPSS0390 were also grown to early exponential phase. 0.2% (w/v) arabinose was then added to cultures to induce expression of the cloned gene for 2 hours. *E. coli* harbouring empty pBAD had a CFU fold increase in cell numbers after 2 hours incubation, while the *E. coli* harbouring pBAD his tagged BPSS0390 decreased in cell numbers over the same period (figure 7.2). *E. coli* strains expressing the G14C, S23G or P41A mutants all decreased in cell numbers. In comparison the *E. coli* MG1655 strains expressing the his tagged H24A or G22C mutants showed an increase in CFU counts by approximately 100 fold, similar to the pBAD negative control. The difference between the CFU fold change with G22C and H24A was significant ($p<0.001$, 1 way ANOVA Dunnett post-test) compared to the his tagged BPSS0390 positive control. This indicated that these mutations either prevented toxicity of BPSS0390 toxin or that the encoded genes were not expressed.

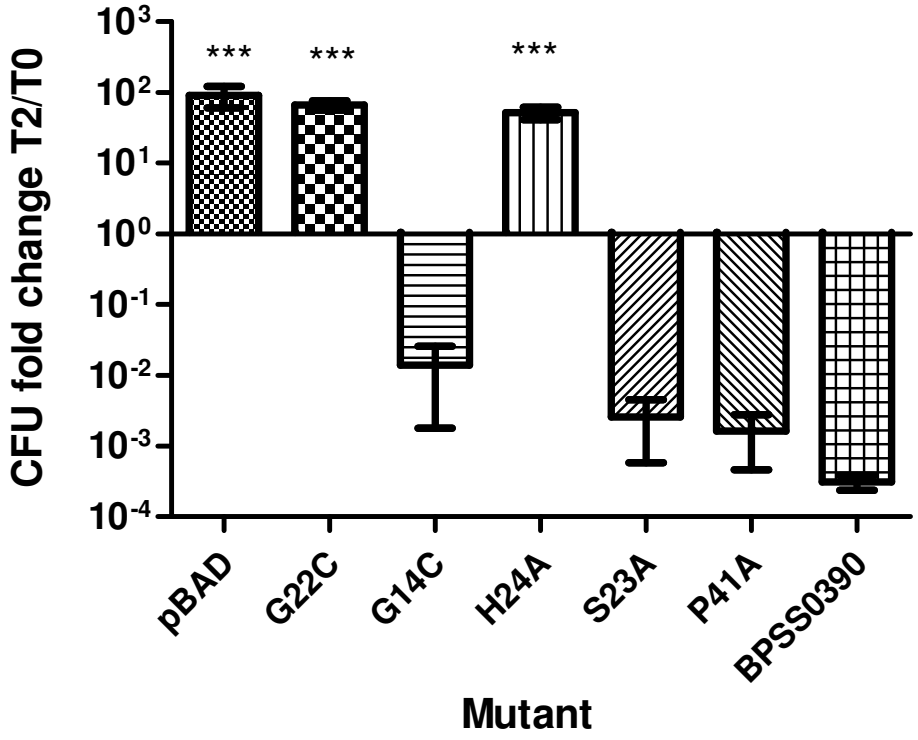

Figure 7.2 CFU fold change following expression of BPSS0390 mutants for 2 hours. Cultures of *E. coli* MG1655 harbouring empty pBAD/his, pBAD/his-BPSS0390 or pBAD/his with a cloned mutant allele were grown to early log phase before inducing expression with 0.2% (w/v) arabinose. CFU was determined by plating cells onto LB agar plates containing 100 µg/ml ampicillin. Data shown are the average of 3 biological repeats. Error bars show SEM, ***=$p<0.001$ following a 1 way Anova and Dunnett post-test using the BPSS0390 strain as a reference.

7.1.4.2 Western blots to check expression of H24A and G22C

E. coli MG1655 harbouring pBAD/his cloned BPSS0390 H24A or G22C were grown to early exponential phase and then 0.2% (w/v) glucose or 0.2% arabinose (w/v) was added for repression or induction of expression from the pBAD promoter and the bacteria were grown for a further 2 hours. A sample of culture was then centrifuged and the cell pellet lysed using Bugbuster, lysozyme and benzonase. A sample of the cell lysate was loaded onto SDS-PAGE gel and electrophoresed before carrying out a Western blot. An anti-xpress 1^{o} antibody was used for protein detection, which is specific against the express epitope in the his tag and a 2^{o} HRP conjugated anti-goat anti-mouse antibody was used for chemilumonescence and binding to the 1^{o} antibody. Under repressed conditions for *E. coli* harbouring either H24A or G22C there was no detectable band on the Western blot following chemiluminescence (figure 7.3). However when arabinose was added to cultures, *E. coli* harbouring either H24A or G22C showed a detectable band at around 13 kDa corresponding to the BPSS0390 tagged mutant toxins. The BPSS0390 mutant toxins ran slightly higher on the gel than expected (Mw ~10kDa) due to the high pI of the protein.

7.1.5 Co-expression of the G14C, S23A or P41A BPSS0390 mutants with BPSS0391

The G14C, S23A and G14C mutants were tested to see if the residues might play a role in antitoxin binding. *E .coli* MG1655 pBAD/his BPSS0390 G14C, S23A or P41A were made calcium competent and then transformed with the pME6032-BPSS0391 construct. Transformants were selected on LB ampicillin tetracycline plates. A negative untransformed control was also plated onto selective plates for each of the

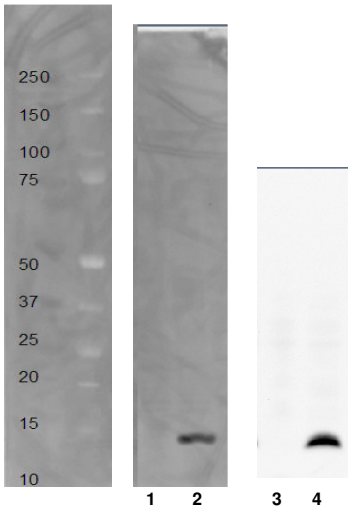

Figure 7.3 Combined Western blot images following repression or expression of H24A (lanes 1 or 2 respectively) or G22C (lane 3 or 4 respectively) from pBAD/his in *E. coli* MG1655. Cultures were grown to early log phase before repression or expression of the pBAD/his cloned mutant gene by 0.2% (w/v) glucose or 0.2% (w/v) arabinose respectively for 3 hours. Cultures were lysed in Bugbuster solution and lysozyme before running samples of the cell lysate on an SDS-PAGE gel at 200V for 40 minutes. Protein on the gel was blotted using an iblot onto a nitrocellulose membrane and blocked with 3% (w/v) BSA. The primary antibody used was an anti-xpress mouse antibody. The secondary antibody used was an HRP conjugated anti-goat anti-mouse. The membrane was visualised using chemiluminescence.

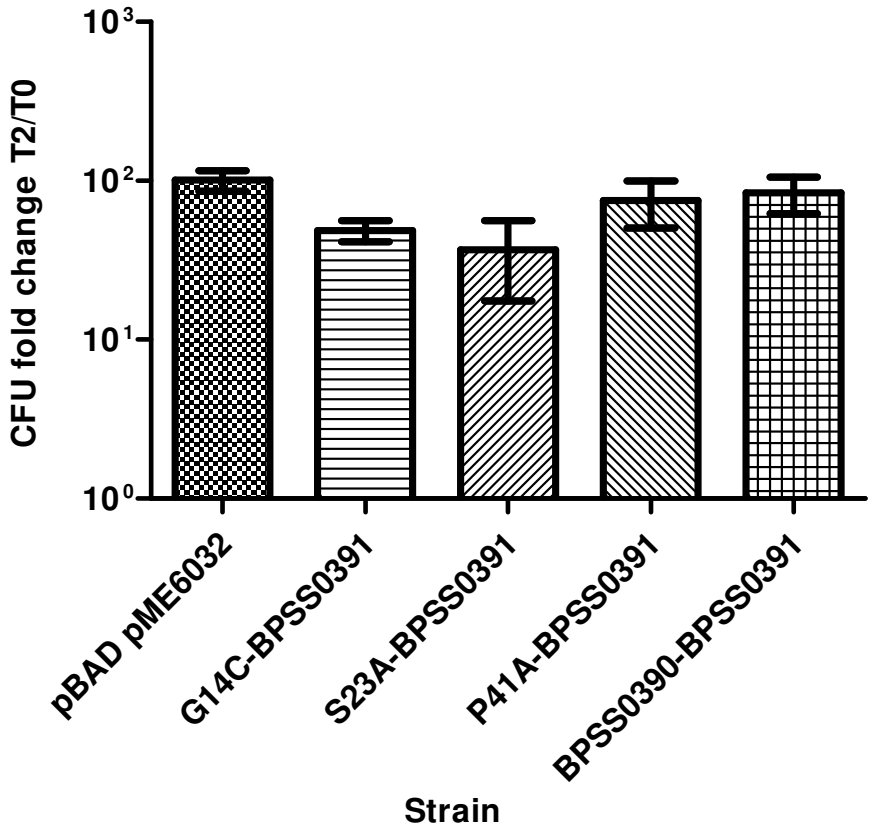

Figure 7.4 CFU fold change in *E. coli* cell numbers following co-expression of BPSS0391 with the BPSS0390 site directed mutants G14C, S23A or P41A. Cultures of *E. coli* MG1655 harbouring pME6032 cloned BPSS0391 and pBAD/his cloned BPSS0390 G14C, S23A or P41A were grown to early exponential phase before adding 0.2% (w/v) arabinose and 25 mM IPTG for 2 hours. *E. coli* /pBAD /pME6032 and *E. coli* /pBAD-BPSS0390 /pME6032-BPSS0391 were used as controls. Data shown are the average of 3 biological repeats and error bars show SEM.

calcium competent strains. All negative control plates had no growth. Plates inoculated with *E. coli* transformed with pME6032-BPSS0391 contained 50+ colonies. *E. coli* MG1655 harbouring pME6032-BPSS0391 and pBAD/his with cloned G14C, S23A or P41A mutants were grown to early exponential phase. 0.2% (w/v) arabinose and 25 mM IPTG were added to induce expression of the cloned toxin and antitoxin genes for 2 hours. Figure 7.4 shows the resulting fold change in CFU counts. The *E. coli* strains harbouring G14C, S23G and P41A showed a 100 fold increase in CFU counts following co-expression with BPSS0391 similar to the *E. coli* pBAD/his-BPSS0390 pME6032-BPSS0391 and *E. coli* pBAD/his pME6032 control strains. This suggested that the BPSS0391 antitoxin was also able to counteract the activity of the mutant toxins and indicates that these residues were not important in antitoxin binding.

7.1.6 Persister assays on *E. coli* MG1655 expressing BPSSS0390 mutants

7.1.6.1 Ciprofloxacin

E. coli MG1655 strains harbouring pBAD/his cloned BPSS0390 G22C, H24A, G14C, S23A, or P41A and pME6032- BPSS0391 along with *E. coli* MG1655 pBAD/his-BPSS0390/ pME6032-BPSS0391 and *E. coli* MG1655 pBAD/pME6032 controls were grown to early exponential phase. Expression of the pBAD/his cloned gene was induced with 0.2% (w/v) arabinose for 3 hours. After this duration cultures were standardised to an OD_{590}nm 0.5 then mixed at a 1:1 ratio with 200 x MIC ciprofloxacin (64 µg/ml) and incubated statically for 24 hours at 37 ^{o}C. Antibiotic was removed by washing and cells were plated onto LB agar supplemented with 1 mM IPTG to induce expression of BPSS0391 to resuscitate non-culturable cells. Figure

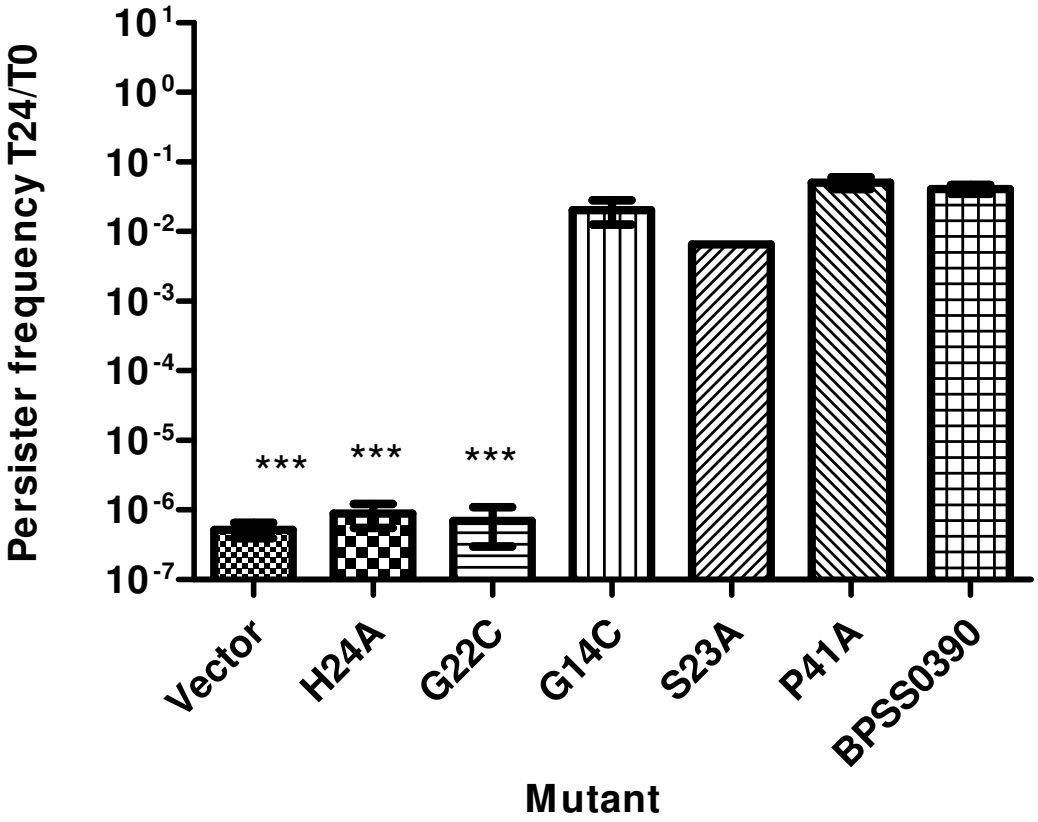

Figure 7.5 Persister frequency of *E. coli* MG1655 strains expressing pBAD/his cloned BPSS0390 H24A, G22C, G14C, S23A or P41A after 100 x MIC (32 µg/ml) ciprofloxacin treatment. Cultures harbouring both pBAD/his cloned BPSS0390 alleles and pME6032 cloned BPSS0391 were grown to early log phase before inducing expression of the pBAD/his cloned alleles for 3 hours by adding 0.2% (w/v) arabinose. Cultures were then standardised to OD_{590}nm 0.5 and incubated with ciprofloxacin for 24 hours in a 24 well plate at 37 ^{o}C. Following incubation cells were washed twice in LB and then plated onto LB agar supplemented with 100 µg/ml ampicillin 15 µg/ml tetracycline and 1 mM IPTG to induce BPSS0391 expression to resuscitate any non-culturable cells. T0 samples were also plated on LB agar containing antibiotic and 1 mM IPTG for resuscitation. Persister frequency was calculated as CFU counts post antibiotic treatment divided by CFU counts pre-treatment. The data shown are the average of 3 biological repeats (except S23A which shows only 1 replicate). Error bars show SEM. ***= $p<0.001$, following a 1 way Anova with a Dunett post-test.

7.5 shows the persister frequencies of the different strains. *E. coli* expressing the G14C, S23A or P41A mutants had persister frequencies similar to the positive control strain expressing his tagged BPSS0390 following ciprofloxacin treatment. In contrast H24A and G22C expression in *E. coli* resulted in persister frequencies of 10^{-6} (the same as the empty vector control), which were significantly different compared to the positive control strain ($p<0.001$, 1 way ANOVA Dunnett post-test).

7.1.6.2 Ceftazidime

E. coli MG1655 strains harbouring pBAD/his cloned G22C, H24A, G14C, S23A, or P41A mutants and pME6032- BPSS0391 along with *E. coli* MG1655 pBAD/his-BPSS0390 pME6032-BPSS0391 and *E. coli* MG1655 pBAD/pME6032 controls were grown to early exponential phase. Expression of the pBAD/his cloned gene was induced with 0.2% (w/v) arabinose for 3 hours. After this duration cultures were standardised to an OD_{590}nm 0.5 then mixed at a 1:1 ratio with 200 x MIC (40 µg/ml) ceftazidime for 24 hours. Cells were then washed to remove antibiotic and plated onto LB agar plates containing 1 mM IPTG to resuscitate non-culturable cells. The *E. coli* strains expressing the P41A, S33G and G14C mutants gave similar persister frequencies to his tagged BPSS0390 positive control strain following ceftazidime treatment. Conversely the *E. coli* MG1655 strains carrying the empty vector or expressing the H24A or G22C mutant toxins gave persister frequencies below detectable levels (figure 7.6).

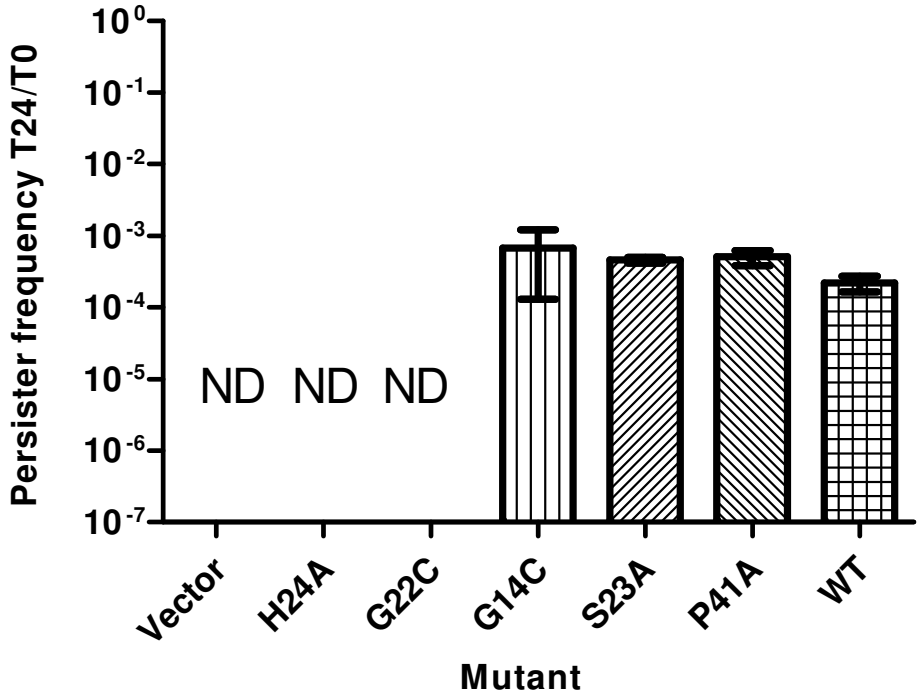

Figure 7.6 Persister frequency of *E. coli* MG1655 strains expressing pBAD/his cloned BPSS0390 H24A, G22C, G14C, S23A or P41A after 100 x MIC (20 µg/ml) ceftazidime treatment. Cultures harbouring both pBAD/his cloned alleles and pME6032 cloned BPSS0391 were grown to early log phase before inducing expression of the pBAD/his BPSS0390 alleles for 3 hours by adding 0.2% (w/v) arabinose. Cultures were then standardised to OD_{590}nm 0.5 and then incubated with ceftazidime for 24 hours in a 24 well plate at 37 ^{o}C. Following incubation cells were washed twice in LB and then plated onto LB agar supplemented with ampicillin 100 µg/ml, tetracycline 15 µg/ml and 1 mM IPTG to induce BPSS0391 expression to resuscitate any non-culturable cells. T0 samples were also plated on LB agar containing antibiotic and 1 mM IPTG for resuscitation. Persister frequencies were calculated as CFU numbers post antbiotic exposure divided by CFU numbers pre antibiotic exposure. The data shown are the average of 3 biological repeats. Error bars show SEM. ND= No detectable colonies.

7.2 Structure determination

7.2.1 Purification of recombinant protein

7.2.1.1 His tagged BPSS0390

E. coli MG1655/pBAD/his-BPSS0390 and the control strains *E. coli* Top10/pBAD/his-LacZ and *E. coli* MG1655/pBAD were grown to an OD_{590}nm of 0.5 before inducing expression of the pBAD/his cloned gene with 0.2% (w/v) arabinose for 3 hours. Cultures were then standardised and harvested by centrifugation. The cell pellet was lysed using the Bugbuster technique and both the soluble cell lysate and insoluble cell debris were analysed by a SDS PAGE gel and Western blotting. His tagged protein was detected using chemiluminescence. Wells containing samples of *E. coli* harbouring empty pBAD gave no visible bands (Figure 7.7). *E. coli* pBAD/his LacZ samples gave a luminescent band at 120kDa in both soluble and insoluble fractions. Neither soluble nor insoluble samples from *E. coli* expressing his tagged BPSS0390 gave a detectable band. This suggested there was no free BPSS0390his protein in the cell lysate or in the insoluble fraction.

In addition to this blot, the samples were also run on higher percentage gels (Bis-Tris 4-12%), blotted onto PVDF membranes and a more sensitive chemiluminescence substrate was used. A his tagged protein band was not detected in any of the samples (data not shown)

7.2.1.2 His tagged H24A mutant

The H24A mutant had previously been detected on a western blot following expression and was non-toxic to the cell, which meant cultures could be grown to high yields. The his tagged H24A mutant was subsequently cloned into the pET26-b vector. The pBAD/his-H24A construct was digested with the *Nco*I and *Eco*RI restriction

enzymes and the purified fragment encoding H24A was cloned into the *Nco*I and *Eco*RI sites of pET26-b to create pET26-b/his H24A. Constructs were transformed into *E. coli* DH5*α* and plasmid DNA re-isolated and the authenticity confirmed by nucleotide sequencing. Correct constructs were transformed into *E. coli* Rosetta (DE3) cells for expression driven by the T7 polymerase.

Overnight cultures of *E. coli* Rosetta (DE3) /pET26-b/his BPSS0390 H24A grown in LB were diluted 1:100 in 5 x 100 ml volumes of autoinduction media supplemented with kanamycin for plasmid selection and grown at 37 ^{o}C, 300 rpm until mid-log phase (OD_{590}nm 0.5). The temperature was then reduced to 20 ^{o}C and cells incubated overnight. Cells were harvested by centrifugation and Bugbuster treated to release the protein. The lysate was then run through a nickel coated affinity column and bound protein was eluted with imidazole. Eluted protein was de-salted using a PD-10 column and then incubated with enterokinase. Following purification through the affinity column the his tagged H24A protein was visible running at approximately 13kDa on an SDS-PAGE gel but there was also some contamination (figure 7.8). The enterokinase did not digest 100% of the H24Ahis protein, indicated by 3 bands on the SDS gel running at 13kDa (uncut H24Ahis), 10kDa (H24A protein) and 6kDa (histidine tag). Running the digested protein through a second nickel affinity column was able to separate the H24A protein from uncut protein and the tag. To further purify the protein, it was then run through a Superdex 75 16/60hr size exclusion column. Following this final purification step the purity of the protein was pure with no visible contaminants.

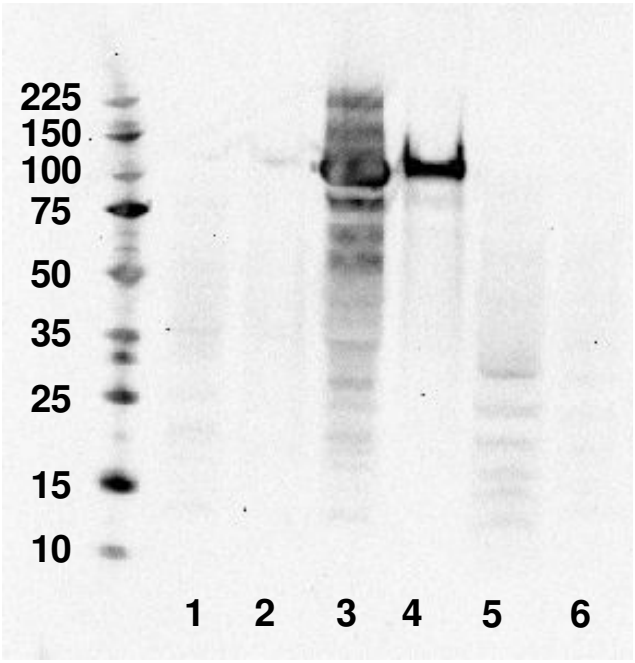

Figure 7.7 Western blot of 0.2% (w/v) arabinose induced *E. coli* MG1655 /pBAD (lanes 1 and 2), *E. coli* MG1655 /pBAD/his-LacZ (lanes 3 and 4) and *E. coli* MG1655 /pBAD/his-BPSS0390 (lanes 5 and 6). Lanes 1, 3 and 5 are soluble cell lysate samples and 2, 4 and 6 are insoluble cell debris samples. Cultures were grown to early exponential phase before inducing expression of cloned pBAD/his genes for 3 hours. A 1 ml sample was lysed in Bugbuster and lysozyme before centrifuging to separate cell lysate and insoluble debris. Samples were run on a 4-12% SDS-PAGE gel and then blotted onto a nitrocellulose membrane. The membrane was blocked with 3% (w/v) BSA before adding the primary anti-xpress anti-mouse antibody followed by a secondary HRP conjugated anti-goat anti-mouse antibody. The membrane was visualised using chemiluminescence. The expected sizes of the his tagged LacZ and BPSS0390 proteins were ~120 and ~10 kDa respectively.

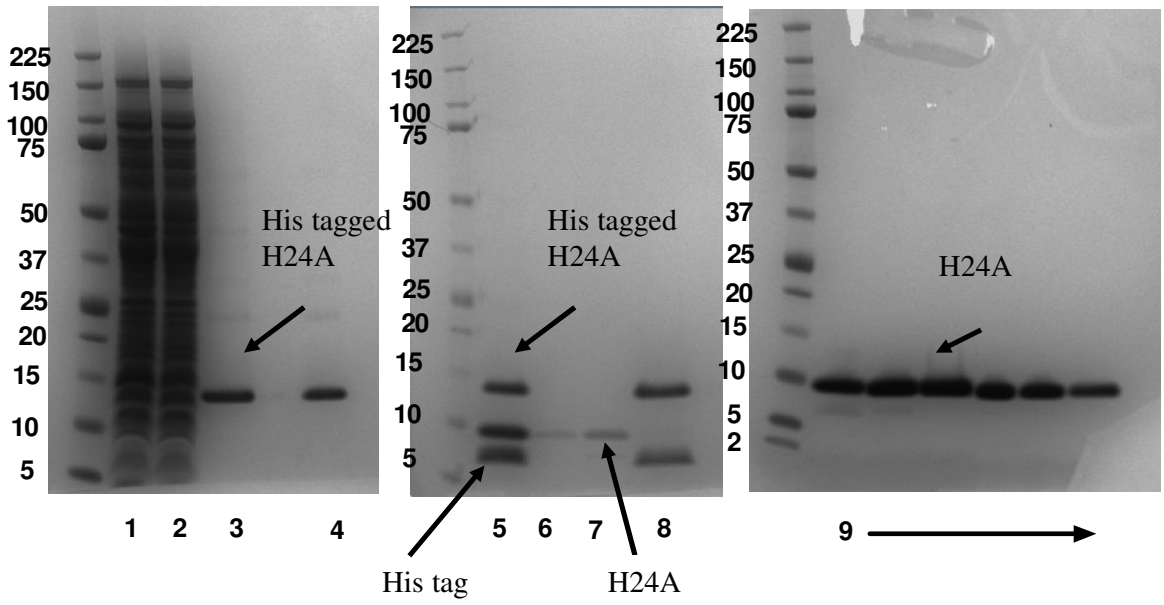

Figure 7.8 SDS-PAGE gels showing the purification steps of the H24A protein. Cultures of *E. coli* Rosetta (DE3) /pET26-b/his-H24Ahis were harvested by centrifugation and lysed by Bugbuster and lysoszyme to release the total protein (lane 1). The cell lysate was run through a nickel affinity his gravi column (GE healthcare) and unbound material was discarded (lane 2). The column was washed with binding buffer and protein bound to the column was eluted using imidazole (lane 3) before de-salting the eluted protein through a PD-10 de-salting column using TBS (lane 4). The purified protein was then digested with enterokinase (lane 5) and the digested protein run down another gravi his column collecting the flow through (lane 6), wash (lane 7) and elution (lane 8). The flow through and wash was combined and run on a Superdex 75 16/60hr size exclusion column. Eluted fractions which contained protein (lanes 9) were run on a gel to confirm purity then combined for downstream use.

7.2.2 Crystallisation trials

Purified H24A protein was concentrated using a 3kDa cut off spin column. Once the protein was at a concentration of approximately 10 mg/ml (measured by the Nanodrop) the protein solution was removed from the spin column. This concentrated protein was then aliquoted using a robot into a 96-well plate and mixed with combinations of buffers and salts for vapour diffusion to promote crystallisation of the protein. The wells were coated with oil and the plate incubated in the fridge up to 5 days. The wells were checked for crystal growth using a bright field microscope after 1, 3 and 5 days. The state of each well following 5 days growth was recorded using a point scoring system. Many of the wells contained precipitated or partially precipitated protein (Table 7.1). Some of the wells contained visible crystals (A11, D9, F1, F8, G12 and H5) but further analysis using a loop revealed these were salt crystals.

Following this unsuccessful screen a second screen was set up with additives but this also resulted in no protein crystal growth.

7.2.3 CD spectrophotometry

Purified his tagged H24A protein eluted in PBS was diluted to a concentration of 0.3 mg/ml and a sample of the protein was sent to King's College London to be analysed by circular dichroism spectroscopy (CD spectroscopy). The spectrum would indicate whether or not the protein was folded. Figure 7.9A shows the UV and CD spectra and figure 7.9B shows the proposed secondary structure composition. The spectra showed the correct curve for a folded protein and the near UV and CD spectra showed the features of predominant single tryptophan indicating that this residue is highly constrained. The structure of the his tagged H24A protein has a high β-sheeted consistency (42.9%) and a low α-helical make up of only 6.7%.

Table 7.1 The condition of the wells in a 96-well plate containing the BPSS0390H24A protein and a range of buffers and salts, following vapour diffusion. Each number refers to a different state. For each well 1 µl of H24A protein at a concentration of 10 mg/ml was mixed with 1 µl of buffer/salt. Plates were covered in mineral oil and incubated at 4 ^{o}C for 5 days. Wells were visualised under a bright field microscope at 40 x magnification.

0 =clear	5=phase separation
1= non protein particles	6= spherulites or microcrystals
2= part precipitation	7= needle
3= precipitation	8= plates
4= gelatinous or particulated precipitate	9=crystals

Well position												
	One	Two	Three	Four	Five	Six	Seven	Eight	Nine	Ten	Eleven	Twelve
A	4	2	1	3	5	2	3	5	5	3	9- salt	1
B	4	3	4	2	6	3	3	3	3	1	5	1
C	3	5	1	3	4	4	5	5	5	5	4	5
D	4	5	3	3	4	4	3	4	3	9-salt	3	4
E	6	3	3	3	3	3	4	5	3	1	1	2
F	9-salt	3	3	3	4	3	2	9-salt	3	3	4	3
G	5	3	2	2	2	2	1	3	3	3	3	9-salt
H	3	3	3	2	9-salt	1	2	3	2	3	3	5

A)

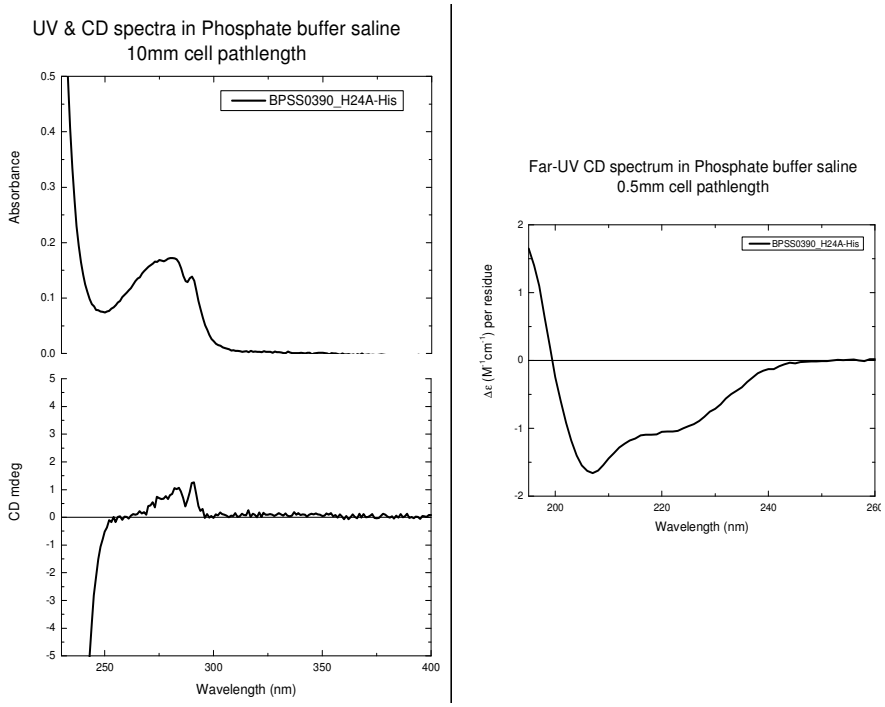

B)

Sample	% α helix	% β-sheet	% other
BPSS030_H24A-His	6.7	42.9	50.4

Figure 7.9 CD spectroscopy of the his tagged H24A protein. A) UV and CD spectra B) predicted composition of secondary structure. All spectra were buffer baseline subtracted and measured at 23 ^{o}C. The far-UV CD data was normalised for concentration and pathlength and expressed in terms of Δε per residue (MWt =113). The CD spectra were smoothed using the *Savitzky–Golay* method with a window factor of 2. The protein secondary structure content was calculated based on the principle component regression method.

7.2.4 Stabilisation experiments

Purified H24A protein at a concentration of 0.133 mg/ml was mixed with a Sypro orange fluorophore dye. A range of salt and additives from a compound library were added to the protein mix in a PCR plate to test if any compounds had a stabilising effect on the protein. The plate was then incubated in a qPCR machine and a heat denaturation gradient from 25-99 ^{o}C was applied to the samples and fluorescence measured. The protein did not show a classic denaturation profile in any of the buffer/compounds or controls and the Tm of the protein could not be calculated using a Boltzmann curve or the derivative at the temperature gradient tested (data not shown). This suggested that the protein was very stable at high temperature.

7.2.5 NMR

7.2.5.1 Sample preparation

For the NMR trial experiment purified H24A protein was diluted to a concentration of 7 mg/ml in a 500µl volume. 10% D_2O was then added before analysing the sample. A 1D screen of the protein showed conventional characteristics of protein structure and subsequent COSY and TOCSY test experiments were run to derive carbon to hydrogen bond information. These data sets gave good spectra and it was decided that ^{15}N labelled H24A protein would be made for further analysis of the structure (data not shown).

To create ^{15}N labelled H24A protein an altered autoinduction media was used replacing the ammonium chloride in the media with ^{15}N ammonium chloride. The labelled protein was concentrated to approximately 7 mg/ml before adding 10% D_20 and carrying out 1D and 2D spectrophotometry on the sample. With the ^{15}N labelled protein a HSQC data set was obtained which gave structural data regarding N-H

amide bonds. TOCSY and NOSEY datasets were also obtained. The data sets obtained in this instance showed some evidence of protein degradation (data not shown). Incubation of the protein at 25 ^{o}C for 1 week and re-testing the protein showed evidence of no subsequent degradation, and it was assumed degradation had occurred during purification. In light of this, another batch of ^{15}N labelled protein was created and 0.1% (w/v) sodium azide was added. Analysis of this batch of labelled protein showed that the protein had not degraded and subsequently sodium azide was added for further purifications of the protein.

Next ^{15}N and ^{13}C labelled H24A protein was produced. *E. coli* Rosetta (DE3) pET26-b BPSS0390H24Ahis strain was grown in 2 litres of LB (5x 400 ml) at 37 ^{o}C 200 rpm until reaching an OD_{590}nm of 0.9. The cultures were then centrifuged and re-suspended in a 500 ml volume of double labelled minimal media. H24A expression was induced with 0.5 mM IPTG. Yields obtained from this method of growth were much lower than unlabelled and single labelled protein and protein could only be concentrated to around 4 mg/ml in a 500 µl volume.

7.2.5.2 NOE assignment

All NMR data, including triple resonance experiments to assign the backbone (HNCA, HNCOCA, HNCACB, HNCO) and sidechains (15N-TOCSY, HCCONH, CCONH, HCCH-TOCSY) are being analysed, by collaborators at Bristol University for structure determination. To date the ^{15}N-HSQC data has been analysed and the majority of NOEs for this data set assigned to the corresponding residues in the H24A structure (figure 7.10).

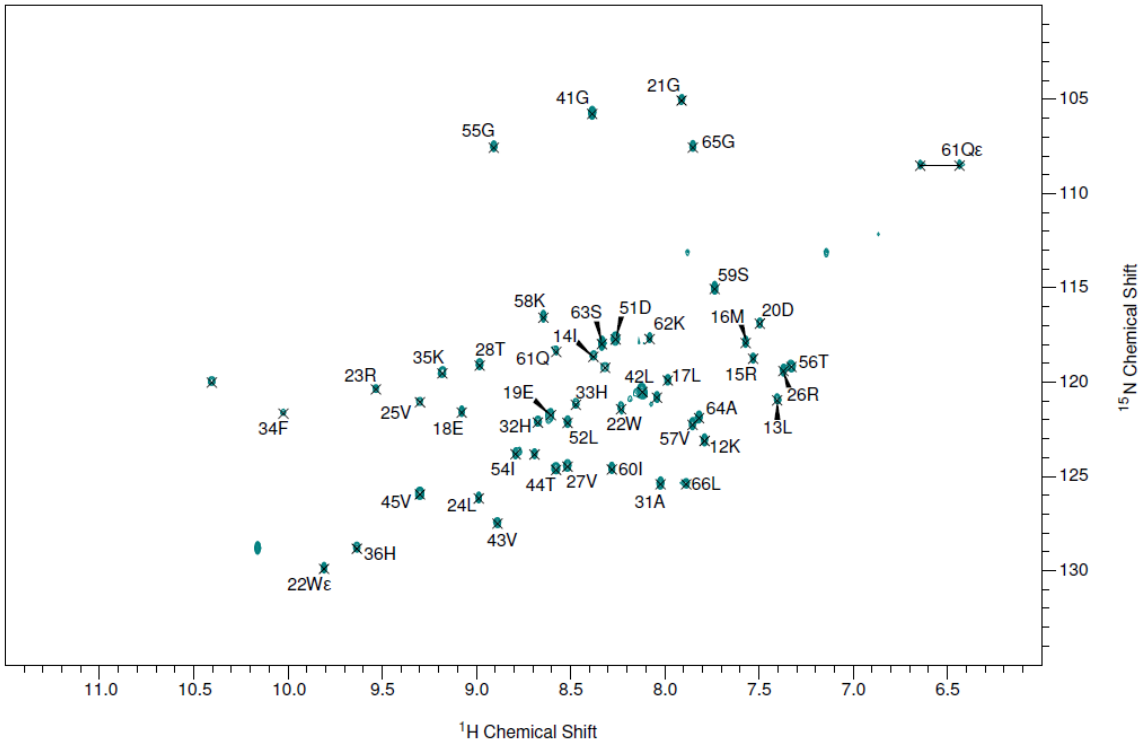

Figure 7.10 15^{N}-HSQC spectra showing the assigned NOEs for the H24A protein. CCPN software was used to analyse and assign the data.

7.3 The BPSS0391 antitoxin and BPSS0390-0391 complex

7.3.1 Identification of key BPSS0391 residues

The BPSS0391 protein sequence was BLASTp searched against the NCBI database and sequences that had an E-value below 0.001 (n=89) were downloaded and aligned with BioEdit software using the BPSS0391 sequence as the reference sequence. Residues that were conserved in at least 75% of the homologues are listed in table 7.2. The most conserved residue in BPSS0391 was a proline residue at position 20. Glycine 24 and alanine 42 were 89% conserved and there were 9 other residues conserved in over 75% of the sequences. 4 conserved residues were close together in the protein sequence and may be in close proximity in the structure (Pro 20, Asp 21, Gly 24 and Cys 25).

7.3.2 Expression and purification of the BPSS0390-0391 complex

The *E. coli* MG1655 /pBAD/his-BPSS0390 /pME6032-BPSS0391 strain was grown to an OD_{590}nm of 0.3 before adding 0.2% (w/v) arabinose and 25 mM IPTG for 4 hours to induce expression of BPSS0390 and BPSS0391 respectively. The culture was pelleted and lysed by Bugbuster and the total cell lysate passed through a nickel affinity column for purification of complex and free BPSS0390 toxin. Samples were taken at each purification step and total protein was detected on a SDS-PAGE gel (figure 7.11A) and Western blotted (figure 7.11B). A protein of approximately 13kDa in size was detected in the total protein by Western blotting. Due to the high pI of the BPSS0390 protein this was its expected size when run on a SDS-PAGE gel. The total protein eluted from the affinity column with imidazole

Table 7.2 The most conserved residues in 89 homologous BPSS0391 protein sequences. The BPSS0391 sequence was BLASTp searched against the NCBI database and sequences that gave a significant E-value of <0.001 were downloaded and aligned in Bioedit software using BPSS0391 as the reference sequence. Residues that were at least 75% conserved are listed in the table.

Residue name/number (based on BPSS0391)	**Species coverage (%)**
Proline 20	94
Glycine 24	89
Alanine 42	89
Arginine 118	84
Aspartate 108	83
Serine 119	80
Asparagine 96	80
Cysteine 25	79
Aspartate 21	77
Isoleucine 107	77
Glutamate 50	76
Phenylalanine 121	75

also contained the 13kDa protein that was detectable both on the SDS-PAGE gel and on the Western blot. This protein was absent from the unbound column flowthrough. A smaller protein band of 10kDa was also present in the total protein and column elute detectable by Western blotting. The column elute also contained a protein band between 50 and 75kDa in size detectable on the SDS-PAGE gel and by Western blotting. This could be a complex of BPSS0390 and BPSS0391 (2 x BPSS0391 + 2 x BPSS0390 ~50kDa) that had resisted denaturation by boiling and SDS. No detectable BPSS0391 band was detectable in the column elution.

7.3.3 Western blots following co-expression of BPSS0391 with G14C, P41A and S23G

As his tagged BPSS0390 could be detected on a Western blot following co-expression with BPSS0391, it was next tested if the G14C, S23A or P41A mutants could be detected on a blot following co-expression with BPSS0391. Figure 7.12 shows combined Western blot images for the 3 different mutants in addition to an empty pBAD pME6032 control strain. The empty vector controls gave no detectable bands following Western blotting. Co-expression of the mutant BPSS0390 toxins G14C, S23A or P41A with BPSS0391 antitoxin in *E. coli* gave detectable bands at ~13kDa which represents the tagged mutant BPSS0390 toxins. Unlike co-expression of BPSS0390 with BPSS0391 there was no high molecular weight signal (possible TA complex). There was no detectable protein band when the S23A protein was expressed independently of the BPSS0391 antitoxin as another negative control.

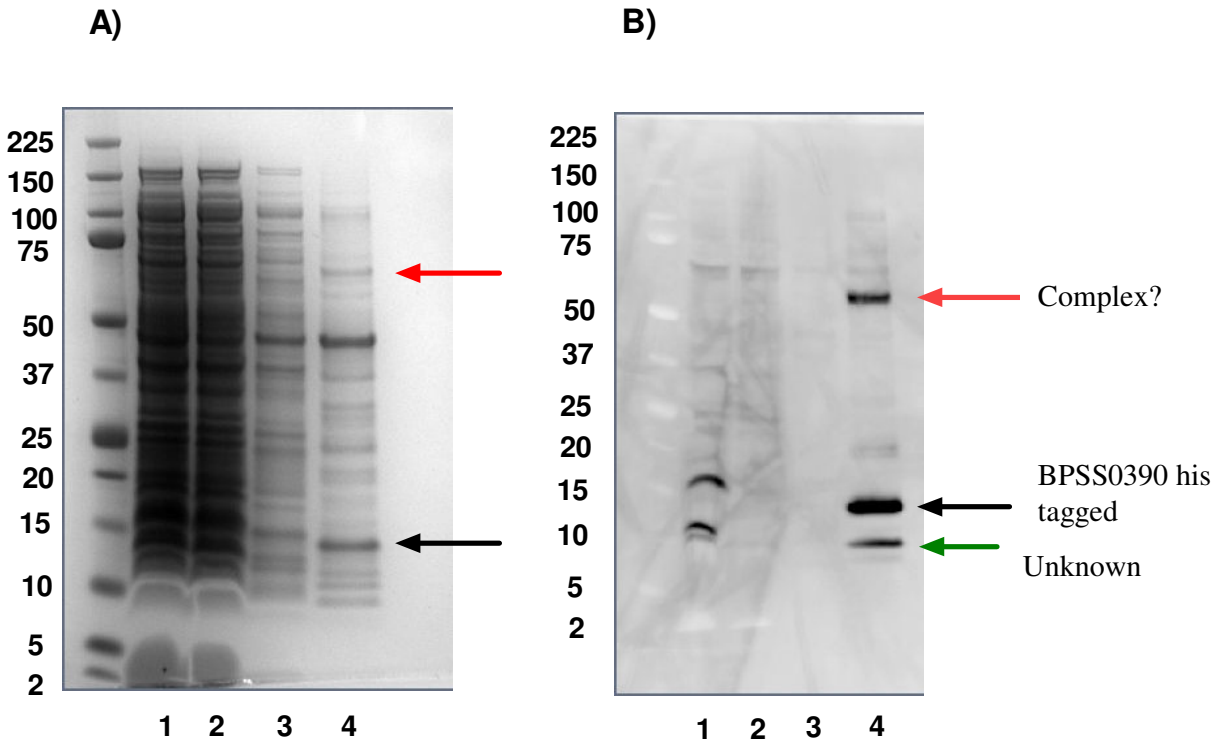

Figure 7.11 Co-expression and purification of his tagged BPSS0390 and BPSS0391. *E. coli* MG1655 /pBAD/his-BPSS0390 /pME6032-BPSS0391 was grown to mid log phase and expression of the cloned genes was induced for 4 hours by addition of 0.2% (w/v) arabinose and 25 mM IPTG. Cells were lysed in Bugbuster and lysozyme and the total cell lysate (lane 1) was run though a nickel affinity his gravi column. Lane 2 shows the total unbound protein and lane 3 shows the total protein following the wash step. Protein eluted from the column after addition of imidazole is shown in lane 4. A) SDS-PAGE gel of the protein samples and B) is the corresponding Western blot using 3% (w/v) BSA, anti-xpres anti-mouse primary antibody and a HRP conjugated anti-goat anti- mouse secondary antibody for chemiluminescence. The red arrow indicates a possible complex of BPSS0390 with BPSS0391. The black arrows indicates his tagged BPSS0390. The green arrow is an unknown protein.

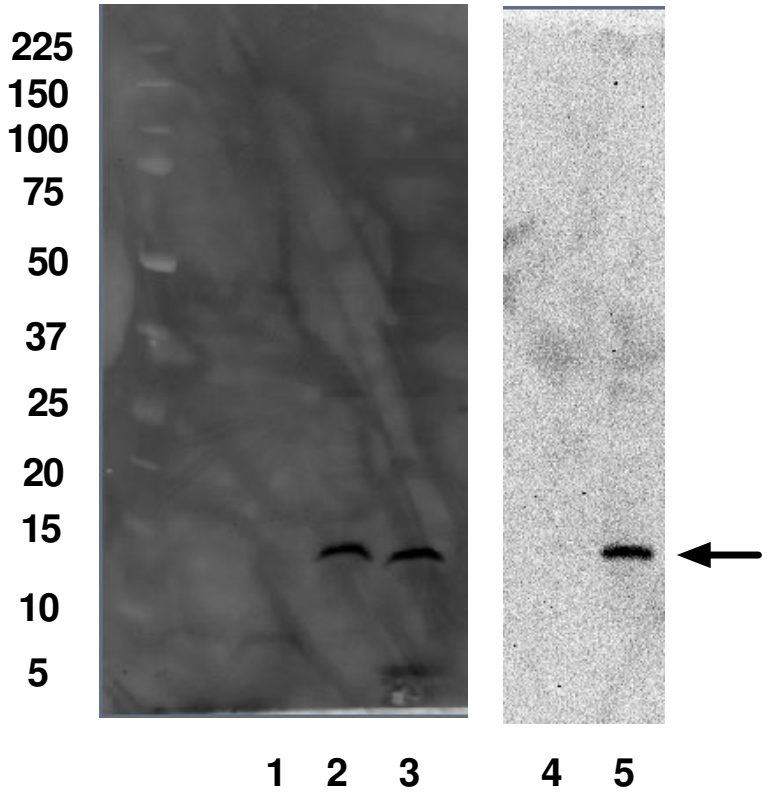

Figure 7.12 Western blots following co-expression of BPSS0391 with the toxic alleles of BPSS0390. *E. coli* MG1655 strains harbouring pME6032-BPSS0391 and the BPSS0390 alleles: G14C (lane 2), P41A (lane 3) and S23A (lane 5) cloned into pBAD/his were co-expressed with 0.2% (w/v) arabinose and 25 mM IPTG for 3 hours. 1 ml of each of the cultures was harvested by centrifugation and lysed in bugbuster and lysozyme. 2 controls were also processed: *E. coli* MG1655 /pBAD/his /pME6032 (lane 1) and *E. coli* MG1655 /pBAD/his-BPSS0390 S23Ahis /pME6032-BPSS0391 where only toxin was induced for 3 hours (lane 4). The black arrow indicates the position on the blot in which the BPSS0390 allele proteins should be located if expressed. The protein was blotted onto a nitrocellulose membrane and detected using chemiluminescence with HRP conjugated anti-goat anti-mouse binding to the express epitope in the his tag via the anti-xpress primary antibody. 3% (w/v) BSA was used for blocking.

7.3.4 Expression and purification of BPSS0391

The BPSS0391 gene was PCR amplified from the pME6032-BPSS0391 plasmid using pME6032 foward and reverse primers to generate a 600bp product. The PCR product was digested with *Xho*I and *Sac*I restriction enzymes. In parallel the pET26-b/his-H24A vector was digested with *Xho*I and *Sac*I to remove the H24A gene. The restriction digested BPSS0391 gene was then cloned into the digested pET26-b/his vector to create the pET26-b/his-BPSS0391 construct. This plasmid was transformed into *E. coli* DH5α cells selecting for transformants on LB agar plates supplemented with kanamyin. Plasmid DNA was re- isolated from transformed colonies and sent for sequencing to confirm the sequence was correct. A sequenced confirmed pET26-b/his-BPSS0391 construct was then transformed into *E. coli* Rosetta (DE3) cells for expression.

Overnight cultures of *E. coli* Rosetta (DE3) pET26-b/his-BPSS0391 grown in LB were diluted 1:100 in autoinduction media and grown to mid exponential phase at 37 ^{o}C, 300 rpm. On reaching this growth phase the temperature was reduced to 20 ^{o}C and cells were incubated overnight. The cells were harvested by centrifugation and lysed using Bugbuster and lysozyme to release the protein. The cell lysate was loaded onto a nickel affinity column and bound protein was eluted with imidazole. The total eluted protein was digested with enterokinase for 16 hours before running through a second nickel affinity column and collecting the flowthrough. The flow through was applied to a size exclusion column in order to remove any contaminants. Following elution from the first affinity column the predominant protein detectable on an SDS-PAGE gel was 20kDa in size (figure 7.13A). This corresponded to the size of his tagged BPSS0391 protein. 4 distinct proteins were eluted from the size exclusion column in various fractions.

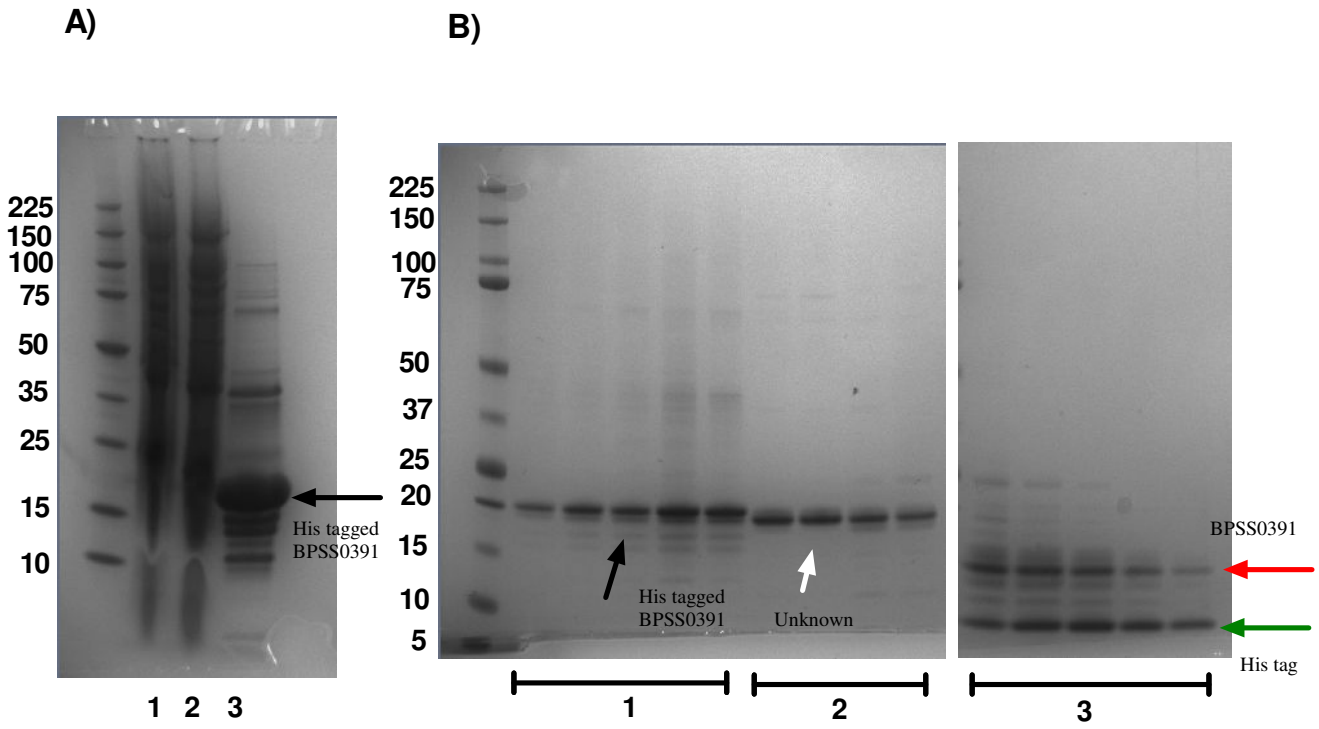

Figure 7.13 SDS-PAGE gels showing the purification steps of the BPSS0391 antitoxin. *E. coli* Rosetta (DE3) /pET26-b/his-BPSS0391 cultures were lysed in Bugbuster and lysozyme and the resulting cell lysate (lane 1, fig 7.13A) was run through a nickel affinity gravi his column. Protein that did not bind to the column (lane 2, fig 7.13A) was discarded and protein eluted from the column with imidazole (lane 3, fig 7.13A) was de-salted and enterokinase treated before running through a second nickel affinity gravi his column. The flowthrough and wash from this second his column were combined and added to a size exclusion chromatography column. The fractions containing protein were loaded onto SDS-PAGE gels B). 3 distinct samples were collected in the different fractions. Fractions 1 shows his tagged BPSS0391 protein at 20kDa (black arrow), fraction 2 shows an unknown protein of 18kDa (white arrow), Fraction 3 shows BPSS0391 at 15kDa (red arrow) and the his tag at 6kDa (green arrow).

In addition there were some fainter bands that could represent degradation (Figure 7.13B). Fractions containing the 20kDa protein (purified his tagged BPSS0391) were combined as were fractions containing the 15kDa protein (tagged removed BPSS0391).

7.3.5 Pull down assay

An alternative approach that was taken to try and prove that BPSS0390 interacts with BPSS0391 was to carry out a pull down assay. *E. coli* DH5α /pME6032-BPSS0391 were grown to early exponential phase in LB and then 25 mM IPTG was added to induce expression of BPSS0391. Cells were harvested by centrifugation and then lysed and centrifuged to isolate total soluble protein (prey protein). Purified his tagged H24A protein (bait) was incubated with nickel coated beads to bind before washing away unbound material and adding the prey protein. Not all of the bait bound to the beads and some was washed through the column (figure 7.14). The bait and prey were incubated overnight for maximum binding before washing away unbound material. Finally the bait and prey were removed from the nickel coated beads by adding imidazole to compete with the his tag to nickel bead interaction. Only 1 protein appeared to be present in elute following removal of the bait and prey protein from the column. This band ran slightly higher on the SDS-PAGE gel compared to the his tagged H24A bait control.

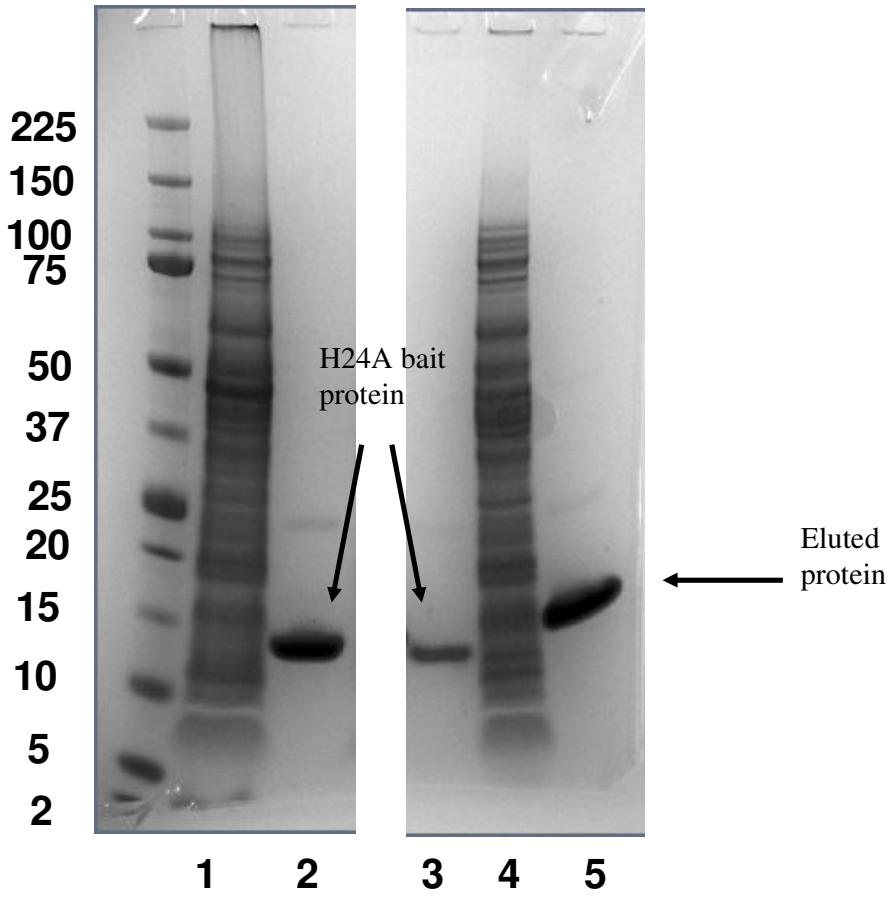

Figure 7.14 SDS-PAGE gel showing the result of a pull down assay using purified his tagged BPSS0390H24A protein as the bait protein and the cell lysate from a 3 hour BPSS0391 induced culture of *E. coli* DH5α /pME6032-BPSS0391 as the prey. BPSS0391 was induced with 25 mM IPTG once the culture reached early exponential phase. Lanes 1 and 2 on the gel show the total cell lysate (prey) and H24Ahis (bait) protein respectively. Lane 3 shows the flow through from washing (1:1 mix of TBS with profound lysis buffer) the column following incubation of the nickel beads with the bait protein. Lane 4 shows the flow though from the column after incubation of the beads and bait protein with the prey cell lysate. Lane 5 shows the total protein eluted from the column after imidazole treatment to remove bound prey and bait from the nickel coated beads.

7.4 RNA binding properties of the BPSS0390 toxin

Purified material following co-expression of his tagged BPSS0390 and BPSS0391 in *E. coli* was used in this experiment, since it contained BPSS0390 protein. Purified H24A protein was also tested along with BSA and RNase H controls. 1µg of MS2 RNA was incubated with protein and water in a 20µl reaction volume for 10 minutes before running the samples on a 1% (w/v) agarose gel to screen for degradation. MS2 RNA incubated with water only or 0.5 µg of BSA protein ran in a similar manner on the gel (Figure 7.15) Incubation with RNaseH caused complete degradation of the RNA, as no RNA was visible on the gel. When incubated with H24A protein the RNA appeared to be shifted down the gel, which could suggest binding but no degradation. When the RNA was incubated with the BPSS0390-0391 purified protein all the RNA appeared to be condensed into one band smaller than 250bp. When this assay was repeated, although the H24A protein gave a similar pattern when incubated with RNA, the BPSS0390-0391 purified protein failed to give the same phenotype. This could be because the protein had partially degraded and lost functionality as it was stored in the fridge between experiments and not freshly prepared.

7.5 Binding of BPSS0390H24A and BPSS0391 to DNA

The left flanking region of the BPSS0390-0391 locus containing the predicted promoter region was PCR amplified from genomic *B. pseudomallei* K96243 DNA using region specific primers to create a 600bp product. 1 mg/ml of either his tagged BPSS0391 or BPSS0391 in PBS was incubated with 500ng of PCR product in a 20µl volume made up with water. Water only, BSA (0.5 mg/ml) and BPSS0390H24A (0.45 mg/ml) were also set up for comparison. When the PCR product was

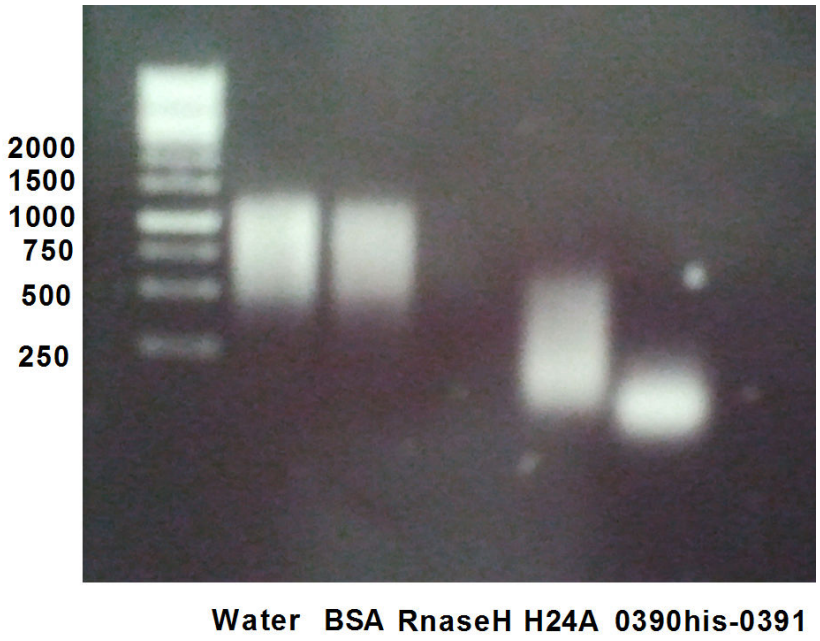

Figure 7.15 Agarose gel showing the migration pattern of MS2 RNA incubated with various proteins. 1 µg of RNA was incubated with water only, BSA, RnaseH, H24A protein or BPSS0390his-0391 purified protein in a 20 µl volume for 10 minutes at RT. The RNA: protein mix was then loaded onto a 1% (w/v) agarose gel containing DNA SYBR safe stain and run for 30 minutes at 180V before visualisation under a UV light. The concentration of BSA was 0.5 mg/ml, H24A was 0.45 mg/ml and BPSS0390-BPSS0391 mix was 0.05 mg/ml.

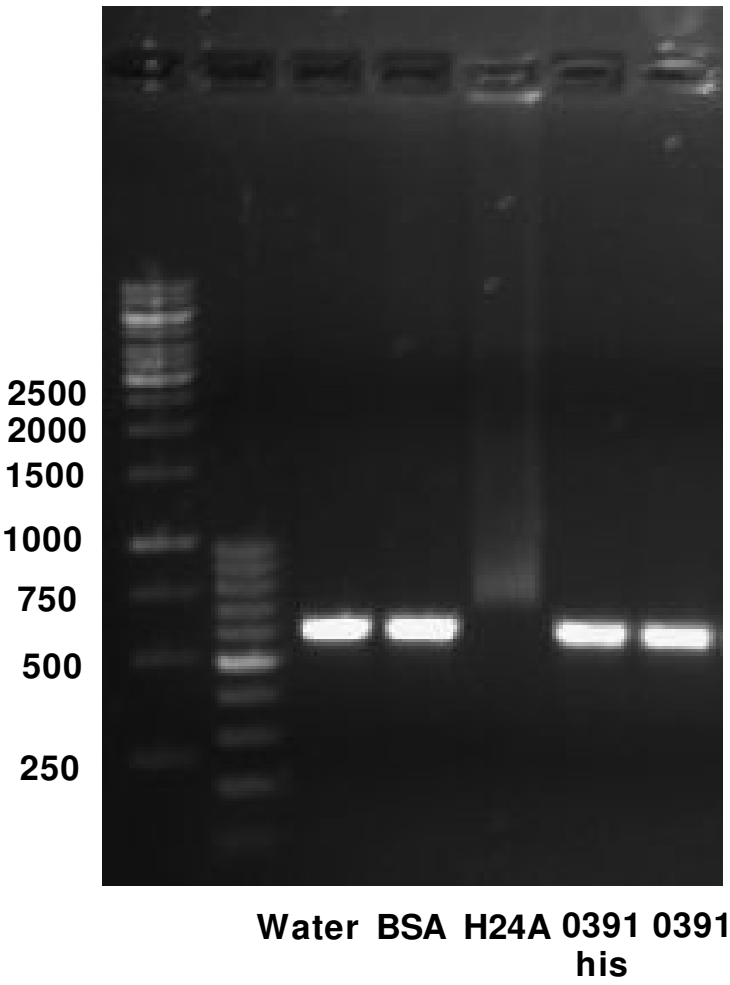

Figure 7.16 EMSA assay incubating purified his tagged BPSS0391 and BPSS0391 protein (1 mg/ml) with a 600bp upstream region of the BPSS0390-0391 locus containing the predicted promoter region. 500ng of DNA was incubated with the protein samples before adding to a reaction volume of 20 µl total for 10 minutes at RT. Samples were run on a 1% (w/v) agarose gel stained with SYBR safe stain for 30 minutes at 180v. Water only, BSA (0.5 mg/ml) and BPSS0390H24A (0.45 mg/ml) acted as controls. DNA was visualised under UV light.

incubated with water only, BSA, his tagged BPSS0391 or BPSS0391 the DNA fragment migrated to the correct size position of 600bp (Figure 7.16). When incubated with BPSS0390H24A there was a shifting pattern, with some of the DNA at approximately 700bp and the rest isolated in the top of the lane.

7.6 Binding of various concentrations of BPSS0390H24A to DNA

The BPSL2333 gene was amplified from genomic *B. pseudomallei* K96243 DNA using gene specific primers to give the 800bp random PCR product. In parallel the left flanking region of the BPSS0390-0391 locus, containing the predicted promoter region, was PCR amplified from genomic *B. pseudomallei* K96243 DNA using region specific primers to create a 600bp upstream product. Varying amounts of purified H24A toxin were incubated with both the random PCR product and the 600bp DNA fragment upstream of the BPSS0390-0391 locus.

500ng of the random PCR product was incubated with 0.45, 0.9, 1.8, or 3.6 mg/ml of the H24A protein (70, 140, 280 or 560nM respectively) for 10 minutes in a final volume of 20µl made up to volume with water. Water only and BSA at 0.5 mg/ml were also incubated with the PCR product as controls. The samples were then run on an agarose gel before visualising the migration of the DNA. When the PCR product was incubated with water only or BSA, the DNA migrated as a 330bp fragment (figure 7.17A). Addition of the H24A protein to the PCR product resulted in a concentration dependent mobility shift of the DNA.

The PCR product derived from the BPSS0390-0391 region also showed a mobility shift in a H24A concentration dependent manner (figure 7.17B).

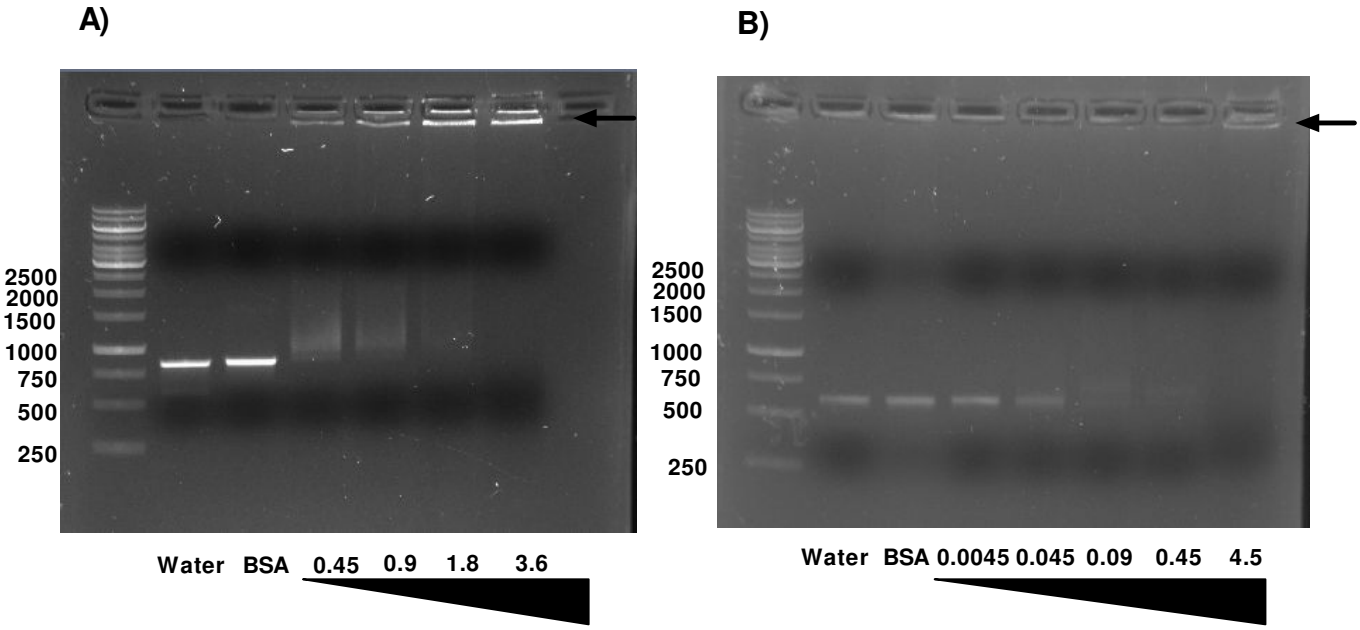

Figure 7.17 EMSA assay incubating BPSS0390H24A protein at various concentrations with either A) 800bp BPSL2333 gene PCR product or B) 600 bp upstream region of BPSS0390-0391 locus containing the predicted promoter region. 500 ng of DNA was incubated with the protein samples (that were diluted in water where necessary) before adding to a reaction volume of 20 µl total for 10 minutes at RT. Numbers show the protein concentration in mg/ml The samples were then run on a 1 % (w/v) agarose gel stained with SYBR safe stain for 30 minutes at 180 v. Water only and BSA (0.5 mg/ml) were used as controls. DNA was visualised under UV light.

7.7 Discussion

Alignment of the BPSS0390 (HicA) protein sequence with homologous protein sequences revealed some highly conserved residues that may have importance in functionality. Indeed mutating 5 of these residues and running the toxin mutants through the toxicity and persister assays revealed that residues histidine 24 and glycine 22 were important in function. Substitution of either of these 2 amino acids with alanine or cystine rendered the protein non-toxic. Based on the model structure generated by Swiss model it is apparent that these 2 residues are present in a protruding loop that may bind to RNA. Histidine residues have importance in RNA binding and degradation in other enzymes. For instance a histidine to alanine point mutation in an archaeal RNA splicing endoribonuclease reduces activity by 28-fold (Calvin*, et al.*, 2008) and histidine mutations in the CPEB RNA binding protein can completely abolish binding (Hake*, et al.*, 1998). 2 histidine residues are also critical in catalysis of RNA cleavage by the ribonuclease A enzyme (Park*, et al.*, 2001). This suggests that His24 in HicA is either important in RNA binding or the catalysis of RNA degradation.

Glycine residues also have importance in RNA binding. For instance the RNA binding domain of the human UA1 protein has reduced RNA binding by 200 fold when a conserved glycine residue is mutated to alanine or valine, suggesting it modulates binding of the protein to the RNA (Showalter & Hall, 2004). Also, 3 glycine residues are important in binding of the bovine immunodeficiency virus Tat protein to the major groove of RNA (Chen & Frankel, 1995). This suggests the Gly22 residue in the HicA protein modulates binding of the toxin to RNA targeted for degradation. Mutation of the other 3 residues did not affect the CFU reduction phenotype or persister frequencies caused by the HicA toxin.

It was previously shown that addition of a histidine tag inactivated the HipA toxin (chapter 3). However, addition of a tag to the HicA toxin did not prevent toxicity of the protein. The histidine tag was used for protein purification and structural studies on the H24A protein. Expression of the wild type HicA his tagged protein could not be detected by Western blot unless co-expressed with the HicB antitoxin. This was not surprising since expression of the toxin inhibited growth and translation. Neutralisation of the his tagged HicA toxin by HicB antitoxin expression allowed cell growth resulting in higher yields of HicA toxin that were detectable on a Western blot and could be purified. Expression of the HicA mutants H24A and G22C could be detected by Western blotting in the absence of HicB as they did not modulate cell growth. G14C, P41A and S23A required co-expression with HicB before expression could be detected.

The *E. coli* strains harbouring HicA mutants G14C, S23A or P41A that were toxic when expressed showed no reduction in CFU or optical binding when co-expressed with HicB. This suggests that the Glycine 14, Serine 23 and Proline 41 residues do not have an important functional role in either substrate or antitoxin binding.

CD spectroscopy analysis revealed the purified his tagged H24A protein was folded and had secondary structure consisting predominantly of beta-sheeted regions comparable to the model structure generated by Swiss model. Degradation experiments also suggested that the HicA H24A protein was stable in a variety of buffer conditions.

As the HicA H24A protein was folded, attempts at crystallising the protein were made but they proved unsuccessful at the concentration trialled. It is possible that further concentration of the protein >10 mg/ml may have proven more successful

at generating protein crystals in 1 or more of the buffer screens. Screening more additives and buffer conditions may also have aided in crystal growth although these procedures may have been time consuming. NMR seemed a more feasible experimental approach considering the H24A protein was small at only 6.6kDa, consisting of 58 amino acids and relatively stable (indicated by the degradation experiments).

Aligning HicB sequences from different bacteria identified many highly conserved residues that may have importance in DNA or HicA binding. Time contraints meant none of these residues could be mutated to confirm activity. When his tagged HicB was overexpressed for purification it appeared to be unstable. Antitoxins are readily degraded by proteases and the *E. coli* HicB toxin is degraded by the Lon protease (Jorgensen*, et al.*, 2008). Lon protease present in the cell lysate was probably responsible for the detectable degradation of the purified HicB antitoxin when run on an SDS-PAGE gel. The protease usually degrades antitoxin at the C-terminus where the structure is looser (Gerdes & Maisonneuve, 2012). Thus adding an N-terminal his tag could not stabilise the protein to prevent degradation.

To confirm that HicA and HicB could interact, a variety of methods were used. Native PAGE was not useful to confirm interaction, as the HicA and HicB proteins are small (approximately 6.6kDa and 15kDa respectively). A pull down assay was performed but there was no obvious HicB band (expected size 15kDa) eluted with the his tagged HicA toxin following incubation. However the his tagged HicA protein did appear to run slightly higher than the controls. If there was a very strong interaction between tagged HicA and a very small peptide, which resists the denaturing conditions, then this might be a complex visible on the gel. The complex appears to be too small to be a complex of HicA and HicB, which would be approximately 25kDa

(15kDa HicB +10kDa tagged HicA) in size. It is possible that the tagged HicA protein bound to another protein in the lysate and perhaps mass spectrometry analysis would have determined the identity of the protein band. The failure to detect a HicB band may also have been the result of salt in the wash buffer. Some protein interactions can be dissolved by salt, so the antitoxin may have been washed away prior to elution. This assay was only performed once and it is possible that repetitive experiments with an alternate method would have shown both HicA and HicB proteins in the elution.

The final assay was to co-express both *hicA* and *hicB* genes and purify the encoded proteins. Running the purified sample on a SDS-PAGE gel and performing a Western blot did detect the HicA toxin along with another 2 bands. The higher band could be a complex of HicAB that resisted denaturation by heat and SDS or oligomerised HicA protein. Looking at the protein gel only, there was no obvious HicB band in the elution but a potential band in the wash, suggesting HicAB interactions could be relatively weak. From these experiments it cannot be concluded that the proteins interact.

Although the H24A mutation abolished the toxic activity of the HicA toxin, incubation studies with MS2 RNA revealed it was able to bind to the RNA. Incubation of the MS2 RNA with purified protein from co-expressed HicA and HicB gave a condensed small band on the gel suggesting the RNA had been digested but not completely degraded. Unfortunately this observation could not be repeated in subsequent experiments

In the Electrophoretic mobility shift assay (EMSA) experiment H24A was able to bind to 2 test PCR products, including 1 that contained the HicAB promoter region, causing a shift of the DNA on an agarose gel. HipA was also previously shown to bind to its DNA promoter region (Black*, et al.*, 1994). As the concentration

of HicA H24A protein was increased the shifting effect was enhanced. This shift in both DNA products suggests the binding activity of the HicA protein for nucleotides is non-specific. All TA systems to date that have had their regulatory mechanism determined appear to be negatively regulated by the antitoxin and/ or TA complex binding to the promoter region (Gerdes*, et al.*, 2005). Incubation of the PCR product containing the predicted promter upstream of the *hicAB* loci with purified HicB or HicB his protein did not cause a shift in the gel. There could be many reasons why no shifting pattern was observed. The protein may have been too degraded to bind and shift the DNA, the amount of protein could have been too low to have caused a shifting effect, HicB antitoxin may require binding to the HicA toxin for DNA binding, or the HicB antitoxin may not have been in the right conditions or had the necessary cofactors. The EMSA method used in these experiments involved relatively high concentrations of DNA. Perhaps using a radiolabelled method would be a more sensitive method. Binding buffers should also have been used that reflect pH and ion levels in the cytoplasm.

As *hicAB* loci have a different gene order compared to most TA systems it could be possible that there is a different regulatory mechanism for this TA system. The only other type II TA system with reversed gene order is HigBA. The HigA antitoxin from this system has also been shown to regulate expression of the TA system so it appears likely that this is also true for HicAB (Fivian-Hughes & Davis, 2010)

Chapter 8
Final Discussion and conclusions

B. pseudomallei causes a high rate of recurrent and relapsing infection in adult melioidosis patients (Chaowagul, et al., 1993). This is often attributed to recrudescence of the initial infecting strain (Hayden, *et al.*, 2012). Bacterial cells isolated from both the primary infection and relapse infections up to 6 years later can have significant genetic changes associated with antibiotic resistance (Hayden, *et al.*, 2012). Recurrent infection may also involve antibiotic tolerant cells (persister cells). Isocitrate lysate has recently been shown to be a persistence factor in *B. pseudomallei*. Inhibiting the activity of this enzyme during a chronic lung infection forces the bacteria into an acute replicating state that become susceptible to antibiotics (van Schaik, *et al.*, 2009). Toxin-antitoxin systems have also been demonstrated to affect persistence in other bacteria. For instance in *M. tuberculosis,* which is also associated with high recurrent chronic disease, overexpression of *relE* can significantly increase the survival of the bacteria to a range of antibiotics, while deletion of *relE* can significantly decrease survival (Singh, *et al.*, 2010). Much work on TA systems has been carried out in *E. coli* and in addition to RelE, the TA toxins MazF, HipA and TisB have all been associated with persistence (Falla & Chopra, 1998, Keren, *et al.*, 2004, Correia, *et al.*, 2006, Korch & Hill, 2006, Vazquez-Laslop, *et al.*, 2006, Dörr, *et al.*, 2010). Elimination of persister cells by understanding the molecular basis for their formation and their location within the host may aid in developing better drug therapy for successful treatment of chronic melioidosis. New evidence suggests that *B. pseudomallei* persisters may reside in the GI tract particularly in the stomach (Goodyear, *et al.*, 2012).

This study aimed to identify and characterise TA systems in *B. pseudomallei.* Of the eight cloned toxin genes the paralogous toxins BPSS1060 (RelE1) and BPSL0175 (RelE2) caused growth arrest when expressed, while the BPSS0390

(HicA) and BPSS1584 (HipA) toxins caused growth arrest and a reduction in the number of culturable bacteria when expressed in *E. coli* MG1655 and *E. coli* MG1655 Δ*hipBA* respectively. This reduction in culturability phenotype was not the result of cell death as cells could be resuscitated by expression of the cognate antitoxin (and in the case of the HicA also by the RelE2 antitoxin), and Live/dead staining revealed there was no significant cell death following toxin expression. This indicated the cells were entering into a non-culturable state and were not completely metabolically inactive. This could be similar to the viable but nonculturable (VBNC) state. Oliver describes the VBNC state as bacteria that fail to grow on routine bacteriological media but are still alive. The bacteria have low metabolic activity but can become culturable on resuscitation (Oliver, 2010). Expression of the HicA toxin was also able to increase persister cell frequencies of *E. coli* to different classes of antibiotics. Since antibiotics target actively growing cells it suggested that HicA was inducing an antibiotic tolerant state. It is possible that persister cells, the VBNC state and toxin induced cells are similar or variants of the same phenotype, since they are all tolerant to antibiotics (Lewis, 2010, Oliver, 2010).

Following expression of the *B. pseudomallei* HipA or HicA toxins in *E.* coli not all cells became nonculturable or antibiotic tolerant. Some possible explanations include cells not expressing the toxin or toxin levels being below a particular threshold needed for the induction of non-culturability/ antibiotic tolerant phenotypes. Moreover there appeared to be an additional quorum sensing based factor or factors that accumulated in stationary phase spent media. This contributed to the switch in phenotype to growth arrest and/or reduction in culturability for HipA, HicA and RelE2. The cell density effect and enhancement of toxicity by spent media was also observed in *B. pseudomallei* in either *B. pseudomallei* or *E. coli* spent media. This

suggested a common factor or factors between the 2 species. Further studies are needed to identify this factor(s), perhaps through column size filtration of spent media and mass spectrometry. Such a factor could be similar to the pentapeptide EDF involved in MazF functionality in *E. coli* or the factor associated with RelE function (Kolodkin-Gal*, et al.*, 2007, Tashiro*, et al.*, 2012).

It appears that there is redundancy and even cross talk between the different TA systems that allow the bacteria to cope with a series of stresses. For instance deletion of the *hipBA* or *hicAB* system from *B. pseudomallei* K96343 did not give a significant difference in persister frequencies in response to a series of stresses that were up regulated in the microarray data. It is possible that other stresses may have given a phenotype. More likely subsequent deletions of many or all TA systems in *B. pseudomallei* are needed to eliminate the persistence phenotype (Maisonneuve*, et al.*, 2011). Knocking out single genes associated with persistence cannot completely eliminate persister cell generation (Lewis, 2010).

As the *B. pseudomallei* TA toxins HipA, HicA, RelE1 and RelE2 could be expressed in *E. coli* it is possible that the toxins could be used as novel growth inhibitors to stop the spread of a range of bacterial infections. Alternatively, inhibitors or compounds could be developed that could inhibit the function of TA toxins to prevent them from inducing persister cells, which may allow for more affective sterilisation by antibiotics. Inhibitors could be developed based on the antitoxin proteins since they already act by binding and inhibiting the toxin protein. By removing protease susceptible domains, the generation of stable antitoxins may be possible. Inhibitors could also be designed to target key catalytic residues. For instance designing an inhibitor that masked the activity of the histidine 24 or glycine 22 residues in the HicA protein would prevent its RNA degradation function.

The RASTA bacteria resource identified many more candidate genes that were not studied in this work. Expression of these candidate genes in the *E. coli* host may give similar phenotypes to HicA, HipA or RelE and increase the repertoire of known type II TA systems within the *B. pseudomallei* K96243 genome. New type II families may also be identified since many of the candidate genes have no homology to currently characterised families.

This work focused solely on type II toxin-antitoxin systems and it is possible that the genome of *B. pseudomallei* K96243 contains a range of type I, III or V toxin-antitoxin systems. At present these groups are relatively understudied although some bioinformatic screening on bacterial genomes has been performed (Blower*, et al.*, 2012). Identification and subsequent expression of these other TA groups may demonstrate functional importance in *B. pseudomallei* survival and persistence in chronic disease. For instance the TisB type I toxin increases persistence to ciprofloxacin in *E. coli* (Dörr*, et al.*, 2010).

All toxin-antitoxin characterisation was carried out in the K96243 strain of *B. pseudomallei.* The RASTA bacteria software predicted additional TA systems that were not present in the genome of K96243 but were present in the genomes of *B. pseudomallei* 1106a, 668 and 1170b strains. Further study into TA systems in other strains would help develop a broader picture of the conservation of different functional TA families and provide a better picture on their role in both environmental and host survival. Some TA systems such as the HipBA system appeared to be highly conserved throughout all strains compared in this study, while others such as the HicAB and RelBE families were less conserved. The HicAB and RelBE systems are located on genomic islands in *B. pseudomallei* and are presumably more susceptible to genetic loss or gain amongst the different strains (Sim*, et al.*, 2008). This could

suggest that the HipBA system has more of a conserved functional role, whereas the other systems are more freely motile providing stress adaptation in different environments. Those TA systems on GIs could be relics of phage elements or selfish DNA that may have no function *in vivo.* However, the *hicAB, relBE1* and *relBE2* genes were up or down regulated in a series of stress related microarray data sets and were associated with clinical strains of *B. pseudomallei* (Sim, et al., 2008). This suggests they provide some adaptive role.

References

Ab E, Atkinson AR, Banci L*, et al.* (2006) NMR in the SPINE Structural Proteomics project. *Acta Crystallogr D Biol Crystallogr* **62**: 1150-1161.

Ahmed K, Enciso HD, Masaki H, Tao M, Omori A, Tharavichikul P & Nagatake T (1999) Attachment of *Burkholderia pseudomallei* to pharyngeal epithelial cells: a highly pathogenic bacteria with low attachment ability. *Am J Trop Med Hyg* **60**: 90-93

Akira S, Uematsu S & Takeuchi O (2006) Pathogen recognition and innate immunity. *Cell* **124**: 783-801.

Allison KR, Brynildsen MP & Collins JJ (2011) Metabolite-enabled eradication of bacterial persisters by aminoglycosides. *Nature* **473**: 216-220.

Amitai S, Yassin Y & Engelberg-Kulka H (2004) MazF-mediated cell death in *Escherichia coli*: a point of no return. *J Bacteriol.* **186**: 8295–8300.

Amitai S, Kolodkin-Gal I, Hananya-Meltabashi M, Sacher A & Engelberg-Kulka H (2009) *Escherichia coli* MazF leads to the simultaneous selective synthesis of both "Death proteins" and "Survival proteins". *PLoS Genetics* **5**.

Arbing MA, Handelman SK, Kuzin AP*, et al.* (2010) Crystal structures of Phd-Doc, HigA, and YeeU establish multiple evolutionary links between microbial growth-regulating toxin-antitoxin systems. *Structure* **18**: 996-1010.

Ashdown LR & Koehler JM (1990) Production of hemolysin and other extracellular enzymes by clinical isolates of *Pseudomonas pseudomallei*. *J Clin Microbiol* **28**: 2331-2334.

Atkins T, Prior RG, Mack K*, et al.* (2002b) A mutant of *Burkholderia pseudomallei*, auxotrophic in the branched chain amino acid biosynthetic pathway, is attenuated and protective in a murine model of melioidosis. *Infect Immun* **70**: 5290-5294.

Atkins T, Prior R, Mack K*, et al.* (2002a) Characterisation of an acapsular mutant of *Burkholderia pseudomallei* identified by signature tagged mutagenesis. *J Med Microbiol* **51**: 539-547.

Attree O & Attree I (2001) A second type III secretion system in *Burkholderia pseudomallei*: who is the real culprit? *Microbiology* **147**: 3197-3199.

Balder R, Lipski S, Lazarus JJ*, et al.* (2010) Identification of *Burkholderia mallei* and *Burkholderia pseudomallei* adhesins for human respiratory epithelial cells. *BMC Microbiol* **10**: 250.

Bigger J (1944) Treatment of *staphylococcal* infections with penicillin. *Lancet* **244**: 497-500.

Black DS, Irwin B & Moyed HS (1994) Autoregulation of hip, an operon that affects lethality due to inhibition of peptidoglycan or DNA synthesis. *J Bacteriol* **176**: 4081-4091.

Black DS, Kelly AJ, Mardis MJ & Moyed HS (1991) Structure and organization of hip, an operon that affects lethality due to inhibition of peptidoglycan or DNA synthesis. *J Bacteriol* **173**: 5732-5739.

Blower TR, Salmond GP & Luisi BF (2011) Balancing at survival's edge: the structure and adaptive benefits of prokaryotic toxin-antitoxin partners. *Curr Opin Struct Biol* **21**: 109-118.

Blower TR, Short FL, Rao F*, et al.* (2012) Identification and classification of bacterial Type III toxin-antitoxin systems encoded in chromosomal and plasmid genomes. *Nucleic Acids Res* **40**: 6158-6173.

Breitbach K, Kohler J & Steinmetz I (2008) Induction of protective immunity against *Burkholderia pseudomallei* using attenuated mutants with defects in the intracellular life cycle. *Trans R Soc Trop Med Hyg* **102 Suppl 1**: S89-94.

Brown BL, Grigoriu S, Kim Y*, et al.* (2009) Three dimensional structure of the MqsR:MqsA complex: a novel TA pair comprised of a toxin homologous to RelE and an antitoxin with unique properties. *PLoS Pathog* **5**: e1000706.

Budde P, Davis B, Yuan J & Waldor M (2006) Characterization of a *higBA* toxin-antitoxin locus in *Vibrio cholerae*. *J Bacteriol.* **189**: 491-500.

Burtnick MN & Woods DE (1999) Isolation of polymyxin B-susceptible mutants of *Burkholderia pseudomallei* and molecular characterization of genetic loci involved in polymyxin B resistance. *Antimicrob Agents Chemother* **43**: 2648-2656.

Butler D (2012) Viral research faces clampdown. *Nature* **490**: 456.

Buts L, Lah J, Dao-Thi M, Wyns L & Loris R (2005) Toxin-antitoxin modules as bacterial metabolic stress managers. *Trends Biochem Sci* **30**: 672-679.

Button JE, Silhavy TJ & Ruiz N (2007) A suppressor of cell death caused by the loss of sigmaE downregulates extracytoplasmic stress responses and outer membrane vesicle production in *Escherichia coli*. *J Bacteriol* **189**: 1523-1530.

Calvin K, Xue S, Ellis C, Mitchell MH & Li H (2008) Probing the catalytic triad of an archaeal RNA splicing endonuclease. *Biochemistry* **47**: 13659-13665.

Cardona ST & Valvano MA (2005) An expression vector containing a rhamnose-inducible promoter provides tightly regulated gene expression in *Burkholderia cenocepacia*. *Plasmid* **54**: 219-228.

Chantratita N, Wuthiekanun V, Limmathurotsakul D*, et al.* (2008) Genetic Diversity and Microevolution of *Burkholderia pseudomallei* in the Environment. *PLoS Negl Trop Dis.* **20**.

Chaowagul W, Simpson AJ, Suputtamongkol Y & White NJ (1999) Empirical cephalosporin treatment of melioidosis. *Clin Infect Dis* **28**: 1328.

Chaowagul W, Suputtamongkol Y, Dance DA, Rajchanuvong A, Pattara-arechachai J & White NJ (1993) Relapse in melioidosis: incidence and risk factors. *J Infect Dis* **168**: 1181-1185.

Chaowagul W, White NJ, Dance DA*, et al.* (1989) Melioidosis: a major cause of community-acquired septicemia in northeastern Thailand. *J Infect Dis* **159**: 890-899.

Chen L & Frankel AD (1995) A peptide interaction in the major groove of RNA resembles protein interactions in the minor groove of DNA. *Proc Natl Acad Sci U S A* **92**: 5077-5081.

Chen YS, Chen SC, Kao CM & Chen YL (2003) Effects of soil pH, temperature and water content on the growth of *Burkholderia pseudomallei*. *Folia Microbiol (Praha)* **48**: 253-256.

Chen YS, Hsiao YS, Lin HH, Liu Y & Chen YL (2006) CpG-modified plasmid DNA encoding flagellin improves immunogenicity and provides protection against *Burkholderia pseudomallei* infection in BALB/c mice. *Infect Immun* **74**: 1699-1705.

Chieng S, Carreto L & Nathan S (2012) *Burkholderia pseudomallei* transcriptional adaptation in macrophages. *BMC Genomics* **13**: 328.

Chierakul W, Winothai W, Wattanawaitunechai C*, et al.* (2005) Melioidosis in 6 tsunami survivors in southern Thailand. *Clin Infect Dis* **41**: 982-990.

Christensen-Dalsgaard M & Gerdes K (2006) Two *higBA* loci in the *Vibrio cholerae* superintegron encode mRNA cleaving enzymes and can stabilize plasmids *Mol Microbiol***62**: 397-411.

Christensen-Dalsgaard M, Jørgensen M & K G (2010) Three new RelE-homologous mRNA interferases of *Escherichia coli* differentially induced by environmental stresses. *Mol Microbiol* **75**: 333-348.

Christensen SK & Gerdes K (2003) RelE toxins from bacteria and Archaea cleave mRNAs on translating ribosomes, which are rescued by tmRNA. *Mol Microbiol* **48**: 1389-1400.

Chua KL, Chan YY & Gan YH (2003) Flagella are virulence determinants of *Burkholderia pseudomallei*. *Infect Immun* **71**: 1622-1629.

Correia F, D'Onofrio A, Rejtar T*, et al.* (2006) Kinase activity of overexpressed HipA is required for growth arrest and multidrug tolerance in *Escherichia coli*. *Journal of Bacteriology* **188**: 8360-8367.

Cruz-Migoni A, Hautbergue GM, Artymiuk PJ*, et al.* (2011) A *Burkholderia pseudomallei* toxin inhibits helicase activity of translation factor eIF4A. *Science* **334**: 821-824.

Cuccui J, Easton A, Chu KK, Bancroft GJ, Oyston PC, Titball RW & Wren BW (2007) Development of signature-tagged mutagenesis in *Burkholderia pseudomallei* to identify genes important in survival and pathogenesis. *Infect Immun* **75**: 1186-1195.

Currie B, Fisher D, Anstey N & Jacups S (2000) Melioidosis: acute and chronic disease, relapse and re-activation. *Trans R Soc Trop Med Hyg.* **94**: 301-304.

Currie BJ & Jacups SP (2003) Intensity of rainfall and severity of melioidosis, Australia. *Emerg Infect Dis* **9**: 1538-1542.

Currie BJ, Fisher DA, Anstey NM & Jacups SP (2000) Melioidosis: acute and chronic disease, relapse and re-activation. *Trans R Soc Trop Med Hyg* **94**: 301-304.

Dao-Thi M, Van Melderen L, De-Genst E, Afif H, Buts L, Wyns L & Loris R (2005) Molecular basis of gyrase poisoning by the addiction toxin CcdB. *J Mol Biol* **348**: 1091-1102.

Datsenko K & Wanner B (2000) One step inactivation of chromosomal genes in *Escherichia coli* K-12 using PCR products. *Proc Natl Acad Sci U S A.* **97**.

Deshazer D (2007) Virulence of clinical and environmental isolates of *Burkholderia oklahomensis* and *Burkholderia thailandensis* in hamsters and mice. *FEMS Microbiol Lett* **277**: 64-69.

DeShazer D, Brett PJ & Woods DE (1998) The type II O-antigenic polysaccharide moiety of *Burkholderia pseudomallei* lipopolysaccharide is required for serum resistance and virulence. *Mol Microbiol* **30**: 1081-1100.

DeShazer D, Brett PJ, Carlyon R & Woods DE (1997) Mutagenesis of *Burkholderia pseudomallei* with Tn5-OT182: isolation of motility mutants and molecular characterization of the flagellin structural gene. *J Bacteriol* **179**: 2116-2125.

Dhiensiri T, Puapairoj S & Susaengrat W (1988) Pulmonary melioidosis: clinical-radiologic correlation in 183 cases in northeastern Thailand. *Radiology* **166**: 711-715.

Donegan NP, Thompson ET, Fu Z & Cheung AL (2010) Proteolytic regulation of toxin-antitoxin systems by ClpPC in *Staphylococcus aureus*. *J Bacteriol* **192**: 1416-1422.

Dörr T, Vulić M & Lewis K (2010) Ciprofloxacin causes persister formation by inducing the TisB toxin in *Escherichia coli*. *PLoS Biol.* **8**: e1000317.

Drevinek P & Mahenthiralingam E (2010) *Burkholderia cenocepacia* in cystic fibrosis: epidemiology and molecular mechanisms of virulence. *Clin Microbiol Infect* **16**: 821-830.

Easton A, Haque A, Chu K, Lukaszewski R & Bancroft GJ (2007) A critical role for neutrophils in resistance to experimental infection with *Burkholderia pseudomallei*. *J Infect Dis* **195**: 99-107.

Engelberg-Kulka H, Hazan R & S A (2005) *mazEF:* a chromosomal toxin-antitoxin module that triggers programmed cell death in bacteria. *J Cell Sci* **118**: 4327-4332.

Erickson JW & Gross CA (1989) Identification of the sigma E subunit of *Escherichia coli* RNA polymerase: a second alternate sigma factor involved in high-temperature gene expression. *Genes Dev* **3**: 1462-1471.

Essex-Lopresti AE, Boddey JA, Thomas R*, et al.* (2005) A type IV pilin, PilA, Contributes To Adherence of *Burkholderia pseudomallei* and virulence in vivo. *Infect Immun* **73**: 1260-1264.

Falla TJ & Chopra I (1998) Joint tolerance to beta-lactam and fluoroquinolone antibiotics in Escherichia coli results from overexpression of hipA. *Antimicrob Agents Chemother* **42**: 3282-3284.

Fiebig A, Castro Rojas CM, Siegal-Gaskins D & Crosson S (2010) Interaction specificity, toxicity and regulation of a paralogous set of ParE/RelE-family toxin-antitoxin systems. *Mol Microbiol* **77**: 236-251.

Fineran PC, Blower TR, Foulds IJ, Humphreys DP, Lilley KS & Salmond GP (2009) The phage abortive infection system, ToxIN, functions as a protein-RNA toxin-antitoxin pair. *Proc Natl Acad Sci U S A* **106**: 894-899.

Fink AL, Calciano LJ, Goto Y, Kurotsu T & Palleros DR (1994) Classification of acid denaturation of proteins: intermediates and unfolded states. *Biochemistry* **33**: 12504-12511.

Fivian-Hughes AS & Davis EO (2010) Analyzing the regulatory role of the HigA antitoxin within *Mycobacterium tuberculosis*. *J Bacteriol* **192**: 4348-4356.

Fozo EM, Hemm MR & G S (2008) Small toxic proteins and the antisense RNAs that repress them. *Microbiol Mol Biol Rev* **72**: 579-589.

Galvani C, Terry J & Ishiguro EE (2001) Purification of the RelB and RelE proteins of *Escherichia coli*: RelE binds to RelB and to ribosomes. *J Bacteriol* **183**: 2700-2703.

Galyov E, Brett p & DeShazer D (2010) Molecular insights in *Burkholderia pseudomallei* and *Burkholderia mallei* pathogenesis. *Annu Rev Microbiol* **64**: 495-517.

Garcia-pino A, Christensen-Dalsgaard M, Wyns L, Yarmolinsky M, Magnuson R,

Gerdes K & Loris R (2008) Doc of Prophage P1 Is Inhibited by Its Antitoxin Partner Phd through Fold Complementation. *J Biol Chem* **283**: 30821-30827.

Garcia-Pino A, Balasubramanian S, Wyns L*, et al.* (2010) Allostery and intrinsic disorder mediate transcription regulation by conditional cooperativity. *Cell* **142**: 101-111.

Gaynor E, Wells DH, Mackichan JK & S F (2005) The *Camplyobacter jejuni* stringent response controls specific stress survival and virulence associated phenotypes. *Mol Microbiol* **56**: 8-27.

Gerdes K & Maisonneuve E (2012) Bacterial persistence and toxin-antitoxin Loci. *Annu Rev Microbiol* **66**: 103-123.

Gerdes K, Christensen S & Lobner-Olesen A (2005) Prokaryotic toxin-antitoxin stress response loci. *Nat Rev Microbiol* **3**: 371-382.

Gerdes K & Wagner E (2007) RNA antitoxins. *Cur Opin Microbiol* **10**: 117-124.

Goodyear A, Bielefeldt-Ohmann H, Schweizer H & Dow S (2012) Persistent gastric colonization with *Burkholderia pseudomallei* and dissemination from the gastrointestinal tract following mucosal inoculation of mice. *PLoS One* **7**: e37324.

Gotfredsen M & Gerdes K (1998) The *Escherichia coli relBE* genes belong to a new toxin-antitoxin gene family. *Mol Microbiol* **29**: 1065-1076.

Goulard C, Langrand S, Carniel E & Chauvaux S (2010) The *Yersinia pestis* Chromosome Encodes Active Addiction Toxins. *J Bacteriol.* **192**: 3669–3677.

Grady R & Hayes F (2003) Axe-Txe, a broad-spectrum proteic toxin-antitoxin system specified by a multidrug-resistant, clinical isolate of *Enterococcus faecium. Mol Microbiol* **47**: 1419-1432.

Grady R & Hayes F (2003) Axe-Txe, a broad-spectrum proteic toxin–antitoxin system specified by a multidrug-resistant, clinical isolate of *Enterococcus faecium. Mol Microbiol* **47**: 1419-1432.

Grant SS, Kaufmann BB, Chand NS, Haseley N & Hung DT (2012) Eradication of bacterial persisters with antibiotic-generated hydroxyl radicals. *Proc Natl Acad Sci U S A* **109**: 12147-12152.

Gronwald W & Kalbitzer HR (2010) Automated protein NMR structure determination in solution. *Methods Mol Biol* **673**: 95-127.

Gupta A (2009) Killing activity and rescue function of genome-wide toxin-antitoxin loci of *Mycobacterium tuberculosis*. *FEMS Microbiol Letts.* **290**: 45-53.

Hake LE, Mendez R & Richter JD (1998) Specificity of RNA binding by CPEB: requirement for RNA recognition motifs and a novel zinc finger. *Mol Cell Biol* **18**: 685-693.

Hansen S, Lewis K & Vulic M (2008) Role of global regulators and nucleotide metabolism in antibiotic tolerance in *Escherichia coli*. *Antimicrob Agents Chemother* **52**: 2718-2726.

Hansen S, Vulic M, Min J, Yen TJ, Schumacher MA, Brennan RG & Lewis K Regulation of the *Escherichia coli* HipBA toxin-antitoxin system by proteolysis. *PLoS One* **7**: e39185.

Haque A, Chu K, Easton A*, et al.* (2006) A live experimental vaccine against *Burkholderia pseudomallei* elicits CD4+ T cell-mediated immunity, priming T cells specific for 2 type III secretion system proteins. *J Infect Dis* **194**: 1241-1248.

Haque A, Easton A, Smith D*, et al.* (2006) Role of T cells in innate and adaptive immunity against murine *Burkholderia pseudomallei* infection. *J Infect Dis* **193**: 370-379.

Hara Y, Mohamed R & Nathan S (2009) Immunogenic *Burkholderia pseudomallei* outer membrane proteins as potential candidate vaccine targets. *PLoS One* **4**: e6496.

Harley VS, Dance DA, Drasar BS & Tovey G (1998) Effects of *Burkholderia pseudomallei* and other *Burkholderia* species on eukaryotic cells in tissue culture. *Microbios* **96**: 71-93.

Hayden HS, Lim R, Brittnacher MJ*, et al.* (2012) Evolution of *Burkholderia pseudomallei* in recurrent melioidosis. *PLoS One* **7**: e36507.

Hayes C & Low D (2009) Signals of growth regulation in bacteria. *Curr Opin Microbiol.* **12**: 1-7.

Hayes F (2003) Toxins-antitoxins:plasmid maintenance, programmed cell death and cell cycle arrest. *Science* **301**: 1496-1499.

Heaton B, Herrou J, Blackwell A, Wysocki V & Crosson S (2012) Molecular structure and function of the novel BrnT/BrnA toxin-antitoxin system of *Brucella abortus*. *J Biol Chem* **287**: 12098–12110.

Hu Y & Coates AR (2005) Transposon mutagenesis identifies genes which control antimicrobial drug tolerance in stationary-phase *Escherichia coli*. *FEMS Microbiol Lett* **243**: 117-124.

Hurley J & Woychik N (2009) Bacterial Toxin HigB Associates with Ribosomes and Mediates Translation-dependent mRNA Cleavage at A-rich Sites. *J Biol Chem* **284**: 18605-18613.

Inglis TJ, Robertson T, Woods DE, Dutton N & Chang BJ (2003) Flagellum-mediated adhesion by *Burkholderia pseudomallei* precedes invasion of *Acanthamoeba astronyxis*. *Infect Immun* **71**: 2280-2282.

Jiang Y, Pogliano J, Helinski DR & Konieczny I (2002) ParE toxin encoded by the broad-host-range plasmid RK2 is an inhibitor of *Escherichia coli* gyrase. *Mol Microbiol* **44**: 971-979.

Joers A, Kaldalu N & Tenson T (2010) The frequency of persisters in *Escherichia coli* reflects the kinetics of awakening from dormancy. *J Bacteriol* **192**: 3379-3384.

Jones SM, Ellis JF, Russell P, Griffin KF & Oyston PC (2002) Passive protection against *Burkholderia pseudomallei* infection in mice by monoclonal antibodies against capsular polysaccharide, lipopolysaccharide or proteins. *J Med Microbiol* **51**: 1055-1062.

Jorgensen M, Pandey D, Jaskola M & Gerdes K (2008) HicA of *Escherichia coli* defines a novel family of translation-independent mRNA interferases in bacteria and archaea. *J Bacteriol.* **191**: 1191-1199.

Jung JW & Lee W (2004) Structure-based functional discovery of proteins: structural proteomics. *J Biochem Mol Biol* **37**: 28-34.

Kamada K & Hanaoka F (2005) Conformational change in the catalytic site of the ribonuclease YoeB toxin by YefM antitoxin. *Mol Cell* **19**: 497-509.

Kawano H, Hirokawa Y & Mori H (2009) Long-term survival of *Escherichia coli* lacking the HipBA toxin-antitoxin system during prolonged cultivation. *Biosci Biotechnol Biochem* **73**: 117-123.

Kawano M, Aravind L & Storz G (2007) An antisense RNA controls synthesis of an SOS-induced toxin evolved from an antitoxin. *Mol Microbiol* **64**: 738-754.

Kawano M, Oshima T, Kasai H & Mori H (2002) Molecular characterization of long direct repeat (LDR) sequences expressing a stable mRNA encoding for a 35-amino-acid cell-killing peptide and a cis-encoded small antisense RNA in *Escherichia coli*. *Mol Microbiol* **45**: 333-349.

Kedzierska B, Lian LY & Hayes F (2007) Toxin-antitoxin regulation: bimodal interaction of YefM-YoeB with paired DNA palindromes exerts transcriptional autorepression. *Nucleic Acids Res* **35**: 325-339.

Keren I, Kaldalu N, Spoering A, Wang Y & Lewis K (2004) Persister cells and tolerance to antimicrobials. *FEMS Microbiol Lett* **230**: 13-18.

Kespichayawattana W, Rattanachetkul S, Wanun T, Utaisincharoen P & Sirisinha S (2000) *Burkholderia pseudomallei* induces cell fusion and actin-associated membrane protrusion: a possible mechanism for cell-to-cell spreading. *Infect Immun* **68**: 5377-5384.

Khoo SK, Loll B, Chan WT, Shoeman RL, Ngoo L, Yeo CC & Meinhart A (2007) Molecular and structural characterization of the PezAT chromosomal toxin-antitoxin system of the human pathogen *Streptococcus pneumoniae*. *J Biol Chem* **282**: 19606-19618.

Kim JS, Heo P, Yang TJ*, et al.* (2011) Selective killing of bacterial persisters by a single chemical compound without affecting normal antibiotic-sensitive cells. *Antimicrob Agents Chemother* **55**: 5380-5383.

Kolodkin-Gal I, Hazan R, Gaathon A, Carmeli S & Engelberg-Kulka H (2007) A linear pentapeptide is a quorum- sensing factor required for mazEF mediated cell death in *Escherichia coli*. *Science.* **318**: 652-658.

Kolodkin-Gal I & H E-K (2008) The extracellular death factor: physiological and genetic factors influencing tts production and response in *Escherichia coli*. *J Bacteriol.* **190**: 3169-3175.

Kolodkin-Gal I, Sat B, Keshet A & H E-K (2008) The communication factor EDF and the toxin-antitoxin module *mazEF* determine the mode of action of antibiotics. *PLoS Biol* **6**.

Koponen MA, Zlock D, Palmer DL & Merlin TL (1991) Melioidosis. Forgotten, but not gone! *Arch Intern Med* **151**: 605-608.

Korbsrisate S, Tomaras AP, Damnin S*, et al.* (2007) Characterization of two distinct phospholipase C enzymes from *Burkholderia pseudomallei*. *Microbiology* **153**: 1907-1915.

Korch S & Hill T (2006) Ectopic overexpression of wild-type and mutant *hipA* genes in *Escherichia coli*: effects on macromolecular synthesis and persister formation. *J Bacteriol.* **188**: 3826-3836.

Korch SB, Henderson TA & Hill TM (2003) Characterization of the *hipA7* allele of *Escherichia coli* and evidence that high persistence is governed by (p)ppGpp synthesis. *Mol Microbiol* **50**: 1199-1213.

Lehnherr H & Yarmolinsky MB (1995) Addiction protein Phd of plasmid prophage P1 is a substrate of the ClpXP serine protease of *Escherichia coli*. *Proc Natl Acad Sci U S A* **92**: 3274-3277.

Leplae R, Geeraerts D, Hallez R, Guglielmini J, Dreze P & Van Melderen L (2011) Diversity of bacterial type II toxin-antitoxin systems: a comprehensive search and functional analysis of novel families. *Nucleic Acids Res.* **39**: 5513-5525.

Leung V & Lévesque C (2012) A stress-inducible quorum-sensing peptide mediates the formation of persister cells with noninherited multidrug tolerance. *J Bacteriol.* **194**: 2265-2274.

Lewis K (2010) Persister cells. *Annu Rev Microbiol* **64**: 357-372.

Li GY, Zhang Y, Inouye M & Ikura M (2009) Inhibitory mechanism of *Escherichia coli* RelE-RelB toxin-antitoxin module involves a helix displacement near an mRNA interferase active site. *J Biol Chem* **284**: 14628-14636.

Lichty JJ, Malecki JL, Agnew HD, Michelson-Horowitz DJ & Tan S (2005) Comparison of affinity tags for protein purification. *Protein Expr Purif* **41**: 98-105.

Liu M, Zhang Y, Inouye M & Woychik NA (2008) Bacterial addiction module toxin Doc inhibits translation elongation through its association with the 30S ribosomal subunit. *Proc Natl Acad Sci U S A* **105**: 5885-5890.

Luidalepp H, Joers A, Kaldalu N & Tenson T (2011) Age of inoculum strongly influences persister frequency and can mask effects of mutations implicated in altered persistence. *J Bacteriol* **193**: 3598-3605.

Madl T, Van Melderen L, Mine N*, et al.* (2006) Structural basis for nucleic acid and toxin recognition of the bacterial antitoxin CcdA. *J Mol Biol* **364**: 170-185.

Maisonneuve E, Shakespeare L, Jorgensen M & Gerdes K (2011) Bacterial persistence by RNA endonucleases. *Proc Natl Acad Sci U S A*. **108**: 13206-13211.

Makarova K, Wolf Y & Koonin E (2009) Comprehensive comparative-genomic analysis of type 2 toxin-antitoxin systems and related mobile stress response systems in prokaryotes. *Biol Direct.* **4**.

Makarova KS, Grishin NV & Koonin EV (2006) The HicAB cassette, a putative novel, RNA-targeting toxin-antitoxin system in archaea and bacteria. *Bioinformatics* **22**: 2581-2584.

Makarova KS, Wolf YI, Snir S & Koonin EV (2011) Defense islands in bacterial and archaeal genomes and prediction of novel defense systems. *J Bacteriol* **193**: 6039-6056.

Mattison K, Wilbur JS, So M & Brennan RG (2006) Structure of FitAB from *Neisseria gonorrhoeae* bound to DNA reveals a tetramer of toxin-antitoxin heterodimers containing pin domains and ribbon-helix-helix motifs. *J Biol Chem* **281**: 37942-37951.

Melderen V & De-Bast (2009) Bacterial Toxin- Antitoxin systems: More than selfish entities. *PLoS Genet* **5**.

Moker N, Dean CR & Tao J (2010) *Pseudomonas aeruginosa* increases formation of multidrug-tolerant persister cells in response to quorum-sensing signaling molecules. *J Bacteriol* **192**: 1946-1955.

Moritz E & Hergenrother P (2006) Toxin- antitoxin systems are ubiquitous and plasmid- encoded in vancomycin-resitant *enterococci*. *Proc Natl Acad Sci U S A* **104**: 311-316.

Moyed HS & Broderick SH (1986) Molecular cloning and expression of *hipA*, a gene of *Escherichia coli* K-12 that affects frequency of persistence after inhibition of murein synthesis. *J Bacteriol* **166**: 399-403.

Muller CM, Conejero L, Spink N, Wand ME, Bancroft GJ & Titball RW (2012) Role of RelA and SpoT in *Burkholderia pseudomallei* virulence and immunity. *Infect Immun* **80**: 3247-3255.

Mutschler H, Gebhardt M, Shoeman R & Meinhart A (2011) A novel mechanism of programmed cell death in bacteria by toxin-antitoxin systems corrupts peptidoglycan synthesis. *PLoS Biol.* **9**: e1001033.

Nariya H & Inouye M (2008) MazF, an mRNA interferase, mediates programmed cell death during multicellular *Myxococcus* development. *Cell* **132**: 55-66.

Nelson M, Prior JL, Lever MS, Jones HE, Atkins TP & Titball RW (2004) Evaluation of lipopolysaccharide and capsular polysaccharide as subunit vaccines against experimental melioidosis. *J Med Microbiol* **53**: 1177-1182.

Neubauer C, Gao YG, Andersen KR*, et al.* (2009) The structural basis for mRNA recognition and cleavage by the ribosome-dependent endonuclease RelE. *Cell* **139**: 1084-1095.

Ngauy V, Lemeshev Y, Sadkowski L & Crawford G (2005) Cutaneous melioidosis in a man who was taken as a prisoner of war by the Japanese during World War II. *J Clin Microbiol* **43**: 970-972.

Oberer M, Zangger K, Gruber K & Keller W (2007) The solution structure of ParD, the antidote of the ParDE toxin antitoxin module, provides the structural basis for DNA and toxin binding. *Protein Sci* **16**: 1676-1688.

Oliver JD (2010) Recent findings on the viable but nonculturable state in pathogenic bacteria. *FEMS Microbiol Rev* **34**: 415-425.

Overgaard M, Borch J & Gerdes K (2009) RelB and RelE of *Escherichia coli* form a tight complex that represses transcription via the ribbon-helix-helix motif in RelB. *J Mol Biol* **394**: 183-196.

Overgaard M, Borch J, Jorgensen MG & Gerdes K (2008) Messenger RNA interferase RelE controls relBE transcription by conditional cooperativity. *Mol Microbiol* **69**: 841-857.

Pan J, Bahar AA, Syed H & Ren D (2012) Reverting Antibiotic Tolerance of *Pseudomonas aeruginosa* PAO1 Persister Cells by (Z)-4-bromo-5-(bromomethylene)-3-methylfuran-2(5H)-one. *PLoS One* **7**: e45778.

Pandey D & Gerdes K (2005) Toxin-antitoxin loci are highly abundant in free-living but lost from host-associated prokaryotes. *Nucleic Acids Res.* **33**: 966-976.

Park C, Schultz LW & Raines RT (2001) Contribution of the active site histidine residues of ribonuclease A to nucleic acid binding. *Biochemistry* **40**: 4949-4956.

Patel N, Conejero L, De Reynal M, Easton A, Bancroft GJ & Titball RW (2011) Development of vaccines against *Burkholderia pseudomallei*. *Front Microbiol* **2**: 198.
Payne GW, Vandamme P, Morgan SH*, et al.* (2005) Development of a recA gene-based identification approach for the entire *Burkholderia* genus. *Appl Environ Microbiol* **71**: 3917-3927.

Pedersen K, Christensen S & Gerdes K (2002) Rapid induction and reversal of a bacteriostatic condition by controlled expression of toxins and antitoxins. *Mol Microbiol.* **45**: 501-510.

Pedersen K, Zavialov A, Pavlov M, Elf J, Gerdes K & Ehrenberg M (2003) The Bacterial Toxin RelE Displays Codon-Specific Cleavage of mRNAs in the Ribosomal A Site. *Cell* **112**: 131-140.

Price EP, Hornstra HM, Limmathurotsakul D*, et al.* (2010) Within-Host Evolution of *Burkholderia pseudomallei* in Four Cases of Acute Melioidosis. *PLoS Pathog* **6**: e1000725.

Pruksachartvuthi S, Aswapokee N & Thankerngpol K (1990) Survival of *Pseudomonas pseudomallei* in human phagocytes. *J Med Microbiol* **31**: 109-114.

Pumirat P, Cuccui J, Stabler RA*, et al.* (2010) Global transcriptional profiling of *Burkholderia pseudomallei* under salt stress reveals differential effects on the Bsa type III secretion system. *BMC Microbiol* **10**: 171.

Rajchanuvong A, Chaowagul W, Suputtamongkol Y, Smith MD, Dance DA & White NJ (1995) A prospective comparison of co-amoxiclav and the combination of chloramphenicol, doxycycline, and co-trimoxazole for the oral maintenance treatment of melioidosis. *Trans R Soc Trop Med Hyg* **89**: 546-549.

Ramage H, Connolly L & Cox J (2009) Comprehensive functional analysis of *Mycobacterium tuberculosis* Toxin-antitoxin systems: implications for pathogenesis, stress response and evolution. *PLoS Genet.* **5**.

Reckseidler-Zenteno SL, DeVinney R & Woods DE (2005) The capsular polysaccharide of *Burkholderia pseudomallei* contributes to survival in serum by reducing complement factor C3b deposition. *Infect Immun* **73**: 1106-1115.

Roberts RC, Strom AR & Helinski DR (1994) The *parDE* operon of the broad-host-range plasmid RK2 specifies growth inhibition associated with plasmid loss. *J Mol Biol* **237**: 35-51.

Rodrigues F, Sarkar-Tyson M, Harding SV*, et al.* (2006) Global map of growth-regulated gene expression in *Burkholderia pseudomallei*, the causative agent of melioidosis. *J Bacteriol* **188**: 8178-8188.

Rotem E, Loinger A, Ronin I*, et al.* (2010) Regulation of phenotypic variability by a threshold based mechanism underlies bacterial persistence. *Proc Natl Acad Sci U S A.* **107**: 12541-12546.

Sarkar-Tyson M, Thwaite JE, Harding SV, Smither SJ, Oyston PC, Atkins TP & Titball RW (2007) Polysaccharides and virulence of *Burkholderia pseudomallei*. *J Med Microbiol* **56**: 1005-1010.

Sarovich DS, Price EP, Limmathurotsakul D*, et al.* (2012) Development of ceftazidime resistance in an acute *Burkholderia pseudomallei* infection. *Infect Drug Resist* **5**: 129-132.

Sayed N, Nonin-Lecomte S, Rety S & Felden B (2012) Functional and structural insights of a *Staphylococcus aureus* apoptotic-like membrane peptide from a Toxin-Antitoxin module. *J Biol Chem*.

Schell MA, Lipscomb L & DeShazer D (2008) Comparative genomics and an insect model rapidly identify novel virulence genes of *Burkholderia mallei*. *J Bacteriol* **190**: 2306-2313.

Schmidt O, Schuenemann VJ, Hand NJ, Silhavy TJ, Martin J, Lupas AN & Djuranovic S (2007) *prlF* and *yhaV* encode a new toxin-antitoxin system in *Escherichia coli*. *J Mol Biol* **372**: 894-905.

Schmidt O, Schuenemann V, Hand N, Silhavy T, Martin J, Lupas A & Djuranovic S (2007) *prlF* and *yhaV* encode a new toxin–antitoxin system in *Escherichia coli*. *J Mol Biol* **372**: 894-905.

Schumacher M, Piro K, Xu W, Hansen S, Lewis K & Brennan R (2009) Molecular mechanisms if HipA -mediated multidrug tolerance and its neutralisation by HipB. *Science.* **323**: 396-401.

Seshadri R, Myers GS, Tettelin H*, et al.* (2004) Comparison of the genome of the oral pathogen *Treponema denticola* with other spirochete genomes. *Proc Natl Acad Sci U S A* **101**: 5646-5651.

Sevillano L, Díaz M, Yamaguchi Y, Inouye M & Santamaría R (2012) Identification of the first functional toxin-antitoxin system in *Streptomyces*. *PLoS one* **7**: e32977.
[172] Sevillano L, Díaz M, Yamaguchi Y, Inouye M & Santamaría R (2012) Identification of the first functional toxin-antitoxin system in Streptomyces. *PLoS one* **7**: e32977.

Sevin E & Barloy-Hubler F (2007) RASTA-bacteria: A web based tool for identifying toxin-antitoxin loci in prokaryotes. *Genome Biol* **8**.

Shah D, Zhang Z, Khodursky A, Kaldalu N, Kurg K & Lewis K (2006) Persisters: a distinct physiological state of *E. coli*. *BMC Microbiol* **6**.

Shao Y, Harrison E, D B, X H, Ou H, Rajakumar K & Deng Z (2011) TADB: a web-based resource for Type 2 toxin-antitoxin loci in bacteria and archaea. *Nucleic Acids Res.* **39**: D606-611.

Showalter SA & Hall KB (2004) Altering the RNA-binding mode of the U1A RBD1 protein. *J Mol Biol* **335**: 465-480.

Sim S, Yu Y, Lin C*, et al.* (2008) The core and accessory genomes of *Burkholderia pseudomallei*: implications for human melioidosis. *PloS Pathog* **10**: e1000178.

Simpson AJ, Suputtamongkol Y, Smith MD*, et al.* (1999) Comparison of imipenem and ceftazidime as therapy for severe melioidosis. *Clin Infect Dis* **29**: 381-387.

Singh R, Barry CE, 3rd & Boshoff HI (2010) The three RelE homologs of Mycobacterium tuberculosis have individual, drug-specific effects on bacterial antibiotic tolerance. *J Bacteriol* **192**: 1279-1291.

Smith JA & Magnuson RD (2004) Modular organization of the Phd repressor/antitoxin protein. *J Bacteriol* **186**: 2692-2698.

Smith MD, Wuthiekanun V, Walsh AL & Pitt TL (1993) Latex agglutination test for identification of *Pseudomonas pseudomallei*. *J Clin Pathol* **46**: 374-375.

Spoering AL & Lewis K (2001) Biofilms and planktonic cells of *Pseudomonas aeruginosa* have similar resistance to killing by antimicrobials. *J Bacteriol* **183**: 6746-6751.

Stevens MP, Wood MW, Taylor LA*, et al.* (2002) An Inv/Mxi-Spa-like type III protein secretion system in *Burkholderia pseudomallei* modulates intracellular behaviour of the pathogen. *Mol Microbiol* **46**: 649-659.

Stevens MP, Haque A, Atkins T*, et al.* (2004) Attenuated virulence and protective efficacy of a *Burkholderia pseudomallei bsa* type III secretion mutant in murine models of melioidosis. *Microbiology* **150**: 2669-2676.

Studier FW (2005) Protein production by auto-induction in high density shaking cultures. *Protein Expr Purif* **41**: 207-234.

Suputtamongkol Y, Chaowagul W, Chetchotisakd P*, et al.* (1999) Risk factors for melioidosis and bacteremic melioidosis. *Clin Infect Dis* **29**: 408-413.

Tan Q, Awano N & Inouye M (2011) YeeV is an *Escherichia coli* toxin that inhibits cell division by targeting the cytoskeleton proteins, FtsZ and MreB. *Mol Microbiol* **79**: 109-118.

Tashiro Y, Kawata K, Taniuchi A, Kakinuma K, May T & Okabe S (2012) RelE-mediated dormancy is enhanced at high cell density in *Escherichia coli*. *J Bacteriol.* **194**: 1169–1176.

Tsilibaris V, Maenhaut-Michel G, Mine N & Melderen L (2007) What is the benefit to *Escherichia coli* is having multiple toxin-antitoxin in its genome? *J Bacteriol.* **189**: 6101-6108.

Tuanyok A, Kim H, Neirman W, Yu, Y, Dunbar J, Moore R, Baker P, Tom M, Ling J & Woods DE (2005) Genome-wide expression analysis of iron aqusition in *Burkholderia pseudomallei* and *Burkholderia mallei* using DNA microarrays. *FEMS Microbiol Letts* **252:** 327-335.

Tuanyok A, Tom M, Dunbar J & Woods DE (2006) Genome-wide expression analysis of *Burkholderia pseudomallei* infection in a hamster model of acute melioidosis. *Infect Immun* **74**: 5465-5476.

Tuanyok A, Leadem BR, Auerbach RK*, et al.* (2008) Genomic islands from five strains of *Burkholderia pseudomallei*. *BMC Genomics* **9**: 566.

Tumapa S, Holden MT, Vesaratchavest M*, et al.* (2008) *Burkholderia pseudomallei* genome plasticity associated with genomic island variation. *BMC Genomics* **9**: 190.

Ulrich RL, Deshazer D, Brueggemann EE, Hines HB, Oyston PC & Jeddeloh JA (2004) Role of quorum sensing in the pathogenicity of *Burkholderia pseudomallei*. *J Med Microbiol* **53**: 1053-1064.

Unoson C & Wagner EG (2008) A small SOS-induced toxin is targeted against the inner membrane in *Escherichia coli*. *Mol Microbiol* **70**: 258-270.

Utaisincharoen P, Tangthawornchaikul N, Kespichayawattana W, Anuntagool N, Chaisuriya P & Sirisinha S (2000) Kinetic studies of the production of nitric oxide (NO) and tumour necrosis factor-alpha (TNF-alpha) in macrophages stimulated with *Burkholderia pseudomallei* endotoxin. *Clin Exp Immunol* **122**: 324-329.

Valade E, Thibault FM, Gauthier YP, Palencia M, Popoff MY & Vidal DR (2004) The PmlI-PmlR quorum-sensing system in *Burkholderia pseudomallei* plays a key role in virulence and modulates production of the MprA protease. *J Bacteriol* **186**: 2288-2294.

van Schaik EJ, Tom M & Woods DE (2009) Burkholderia pseudomallei isocitrate lyase is a persistence factor in pulmonary melioidosis: implications for the development of isocitrate lyase inhibitors as novel antimicrobials. *Infect Immun* **77**: 4275-4283.

Vatcharapreechasakul T, Suputtamongkol Y, Dance DA, Chaowagul W & White NJ (1992) *Pseudomonas pseudomallei* liver abscesses: a clinical, laboratory, and ultrasonographic study. *Clin Infect Dis* **14**: 412-417.

Vazquez-Laslop N, Lee H & Neyfakh AA (2006) Increased persistence in Escherichia coli caused by controlled expression of toxins or other unrelated proteins. *J Bacteriol* **188**: 3494-3497.

Vega NM, Allison KR, Khalil AS & Collins JJ (2012) Signaling-mediated bacterial persister formation. *Nat Chem Biol* **8**: 431-433.

Walsh AL & Wuthiekanun V (1996) The laboratory diagnosis of melioidosis. *Br J Biomed Sci* **53**: 249-253.

Wang X, Lord DM, Cheng HY*, et al.* (2012) A new type V toxin-antitoxin system where mRNA for toxin GhoT is cleaved by antitoxin GhoS. *Nat Chem Biol*.

Waterfield NR, Ciche T & Clarke D (2009) Photorhabdus and a host of hosts. *Annu Rev Microbiol* **63**: 557-574.

White NJ (2003) Melioidosis. *Lancet* **361**: 1715-1722.

White NJ, Dance DA, Chaowagul W, Wattanagoon Y, Wuthiekanun V & Pitakwatchara N (1989) Halving of mortality of severe melioidosis by ceftazidime. *Lancet* **2**: 697-701.

Wibulpolprasert B & Dhiensiri T (1999) Visceral organ abscesses in melioidosis: sonographic findings. *J Clin Ultrasound* **27**: 29-34.

Wiersinga W, van der Poll T, White N, Day N & SJ P (2006) Melioidosis: insights into the pathogenicity of *Burkholderia pseudomallei*. *Nat Rev Microbiol* **4**: 273-282.

Wiersinga WJ & van der Poll T (2009) Immunity to *Burkholderia pseudomallei*. *Curr Opin Infect Dis* **22**: 102-108.

Wiersinga WJ, Currie BJ & Peacock SJ (2012) Melioidosis. *N Engl J Med* **367**: 1035-1044.

Wiersinga WJ, Wieland CW, Roelofs JJ & van der Poll T (2008) MyD88 dependent signaling contributes to protective host defense against *Burkholderia pseudomallei*. *PLoS One* **3**: e3494.

Wiersinga WJ, Meijers JC, Levi M, Van 't Veer C, Day NP, Peacock SJ & van der Poll T (2008) Activation of coagulation with concurrent impairment of anticoagulant mechanisms correlates with a poor outcome in severe melioidosis. *J Thromb Haemost* **6**: 32-39.

Wiersinga WJ, Wieland CW, van der Windt GJ*, et al.* (2007) Endogenous interleukin-18 improves the early antimicrobial host response in severe melioidosis. *Infect Immun* **75**: 3739-3746.

Williams JJ & Hergenrother PJ (2012) Artificial activation of toxin-antitoxin systems as an antibacterial strategy. *Trends Microbiol* **20**: 291-298.

Wong KT, Puthucheary SD & Vadivelu J (1995) The histopathology of human melioidosis. *Histopathology* **26**: 51-55.

Wu Y, Vulic M, Keren I & Lewis K (2012) Role of oxidative stress in persister tolerance. *Antimicrob Agents Chemother* **56**: 4922-4926.

Wuthiekanun V, Suputtamongkol Y, Simpson AJ, Kanaphun P & White NJ (2001) Value of throat swab in diagnosis of melioidosis. *J Clin Microbiol* **39**: 3801-3802.
Yamaguchi Y, Park J & Inouye M (2011) Toxin-antitoxin systems in Bacteria and Archaea. *Ann Rev Genet.* **45**: 61-79.

Yang H, Kooi CD & Sokol PA (1993) Ability of *Pseudomonas pseudomallei* malleobactin to acquire transferrin-bound, lactoferrin-bound, and cell-derived iron. *Infect Immun* **61**: 656-662.

Zhang J, Zhang Y & Inouye M (2003) Characterization of the Interactions within the *mazEF* Addiction Module of *Escherichia coli*. *Journal Biol Chem* **278**: 32300-32306.

Zhang Y & Inouye M (2009) The inhibitory mechanism of protein synthesis by YoeB, an *Escherichia coli* toxin. *J Biol Chem* **284**: 6627-6638.

Zhang Y, Zhang J, Hoeflich KP, Ikura M, Qing G & Inouye M (2003) MazF cleaves cellular mRNAs specifically at ACA to block protein synthesis in *Escherichia coli*. *Mol Cell* **12**: 913-923.

Zhu L, Sharp JD, Kobayashi H, Woychik NA & Inouye M (2010) Noncognate *Mycobacterium tuberculosis* toxin-antitoxins can physically and functionally interact. *J Biol Chem* **285**: 39732-39738.

Appendix

Primer name	Sequence
BpshipA_fwd (rh)	ACTAGTGCGGGAGGACTGGTGA
BpshipA_rv (rh)	GGATCCTTGCGTGCCGATTGCA
BPSS1060_fwd(rh)	actagtatgttgtcccttatgggttacaattctcgcatg
BPSS1060_rv (rh)	ggatcctcaatcctccagttcgccagcgat
BPSS0390_fwd (rh)	actagtATGAACTCATCGAAGCTGATCC
BPSS0390_Rv (rh)	ggatccTCACAGGCCGGCGGATTTC
BPSL0174 Fw	GAGCTCCGAACTGGAGGATTGAGTAT
BPSL0174Rv	CCATGGTGTGACGTTCGACGATTA
BPSS0391 Fw	GAGCTCATGGAATTTCCCATCGCAGTG
BPSS0391 rv	CCATGGTTATGCGTGCCTAACTTTGCC
paraBPSS0390BAD Fw	GAGCTCCTCTACTGTTTCTCCATACCC
paraBPSS0390BAD rv	CCGCGGTCTGCGTTCTGATTTAATCTG
BPSL0175 fwd	GAGCTCGCCATGGCGTTGTCCCTTATGGGTTACAATTCTCGCAT
BPSL0175 rv	GCGAATTCTCAATCCTCCAGTTCGCCAGCGATTT
BPSL2136_fwd	GGCCATGGTGATGGCAGATGTCCAGAAAACCG
BPSL2136_rv	ATAAGCTTTCACCCCTTGCCGTAGCG
BPSL2135_fwd	CCATGGTCAGCGCGAATCCTTCGGCAG
BPSL2135_rv	GCGGAATTCATGCCGAAGGTCCAGGTCTG
BPSS0390 N tag_fwd	CGCCGAGCTCATGAACTCATCGAAGCTGATCC
H24A_fwd	gttcgagtgacaggcagcgctcatcatttcaaacaccc
H24A rv	gggtgtttgaaatgatgagcgctgcctgtcactcgaac
S23A_fwd	gttggttcgagtgacaggcgcccatcatcatttcaaacac
S23A_rv	gtgtttgaaatgatgatgggcgcctgtcactcgaaccaac
G22C_fwd	tggaggttggttcgagtgacatgcagccatcat
G22C rv	atgatggctgcatgtcactcgaaccaacctcca
G14C_fwd	ccggatgcttgaggaagattgctggaggttg
G14C_rv	caacctccagcaatcttcctcaagcatccgg
P41A_fwd	gacggttccccacgcgaagaaggacct
P41A_rv	aggtccttcttcgcgtggggaaccgtc
BPSS1060_fwd	GAGCTCGCCATGGGAATGTCCCTTATGGGTTACAATTCTC
BPSS1060_rv	GAATTCCTCAATCCTCCAGTTCGCCAGCGATTTGC
BPSL3261_fwd	GAGCTCGCTAGCATGGCAACCATGCACGATA
BPSL3261_Rv	CGGAAGCTTCGTCATGACCATGCCTCGTTA
nativeBps-hipA_ fwd 2	TTAAACCATGGGTGTGAGCGCCCGCCGCGCA
nativeBps-hipA_ rv 2	ATGAATTCTCATGGCGCGCGCGC
H24A pET fwd	GGCCCATATG-AGGAGGAATTAACCATGGG
H24A pET rv	AATTGAATTC-CTCACAGGCCGGCGGATTTC
HipB_F	CCGAATTCATGGCCATCCTCATCGAGCAC
HipB_Rv	CCATGGTCACCAGTCCTCCCGCTTT
BPSS1061_fwd	GAGCTCGACGCAGAAGAAGGACATCA
BPSS1061_rv	CCATGGGACGTTCGACGATTACGAGA
BPSL0559 fwd	GAGCTCGCCATGGCTATGGCGACGACAAAAAAAGC
BPSL0559 rv	CGCGGAATTCTTACATGACGTCGGTCCACTCG
BPSL2333 fwd	GAGCTCGCCATGGCTATGGCCGAGGAAGACCTGTTGTG
BPSL2333 rv	GAATTCTCACGGCCATTCTTGGCGCGCATGCTTGA

BPSS0394 fwd	GAGCTCGCCATGGCTATGTCGAGCAAGCGTAAGATC
BPSS0394 rv	GGGAATTCCTACGCAGGCTGATGTTCC
BPSS0395 fwd	GAGCTCGCCATGGCTATGGAGTGTCGTTGGCGCTTG
BPSS0395 rv	GGCGCGGAATTCTTACGCTTGCTCGACATAGC
BPSL0175 fwd	GAGCTCGCCATGGCGTTGTCCCTTATGGGTTACAATTCTCGCAT
BPSL0175 rv	GCGAATTCTCAATCCTCCAGTTCGCCAGCGATTT
BPSS0390 fwd	GGAGCTCGCCATGGCTATGAACTCATCGAAGCTGATCC
BPSS0390 rv	GAATTCTCACAGGCCGGCGGATTTC
HipBA rv	cttataatatccccttaagcggataaacttgctgtggacgtatgacatggtgtaggctggagctgctt
HipBA fw	cggtcatgattgtcatgctcattaacaatgaccaaaccccatatctcacatatgaatatcctccttttagttccta
HipA-EcoRI	GCCCGGAATTCTCACTTACTACCGTATTC
HipA-SacI	CGGGAGCTCATGCCTAAACTTGTCACTTGG
HipA-NcoI	CGGCCATGGCTATGCCTAAACTTGTCACTTGG
paraBADBpshipA_ fwd	GAGCTCCACCAGATGGGCATTAAACG
paraBADBpshipA_rv	CACGATGGTGCAGCCAAGCTTCGAATTCTC
pBHR_fwd	AATACGGTCATACTGGCCTCCT
pBHR_rv	CGCGCAATTAACCCTCACTA
Pdm4 0390_1	ATATAACCCGGGTCTCGTGCTGACCGGCCC
Pdm4 0390_2	cgatatttagcggccgccattagctcccccgaatgtc
Pdm4 0390_3	gagctaatggcggccgctaaatatcgcgtgcgcctgta
Pdm4 0390_4	GAGCTCatggtcgctggattgggtgt
pDM4 up confirm	GTCTGGCCGTCTGCTGACGT
pDM4 gene confirm	ACAAGGCCTGGCTTCTTGGG
pDM4 down confirm	ACTCTTCCTGGTCTCGTGTG
BPSS0390 k/0 fw	GATATCCCGGATGAGTGCAGAACCC
BPSS0390 k/0 rv	CCGCGGAAATGATGATGGCTGCCTG
pME6032-fwd	CGTGATCGAAATCCAGATCC
pME6032-rv	TTGCGCCGACATCATAAC
Pscrhab3_fwd	TCTTTCCCTGGTTGCCAATG
Pscrhab3_rv	CCGCTTCTGCGTTCTGATTT

# ©2009 B@sic - UMR6026 CNRS / Université de Rennes1 - RASTA version 2.12										
BURPS1106A_3427	1	3338860	3339129	89	55.3	28.29	BURPS1106A_3426 Rorf_35135	0		hypothetical protein
# Result File for Burkholderia pseudomallei 1106a chromosome I: complete genome.										
BURPS1106A_3572	1	3479765	3480032	89	55.3	28.29	Rorf_36704	0		hypothetical protein
# [NC_009076.gbk Submitted on Fri Nov 13 11:45:12 2009]										
rpsT	-1	906842	907120	92	55.3	28.26	Rorf_9341 Rorf_9348	0		30s ribosomal protein s20
Gene	Strand	Left_End	Right_End	Length	Score	SizeScore	Possible_Partners	DomainScore	ConservedDomain	Product
BURPS1106A_1574	-1	1530042	1530320	92	55.3	28.26	Rorf_15973 Rorf_15986	0		hypothetical protein
BURPS1106A_3682	-1	3598216	3598467	83	76.4	27.55	Rorf_38213 Rorf_38214	21.9	HTH_3/HTH_XRE	prophage cp4-57 regulatory protein
BURPS1106A_1598	-1	1549031	1549309	92	55.3	28.26	Rorf_16229	0		hypothetical protein
BURPS1106A_0095	1	87362	87685	107	75	23.84	Rorf_936 Rorf_949	24.2	HTH_XRE/HTH_XRE/HTH_3/HipB	xre family transcriptional regulator
BURPS1106A_2037	1	2020016	2020294	92	55.3	28.26	Rorf_20952	0		transposase
BURPS1106A_0146	-1	140092	140493	133	73.7	24.23	Rorf_1730 Rorf_1727	22.5	HTH_XRE/HTH_3/HTH_XRE	addiction module antidote protein
BURPS1106A_0383	-1	350382	350648	88	55.1	28.13	Rorf_3938	0		sensor histidine kinase
BURPS1106A_2169	-1	2154644	2154976	110	72.9	23	Rorf_22608 BURPS1106A_2170	22.9	HTH_XRE/HTH_XRE/HTH_3	hypothetical protein
BURPS1106A_0407	1	371537	371803	88	55.1	28.13	Rorf_4165	0		hypothetical protein
Rorf_28041	-1	2678247	2678525	92	69.4	28.26	Rorf_28034 Rorf_28036 BURPS1106A_2709 Rorf_28048	24.2	Plasmid_stabil/ParE	
BURPS1106A_0640	-1	611541	611807	88	55.1	28.13	Rorf_6464	0		hypothetical protein
BURPS1106A_3691	-1	3606462	3606740	92	66.7	28.26		23.4	HTH_XRE/HTH_XRE/HTH_3/HipB	xre family transcriptional regulator
BURPS1106A_0790	-1	776101	776367	88	55.1	28.13	Rorf_8043 Rorf_8048	0		hypothetical protein
BURPS1106A_1009	1	987580	987876	98	66.7	26.68	BURPS1106A_1008 Rorf_10185 Rorf_10186	0		hypothetical protein
BURPS1106A_1101	-1	1082675	1082941	88	55.1	28.13	Rorf_11109	0		hypothetical protein
BURPS1106A_0797	-1	784375	784605	76	65.3	25.26	BURPS1106A_0796 Rorf_8130	0		hypothetical protein
BURPS1106A_1118	1	1097049	1097315	88	55.1	28.13	Rorf_11274 BURPS1106A_1120 Rorf_11285	0		hypothetical protein
Rorf_25404	-1	2410521	2410772	83	64.5	27.55	Rorf_25400	20	HicB/HicB	
Rorf_42105	-1	3887477	3887851	124	63.1	22.68	Rorf_42100 Rorf_42101	23.4	HTH_XRE/HTH_XRE/HTH_3/HipB	
Rorf_41135	1	3805982	3806314	110	62.8	23	Rorf_41132	22.8	HTH_4	
# ©2009 B@sic - UMR6026 CNRS / Université de Rennes1 - RASTA version 2.12										
Rorf_42142	1	3889222	3889656	144	61.5	21.42	Rorf_42150	23.1	HTH_XRE/HTH_XRE/HTH_3	
# Result File for Burkholderia pseudomallei 1106a chromosome II: complete genome.										
Rorf_25388	1	2410356	2410668	136	60.5	23.55	Rorf_25389 Rorf_25407	20	HicB/HicB	
# [NC_009078.gbk Submitted on Fri Nov 13 11:48:14 2009]										
Rorf_14761	1	1407066	1407299	77	55.6	25.58	Rorf_14698 BURPS1106A_1448 Rorf_14703	0		
Gene	Strand	Left_End	Right_End	Length	Score	SizeScore	Possible_Partners	DomainScore	ConservedDomain	Product
BURPS1106A_0993	1	974356	974628	90	55.4	28.39	Rorf_10048	0		hypothetical protein
BURPS1106A_A0075	-1	65894	66289	131	74.6	24.1	Rorf_792 BURPS1106A_A0076	23.5	COG3609	klua
BURPS1106A_2606	-1	2569742	2570014	90	55.4	28.39	Rorf_806 Rorf_803 Rorf_26951	0		hypothetical protein
BURPS1106A_A2904	-1	2837319	2837858	179	71.2	20.03	BURPS1106A_A2905	24.2	HTH_XRE/HTH_XRE/HTH_3/HipB	dna-binding protein
BURPS1106A_3022	1	2956190	2956462	90	55.4	28.39	BURPS1106A_3021 Rorf_30975	0		hypothetical protein
BURPS1106A_A2936	1	2864320	2864787	155	69.5	20.68	Rorf_31172	21.9	HTH_XRE/HTH_XRE/HTH_3	hypothetical protein
BURPS1106A_3315	1	3232248	3232520	90	55.4	28.39	Rorf_34135 Rorf_34132	0		hypothetical protein
BURPS1106A_A2905	-1	2837884	2838129	81	66.7	26.68	BURPS1106A_A2904 Rorf_30893 BURPS1106A_A2906	0		hypothetical protein
rpsQ	-1	3700381	3700653	90	55.4	28.39	rpmC	0		30s ribosomal protein s17
Rorf_12565	-1	1116982	1117224	80	66.5	26.22	Rorf_12560	23.3	HTH_XRE/HTH_XRE/HTH_3/HipB	
BURPS1106A_2354	-1	2330504	2330779	91	55.4	28.35	Rorf_24357 BURPS1106A_2355 Rorf_24362	0		hypothetical protein
Rorf_9030	-1	802718	803059	113	62.5	23.1	Rorf_9026	22.4	Phd	
BURPS1106A_2996	-1	2936902	2937177	91	55.4	28.35	Rorf_30725	0		hypothetical protein
BURPS1106A_A0003	-1	2488	2931	147	61.5	21.52	Rorf_38 BURPS1106A_A0004	0		hypothetical protein
BURPS1106A_3151	-1	3071856	3072131	91	55.4	28.35	Rorf_32237	0		rubredoxin
BURPS1106A_A0076	-1	66296	66838	180	60.1	20.1	BURPS1106A_A0075 Rorf_811 Rorf_812	0		hypothetical protein
rpsS	-1	3702427	3702702	91	55.4	28.35	rplV	0		30s ribosomal protein s19
BURPS1106A_A1538	1	1486326	1486556	76	58.5	25.26		23.3	HTH_4	hypothetical protein
osmB	-1	1375777	1376046	89	55.3	28.29	Rorf_14315 Rorf_14313	0		osmotically inducible
Rorf_803	-1	66220	66492	90	58.4	28.39	BURPS1106A_A0075	0		lipoprotein b
BURPS1106A_2120	1	2112851	2113120	89	55.3	28.29	BURPS1106A_A0076 Rorf_22219 BURPS1106A_2121	0		hypothetical protein
BURPS1106A_A2151	1	2107687	2108097	136	56.9	23.55		23.4	HTH_3/HTH_XRE/HTH_XRE/HipB	putative transcriptionl regulator hipb

BURPS1106A_A0999	1	971025	971297	90	55.4	28.39	Rorf_10999	0		hypothetical protein
BURPS1106A_A1892	-1	1856514	1856786	90	55.4	28.39	BURPS1106A_A1891	0		hypothetical protein
BURPS1106A_A2330	-1	2308420	2308692	90	55.4	28.39	Rorf_24613	0		tpr repeat-containing protein
BURPS1106A_A0451	-1	443912	444187	91	55.4	28.35	Rorf_5056 BURPS1106A_A0450	0		hypothetical protein
BURPS1106A_A0613	-1	598751	599026	91	55.4	28.35	BURPS1106A_A0614	0		hypothetical protein
BURPS1106A_A2356	1	2332467	2332742	91	55.4	28.35	Rorf_24887 Rorf_24889	0		hypothetical protein
BURPS1106A_A2681	1	2617434	2617709	91	55.4	28.35	BURPS1106A_A2680 Rorf_28009	0		hypothetical protein
BURPS1106A_A2910	1	2842460	2842735	91	55.4	28.35	Rorf_30938	0		hypothetical protein
BURPS1106A_A0442	-1	437796	438065	89	55.3	28.29	BURPS1106A_A0441 Rorf_5000 Rorf_5001 BURPS1106A_A0443	0		hypothetical protein
BURPS1106A_A1062	1	1021708	1021977	89	55.3	28.29	BURPS1106A_A1063	0		hypothetical protein
BURPS1106A_A1257	1	1190640	1190909	89	55.3	28.29	Rorf_13401 Rorf_13403 Rorf_13402	0		hypothetical protein
BURPS1106A_A1851	-1	1820763	1821032	89	55.3	28.29	BURPS1106A_A1852 Rorf_19562	0		hypothetical protein
BURPS1106A_A1882	-1	1844750	1845019	89	55.3	28.29	Rorf_19804 Rorf_19803	0		hypothetical protein
BURPS1106A_A2126	-1	2082175	2082444	89	55.3	28.29	Rorf_22309	0		hypothetical protein
BURPS1106A_A2409	-1	2387048	2387317	89	55.3	28.29	BURPS1106A_A2410 Rorf_25579	0		hypothetical protein
BURPS1106A_A2747	1	2684870	2685139	89	55.3	28.29	Rorf_28855	0		hypothetical protein
BURPS1106A_A3003	-1	2926223	2926492	89	55.3	28.29	Rorf_31752	0		hypothetical protein
BURPS1106A_A3061	1	2975681	2975950	89	55.3	28.29	Rorf_32235	0		hypothetical protein
BURPS1106A_A0227	-1	210832	211110	92	55.3	28.26	Rorf_2779	0		hypothetical protein
BURPS1106A_A1641	1	1612030	1612308	92	55.3	28.26	Rorf_17565 Rorf_17573	0		hypothetical protein
BURPS1106A_A1886	-1	1852128	1852406	92	55.3	28.26	BURPS1106A_A1887	0		hypothetical protein
BURPS1106A_A0880	1	866635	866901	88	55.1	28.13	BURPS1106A_A0879 Rorf_9693	0		hypothetical protein
BURPS1106A_A1003	1	973060	973326	88	55.1	28.13	Rorf_11017 Rorf_11022	0		hypothetical protein
BURPS1106A_A1705	1	1670108	1670374	88	55.1	28.13	Rorf_18102	0		hypothetical protein
BURPS1106A_A2412	1	2388755	2389021	88	55.1	28.13	Rorf_25608 Rorf_25622	0		hypothetical protein

# ©2009 B@sic - UMR6026 CNRS / Université de Rennes1 - RASTA version 2.12										
# Result File for Burkholderia pseudomallei 668 chromosome I: complete sequence.										
# [NC_009074.gbk Submitted on Fri Nov 13 11:45:31 2009]										
Gene	Strand	Left_End	Right_End	Length	Score	SizeScore	Possible_Partners	DomainScore	ConservedDomain	Product
Rorf_27309	-1	2630364	2630642	92	69.3	28.3	Rorf_27301 Rorf_27303 BURPS668_2652 Rorf_27315 Rorf_27317	24.1	Plasmid_stabil/ParE	
BURPS668_0785	-1	769005	769256	83	67.5	27.5	BURPS668_0784 Rorf_7872	0		hypothetical protein
BURPS668_1002	1	978485	978781	98	66.7	26.7	BURPS668_1001 Rorf_9950 Rorf_9951	0		hypothetical protein
Rorf_31465	1	2995926	2996324	132	65	24.1	Rorf_31458 Rorf_31460 Rorf_31473	23.9	HTH_XRE/HTH_XRE/HTH_3/HipB	
Rorf_31234	-1	2985289	2985609	106	64.7	23.9	Rorf_31244	23.7	HTH_XRE/HTH_XRE/HTH_3/HipB	
Rorf_22246	-1	2135065	2135418	117	64.5	22.7	Rorf_22240 Rorf_22241 Rorf_22254	24.8	HTH_XRE/HTH_3/HTH_XRE/HipB	
Rorf_40891	-1	3801661	3802035	124	63.1	22.7	Rorf_40886 Rorf_40887	23.4	HTH_XRE/HTH_XRE/HTH_3/HipB	
BURPS668_3910	-1	3809644	3810012	122	62.4	22.4	BURPS668_3909 Rorf_41054 Rorf_41055	0		abc-type co2+ transport system
Rorf_41122	1	3813820	3814254	144	61.5	21.4	Rorf_41130	23.1	HTH_XRE/HTH_XRE/HTH_3	
BURPS668_3905	-1	3803199	3803681	160	60.5	20.5	Rorf_40915 Rorf_40920 BURPS668_3906 Rorf_40934 Rorf_40926	0		hypothetical protein
Rorf_12626	1	1241496	1241999	167	60.1	20.3	Rorf_12624	22.7	VapC	
Rorf_22254	-1	2135432	2135704	90	58.4	28.4	Rorf_22246	0		
Rorf_38029	1	3568085	3568372	95	58	28	Rorf_38033 Rorf_38034	0		
BURPS668_1097	-1	1073941	1074213	90	55.4	28.4	Rorf_10864	0		hypothetical protein
BURPS668_1205	-1	1188265	1188537	90	55.4	28.4	Rorf_12123 Rorf_12130	0		hypothetical protein
BURPS668_2554	-1	2524549	2524821	90	55.4	28.4	Rorf_26276	0		hypothetical protein
BURPS668_2956	1	2908974	2909246	90	55.4	28.4	BURPS668_2955 Rorf_30255	0		hypothetical protein
BURPS668_3282	1	3216035	3216307	90	55.4	28.4	Rorf_34117 Rorf_34113	0		hypothetical protein
rpsQ	-1	3653169	3653441	90	55.4	28.4	rpmC	0		30s ribosomal protein s17
BURPS668_3899	-1	3797729	3798001	90	55.4	28.4	Rorf_40818	0		hypothetical protein
BURPS668_2125	1	2117421	2117696	91	55.4	28.4	BURPS668_2126	0		hypothetical protein
BURPS668_2502	-1	2465416	2465691	91	55.4	28.4	Rorf_25700	0		hypothetical protein
BURPS668_3115	-1	3056433	3056708	91	55.4	28.4	Rorf_32226	0		rubredoxin
rpsS	-1	3655215	3655490	91	55.4	28.4	rplV	0		30s ribosomal protein s19
BURPS668_3805	-1	3717675	3717950	91	55.4	28.4	BURPS668_3804 Rorf_39891 Rorf_39901 Rorf_39903 BURPS668_3806	0		hypothetical protein

BURPS668_0299	-1	282469	282738	89	55.3	28.3	Rorf_3122 Rorf_3130	0		hypothetical protein
BURPS668_0366	-1	337881	338150	89	55.3	28.3	Rorf_3707 Rorf_3719	0		hypothetical protein
BURPS668_0847	1	825357	825626	89	55.3	28.3	Rorf_8474	0		hypothetical protein
BURPS668_1341	-1	130876	130932	89	55.3	28.3	Rorf_13512	0		hypothetical protein
BURPS668_1360	1	132573	132601	89	55.3	28.3	Rorf_13715 Rorf_13716	0		hypothetical protein
BURPS668_1394	-1	136558	136849	89	55.3	28.3	Rorf_14081 Rorf_14079	0		surface antigen-like protein
BURPS668_2065	1	205653	205680	89	55.3	28.3	Rorf_21359 BURPS668_2066	0		hypothetical protein
BURPS668_3392	1	332101	332128	89	55.3	28.3	Rorf_35083	0		hypothetical protein
Rorf_27301	-1	263012	263035	76	55.3	25.3	Rorf_27297 Rorf_27298 Rorf_27309	0		
rpsT	-1	898830	899108	92	55.3	28.3	Rorf_9125 Rorf_9134	0		30s ribosomal protein s20
BURPS668_1550	-1	151976	152039	92	55.3	28.3	Rorf_15793 Rorf_15806	0		hypothetical protein
BURPS668_1573	-1	153872	153899	92	55.3	28.3	Rorf_16049	0		hypothetical protein
BURPS668_1971	1	194867	194952	92	55.3	28.3	Rorf_20244 Rorf_20255	0		hypothetical protein
BURPS668_2071	-1	206278	206302	92	55.3	28.3	Rorf_21417	0		hypothetical protein
BURPS668_3207	-1	313937	313954	92	55.3	28.3	Rorf_33149 BURPS668_3208	0		putative lipoprotein
BURPS668_3387	-1	331870	331898	92	55.3	28.3	BURPS668_3386	0		hypothetical protein
BURPS668_0625	-1	596554	596820	88	55.1	28.1	Rorf_6190	0		hypothetical protein
BURPS668_0730	1	707059	707325	88	55.1	28.1	Rorf_7284	0		hypothetical protein
BURPS668_0778	-1	760930	761196	88	55.1	28.1	Rorf_7788 Rorf_7793	0		hypothetical protein
BURPS668_1096	-1	1073548	1073814	88	55.1	28.1	Rorf_10864	0		hypothetical protein
BURPS668_1558	1	1525314	1525580	88	55.1	28.1	BURPS668_1559	0		hypothetical protein
BURPS668_1594	1	1565141	1565407	88	55.1	28.1	Rorf_16406	0		transposase
BURPS668_2671	1	2647237	2647503	88	55.1	28.1	Rorf_27480 Rorf_27481	0		hypothetical protein
BURPS668_2895	1	2853418	2853684	88	55.1	28.1	Rorf_29658	0		hypothetical protein
BURPS668_3053	-1	2997463	2997729	88	55.1	28.1	Rorf_31502 Rorf_31501	0		hypothetical protein
# ©2009 B@sic - UMR6026 CNRS / Université de Rennes1 - RASTA version 2.12										
# Result File for Burkholderia pseudomallei 668 chromosome III: complete sequence.										

# [NC_009075.gbk Submitted on Fri Nov 13 11:48:20 2009]										
Gene	Strand	Left_End	Right_End	Length	Score	SizeScore	Possible_Partners	DomainScore	ConservedDomain	Product
BURPS668_A1246	-1	1179532	1179774	80	76.5	26.2	Rorf_13604	23.3	HTH_XRE/HTH_XRE/HTH_3/HipB	dna-binding protein
BURPS668_A0093	-1	83135	83530	131	74.6	24.1	Rorf_1165 BURPS668_A0094	23.5	COG3609	hypothetical protein
BURPS668_A3020	-1	2868878	2869417	179	71.2	20	BURPS668_A3021	24.2	HTH_XRE/HTH_XRE/HTH_3/HipB	dna-binding protein
BURPS668_A3062	1	2905998	2906465	155	69.5	20.7	Rorf_31813 Rorf_31814 Rorf_31826	21.9	HTH_XRE/HTH_XRE/HTH_3	hypothetical protein
BURPS668_A3021	-1	2869443	2869688	81	66.7	26.7	BURPS668_A3020 Rorf_31446 BURPS668_A3022 Rorf_31445	0		hypothetical protein
Rorf_352	1	25140	25532	130	64.7	24	Rorf_362	23.7	HTH_XRE/HTH_XRE/HTH_3/HipB	
BURPS668_A0094	-1	83537	83944	135	64	24	BURPS668_A0093 Rorf_1178	0		hypothetical protein
Rorf_10194	-1	877606	877953	115	62.3	23	Rorf_10189 Rorf_10192	22.4	Phd	
BURPS668_A0003	-1	2488	2931	147	61.5	21.5	Rorf_38 BURPS668_A0004	0		serine/threonine protein kinase
BURPS668_A1623	1	1551280	1551510	76	58.5	25.3		23.3	HTH_4	hypothetical protein
Rorf_308	-1	23158	23436	92	58.3	28.3	Rorf_307 BURPS668_A0033	0		
Rorf_25089	1	2300233	2300517	94	57.9	27.9	BURPS668_A2366 Rorf_25095	0		
Rorf_13604	-1	1179261	1179524	87	57.7	27.7	BURPS668_A1246	0		
Rorf_24691	-1	2275055	2275558	167	57.3	20.3	Rorf_24699	20	HicB	
BURPS668_A2236	1	2168839	2169249	136	56.9	23.5		23.4	HTH_3/HTH_XRE/HTH_XRE/HipB	putative transcriptionl regulator hipb
Rorf_10189	-1	877300	877602	100	55.7	25.7	Rorf_10194 Rorf_10195	0		
BURPS668_A0256	1	227493	227765	90	55.4	28.4	Rorf_3277 Rorf_3279 BURPS668_A0255	0		hypothetical protein
BURPS668_A1085	1	1046114	1046386	90	55.4	28.4	Rorf_12174	0		hypothetical protein
BURPS668_A1984	-1	1922406	1922678	90	55.4	28.4	Rorf_21144	0		hypothetical protein
BURPS668_A2390	1	2310600	2310872	90	55.4	28.4	BURPS668_A2388	0		prophage cp4-57 regulatory protein (alpa)
BURPS668_A2468	-1	2385626	2385898	90	55.4	28.4	Rorf_26028	0		tpr repeat-containing protein
BURPS668_A2541	-1	2454119	2454391	90	55.4	28.4	Rorf_26879	0		hypothetical protein
BURPS668_A3094	1	2934224	2934496	90	55.4	28.4	Rorf_32080	0		hypothetical protein
BURPS668_A0255	1	227332	227607	91	55.4	28.4	Rorf_3262 BURPS668_A0256 Rorf_3274 Rorf_3275 Rorf_3264	0		hypothetical protein
BURPS668_A2828	1	2690611	2690886	91	55.4	28.4	BURPS668_A2827 Rorf_29349	0		hypothetical protein
BURPS668_A0117	1	100087	100356	89	55.3	28.3	Rorf_1406 Rorf_1420	0		hypothetical protein
BURPS668_A1329	1	1253422	1253691	89	55.3	28.3	Rorf_14454 Rorf_14456 Rorf_14455	0		hypothetical protein

BURPS668_A1942	-1	1886861	1887130	89	55.3	28.3	BURPS668_A1943 Rorf_20712 Rorf_20709	0		hypothetical protein
BURPS668_A2213	-1	2143478	2143747	89	55.3	28.3	Rorf_23376	0		hypothetical protein
BURPS668_A0659	1	630425	630703	92	55.3	28.3	Rorf_7645	0		hypothetical protein
BURPS668_A1730	1	1678801	1679079	92	55.3	28.3	Rorf_18720 Rorf_18726	0		hypothetical protein
BURPS668_A1979	-1	1918020	1918298	92	55.3	28.3	BURPS668_A1980	0		hypothetical protein
BURPS668_A2867	-1	2724690	2724968	92	55.3	28.3	BURPS668_A2866 Rorf_29763	0		hypothetical protein
BURPS668_A1147	1	1093081	1093347	88	55.1	28.1	BURPS668_A1148	0		hypothetical protein
BURPS668_A2357	-1	2295072	2295338	88	55.1	28.1	Rorf_25003 Rorf_25001	0		hypothetical protein
BURPS668_A2522	1	2436014	2436280	88	55.1	28.1	BURPS668_A2523 Rorf_26659	0		bbp50
BURPS668_A2523	1	2436220	2436486	88	55.1	28.1	Rorf_26673 BURPS668_A2522	0		bbp50
BURPS668_A2848	-1	2707927	2708193	88	55.1	28.1	Rorf_29552	0		hypothetical protein

# ©2009 B@sic - UMR6026 CNRS / Université de Rennes1 - RASTA version 2.12										
# Result File for Burkholderia pseudomallei 1710b chromosome I: complete sequence.										
# [NC_007434.gbk Submitted on Fri Nov 13 11:45:24 2009]										
Gene	Strand	Left_End	Right_End	Length	Score	SizeScore	Possible_Partners	DomainScore	ConservedDomain	Product
staB	-1	3090058	3090333	91	79.6	28.4	BURPS1710b_2786 Rorf_34595	24.29	Plasmid_stabil/ParE	stab
BURPS1710b_0117	-1	122160	122534	124	73.1	22.7	Rorf_1530 Rorf_1531 Rorf_1545 BURPS1710b_0118	23.44	HTH_XRE/HTH_XRE/HTH_3/HipB	putative dna-binding protein
BURPS1710b_2300	-1	2567261	2567593	110	72.9	23	Rorf_29174 BURPS1710b_2301	22.95	HTH_XRE/HTH_XRE/HTH_3	putative transcriptional regulatory protein
BURPS1710b_1676	-1	1795833	1796300	155	71.4	20.7	Rorf_20058 Rorf_20059 Rorf_20061	23.71	HTH_3/HTH_XRE/HTH_XRE/HipB/COG5499	gp68
Rorf_44654	-1	4000053	4000331	92	68.7	28.3	Rorf_44649 Rorf_44658 Rorf_44659	23.43	HTH_XRE/HTH_XRE/HTH_3/HipB	
BURPS1710b_1721	1	1851666	1852124	152	68	21	Rorf_21057 Rorf_21061 Rorf_21077	20	COG1598	copg family dna-binding protein
BURPS1710b_1163	1	1208733	1209029	98	66.7	26.7	BURPS1710b_1162 Rorf_12949 Rorf_12950	0		hypothetical protein
Rorf_20753	1	1837120	1837386	88	65.1	28.1	Rorf_20759	20	HicB	
Rorf_32016	-1	2824322	2824573	83	64.5	27.5	Rorf_32012	20	HicB/HicB	
BURPS1710b_0118	-1	122485	122805	106	63.9	23.9	BURPS1710b_0117 Rorf_1539	0		putative bacteriophage protein
Rorf_1572	1	123905	124339	144	61.5	21.4	Rorf_1580	23.11	HTH_XRE/HTH_XRE/HTH_3	
Rorf_32010	-1	2824059	2824469	136	60.5	23.5	Rorf_32001 Rorf_32019	20	HicB/HicB	
Rorf_19740	-1	1779222	1779722	166	60.4	20.3	Rorf_19752	23.05	HTH_XRE	
Rorf_1580	1	124336	124629	97	57.2	27.2	Rorf_1572	0		
BURPS1710b_2690	-1	2983584	2983856	90	55.4	28.4	Rorf_33554	0		hypothetical protein
BURPS1710b_3055	1	3366508	3366780	90	55.4	28.4	Rorf_37499 Rorf_37512	0		integrase
rpsQ	-1	4097456	4097728	90	55.4	28.4	rpmC	0		30s ribosomal protein s17
BURPS1710b_1657	1	1766280	1766555	91	55.4	28.4	BURPS1710b_1656	0		hypothetical protein
rpsS	-1	4099502	4099777	91	55.4	28.4	rplV	0		30s ribosomal protein s19
BURPS1710b_1527	-1	1614485	1614754	89	55.3	28.3	Rorf_17422 Rorf_17420	0		putative lipoprotein
BURPS1710b_2260	1	2525671	2525940	89	55.3	28.3	Rorf_28782 BURPS1710b_2261	0		hypothetical protein
BURPS1710b_3430	1	3748114	3748383	89	55.3	28.3	Rorf_41636	0		hypothetical protein
rpsT	-1	1130138	1130416	92	55.3	28.3	Rorf_12134 Rorf_12142	0		30s ribosomal protein s20
BURPS1710b_1286	1	1344293	1344571	92	55.3	28.3	Rorf_14486 Rorf_14492	0		hypothetical protein
BURPS1710b_1656	1	1766023	1766301	92	55.3	28.3	Rorf_19477 Rorf_19482 BURPS1710b_1657	0		gp36-related protein

BURPS1710b_0952	-1	998307	998573	88	55.1	28.1	Rorf_10813 Rorf_10818	0		hypothetical protein
BURPS1710b_1255	-1	1303823	1304089	88	55.1	28.1	Rorf_13862	0		hypothetical protein
BURPS1710b_1775	1	1931956	1932222	88	55.1	28.1	Rorf_22080	0		transposase
# ©2009 B@sic - UMR6026 CNRS / Université de Rennes1 - RASTA version 2.12										
# Result File for Burkholderia pseudomallei 1710b chromosome I: complete sequence.										
# [NC_007434.gbk Submitted on Fri Nov 13 11:45:24 2009]										
Gene	Strand	Left_End	Right_End	Length	Score	SizeScore	Possible_Partners	DomainScore	ConservedDomain	Product
staB	-1	3090058	3090333	91	79.6	28.4	BURPS1710b_2786 Rorf_34595	24.29	Plasmid_stabil/ParE	stab
BURPS1710b_0117	-1	122160	122534	124	73.1	22.7	Rorf_1530 Rorf_1531 Rorf_1545 BURPS1710b_0118	23.44	HTH_XRE/HTH_XRE/HTH_3/HipB	putative dna-binding protein
BURPS1710b_2300	-1	2567261	2567593	110	72.9	23	Rorf_29174 BURPS1710b_2301	22.95	HTH_XRE/HTH_XRE/HTH_3	putative transcriptional regulatory protein
BURPS1710b_1676	-1	1795833	1796300	155	71.4	20.7	Rorf_20058 Rorf_20059 Rorf_20061	23.71	HTH_3/HTH_XRE/HTH_XRE/HipB/COG5499	gp68
Rorf_44654	-1	4000053	4000331	92	68.7	28.3	Rorf_44649 Rorf_44658 Rorf_44659	23.43	HTH_XRE/HTH_XRE/HTH_3/HipB	
BURPS1710b_1721	1	1851666	1852124	152	68	21	Rorf_21057 Rorf_21061 Rorf_21077	20	COG1598	copg family dna-binding protein
BURPS1710b_1163	1	1208733	1209029	98	66.7	26.7	BURPS1710b_1162 Rorf_12949 Rorf_12950	0		hypothetical protein
Rorf_20753	1	1837120	1837386	88	65.1	28.1	Rorf_20759	20	HicB	
Rorf_32016	-1	2824322	2824573	83	64.5	27.5	Rorf_32012	20	HicB/HicB	
BURPS1710b_0118	-1	122485	122805	106	63.9	23.9	BURPS1710b_0117 Rorf_1539	0		putative bacteriophage protein
Rorf_1572	1	123905	124339	144	61.5	21.4	Rorf_1580	23.11	HTH_XRE/HTH_XRE/HTH_3	
Rorf_32010	-1	2824059	2824469	136	60.5	23.5	Rorf_32001 Rorf_32019	20	HicB/HicB	
Rorf_19740	-1	1779222	1779722	166	60.4	20.3	Rorf_19752	23.05	HTH_XRE	
Rorf_1580	1	124336	124629	97	57.2	27.2	Rorf_1572	0		
BURPS1710b_2690	-1	2983584	2983856	90	55.4	28.4	Rorf_33554	0		hypothetical protein
BURPS1710b_3055	1	3366508	3366780	90	55.4	28.4	Rorf_37499 Rorf_37512	0		integrase
rpsQ	-1	4097456	4097728	90	55.4	28.4	rpmC	0		30s ribosomal protein s17
BURPS1710b_1657	1	1766280	1766555	91	55.4	28.4	BURPS1710b_1656	0		hypothetical protein
rpsS	-1	4099502	4099777	91	55.4	28.4	rplV	0		30s ribosomal protein s19
BURPS1710b_1527	-1	1614485	1614754	89	55.3	28.3	Rorf_17422 Rorf_17420	0		putative lipoprotein

BURPS1710b_2260	1	2525671	2525940	89	55.3	28.3	Rorf_28782 BURPS1710b_2261	0		hypothetical protein
BURPS1710b_3430	1	3748114	3748383	89	55.3	28.3	Rorf_41636	0		hypothetical protein
rpsT	-1	1130138	1130416	92	55.3	28.3	Rorf_12134 Rorf_12142	0		30s ribosomal protein s20
BURPS1710b_1286	1	1344293	1344571	92	55.3	28.3	Rorf_14486 Rorf_14492	0		hypothetical protein
BURPS1710b_1656	1	1766023	1766301	92	55.3	28.3	Rorf_19477 Rorf_19482 BURPS1710b_1657	0		gp36-related protein
BURPS1710b_0952	-1	998307	998573	88	55.1	28.1	Rorf_10813 Rorf_10818	0		hypothetical protein
BURPS1710b_1255	-1	1303823	1304089	88	55.1	28.1	Rorf_13862	0		hypothetical protein
BURPS1710b_1775	1	1931956	1932222	88	55.1	28.1	Rorf_22080	0		transposase

# ©2009 B@sic - UMR6026 CNRS / Université de Rennes1 - RASTA version 2.12										
# Result File for Burkholderia pseudomallei K96243 chromosome 1: complete sequence.										
# [NC_006350.gbk Submitted on Wed Oct 7 10:27:18 2009]										
Gene	Strand	Left_End	Right_End	Length	Score	SizeScore	Possible_Partners	DomainScore	ConservedDomain	Product
BPSL2333	-1	2820136	2820411	91	79.6	28.4	Rorf_30837 BPSL2334 Rorf_30846	24.29	Plasmid_stabil/ParE	hypothetical protein
BPSL3260	-1	3876826	3877212	128	74.9	23.5	BPSL3259 BPSL3261	24.33	VapI/MazE/HTH_XRE/HTH_XRE	hypothetical protein
BPSL0549A	-1	606593	607036	147	73.3	21.5	Rorf_6398 Rorf_6413	24.83	HipB/HipB/HTH_XRE/HTH_XRE/HTH_XRE/HTH_XRE/HTH_3/HTH_3	putative dna-binding protein
BPSL1564	1	1814641	1814973	110	72.9	23	Rorf_20079 BPSL1563	22.95	HTH_XRE/HTH_XRE/HTH_3	putative transcriptional regulatory protein
BPSL0756	-1	873400	873873	157	71.3	20.6	Rorf_9794 Rorf_9790	23.75	HTH_XRE/HTH_XRE/HTH_3/HipB	putative dna-binding protein
BPSL0141	1	153537	154043	168	70.8	20.3	Rorf_1795	23.5	HTH_XRE/HipB/HTH_XRE/HTH_3	putative phage dna-binding protein
BPSL0079	-1	90207	90668	153	69.8	20.9	Rorf_907	21.85	HTH_XRE/HTH_3/HTH_XRE	hypothetical protein
BPSL3261	-1	3877164	3877472	102	65.4	25.4	BPSL3260 Rorf_42693	0		hypothetical protein
Rorf_43830	-1	3966098	3966430	110	63.4	23	Rorf_43826 Rorf_43838 Rorf_43839	23.44	HTH_XRE/HTH_XRE/HTH_3/HipB	
BPSL0562	1	615675	616079	134	62.9	24.2		23.75	HTH_XRE/HTH_XRE/HTH_3/HipB	putative dna-binding protein
BPSL3259	-1	3876611	3876817	68	62.2	22.2	Rorf_42667 Rorf_42669 Rorf_42670 BPSL3260	0		putative plasmid conjugal transfer protein
BPSL0558	1	612984	613364	126	61	22.9		23.1	HTH_XRE/HTH_XRE/HTH_3/HipB	putative dna-binding protein
BPSL0938A	1	1090254	1090730	158	60.6	20.6	BPSL0938 Rorf_12168	0		hypothetical protein
Rorf_17383	-1	1561823	1562290	155	60.3	20.7	Rorf_17386 Rorf_17387	22.59	RelE	
BPSL0733	-1	847318	847833	171	60.2	20.2	Rorf_9276 BPSL0734	0		hypothetical protein
Rorf_20353	-1	1844766	1845185	139	59.5	22.5	Rorf_20351 Rorf_20354	20	HicB/HicB	
Rorf_1795	1	153268	153540	90	58.4	28.4	Rorf_1787 Rorf_1789 BPSL0141	0		
Rorf_17387	-1	1562312	1562578	88	58.1	28.1	Rorf_17383 Rorf_17393	0		
Rorf_40671	1	3718975	3719262	95	58	28	BPSL3115 Rorf_40676	0		
Rorf_17386	-1	1562307	1562555	82	57.1	27.1	Rorf_17383 Rorf_17393	0		
Rorf_12159	1	1090217	1090513	98	56.7	26.7	BPSL0938 Rorf_12162 Rorf_12163	0		
Rorf_6398	-1	606353	606589	78	55.8	25.8	Rorf_6403 BPSL0549A	0		
BPSL0164	-1	171289	171561	90	55.4	28.4	Rorf_2037 BPSL0165	0		putative phage-encoded membrane protein
BPSL2251	-1	2713542	2713814	90	55.4	28.4	Rorf_29795	0		hypothetical protein
rpsQ	-1	380403	380415	90	55.4	28.4	rpmC	0		30s ribosomal protein s17

Rorf_9283	-1	847656	847964	102	55.4	25.4	BPSL0734 Rorf_9287	0		
BPSL0161	-1	169931	170206	91	55.4	28.4	BPSL0160 Rorf_2024	0		hypothetical protein
BPSL1151	-1	1333713	1333988	91	55.4	28.4	BPSL1150 Rorf_14920 BPSL1152	0		hypothetical protein
BPSL2326	1	2811918	2812193	91	55.4	28.4	Rorf_30751	0		hypothetical protein
BPSL2573	-1	3099960	3100235	91	55.4	28.4	BPSL2572 BPSL2574	0		hypothetical protein
rubA	-1	3221882	3222157	91	55.4	28.4	Rorf_35192	0		rubredoxin
rpsS	-1	3806089	3806364	91	55.4	28.4	rplV	0		30s ribosomal protein s19
osmB	-1	1501627	1501896	89	55.3	28.3	Rorf_16810 Rorf_16808	0		osmotically inducible lipoprotein b precursor
BPSL1602	-1	1856701	1856970	89	55.3	28.3	BPSL1601 Rorf_20468	0		hypothetical protein
BPSL2920	1	3488481	3488750	89	55.3	28.3	Rorf_38070	0		hypothetical protein
rpsT	-1	1011098	1011376	92	55.3	28.3	Rorf_11339 Rorf_11347	0		30s ribosomal protein s20
BPSL2072	1	2479511	2479789	92	55.3	28.3	Rorf_27464 Rorf_27457	0		hypothetical protein
BPSL0844a	1	983711	983977	88	55.1	28.1	Rorf_11080	0		hypothetical protein
BPSL1038	-1	1207929	1208195	88	55.1	28.1	Rorf_13549	0		hypothetical protein
# ©2009 B@sic - UMR6026 CNRS / Université de Rennes1 - RASTA version 2.12										
# Result File for Burkholderia pseudomallei K96243 chromosome II: complete sequence.										
# [NC_006351.gbk Submitted on Wed Oct 7 10:30:07 2009]										
Gene	Strand	Left_End	Right_End	Length	Score	SizeScore	Possible_Partners	DomainScore	ConservedDomain	Product
BPSS0390	1	535656	536156	166	80.3	20.3	Rorf_6322 Rorf_6326 BPSS0391 Rorf_6342 Rorf_6344	20	COG1724	hypothetical protein
BPSS0380	1	521052	521324	90	79.1	28.4	Rorf_6038	23.71	HTH_XRE/HTH_3/HTH_XRE/HipB	dna-binding regulatory protein
BPSS0381	1	522433	522720	95	78.7	28	Rorf_6072	23.71	HTH_XRE/HTH_3/HTH_XRE/HipB/VapI	dna-binding regulatory protein
msr0960	-1	1134960	1135202	80	76.5	26.2	Rorf_13003	23.27	HTH_XRE/HTH_XRE/HTH_3/HipB	dna-binding protein
BPSS1152	1	1538943	1539173	76	75.5	25.3	BPSS1153	23.29	HTH_4	copg family protein
BPSS1056	1	1433991	1434272	93	74.7	27.7	Rorf_16048 Rorf_16042	20	HicB/HicB	copg family protein
BPSS0059	-1	63800	64195	131	74.6	24.1	Rorf_770 Rorf_780 Rorf_781	23.51	COG3609	hypothetical protein
BPSS1047	-1	1426470	1426814	114	72.5	23	Rorf_15901 Rorf_15916	22.51	HTH_3/HTH_XRE/HTH_XRE/VapI	hypothetical protein
BPSS2142	-1	2900290	2900829	179	71.2	20	Rorf_32138 Rorf_32139	24.17	HTH_XRE/HTH_XRE/HTH_3/HipB	merr family transcriptional regulator
BPSS2172	1	2937924	2938391	155	69.5	20.7	Rorf_32521 Rorf_32534	21.85	HTH_XRE/HTH_XRE/HTH_3	hypothetical protein

BPSS0003	-1	2471	2929	152	61	21	Rorf_37 BPSS0004	0		hypothetical protein
Rorf_6309	1	534710	534865	51	58.7	20.5	Rorf_6313 Rorf_6315	21.25	MazF	
Rorf_13003	-1	1134689	1134952	87	57.7	27.7	msr0960	0		
hipB	1	2155047	2155451	134	57.6	24.2		23.38	HTH_XRE/HTH_3/HTH_XRE/HipB	transcription regulator
Rorf_32138	-1	2900855	2901100	81	56.7	26.7	BPSS2142 Rorf_32144	0		
BPSS1071	1	1444964	1445236	90	55.4	28.4	BPSS1070 Rorf_16200	0		bacteriophage membrane protein
BPSS1048d	1	1428598	1428873	91	55.4	28.4	Rorf_15958 Rorf_15965 BPSS1048c	0		hypothetical protein
BPSS1073A	1	1446319	1446594	91	55.4	28.4	BPSS1074	0		hypothetical protein
BPSS1226	1	1658338	1658616	92	55.3	28.3	Rorf_18407 Rorf_18416	0		hypothetical protein
BPSS0118	1	151019	151285	88	55.1	28.1	Rorf_2087 Rorf_2101 Rorf_2102	0		hypothetical protein
BPSS0406	1	548784	549050	88	55.1	28.1	Rorf_6592	0		hypothetical protein
BPSS1053	1	1432704	1432970	88	55.1	28.1	BPSS1054	0		bacteriophage-acquired protein